ISSN 0021-9673

VOL. 543 NO. 1 APRIL 26, 1991

RNAL OF HROMATOGRAPHY

LUDING ELECTROPHORESIS AND OTHER SEPARATION METHODS

ELSEVIER

JOURNAL OF CHROMATOGRAPHY

Scope. The *Journal of Chromatography* publishes papers on all aspects of chromatography, electrophoresis and related methods. Contributions consist mainly of research papers dealing with chromatographic theory, instrumental development and their applications. The section *Biomedical Applications*, which is under separate editorship, deals with the following aspects: developments in and applications of chromatographic and electrophoretic techniques related to clinical diagnosis or alterations during medical treatment; screening and profiling of body fluids or tissues with special reference to metabolic disorders; results from basic medical research with direct consequences in clinical practice; drug level monitoring and pharmacokinetic studies; clinical toxicology; analytical studies in occupational medicine.

Submission of Papers. Manuscripts (in English; *four* copies are required) should be submitted to: Editorial Office of *Journal of Chromatography*, P.O. Box 681, 1000 AR Amsterdam, The Netherlands, Telefax (+31-20) 5862 304, or to: The Editor of *Journal of Chromatography, Biomedical Applications*, P.O. Box 681, 1000 AR Amsterdam, The Netherlands. Review articles are invited or proposed by letter to the Editors. An outline of the proposed review should first be forwarded to the Editors for preliminary discussion prior to preparation. Submission of an article is understood to imply that the article is original and unpublished and is not being considered for publication elsewhere. For copyright regulations, see below.

Subscription Orders. Subscription orders should be sent to: Elsevier Science Publishers B.V., P.O. Box 211, 1000 AE Amsterdam, The Netherlands, Tel. (+31-20) 5803 911, Telex 18582 ESPA NL, Telefax (+31-20) 5803 598. The *Journal of Chromatography* and the *Biomedical Applications* section can be subscribed to separately.

Publication. The *Journal of Chromatography* (incl. *Biomedical Applications*) has 38 volumes in 1991. The subscription prices for 1991 are:

J. Chromatogr. (incl. *Cum. Indexes, Vols. 501–550*) + *Biomed. Appl.* (Vols. 535–572):
Dfl. 7220.00 plus Dfl. 1140.00 (p.p.h.) (total *ca.* US$ 4976.25)

J. Chromatogr. (incl. *Cum. Indexes, Vols. 501–550*) only (Vols. 535–561):
Dfl. 5859.00 plus Dfl. 810.00 (p.p.h.) (total *ca.* US$ 3969.75)

Biomed. Appl. only (Vols. 562–572):
Dfl. 2387.00 plus Dfl. 330.00 (p.p.h.) (total *ca.* US$ 1617.25).

Our p.p.h. (postage, package and handling) charge includes surface delivery of all issues, except to subscribers in Argentina, Australia, Brasil, Canada, China, Hong Kong, India, Israel, Malaysia, Mexico, New Zealand, Pakistan, Singapore, South Africa, South Korea, Taiwan, Thailand and the U.S.A. who receive all issues by air delivery (S.A.L. — Surface Air Lifted) at no extra cost. For Japan, air delivery requires 50% additional charge; for all other countries airmail and S.A.L. charges are available upon request. Back volumes of the *Journal of Chromatography* (Vols. 1–534) are available at Dfl. 208.00 (plus postage). Claims for missing issues will be honoured, free of charge, within three months after publication of the issue. Customers in the U.S.A. and Canada wishing information on this and other Elsevier journals, please contact Journal Information Center, Elsevier Science Publishing Co. Inc., 655 Avenue of the Americas, New York, NY 10010, U.S.A., Tel. (+1-212) 633 3750, Telefax (+1-212) 633 3990.

Abstracts/Contents Lists published in Analytical Abstracts, Biochemical Abstracts, Biological Abstracts, Chemical Abstracts, Chemical Titles, Chromatography Abstracts, Clinical Chemistry Lookout, Current Contents/Life Sciences, Current Contents/Physical, Chemical & Earth Sciences, Deep-Sea Research/Part B: Oceanographic Literature Review, Excerpta Medica, Index Medicus, Mass Spectrometry Bulletin, PASCAL-CNRS, Pharmaceutical Abstracts, Referativnyi Zhurnal, Research Alert, Science Citation Index and Trends in Biotechnology.

See inside back cover for Publication Schedule, Information for Authors and information on Advertisements.

0021-9673/91/$03.50

Printed in The Netherlands

VOL. 543, NO. 1 JOURNAL OF CHROMATOGRAPHY APRIL 26, 1991

CONTENTS

(Abstracts/Contents Lists published in Analytical Abstracts, Biochemical Abstracts, Biological Abstracts, Chemical Abstracts, Chemical Titles, Chromatography Abstracts, Current Contents/Life Sciences, Current Contents/Physical, Chemical & Earth Sciences, Deep-Sea Research/Part B: Oceanographic Literature Review, Excerpta Medica, Index Medicus, Mass Spectrometry Bulletin, PASCAL-CNRS, Referativnyi Zhurnal, Research Alert and Science Citation Index)

REGULAR PAPERS

Column Liquid Chromatography

(Continued overleaf)

In articles with more than one author, the name of the author to whom correspondence should be addressed is indicated in the article heading by a 6-pointed asterisk (*)

Journal of Chromatography Library, 50

Liquid Chromatography in Biomedical Analysis

edited by **T. Hanai,** *International Institute of Technological Analysis, Health Research Foundation, Kyoto, Japan*

This book presents a guide for the analysis of biomedically important compounds using modern liquid chromatographic techniques. After a brief summary of basic liquid chromatographic methods and optimization strategies, the main part of the book focuses on the various classes of biomedically important compounds: amino acids, catecholamines, carbohydrates, fatty acids, nucleotides, porphyrins, prostaglandins and steroid hormones. The different chapters discuss specialized techniques pertaining to each class of compounds, such as sample pretreatment, pre- and post-column derivatization, detection and quantification.

1991 xii + 296 pages
Price: US $ 154.50 / Dfl. 270.00
ISBN 0-444-87451-8

Contents:

Elsevier Science Publishers

P.O. Box 211, 1000 AE Amsterdam, The Netherlands
P.O. Box 882, Madison Square Station, New York, NY 10159, USA

ANATECH '92

3rd International Symposium on Analytical Techniques for Industrial Process Control

Atlanta, 6-8 April 1992

MORE INFORMATION FROM:

Infoscience Services Inc
3000 Dundee Road, Suite 313
Northbrook, IL. 60062, USA
Tel: (708) 291-9161
Fax: (708) 291-0097

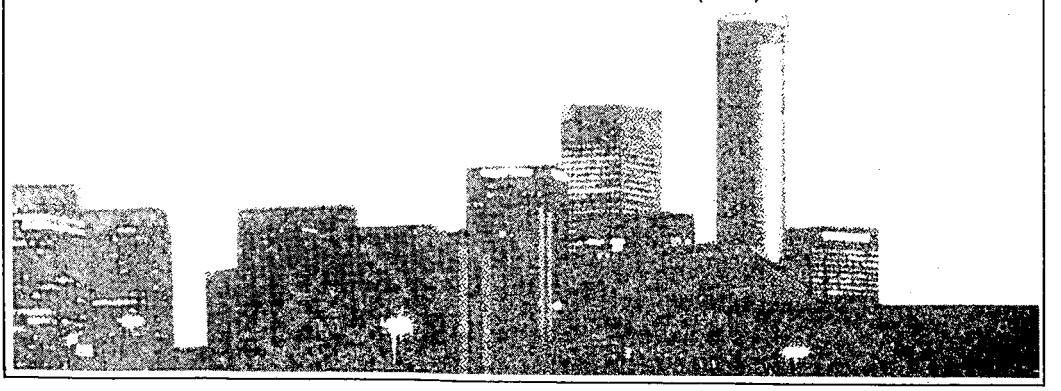

Selective Sample Handling and Detection in High-Performance Liquid Chromatography

Journal of Chromatography Library, 39

part A

edited by **R.W. Frei†**, *Free University, Amsterdam, The Netherlands, and* **K. Zech**, *Byk Gulden Pharmaceuticals, Konstanz, FRG*

Part A of this two-volume project attempts to treat the sample handling and detection processes in a liquid chromatographic system in an integrated fashion. The need for more selective and sensitive chromatographic methods to help solve the numerous trace analysis problems in complex samples is undisputed. However, few workers realize the strong interdependence of the various steps - sample handling, separation and detection - which must be considered if one wants to arrive at an optimal solution. By introducing a strong element of selectivity and trace enrich- ment in the sample preparation step, fewer demands are placed on the quality of the chromatography and often a simple UV detector can be used. By using a selective detection mode, i.e. a reaction detector, the sample handling step can frequently be simplified and more easily automated. The impact of such a "total system" approach on handling series of highly complex samples such as environmental specimens or biological fluids can be easily imagined.

1988 xii + 458 pages
US$ 123.00 / Dfl. 240.00
ISBN 0-444-42881-X

part B

edited by **K. Zech**, *Byk Gulden Pharmaceuticals, Konstanz, FRG, and* **R.W. Frei†**, *Free University, Amsterdam, The Netherlands*

Part B completes the treatment of the handling, separation and detection of complex samples as an integrated, interconnected process. On the basis of this philosophy the editors have selected those contributions which demonstrate that optimal sample preparation leads to a simplification of detection or reduced demands on the separation process. Throughout the book emphasis is on chemical principles with minimum discussion of the equipment required - an approach which reflects the editors' view that the limiting factor in the analysis of complex samples is an incomplete knowledge of the underlying chemistry rather than the hardware available. This lack of knowledge becomes more evident as the demands for lower detection limits grow, as solving complex matrix problems requires a greater understanding of the chemical interaction between the substance to be analysed and the stationary phase.

1989 xii + 394 pages
US$ 136.00 / Dfl. 265.00
ISBN 0-444-88327-4

Written by experienced practitioners, these volumes will be of interest to investigators in many areas of application, including environmental scientists and those active in the clinical, pharmaceutical and bioanalytical fields.

For more information, please write to:

Elsevier Science Publishers
P.O. Box 211, 1000 AE Amsterdam, The Netherlands
P.O. Box 882, Madison Square Station, New York, NY 10159, USA

JOURNAL OF CHROMATOGRAPHY

VOL. 543 (1991)

JOURNAL of CHROMATOGRAPHY

INCLUDING ELECTROPHORESIS AND OTHER SEPARATION METHODS

ELSEVIER

AMSTERDAM — OXFORD — NEW YORK — TOKYO

0021-9673/91/$03.50

Printed in The Netherlands

Journal of Chromatography, 543 (1991) 1–7
Elsevier Science Publishers B.V., Amsterdam

CHROM. 23 096

Chromatographic stability of silica-based aminopropyl-bonded stationary phases

B. PORSCH*
Institute of Macromolecular Chemistry, Czechoslovak Academy of Sciences, 162 06 Prague 6 (Czechoslovakia)
and
J. KRÁTKÁ
Research Institute for Plant Production, Ruzyně 507, 161 06 Prague 6 (Czechoslovakia)
(First received July 26th, 1990; revised manuscript received December 27th, 1990)

ABSTRACT

Causes of frequently observed changes in the properties of columns packed with silica modified with primary amino groups were investigated chromatographically, and it was confirmed that the initial instability of new columns appears to be due to the gradual desorption of the respective silane. Further changes in the chromatographic properties during the operation ensue from deactivation of the surface with impurities capable of reacting with the primary amino group. The main source of these impurities is the mobile phase. Simple prevention can be achieved with a protective column packed with the same sorbent and placed between the pump and the injection valve, which allows the column to be used for several months without changes in its chromatographic properties.

INTRODUCTION

Silica modified with chemically bonded primary amino groups is one of the most widely used column packings for the high-performance liquid chromatography (HPLC) of sugar mixtures [1]. In addition to this main field of application, it is also of advantage in some other instances [2]. A frequent, though by no means unanimous, objection to its application is the insufficient chemical stability and the short lifetime of the columns. There is a broad range of views between such extremes, from uselessness of the packing owing to its decomposition, on the one hand [3], and a considerable durability in the case of proper treatment, on the other [4].

Gradual dissolution of the primary amino phase matrix in aqueous mobile phases explains its settling in the column and the decrease in efficiency [5]. Moreover, this sorbent occupies a special position among the various bonded phases, because it is a chemically reactive material [1,2]. The primary amino group may react with many impurities from the mobile phase or the sample and may become deactivated, which in turn may cause changes in the chromatographic properties, *i.e.*, capacity factors and selectivity. In contrast to deactivation by sorption, where in most instances conditions can be found for the desorption of impurities, the amino phase may be regenerated only exceptionally, if the reacting impurity is known [6].

0021-9673/91/$03.50

Knowledge regarding the chromatographic stability of columns packed with primary amino phases is incomplete [7]. Changes in the content of the stationary phase and in the dissolution of the matrix can be followed by employing suitable analytical procedures [8,9] or spectral analysis [10]. It has been shown [11] that dissolution of the silica matrix takes place also with bonded phases, especially at lower pH. The bonded groups protect the matrix; the extent of this protection depends on the size and length of the organic groups and on the bonding chemistry. Hence the gradual dissolution of the silica gel matrix in water-containing mobile phases should be accepted as a fact [12], but the essential features for practical application are a sufficiently long lifetime and the chromatographic stability of the columns.

For this reason, this study considered with the chromatographic stability of the sorbent from the practical point of view, *i.e.*, with the effect of changes in the content of the stationary phase due to washing in water on chromatographic properties in a non-aqueous medium and in the separation of sugar mixtures. Using identical chromatographic conditions, consequences of the chemical deactivation of the sorbent's surface by impurities reacting with the primary amino group were established.

EXPERIMENTAL

Materials

Two types of silica were used (mean particle diameter d_p = 10 μm) with chemically bonded primary amino groups: Separon SIX NH_2 (Laboratory Instruments, Prague, Czechoslovakia; present manufacturer, Tessek, Prague, Czechoslovakia) and LiChrosorb NH_2 (E. Merck, Darmstadt, Germany), specific surface area 480 and 300 m^2/g, respectively. Xylose, arabinose, fructose, glucose, saccharose, maltose, lactose, nitrobenzene, *o*-, *m*- and *p*-chloronitrobenzene and acetonitrile (all analytical-reagent grade) were obtained from Fluka (Buchs, Switzerland) and toluene and heptane (technical and analytical-reagent grade) from Lachema (Brno, Czechoslovakia).

Apparatus, columns and procedures

The liquid chromatograph consisted of a VCM 300 reciprocal membrane pump (CSAS Development Works, Prague, Czechoslovakia), a stop-flow injection valve made at the Institute of Macromolecular Chemistry, an R 401 differential refractometer (Waters Assoc., Milford, MA, U.S.A.) and a Servogor 2S recorder (Goerz Electro, Vienna, Austria). Stainless-steel columns made at the Institute of Macromolecular Chemistry (100 × 6 mm I.D.) and glass columns (150 × 3.3 mm I.D.) (CGC system; Laboratory Instruments, present manufacturer, Tessek) were packed by the slurry technique at 40 MPa with methanol–dioxane as the slurry liquid. The content of amino groups was determined by acid–base titration with perchloric acid in anhydrous acetic acid [13]. The sorbents were washed by stirring or boiling a 2% suspension for 2 h in water.

RESULTS AND DISCUSSION

To investigate the hydrolytic stability of a amino-bonded stationary phase, one must be sure that the surface is covered with really chemically bonded groups. In practice, it is usual to regard as chemically bonded those compounds or groups which

cannot be extracted [14] (usually by a series of solvents at the boiling point). With modification of silica gel with γ-aminopropyltriethoxysilane, which is a basic compound (a 5% aqueous solution has pH = 10.7), the reagent was found to be strongly sorbed on the surface [10,15]. It is possible that during the preparation of the amino-bonded phase in dry organic solvents (in order to prevent the formation of a polymeric layer) the resulting sorbent contains [15] unreacted sorbed silane, which is gradually washed out only if the chromatographic run is taking place in an aqueous solution.

To elucidate these relationships further, changes in the content of the bonded phase and primary amino groups during washing of the amino phases in cold water and after boiling in water, when deeper changes such as oxidation of the amino group can be expected, were investigated by elemental analysis. The results are summarized in Table I. It can be seen that washing in cold water is followed by a decrease in the content of the organic phase and amino groups in both sorbents, which suggests that mainly adsorbed silane is being washed out [10,15]. No further decrease in the C, H, N and NH_2 content was found, within experimental error, after the second wash in cold water.

TABLE I

CHANGES IN THE CONTENT OF THE STATIONARY PHASE AFTER WASHING FOR 2 h IN WATER: COMPARISON BETWEEN SEPARON SIX NH_2 AND LICHROSORB NH_2

Sample	Conditions	Elemental analysis			NH_2 content	
		C (%)	H (%)	N (%)	mmol/g	μmol/m²
LiChrosorb NH_2	Original	3.5	0.94	1.04	0.85	2.83
1	25°C	2.92	0.81	0.89	0.67	2.23
2	100°C	2.47	0.72	0.79	0.558	1.86
Separon SIX NH_2	Original	5.45	1.40	2.06	1.29	2.69
1	25°C	4.98	1.32	1.78	1.16	2.42
2	100°C	3.55	1.07	1.18	0.56	1.17
3	100°C	3.50	1.01	1.09	0.53	1.11

After boiling in water, the decrease in the content of the organic phase and amino groups in both sorbents continues. The results indicate that both sorbents behave very similarly during washing; the only difference is a lower content of the organic phase in LiChrosorb NH_2, which may be due to the different specific surface area of the starting silicas, as follows from the content of amino groups related to the surface area in Table I. The surface coverage is also very similar with both packings, and may be compared with its maximum value [15] of 4.7 μmol/m². From the values of the C/N ratio of the lost material after extraction at 25°C (LiChrosorb NH_2 3.9, Separon SIX NH_2 1.8) and at 100°C (LiChrosorb NH_2 4.1, Separon SIX NH_2 2.2), is possible to conclude that hydrolysed silane is washed out (the C/N ratios of the unhydrolysed and hydrolysed silane are 7.7 and 2.6, respectively). The differences between the two packings at both temperatures probably lie within the experimental error of the Perkin-Elmer 2400 C,H,N analyzer used (± 0.3%) owing to the low content of carbon and especially of nitrogen. Therefore, no further conclusions can be

drawn. Different layers of ^{14}C-labelled γ-aminopropylsilane were found in sorption studies on Pyrex glass [16]. Three layers were described; one of them could be removed by a cold water rinse, the second was extractable by hot water and the remainder was non-removable. Although the experimental conditions and aim of these experiments were different, there is a strong similarity with our experiments.

In order to compare variously washed variants, Separon SIX NH_2 was used and chromatographic tests were carried out with toluene–nitrobenzene and *o*-, *m*- and *p*-chloronitrobenzene mixtures in anhydrous heptane (Table II). Compared with Separon SIX NH_2, the original LiChrosorb NH_2 has lower values of the capacity factors k' and separation factor ($\alpha = k'_2/k'_1$) for the selected pairs of compounds undergoing separation. The k' values of nitrobenzene increased after washing at 25°C with Separon SIX NH_2 while the efficiency decreased (the asymmetry of the peak increased); this again suggests that the mainly sorbed silane has been washed out and that further silanol groups capable of interaction with molecules of nitrobenzene have been made accessible [15]. Nitrobenzene was used as a silanol marker; a higher retention indicates increased silanol activity [17]. The k' values of the individual chloronitrobenzenes also increased after washing in cold water, whereas the selectivity between the *m*- and *p*-isomers decreased. On boiling in water there was a distinct change in the chromatographic properties: at a considerably decreased content of the amino groups the k' values of all three chloronitrobenzenes decreased to about half the original value, and the k' value of nitrobenzene also decreased. Moreover, the *p*- and *m*-isomers remained virtually unseparated. It is likely, therefore, that boiling in water does indeed bring about deeper changes on the sorbent's surface (oxidation of amino groups, or even splitting of the ligand's bonds) than a mere washing out of the mainly unbound silane. The origin of retention changes after the hot water extraction is unclear; some transformation and/or loss of primary amine functionality resulting in

TABLE II

CHROMATOGRAPHIC COMPARISON BETWEEN LICHROSORB NH_2 AND SEPARON SIX NH_2 WITH VARIOUSLY WASHED VARIANTS OF SEPARON SIX NH_2 IN ANHYDROUS HEPTANE

Sorbent	k'					α (*m*-/*p*-isomer)
	Nitrobenzene	Toluene	Chloronitrobenzenes			
			p-	*m*-	*o*-	
LiChrosorb NH_2	1.76	0.16	1.36	1.83	3.97	1.35
Separon SIX NH_2, original	2.83	0.23	1.79	2.63	6.05	1.47
Separon washed I[a]	4.82	0.32	3.09	4.04	9.68	1.31
Separon washed II[b]	3.03	0.22	2.25	2.33	4.65	1.03
Separon washed III[c]	4.78	0.35	2.99	3.85	9.80	1.29

[a] Water, 25°C.

[b] Boiled in water.

[c] Washed wit 2.5 l of acetonitrile-water (80:20) with a protective column packed with Separon SIX NH_2.

increased hydrophobicity of the surface may be suggested as one possible explanation. Good resolution of *m*- and *p*-chloronitrobenzene seems to be typical of amino phases; the more hydrophobic cyanoethylated silica with a similar content of organic phase exhibits a lower retention in comparison with a corresponding amino-phase and separates *m*- and *p*-isomers much more poorly [18].

The last line in Table II is the most interesting; after washing of the column with 2.5 l of acetonitrile–water followed by transfer into anhydrous heptane, both the k' and the α values of the original Separon SIX NH_2 virtually coincide with those obtained after washing of the sorbent with cold water. Consequently, the changes in retention observed with new columns [7,8] with the amino phase can also be explained [15] mainly by washing out of the sorbed silane.

In Table III it can be seen that washing of these sorbents affects their properties in the most common application, *i.e.*, separation of sugar mixtures, to a much smaller extent. The difference between the original LiChrosorb NH_2 and Separon SIX NH_2 consists only in lower k' values; the same applies after boiling in water. Hence, it can be concluded that, unlike the separation of isomeric chloronitrobenzenes, a considerably lower content of amino groups in the analysis of sugars is also sufficient for maintaining a satisfactory selectivity.

TABLE III

CHROMATOGRAPHIC COMPARISON BETWEEN LICHROSORB NH_2 AND SEPARON SIX NH_2, ON THE ONE HAND, AND VARIOUSLY WASHED VARIANTS OF SEPARON SIX NH_2, ON THE OTHER, IN THE ANALYSIS OF A MIXTURE OF SUGARS IN THE MOBILE PHASE ACETONITRILE–WATER (80:20, v/v)

Sorbent	k'							α		
	1 xylose	2 arabinose	3 fructose	4 glucose	5 saccharose	6 maltose	7 lactose	2/1	4/3	7/6
LiChrosorb NH_2	1.12	1.30	1.64	2.25	4.20	5.77	6.35	1.16	1.37	1.10
Separon SIX NH_2	1.55	1.89	2.29	3.11	5.66	7.77	8.97	1.22	1.36	1.15
Separon washed I[a]	1.22	1.47	1.78	2.38	4.31	5.81	6.70	1.20	1.34	1.20
Separon washed II[b]	0.92	1.14	1.71	1.84	3.28	4.38	5.28	1.24	1.31	1.20

[a] Water, 25°C.
[b] Boiled in water.

In the usual application of columns packed with Separon SIX NH_2 washed in water, changes in the k' values were observed also after prolonged use. After the columns had been emptied there was usually a higher content of the organic phase and a lower content of primary amino groups. To ensure that the cause is really impurities fixed at the beginning of the sorbent column, we used two glass CGC columns packed with fresh Separon SIX NH_2 which before and after being connected in series had been tested with nitrobenzene in analytical-reagent grade heptane containing 0.05% of isopropanol (Table IV). Subsequently, analytical-reagent grade heptane was replaced with technical grade heptane and the test mixture was injected repeatedly. It appeared that the k' value of nitrobenzene increased continuously depending on the amount of the mobile phase that had passed through the joined

TABLE IV

EFFECT OF IMPURITIES FROM MOBILE PHASES ON THE CHROMATOGRAPHIC BEHAVIOUR OF THE CGC SYSTEM IN ANALYTICAL-REAGENT GRADE HEPTANE CONTAINING 0.05% OF ISOPROPANOL

Column	k'(nitrobenzene)		
	1[a]	2[b]	3[c]
I	1.14	1.93	1.17
II	1.10	1.14	1.10
I + II	1.31	1.85	1.36

[a] Freshly packed columns.

[b] After using 75 ml of technical grade heptane as the mobile phase (see text).

[c] After 3 weeks of chromatographic analysis of sugars; column re-equilibrated in heptane after methanol–dioxane (1:1) wash.

columns until it reached 1.85 at a total amount of the mobile phase of 75 ml. At the same time, the colour of the sorbent on the inlet side of the first column changed, while in Table IV it can be seen that the properties of the second column remained the same. All attempts at washing out (*i.e.*, desorption in the sense of ref. 14) failed. Another pair of columns connected in a series and packed with an identical charge of Separon SIX NH_2 was used for about 3 weeks for the chromatography of sugar mixtures in the mobile phase [19] acetonitrile–phosphate buffer (pH 5.9) (80:20, v/v) to prevent glycosylamine formation, with a protective column also containing Separon SIX NH_2 placed between the pump and injection valve. Table IV shows that the subsequent test of both the connected and separate columns by using nitrobenzene in heptane containing 0.05% of isopropanol gave k' values which were virtually identical with those obtained for freshly packed columns.

The results suggest that deactivation is indeed due to the chemically bonded impurities from the mobile phase. To these, air oxygen should also be added if the mobile phase has not been helium degassed. The amino group can be protected from oxidation [20] and some other reactions [21] by conversion into a salt, but it is necessary to check whether this change would affect the separation because, *e.g.*, after the conversion of the amino phase into the sulphate form separation of anomers of the respective sugars occurs [22]. Also, with the purest (HPLC-grade) solvents, where transparency to UV radiation is the priority requirement, one cannot expect all impurities able to deactivate the amino group to have been removed.

CONCLUSIONS

Causes underlying the frequently observed changes in the chromatographic behaviour of amino-bonded phases are of twofold in nature: in new columns they are mainly due to desorption of the sorbed silane, whereas on further use the amino groups are deactivated by chemical reactions with impurities, especially those from the mobile phase. In isocratic separations of sugars a protective column with the amino-bonded phase between the pump and the injection valve provides simple pre-

vention against the effect of impurities in the solvents. If reactive impurities may also occur in the samples, a precolumn can be suitably added and to prevent reaction with aldoses the mobile phase should be buffered [19]. At the same time, such a protective column represents a saturation column [9], which also prevents dissolution of the matrix, and the column can be applied for several months without any changes in its chromatographic properties.

REFERENCES

1 R. E. Majors, *J. Chromatogr. Sci.*, 18 (1980) 488.
2 S. R. Abbott, *J. Chromatogr. Sci.*, 18 (1980) 540.
3 H. Engelhardt and D. Mathes, *J. Chromatogr.*, 142 (1977) 311.
4 E. Rajakylä, *J. Chromatogr.*, 353 (1986) 1.
5 F. M. Rabel, *J. Chromatogr. Sci.*, 18 (1980) 394.
6 D. Karlesky, D. C. Shelly and I. Warner, *Anal. Chem.*, 53 (1981) 2146.
7 D. M. Wonnacott and E. V. Patton, *J. Chromatogr.*, 389 (1987) 103.
8 T. G. Waddell, D. E. Leyden and M. T. DeBello, *J. Am. Chem. Soc.*, 103 (1981) 5303.
9 J. G. Atwood, G. J. Schmidt and W. Slavin, *J. Chromatogr.*, 171 (1979) 109.
10 S. R. Culler, H. Ishida and J. L. Koenig, *J. Colloid Interface Sci.*, 106 (1985) 334.
11 J. J. Kirkland, J. L. Glajch and R. D. Farlee, *Anal. Chem.*, 61 (1989) 2.
12 K. K. Unger, *Porous Silica (Journal of Chromatography Library*, Vol. 16), Elsevier, Amsterdam, 1979.
13 N. D. Cheronis and T. S. Ma, *Organic Functional Group Analysis*, Interscience, New York, 1964.
14 P. P. Wickramanayake and W. A. Aue, *J. Chromatogr.*, 195 (1980) 25.
15 H. Engelhardt and P. Orth, *J. Liq. Chromatogr.*, 10 (1987) 1999.
16 E. Plueddemann, *Silane Coupling Agents*, Plenum Press, New York, 1982, p. 87.
17 L. C. Sander, *J. Chromatogr. Sci.*, 26 (1988) 380.
18 R. V. Vivilecchia, R. L. Cotter, R. J. Limpert, N. Z. Thimot and J. N. Little, *J. Chromatogr.*, 99 (1974) 407.
19 B. Porsch, *J. Chromatogr.*, 253 (1982) 49.
20 E. Müller (Editor), *Houben-Weil Methoden der Organischen Chemie*, Georg Thieme, Stuttgart, 1958, Band XI/2, p. 181.
21 E. Müller (Editor), *Houben-Weil Methoden der Organischen Chemie*, Georg Thieme, Stuttgart, 1958, Band XI/1, p. 1007.
22 V. Kahle and K. Tesařík, *J. Chromatogr.*, 191 (1980) 121.

Journal of Chromatography, 543 (1991) 9–16
Elsevier Science Publishers B.V., Amsterdam

CHROM. 23 075

Coated silica and its behaviour in dye-affinity chromatography

DANICA MISLOVIČOVÁ*
Institute of Chemistry, Slovak Academy of Sciences, Dúbravská cesta 9, 842 38 Bratislava (Czechoslovakia)
IVAN NOVÁK
Polymer Institute, Slovak Academy of Sciences, Dúbravská cesta 9, 842 36 Bratislava (Czechoslovakia)
and
MIKULÁŠ PAŠTEKA
Institute of Chemistry, Slovak Academy of Sciences, Dúbravská cesta 9, 842 38 Bratislava (Czechoslovakia)
(First received July 16th, 1990; revised manuscript received December 17th, 1990)

ABSTRACT

Cellulose-coated silica as a support for the high-performance affinity liquid chromatography of proteins was prepared. Cibacron Blue 3G-A as an affinity ligand was grafted onto silica beads coated with cellulose in one or two steps. The prepared supports were used for the purification of lactate dehydrogenase from a crude bovine extract using solutions of potassium chloride, NADH and Cibacron Blue–dextran T 10 as eluents of the bound enzyme. The sorption capacities of the dyed cellulose-coated silica for lactate dehydrogenase from bovine muscle were found to be much lower than those of Cibacron Blue–bead cellulose. The comparison of un-coated and coated silica supports showed that the non-specific interactions between the enzyme and the silica coated with cellulose were considerably reduced.

INTRODUCTION

Polysaccharide matrices such as cross-linked dextrans, agarose and cellulose as chromatographic supports for affinity chromatography of proteins [1] have been known for many years. During the last 15 years of the development of supports amenable to the demands of high-performance (pressure) affinity chromatography (HPAC), the time required for protein purification has decreased from hours to minutes [5] while the purity of the final product has increased. The traditional dextran and agarose supports used for affinity chromatography (AC) are not practical for HPAC owing to their mechanical instability with high-pressure flows.

The first practical HPAC systems for protein separation were based on porous silica beads [2] because they have excellent mechanical properties. However, the non-specific interaction between silanols and proteins on the silica surface requires a modification of these materials to decrease these interaction and to introduce functional groups for affinity ligand binding before their use as chromatographic supports [3,4]. For example, functional silane [5], poly(9-vinyladenine) [6], crown ethers–neutral macrocyclic polymers [7] and polyethyleneimines [8–10] have been used for coat-

ing the surface of silica and silica beads have been coated with polysaccharides (dextran or agarose) substituted by a calculated amount of positively charged diethylaminoethyl functions [3,11,12]. The last support (silica–DEAE-dextran) with the grafted reactive dye Procion Blue HE-GN was used in the dye-affinity chromatography of 6-phosphogluconate dehydrogenase [13]. Dextran-coated silica beads could be used in place of dextran- or agarose-based supports for the preparation of immobilized dye chromatographic supports with kinetically limited enzyme–dye interactions. Their capacity however, is, much lower than that found with agarose supports.

The characteristics of cellulose, such as reactivity, hydrophilicity, mechanical and microbial stabilities, absence of non-specific interaction and low price, are essential for supports for the affinity chromatography of proteins. The ability of cellulose to form solutions and a good sol–gel transition are very important for coating. The non-specific sorption of proteins on bead cellulose and the decrease in these non-specific interactions were studied in our previous work [14–16]. On the basis of this knowledge, we decided to examine cellulose as a coating material. We prepared cellulose triacetate-coated silica which was subsequently deacetylated. This support was used in the dye-affinity chromatography of lactate dehydrogenase (LDH).

EXPERIMENTAL

Materials

Silica gel (SG-100Na) was prepared in the laboratory with surface area 190 m^2 g^{-1} irregular, particle size 120–250 μm, mean pore diameter 25 nm and pore volume 1.15 cm^3 g^{-1}. Acetyl-cellulose (Rhodiafil Acetat-Faser, degree of substitution (DS) = 2.64, Deutsche Rhodiaceta, Freiburg, Germany) and Cibacron Blue 3G-A (CB) (C.I. Reactive Blue 2) were kindly provided by Ciba-Geigy (Basle, Switzerland) and Coomasie Blue G-250 by Serva (Heidelberg, Germany). Dextran T 10 was obtained from Pharmacia (Uppsala, Sweden) and was derivatized with Cibacron Blue 3G-A [14] (degree of substitution 106.3 μmol g^{-1}). Lyophilized LDH prepared from beef flank muscle [15] contained *ca.* 4.8 units of LDH (lactate:NAD oxidoreductase, E.C. 1.1.1.27) per milligram of solid material. The proteins used were bovine serum albumin (SEVAC, Prague, Czechoslovakia), ovalbumin (Fluka, Buchs, Switzerland), γ-globulin (IMUNA, Šarišské Michal'any, Czechoslovakia) and hog trypsin (Koch-Light, Colnbrook, U.K.).

Methods

The activity of LDH was established spectrophotometrically [14,17] and the protein content according to the method of Bradford [18].

Preparations of cellulose-coated silica

For single coating, 7 g of silica gel were mixed and soaked with 12 ml of acetone solution containing 2 g of cellulose triacetate. After drying, the material was hydrolysed in 30 ml of 0.5 *M* sodium hydroxide solution at 20°C for 1 h, washed and dried. The cellulose content was 22% (w/w). For double coating, an additional 3 ml of acetone solution containing 0.3 g of cellulose triacetate were added to 4.2 g of the single-coated silica and then the subsequent steps as in the procedure described above were followed. The cellulose content was 31.3% (w/w).

Preparation of silica–CB

Wide-pore silica (pore diameter 200 nm, surface area 18 $m^2 g^{-1}$, particle diameter 60–120 μm), modified with aminopropyltriethoxysilane, was treated with an excess of a 1% ethanolic solution of Cibacron Blue 3G-A at 60°C for 30 min, washed and dried.

Preparation of CB dyed silica–cellulose

The technique used for the attachment of dyes to bead cellulose [14] was applied to the preparation of the cellulose-coated silica: 2 g of silica–cellulose (SG–CEL) were suspended in 32 ml of water, then 0.12 g of CB in 2 ml water and 2.4 g of sodium chloride were added and the suspension was stirred at 60°C for 30 min. The temperature was subsequently elevated to 80°C, then 6 ml of 6% (w/w) sodium carbonate solution were added and the reaction was allowed to proceed for 2 h at the same temperature. The reaction mixture was neutralized and the unbound dye was washed out until the filtrate was colourless. The degree of substitution was determined spectrophotometrically at 630 nm [14] after the dissolution of CB-cellulose in cadmium tris(ethylenediamine)hydroxide solution.

Elution experiments

Dye-affinity chromatography of LDH on CB–SG–CEL (single-coated, DS = 5.8 μmol g^{-1} CB, and double-coated, DS = 8.4 μmol g^{-1} CB) was performed at ambient temperature using a column (2.5 × 1.1 cm I.D.) equilibrated with 20 m*M* phosphate buffer (pH 8.5). The solution of 0.2 ml of crude LDH (50 U, 8.2 mg protein) was applied. The unbound proteins were washed out with the equilibration buffer, followed by elution with 2 *M* potassium chloride in the equilibration buffer and finally with 1 m*M* NADH (or 50 μ*M* CB–dextran T 10) in the equilibration buffer. The flow-rate was 30 ml h^{-1} and both the total enzyme activity and the protein content were determined in 2-ml fractions.

The non-specific interaction SG–CEL–LDH was determined using a column (2.5 × 1.1 cm I.D.) with undyed support. After loading the same amount of crude LDH or other proteins the elution was performed only with the equilibration buffer.

Loading experiments and determination of binding capacity

The loading experiments were performed on the same columns as the elution experiments. After equilibration the columns were loaded with the solution of crude LDH (5 mg ml^{-1}) in the equilibration buffer at a flow-rate of 20 ml h^{-1}. The activity and protein content in effluent were determined as described above. When the column was saturated, the excess of the enzyme was washed out with the equilibration buffer and the bound LDH was eluted with 50 μ*M* CB-dextran T 10.

RESULTS AND DISCUSSION

Polymer-coated silica supports are potentially good stationary phases for HPAC separations of proteins. The hydrophilic polysaccharide layer neutralizes the negative properties of silica which might lead to, *e.g.*, non-specific interactions with proteins, sensitivity in alkaline media and low reactivity. In the present investigation we covered the surface of the macroporous silica with cellulose according to the

experimental procedure described above. Silica gel was mixed in an acetone solution of cellulose acetate and, after removing acetone, the coated silica gel was dried and the cellulose film was regenerated by saponification with a solution of sodium hydroxide. Silica coated with regenerated cellulose was then dried, whereby the secondary intermolecular bindings or hydrogen bridges were formed. The coating process is so mild that it does not influence the silica gel structure; this was confirmed by leaching out the deposited cellulose with 72% sulphuric acid, which fully restored the original silica gel surface. The silica was coated in one or two steps and thus supports with a lower non-specific interaction with proteins were prepared. The results of elution of crude LDH on three types of silica either coated or not coated with cellulose are given in Table I. The surface areas of cellulose-coated silica reveal that probably only part of the silica porous surface is covered with cellulose. Double coating has no influence on further decreasing the surface area. This finding is in contrast with the observation that the lowest non-specific sorption of the enzyme was found on the column with SG–CEL 2. Nevertheless, important differences between SG–CEL 2 and SG–CEL 1 were not found.

TABLE I

COMPARISON OF NON-SPECIFIC INTERACTIONS OF SILICA SUPPORTS

Silica support	Cellulose content (%, w/w)	Surface area ($m^2\ g^{-1}$)	Elution with equilibration buffer	
			LDH activity (%)	Proteins (%)
SG–100 Na	0	190	16.03	19.54
SG–CEL 1	22.0	131	89.0	79.0
SG–CEL 2	31.3	134	90.3	86.04

However, different non-specific sorptions of several proteins were observed, *e.g.*, about 44% of ovalbumin (p*I* 4.6), 1% of bovine serum albumin (p*I* 4.8), 58% of γ-globulin (p*I* 5.8) and 87% of trypsin (p*I* 10.8) were adsorbed on single-coated silica under the same conditions (20 m*M* phosphate buffer, pH 8.5). The results indicate that the non-specific interactions are not exclusively ionic in nature. Only the very strong sorption with trypsin might be explained by electrostatic effects (high p*I*). The lower non-specific sorption of proteins on SG–CEL 2 than on SG–CEL 1 (Table I) and the previous results suggest that the single-coated silica contains some accessible silanol groups.

Wide-pore silica (activated with aminopropyltriethoxysilane) and both coated supports (SG–CEL 1 and 2) were derivatized with the dye Cibacron Blue 3G-A. Derivatization of coated silica is based on etherification of the cellulose hydroxyl groups with the reactive dye under alkaline conditions. The bond between CB and cellulose is of high stability [19,20]. All dye-affinity chromatographic supports were then examined for the elution profile of crude LDH (Table II). The difficulties with the elution of enzyme and accompanying proteins from CB-silica were due to the non-specific interaction mentioned before. Neither wide pores nor modification of the surface with silane affected the elution of proteins. Protection of the silica surface

TABLE II

ELUTION OF LDH FROM CB–SILICA–CELLULOSE COLUMN

Sorbent	Content of CB (μmol g^{-1})	Elution with					
		Equilibration buffer		2 *M* KCl		1 m*M* NADH	
		LDH activity (%)	Proteins (%)	LDH activity (%)	Proteins (%)	LDH activity (%)	Proteins (%)
Silica–CB	–	45.0	22.3	0.9	0.1	12.0	3.0
CB–SG–CEL 1	5.9	5.5	54.5	3.9	1.0	96.5	13.4
CB–SG–CEL 2	8.4	17.7	65.0	33.9	2.9	48.0	7.6

with cellulose reduced these effects, as confirmed by the decreased elution of LDH (biospecific effects) and increased elution of proteins from CB–SG–CEL when using equilibration buffer as the elution agent. In contrast, elution of LDH with the biospecific eluent NADH (Table II) and with CB-dextran T 10 (not shown) was very effective. The elution characteristics of LDH from CB-coated silicas (Fig. 1a and b) indicated the differences between their sorption behaviour. Important differences were observed between the amounts of biospecifically bound enzyme on CB–SG–CEL 1 and 2. Whereas from CB–SG–CEL 2 the bound LDH was eluted with 2 *M* potassium chloride solution in good yield (almost 34%), from CB–SG–CEL 1 the yield was only 3.9%. On the other hand, the biospecific elution with 1 m*M* NADH (or alternatively with CB–dextran T 10) released the bound LDH quickly and completely from both supports.

Fig. 2 shows the frontal analysis profile for LDH on the dyed coated silicas. It can be seen that saturation of the coated columns with proteins depended on whether the surface was covered once or twice. The single-coated silica in CB-form was able to bind a greater amount of enzyme (9.06 nmol of LDH per gram of sorbent) than the double-coated silica (Table III). The concentrations of the accessible immobilized dye were determined on the basis of the saturation results under the conditions of monovalent interaction (LDH–dye). The values obtained were very low (0.15% or 0.1% of the total bound dye), much lower than those with bead cellulose supports (4.3% accessible dye from 6.03 μmol of total CB per gram of sorbent) [21]. This conclusion is in agreement with the results of Kroviarsky *et al.* [13], who compared dye–agarose with silica coated with dyed agarose or dextran supports in the binding of 6-phosphogluconate dehydrogenase. Clonis [22] compared the loading capacity of various dyed matrices, namely Procion Blue MX-R derivatives of wide-pore silica, TSK 65000 PW and Dynospheres XP-3507, for loading of LDH originating from crude muscle extract. The results showed that the capacities of silica gels were markedly lower (above 100 U ml^{-1} in the concentration range of the immobilized dye 5-10 μmol g^{-1}) than those of the other two matrices. This value is very close to the binding capacities of LDH to our coated silicas.

The results obtained indicate that cheap cellulose-coated silica can be prepared from cellulose triacetate by a very simple method and used as a support for the dye-affinity chromatography of enzymes. The dyed matrix is highly stable, as appar-

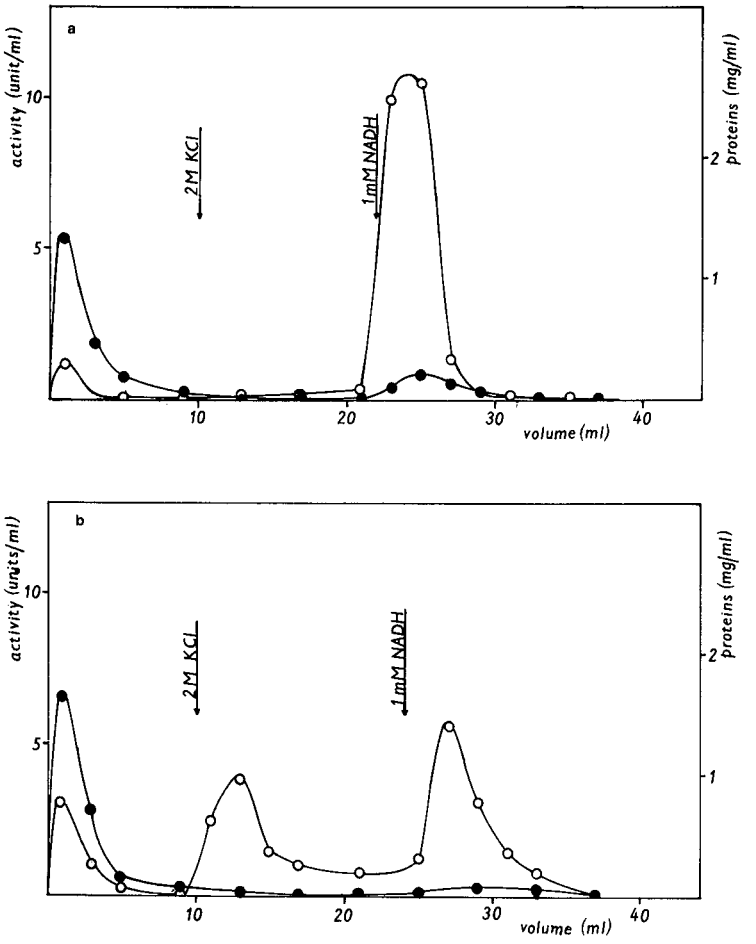

Fig. 1. Elution of LDH from CB–silica–cellulose columns: (a) CB–SG–CEL 1; (b) CB–SG–CEL 2. The procedure was performed on the columns of 2.5 × 1.1 cm I.D.; 0.2 ml of crude LDH (50 U, 8.2 mg protein) was loaded and after removing the unbound protein with the equilibration buffer, LDH was eluted with 2 *M* potassium chloride solution and 1 m*M* NADH. The LDH activity (○) and protein content (●) were determined.

TABLE III

SATURATION PROCESS OF LDH

Sorbent	Concentration of total CB (μmol g^{-1})	Concentration of sorbed LDH (nmol g^{-1})	Accessible dye (%)	Specific activity of LDH (U mg^{-1})
CB–SG–CEL 1	5.9	9.06	0.15	188
CB–SG–CEL 2	8.4	8.69	0.10	227

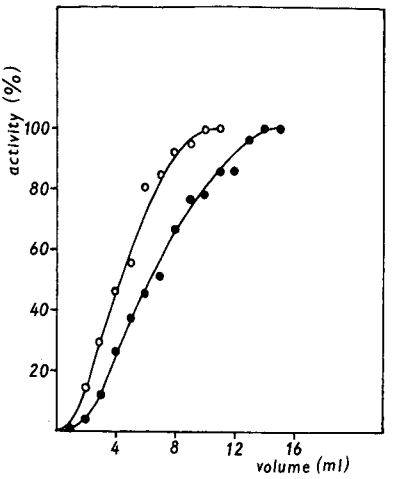

Fig. 2. Saturation process. The size of the column was as in the elution experiments. The supports were loaded with the solution of crude LDH (5 mg/ml, 20 U/ml) using a flow-rate of 20 ml/h. The activity of LDH was determined in 2-ml fractions. Support: (●) CB–SG–CEL 1; (○) CB–SG–CEL 2.

ent changes in its behaviour and release of the dye into the effluent were not observed even after many experiments performed on the same column. The protection of the silica surface with cellulose may prevent non-specific interactions with proteins and facilitate the binding of the reactive dye on the surface of the support. When the coating with cellulose was performed in two steps, the non-specific sorption of the proteins and the binding capacity of LDH to the dyed support were lower, but the separated product was purer (Table III). The present study was performed under low-pressure conditions and it would be of interest to perform experiments with cellulose-coated silica under high-performance liquid chromatographic conditions.

REFERENCES

1 P. D. G. Dean, S. S. Johnson and E. A. Middle, *Affinity Chromatography: a Practical Approach*, IRL Press, Oxford, 1985, p. 1.
2 P. O. Larsson, M. Glad, L. Hansson, M. O. Mansson, S. Ohlson and K. Mosbach, *Adv. Chromatogr.*, 21 (1983) 41.
3 X. Santerelli, D. Muller and J. Jozefonvicz, *J. Chromatogr.*, 443 (1988) 55.
4 P. O. Larsson, *Methods Enzymol.*, 104 (1984) 221.
5 F. E. Regnier and R. Noel, *J. Chromatogr. Sci.*, 14 (1980) 316.
6 M. Akashi, M. Yamaguchi, H. Miyata, M. Hayashi, E. Yashima and U. Miyauchi, *Chem. Lett.*, (1988) 1093.
7 D. Josic and W. Reutter, *J. Chromatogr.*, 476 (1989) 309.
8 A. J. Alpert and F. E. Regnier, *J. Chromatogr.*, 185 (1979) 375.
9 M. Flasher, H. Ramsden and L. J. Crane, *Anal. Biochem.*, 135 (1983) 340.
10 K. M. Gooding and M. N. Schmuck, *J. Chromatogr.*, 327 (1985) 139.
11 F. L. Zhou, D. Muller, X. Santarelli and J. Jozefonvicz, *J. Chromatogr.*, 476 (1989) 195.
12 F. L. Zhou, D. Muller and J. Jozefonvicz, *J. Chromatogr.*, 510 (1990) 71.

13 Y. Kroviarski, X. Santarelli, S. Cochet, D. Muller, T. Arnaud, P. Boivin and O. Bertrand, in M. A. Vijayalakshmi and O., Bertrand (Editors), *Protein–Dye Interactions: Development and Applications*, Elsevier, London, 1989, p. 115.
14 P. Gemeiner, D. Mislovičová, J. Zemek and Ľ. Kuniak, *Collect. Czech. Chem. Commun.*, 46 (1981) 419.
15 A. Pesce, R. H. McKay, F. Stalzenbach, R. D. Cahn and N. O. Kaplan, *J. Biol. Chem.*, 239 (1964) 1753.
16 D. Mislovičová, P. Gemeiner, Ľ. Kuniak and J. Zemek, *J. Chromatogr.*, 194 (1980) 95.
17 H. U. Bergmeyer, *Methoden der Enzymatischen Analyse*, Vol. 1, Verlag Chemie. Weinheim, 2nd ed., 1970, p. 441.
18 M. M. Bradford, *Anal. Biochem.*, 72 (1976) 248.
19 A. Atkinson, J. E. McArdell, M. D. Scaven, R. F. Sherwood and D. A. P. Small, *Affinity Chromatography and Related Techniques*, Elsevier, Amsterdam 1982, p. 399.
20 Ch. R. Lowe and J. C. Pearson, *Methods Enzymol.* 104 (1984) 97.
21 D. Mislovičová, P. Gemeiner and V. Ďurišová, *Collect. Czech. Chem. Commun.*, 55 (1990) 581.
22 Y. D. Clonis, *J. Chromatogr.*, 407 (1987) 179.

Journal of Chromatography, 543 (1991) 17–38
Elsevier Science Publishers B.V., Amsterdam

CHROM. 23 091

New ligands for boronate affinity chromatography

Synthesis and properties[a]

RAM P. SINGHAL*, B. RAMAMURTHY[b], N. GOVINDRAJ and Y. SARWAR
Department of Chemistry, Wichita State University, Wichita, KS 67208-1595 (U.S.A.)
(First received January 30th, 1989; revised manuscript received September 18th, 1990)

ABSTRACT

In order for a boronate ligand to be useful in affinity chromatography for the purification of biomolecules, it must be able to form a stable complex in an environment (pH) in which the affinity molecule is stable. A major limitation of the widely used ligand, 3-aminophenylboronate, is its high ionization constant (pK_a 8.75). To make this complex under more favorable pH conditions, different methods have been explored here in order to introduce an electron-withdrawing (nitro) group in the phenyl ring. Reagents and procedures for the preparation of *ortho*-, *meta*- and *para*-nitro derivatives of succinamidophenylboronic acid using nitronium trifluoromethanesulfonate are described. Preferential substitution of the nitro functionality into the *ortho* position of the boronic acid is exploited by selective use of acetic anhydride for the reaction medium. This method yields mostly an *ortho*-nitro derivative (pK_a 7.4) under selected reaction conditions. The ionization and solute–ligand interaction of several phenylboronates are studied in solution by using ^{11}B NMR and spectrophotometric methods. The results indicate the presence of specific chemical shifts for the neutral (δ 30), the boronate anions (δ 3), and the *cis*-diol-complexed boronate species (δ 7.5). In the presence of a *cis*-diol derivative, the complex formation is favored over anionization of neutral species. Moreover, the complex is formed approximately one pH unit below the ionization constant of the ligand and is stable, *i.e.* fails to break down in boronate anion, even when the solution pH is raised appreciably. Two boronate affinity column matrices were examined for their binding capacity and apparent dissociation constant. The results clearly indicate that the formation and also the breakdown of the complex are greatly enhanced because of the presence of the electron-withdrawing group in the boronate ligand. The results further demonstrate that small structural differences in affinity molecules have significant differences on their binding capacities. A comparison of binding between alkyl-*cis*-diols and aryl-*cis*-diols to different boronate matrices indicates that the aryl affinity molecules not only form a complex but do so very effectively. The *significance* of this work lies in the demonstration that the best environment for the ligand–solute interaction can be established by carrying out studies in solution, without prior immobilization of the ligand. The results derived from in-solution studies and those from the affinity columns are in very good agreement. The new nitrophenylboronate matrix offers enhanced binding of most affinity molecules over those examined with the phenylboronate matrix. In addition, the new matrix offers chromatographic separations of alkali-unstable biomolecules.

[a] This work was in part presented at the *12th International Symposium on Column Liquid Chromatography, Washington, DC, June 19–24, 1988* and also at the *14th International Symposium on Column Liquid Chromatography, Boston, MA, May 20–25, 1990.*

[b] Present address: Organic Chemistry Department, Southern Research Institute, 2000 9th Avenue, South, Birmingham, AL 35255, U.S.A.

0021-9673/91/$03.50

INTRODUCTION

Boronate matrices have been employed successfully for the separation of a wide variety of biomolecules. A few examples of their applications in recent years include: the separation of ribonucleosides, nucleotides, and oligonucleotides from their deoxy derivatives in different situations [1–10]; the separation and assay of modified nucleosides from common nucleosides [11]; nucleotides from 3′,5′-cyclic AMP (cAMP) [12]; the assay of benzo[*a*]pyrene-DNA adducts in cells [13]; the isolation of the nucleotidyl-peptides [14]; the assay of catechols [15]; catechol estrogens and other hormones [16]; the separation of different sugars [17]; the isolation of a specific tRNA [aminoacyl–tRNA (AA-tRNA)] from 19 other tRNAs [11,18–20]; the separation of capped from uncapped mRNA [21]; the separation of ADP-ribosyl-protein from common proteins [22]; the separation of γ-interferon and immunoglobulin G (IgG) [23]; the characterization of specific membrane glycoproteins [24]; the separation of glycosylated proteins [25]; and the purification of serine proteases from other enzymes [26].

The phenylboronate matrix has also been useful for several clinical studies. For example, glycosylated hemoglobins are used increasingly for the assessment of glycemia [27]. Immobilized phenylboronates have been used to measure the level of glycosylated hemoglobin [28–30]. The levels of nucleosides and other metabolites have been measured in the gastro-intestinal mucosa of normal individuals and cancer patients in which greater amounts of specific metabolites are claimed to be indicative of gastric cancer. Similarly, hypoxanthine, uridine, and inosine have been linked to other disorders [31,32]. Substituted phenylboronates have even been shown to exhibit significant antimicrobial activity against common pathogens [33]. Thus, the boronate ligands have been employed for a wide variety of applications involving basic biochemistry and clinical medicine.

The presently available boronate matrices are unstable, function only for a few compounds, and do not work under acidic conditions in which most metabolites are relatively more stable, especially catecholamines and AA-tRNAs. The mechanism of boronate complex formation with compounds of different complexities is largely unknown. Except for the pH, very little is known about controlling factors enhancing adsorption and desorption of the desired molecules from the phenylboronate columns. To fill this void, we have synthesized several boronate affinity ligands and studied their interaction with *cis*-diol model compounds.

A boronate ligand should possess several major characteristics in order to be considered useful in affinity chromatography for the purification of biomolecules. A major limitation of the use of phenylboronate ligands for affinity chromatography is their high ionization constant. The most commonly used ligand, 3-Aminophenylboronic acid (abbreviated here as 3aPBA), has a relatively lower ionization constant (pK_a 8.75) because of the amine group in the *meta* position. Several attempts have been made to synthesize boronate ligands having lower pK_a values. In this study an electron-withdrawing (nitro) group has been introduced into the phenyl ring to make boronate more acidic. The reaction of 3aPBA and its nitro derivative N-(6-nitro-3-dihydroxyborylphenyl)succinamic acid (6nsPBA) with a variety of *cis*-diols is studied here in detail because this compound and its derivatives are used extensively for the design of affinity material by making use of the amino functional group for attachment to a spacer arm or directly to an affinity matrix [2,11].

Chemical shifts of ^{11}B NMR of anionic boronate species, neutral boronic acid and complexed-anionic species are expected to change after reaction with *cis*-diols, due to differential electronic shielding of the ^{11}B atom among these molecules. We realize the potential of the ^{11}B NMR for studying the reaction mechanism of the complex formation with different phenylboronates. In this study, ^{11}B NMR spectroscopy and absorption spectrophotometry techniques are employed to study the boronate complex formation in solution. The results of in-solution complex formation are compared with those derived from binding of affinity molecules with boronate column matrices.

EXPERIMENTAL

Materials

Phenylboronic acid (PBA), obtained from Aldrich, was crystallized from water. 3-Aminophenylboronic acid hemisulfate, also from Aldrich, was converted to its free acid by neutralization followed by crystallization from water. *o*-Nitrophenylboronic acid (2nPBA), *m*-nitrophenylboronic acid (3nPBA), and *p*-nitrophenylboronic acid (4nPBA), were prepared by the reported procedures [34]. *o*-Nitrosuccinamidophenylboronic acid (4nsPBA), *m*-nitrosuccinamidophenylboronic acid (5nsPBA), and *p*-nitrosuccinamidophenylboronic acid (6nsPBA), were synthesized as described in a section below. β-Methylribofuranoside (mRib) and α-O-methylglucopyranoside (mGlc) were purchased from Sigma. Not all the ligands used for NMR studies were used for spectrophotometric studies or were immobilized to the matrix. This is because some of these phenylboronate derivatives are only partially soluble in the medium due to the presence of a spacer arm in their structure.

Solutions for spectrophotometry

Stock solutions of phenylboronic acid derivatives were prepared in glass-distilled deionized water. Appropriate dilutions of stock solutions were made in 50 m*M* buffers of various pH values. The samples were diluted to yield an absorbance of approximately one unit at λ_{max} and pH 4.0. Molar concentrations of mRib and mGlc used were five times greater than those of the phenylboronic acids in order to evaluate the effect of these polyalcohols on pK_a values of the boronate derivatives.

Determination of pK_a by spectrophotometry

A microprocessor-controlled spectrophotometer (Ciba-Corning Gilford Systems, Oberlin, OH, U.S.A., Model Response II) was used for the absorption spectroscopy work. The analytical wavelength for different boronate derivatives was selected so that there was a significant difference in the absorbance between the neutral and the anionic species. The spectrum of the ligand was established for the neutral (A_m) and the ionic (A_i) species, using an identical concentration of the material at pH 4 and pH 10, respectively. The following equations were used for pK_a determinations:

$$\text{if } A_i > A_m, \text{ then: } pK_a = pH + \log [(A_i - A)/(A - A_m)]$$

$$\text{if } A_m > A_i, \text{ then: } pK_a = pH + \log [(A - A_i)/(A_m - A)]$$

where A was the absorbance of the boronate ligand at any given pH value [35]. The concentration of boronate anions (free boronate and those complexed with *cis*-diols) was determined from changes in the absorbance at two selected analytical wavelengths using the following equation:

$$C_{B^-} = \{A_{\lambda_2} - [(\varepsilon^{B^0}_{\lambda_2} \cdot A_{\lambda_1})/\varepsilon^{B^0}_{\lambda_1}]\}/\{\varepsilon^{B^-}_{\lambda_2} - [(\varepsilon^{B^0}_{\lambda_2} \cdot \varepsilon^{B^-}_{\lambda_1})/\varepsilon^{B^0}_{\lambda_1}]\}$$

where C_{B^-} indicates moles of the boronate anion; A_{λ_1} and A_{λ_2} are variable absorptions at the two selected wavelengths, λ_1 and λ_2; $\varepsilon^{B^0}_{\lambda_1}$ and $\varepsilon^{B^0}_{\lambda_2}$ are the molar extinction coefficients of the neutral species of the boronate ligand determined at λ_{max_1} and λ_{max_2} values; and similarly, $\varepsilon^{B^-}_{\lambda_1}$ and $\varepsilon^{B^-}_{\lambda_2}$ are those of the anionic species at the two wavelengths.

^{11}B NMR spectroscopy

NMR spectra were recorded at 22°C, using a Varian XL-300 spectrometer at 96.248 MHz. Boronate derivatives were dissolved in ^2H_2O while maintaining the sample volume to 0.5 ml. The pH was adjusted with NaO^2H in ^2H_2O and measured with a combination micro-pH electrode (Model PHR-146, Lazar, Los Angeles, CA, U.S.A.). Typically, a 50-m*M* solution of a PBA in ^2H_2O was used for the NMR spectra and the p^2H of the solution controlled using ^2HCl and NaO^2H (the solution p^2H was carefully measured inside the NMR tube). Chemical shifts were measured using $BF_3O(C_2H_5)_2$ as the external standard. ^{11}B chemical shifts were measured above the boron background present in the NMR probe. The chemical shifts appeared as sharp peaks above the dome-shaped boron background. Results are plotted here as chemical shifts *versus* p^2H of the solution in bar graphs, where bar heights bear no significance.

Synthesis of boronate ligands

A nitrating reagent consisting of nitronium trifluoromethanesulfonate and hydronium trifluoromethanesulfonate mixture ($NO_2^+CF_3SO_3^- - H_3O^+CF_3SO_3^-$ in a 1:1 proportion) was used [36,37]. Three reaction conditions of nitration were employed (*Methods A, B* and *C*, see below). Synthesis and recovery of the nitro isomers were influenced by small differences in reaction conditions. The best results were obtained by conducting the reaction in anhydrous conditions, using a freshly-distilled acetic anhydride, and observing the order in which the nitrating reagent and N-(3-dihydroxyborylphenyl)succinamic acid (sPBA) were added to the flask while carefully controlling the reaction temperature. Reaction products were characterized by liquid chromatographic and spectroscopic methods. (Mass spectroscopic and elemental analyses could not be relied on because phenylboronic acid molecules easily transform into anhydrides in variable amounts upon drying.) Isomers were further identified by deboronation. For example, in compound 4nsPBA, the boron–carbon bond was eliminated by treating it with an ammoniacal silver nitrate solution and the product characterized as N-(4-nitrophenyl)succinamic acid, thus confirming the presence of the nitro group in position 4 of 4nsPBA. Ionization constants of different derivatives were determined by spectrophotometric methods. Melting points were determined with a Fisher–Johns apparatus and were not corrected. IR spectra were obtained using a Perkin-Elmer (Model 1330) spectrometer. High-performance liquid

chromatography (HPLC) analyses were performed with the help of a microprocessor-controlled liquid chromatograph linked to a minicomputer and equipped with a multi-step gradient elution pump (Perkin-Elmer, Model series 4), a diode-array detector (LKB-Bromma, Model 2140), and a C_{18} reversed-phase column (25 cm × 4.5 mm I.D., Separation Group, Hesperia, CA, U.S.A. Model Vydac 201HS54) [38–40]. A two-step linear gradient of methanol with 20 m*M* sodium succinate buffer (pH 5.3) was used for elution and simultaneous characterization of the different isomers.

3aPBA. A stirring suspension of hemisulfate salt of 3aPBA (5.58 g, 30 mmol) in water (50 ml) was adjusted to pH 7 by dropwise addition of 1 *M* NaOH. The free base was extracted with ethyl acetate (3 × 40 ml), dried over $MgSO_4$, the organic solvent evaporated *in vacuo*, and the crude 3aPBA thus obtained was crystallized from water. Yield: 3.2 g (78%), m.p. 170–171°C (*cf.* 164–165°C [2]). IR (KBr): = 3470, 3450, 3140 cm^{-1}. UV (H_2O): λ_{max} = 295 nm. ^1H NMR ([$^2H_6$]dimethyl sulfoxide, DMSO-d_6): δ = 4.98 (Br, 2H, NH_2); 6.61 (m, 1H, H_{arom} 5); 6.97 (m, 3H, H_{arom} 2, 4, and 6).

sPBA. This compound was essentially prepared by the procedure of Weith *et al.* [2]. The reaction was carried out in a nitrogen atmosphere and the product crystallized from water. Yield: 75%, m.p. 174–175°C (*cf.* 173–174°C [2]). IR (KBr) 3000–2680 cm^{-1}, 1650 cm^{-1}. UV (H_2O) λ_{max} = 243 nm. ^1H NMR (DMSO-d_6): δ = 2.53 (m, 4H, CH_2CH_2); 7.24 (m, 1H, H_{arom} 5); 7.45 (d, 1H, J = 8.1 Hz, H_{arom} 4); 7.70 (d, 1H, J = 8.1 Hz, H_{arom} 6); 7.83 (S, 1H, H_{arom} 2); 8.0 [S, 2H, $B(OH)_2$]; 9.88 (S, 1H, CONH); 12.14 (S, 1H, COOH).

Nitration of sPBA

Method A. The nitrating reagent (a mixture of $NO_2^+CF_3SO_3^-$–H_3O^+ $CF_3SO_3^-$ in a 1:1 proportion; 0.5 g, 1.38 mmol) was added to a three-neck round-bottom flask (50 ml), fitted with a $CaCl_2$ drying tube, nitrogen inlets, and a thermometer, and then cooled to −12°C. While stirring this solution at −12°C, trifluoromethanesulfonic acid (0.2 ml) was added with 100% H_2SO_4 (1.0 ml) and dry CH_2Cl_2 (5.0 ml), and then sPBA (0.3 g, 1.3 mmol). After stirring the mixture for 0.5 h, the temperature was gradually raised to 20–22°C and stirred for an additional 1 h. The reaction mixture, free of organic solvent, was poured onto ice. The crude product was extracted with ethyl acetate (4 × 25 ml) and the combined extracts were washed with a saturated NaCl solution (3 × 25 ml), then dried ($MgSO_4$) and the organic solvent evaporated *in vacuo*. The red solid product (0.18 g) obtained showed a spectrum with a λ_{max} at 324.5 nm; it was crystallized from benzene–ethyl acetate (1:1) to yield yellow crystals (0.015 g). IR and NMR analyses confirm the product was 4nsPBA. IR (KBr): 3800–2700, 1690, 1500 cm^{-1}. ^1H NMR (DMSO-d_6): δ = 2.51 (m, 4H, CH_2CH_2); 7.83 (S, 1H, H_{arom} 2); 8.17 (S, 1H, H_{arom} 4); 8.34 (S, 1H, H_{arom} 6); 10.4 (S, 1H, CONH); 12.1 (Br, 1H, COOH). After crystallization of 4nsPBA, the filtrate was evaporated to dryness. HPLC analysis of the solid showed three compounds and NMR data also confirmed the presence of all three nitro derivatives. No further attempts were made to isolate the isomers.

Method B. The sPBA (0.5 g, 2.1 mmol) was suspended in dry, distilled acetic anhydride (5.0 ml) and placed into a flask equipped as in *Method A*. To the cold stirring mixture, the nitrating reagent (1.42 g, 4.0 mmol) was added in small portions at such a rate that the reaction temperature remained below 15°C. All additions were completed within 0.5 h, while the mixture gradually turned dark yellow. The reaction

mixture was further stirred at 20–22°C for 3 h, quenched with ice cold water and extracted with ethyl acetate (4 × 40 ml). The combined ethyl extracts were washed with a saturated NaCl solution (4 × 30 ml). Evaporation of the organic solvent *in vacuo* changed the product into a viscous, orange-red oil. The oily substance was purified on an acidic alumina column while eluting it with an ethyl acetate–methanol mixture (97:3). Fractions rich in the compound of interest were pooled, evaporated, and the resultant semisolid substance was triturated with methanol to obtain a solid material. This material was crystallized from methanol and a pure sample of N-(3-nitro-3-dihydroxyborylphenyl)succinamic acid (3nsPBA) was obtained (130 mg, 0.46 mmol); m.p. 146–147°C. IR (KBr) : 3445, 3220, 1520 cm^{-1}. UV (H_2O): λ_{max} = 325 nm. ^1H NMR (DMSO-d_6): δ = 2.57 (m, 4H, CH_2CH_2); 7.62 (S, 1H, H_{arom} 2); 7.76 (d, 1H, J = 8.4 Hz, H_{arom} 6); 8.10 (d, 1H, J = 8.4 Hz, H_{arom} 5); 8.16 [S, 2H, $B(OH)_2$]; 10.49 (S, 1H, CONH); 12.15 (S, 1H, COOH). The methanol filtrate was evaporated after crystallization of the above compound. A semisolid material obtained upon crystallization from the methanol–ethyl acetate mixture (1:1) was characterized as 6nsPBA (30 mg, 0.11 mmol). 1H NMR (DMSO-d_6): δ = 2.6 (m, 4H, CH_2CH_2); 7.48 (S, 1H, H_{arom} 2); 7.55 (d, 1H, J = 9.9 Hz, H_{arom} 4); 7.96 (d, 1H, J = 9.9 Hz, H_{arom} 5).

Method C. The nitrating reagent (3.63 g, 10 mmol), cooled to −30°C, was placed into a three-neck round-bottom flask (125 ml) equipped as in *Method A*. Dry acetic anhydride (15.0 ml) and then sPBA (0.592 g, 2.5 mmol) were added while stirring the mixture. The reaction temperature was gradually raised to −10°C and maintained for 2 h. The mixture was then poured onto ice and the crude product was extracted with ethyl acetate (4 × 40 ml). The combined ethyl acetate extracts were washed with a saturated NaCl solution (4 × 30 ml), dried (Na_2SO_4) and the organic solvent removed *in vacuo*. The semisolid material thus obtained was triturated with CH_2Cl_2 and the yellow solid product was recovered by filtration. This impure product was purified by silica gel chromatography while eluting the column with ethyl acetate. Evaporation of the ethyl acetate fractions gave the *para*-nitro derivative (6nsPBA) (15 mg; 53 μmol). The column, after elution with ethyl acetate, was further eluted with an ethyl acetate–ethanol (95:5) mixture. Evaporation of the pooled fractions gave the *ortho*-nitro derivative (4nsPBA) (160 mg; 57 mmol). HPLC and spectrophotometric analyses confirmed the structure of the two compounds.

Deboronation of 4nsPBA. To a one-neck round-bottom flask (equipped as in *Method A*), 4nsPBA (20 mg, 70 μmol) was added and then a solution of silver nitrate (14 mg, 80 μmol) dissolved in 2% NH_4OH (10 ml). The reaction mixture was gently heated to the reflux temperature for 20 min, cooled, and extracted with ethyl acetate (3 x 20 ml). Combined extracts were dried ($MgSO_4$), filtered, and evaporated to dryness to yield a yellow solid of N-(4-nitrophenyl)succinamic acid (15 mg), m.p. 92–93°C (*cf.* 96–97°C [41]). IR (KBr): 3340, 1690, 1535 cm^{-1}. ^1H NMR (DMSO-d_6): δ = 2.58 (m, 4H, CH_2CH_2); 7.84 (d, 2H, J = 9.3 Hz, H_{arom} 2); 8.22 (d, 2H, J = 9.3 Hz, H_{arom} 3).

Immobilization of boronate ligands on a hydrophilic vinyl polymer

Toyopearl, a product of TosoHaas (Bioseparation Specialists, Supelco, Bellefonte, PA, U.S.A.), is a porous and semirigid spherical gel of vinyl polymer. The AF-Amino Toyopearl 650 matrix used in this work had the structure of Gel–CH_2–CH(OH)–CH_2–NH_2 and contained *ca.* 100 μmol of amine per ml of gel. The matrix

was coupled with sPBA (using 126 μmol of sPBA per ml of gel) and nsPBA (using 68 μmol of nsPBA per ml of gel). The coupling reaction was carried out according to the method of Weith *et al.* [2], but using a different carbodiimide and with small differences in experimental conditions. A 15-ml sample of the Toyopearl gel suspended in 20 ml of water, was mixed with 1.7 mmol of sPBA, which was dissolved in 50% aqueous tetrahydrofuran (THF) (10 ml). To the mixture, cooled in an ice bath and the pH adjusted to *ca.* 6, 2 mmol of 1-ethyl-3(3-dimethylaminopropyl)carbodiimide (EDAC) were added and the suspension stirred while maintaining the solution pH ≈ 6 by the addition of 2 *M* HCl. After 4 h, the temperature of the reaction mixture was raised to 22°C and stirred for another 4 h, and then the product was washed with 10 ml each of 50% aqueous solutions of THF followed with dimethylformamide, and finally with water until the washings were free of the reactants. The coupling of nsPBA to the gel matrix was carried out similarly. Each matrix was acetylated in order to block any unreacted amine in the gel. In a typical reaction the gel, suspended in water in an ice bath and adjusted to pH 9, was mixed dropwise with acetic anhydride (140 μmol per ml of gel). The suspension was stirred and pH maintained at *ca.* 9 for 1 h and then the product washed with a 50 m*M* sodium acetate buffer (pH 4.5) containing 0.1 *M* NaCl.

Liquid chromatography

The chromatographic system consisted of: (a) a manual injection valve (Rheodyne, Cotati, CA, U.S.A., Model 7125), (b) a programmable mobile phase gradients pump (Perkin-Elmer, Norfolk, CT, U.S.A., gradient pump, Series LC4), and (c) a diode-array effluent monitor (LKB, Bromma, Sweden, Model 2140 Rapid Spectral Detector). A microcomputer (Zenith Data Systems, St. Joseph, MI, U.S.A., Model Z-248, IBM AT-compatible) was used to operate the detection unit and also to collect and store the absorption spectrum of the effluent every 0.3 s (for example, from 220–300 nm) with the aid of a software program (LKB-Produkter, Bromma, Sweden, Model Wavescan-EG). To test the purity of boronate ligands, a silica-based reversed-phase (C_{18}) matrix (5-μm beads) was used and the column eluted with a pH 5.5 buffer and methanol gradient at 40°C.

For boronate affinity chromatography, glass (6.34 mm diameter) columns, fitted with movable pistons on both ends and jacketed for 6°C temperature control were used. The boronate columns were eluted in three different ways. One, the column was equilibrated and the sample was applied in an alkaline buffer to form the boronate complex, and then eluted with an acid buffer to break the complex. Two, the sample was applied in the buffer of a selected pH and eluted with the same buffer, but also containing 5 m*M* sorbitol. Three, the sample was applied and the column was eluted in the same buffer without any change in the buffer composition. The first method gave inconsistent results and reduced the column life. The second method, although producing sharper peaks, was cumbersome and had little advantage over the third method. The third method was simple to follow and gave the true value of the retention time (k'). The results in this study are reported by using the last procedure.

Determination of binding capacity of affinity columns by frontal analysis. The frontal analysis method was used to determine the binding capacity and binding constant of the affinity matrix [43]. A buffer containing the affinity molecule (*e.g.* adenosine, A) was applied continuously to the column packed with the affinity ma-

trix. This was performed in an environment in which adenosine could freely bind to the boronate matrix, such as at pH 8.5. The application was continued until all binding sites of the matrix were saturated with the affinity molecule and the effluent concentration of the molecule became equal to the concentration of the feed solution. The column was washed until all bound molecules were eluted from the matrix, and then a buffer containing the same concentration of the molecule (A) was applied in a non-binding environment, such as at pH 5.5. The frontal volume (V_f) was derived from differences in the elution volume between a 50%-saturation point of A for binding and non-binding conditions. The binding capacity was calculated from the values of frontal volume (V_f), total column volume (V_t), adenosine concentration in the feed solution [A], and by the following equation:

$$\text{Binding Capacity} = (V_f\,[A])/V_t$$

The apparent dissociation constant was determined from the ligand concentration [L] in the matrix and by using the following equation [44].

$$K_{diss.}\ (\text{apparent}) = (V_t\,[L] - V_f\,[T])/V_f$$

RESULTS

Synthesis of novel boronate ligands

Different methods for nitration of sPBA were examined. First, we followed the published procedure [43]. It involved acylation of 3aPBA to protect the amino group against oxidation, followed by nitration, and then removal of the protecting group. The last step required the use of a hot HCl treatment, therefore it caused extensive deboronation of the nitro isomers. The product contained a very small amount of the desired product and scores of other derivatives [very complex HPLC and gas chromatography (GC) results]. (The deboronation under acidic conditions is well documented [45–50].) The second method involved the use of fuming HNO_3 for nitration. It gave a resinous material even under mild reaction conditions. The third method involved the use of a commercially available nitrating agent [50,51], nitronium tetrafluoroborate ($NO_2^+BF_4^-$). This reagent produced only 3% of the nitrophenyl derivatives. Finally, a nitrating reagent consisting of a mixture of nitronium trifluoromethane and hydronium trifluoromethanesulfonate ($NO_2^+CF_3SO_3^- - H_3O^+CF_3SO_3^-$, 1:1) was employed. Prior to nitration, succinylation of the amino group in 3aPBA offered protection and also provided a carboxyl group linked to a small spacer arm needed for immobilization (Fig. 1). Nitration of sPBA with this reagent in different solvents was examined to maximize the yield of *ortho*- and *para*-nitro derivatives. A mixture of all three isomers was produced in each of CH_2Cl_2, CF_3SO_3H and 100% H_2SO_4. However, only the two desired nitro isomers were formed in acetic anhydride medium (4nsPBA and 6nsPBA). In two sets of reaction conditions (*Method B* and *Method C*), the *ortho* derivative was the predominant isomer (Fig. 1a). The use of acetic anhydride had a distinct advantage. For example, the ratio of 4nsPBA to 6nsPBA was 4.3 in CH_2Cl_2 (*Method A*) (Fig. 1b), but it increased to 11 in acetic anhydride.

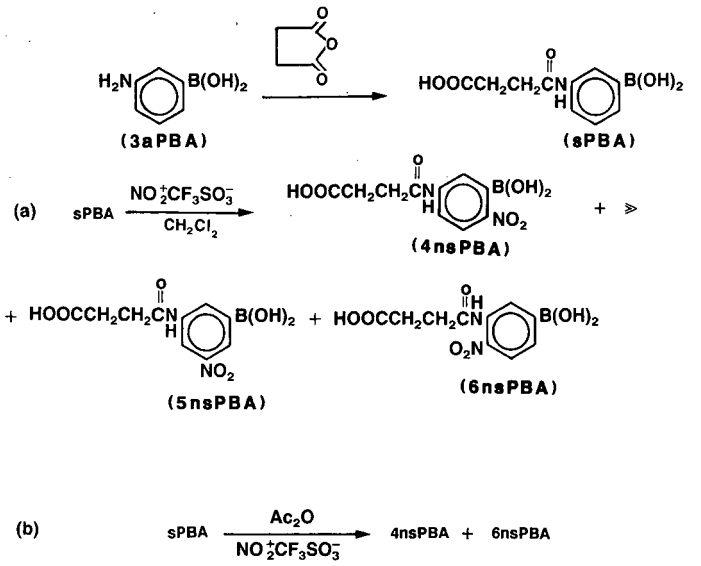

Fig. 1. The nitration of phenylboronate derivatives carried out by (a) *Method A*; and (b) by *Method B* or *Method C*. Ac = Acetyl; 3aPBA = 3-aminophenylboronic acid; sPBA = N-(3-dihydroxyborylphenyl)-succinamic acid; 4nsPBA = N-(4-nitro-3-dihydroxyborylphenyl)succinamic acid; 5nsPBA = N-(5-nitro-3-dihydroxyborylphenyl)succinamic acid; 6nsPBA = N-(6-nitro-3-dihydroxyborylphenyl)succinamic acid (see text for details).

2. Ionization and complex formation of boronate ligands

Studied by spectrophotometry. The boronate complex formation greatly depends on the ionization characteristic of the boronate ligand. A two-wavelength procedure, as described in Experimental, was used to determine the ionization constants of important phenylboronate derivatives. Results in Table I indicate, while PBA and 3aPBA have similar pK_a values, introduction of a nitro group to the phenyl ring substantially lowers the pK_a of the product. A nitro substitution in the *para*-position, as expected, showed a slightly lower pK_a value than in the *meta*-position of the phenyl ring. However, a higher pK_a value for the *ortho* derivatives (2nPBA and 4nsPBA) was observed by this method. (See the next section for explanation of these unexpected results.)

A change in the absorption spectrum of the phenylboronate occurs when it is complexed with a *cis*-diol, because the boron atom acquires an anionic charge in the complexed form. To assess the effect of nitro substitution, this property was used to study the affect of complex formation on the ionization of different ligands. The changes in spectra were examined *before* (boronic acid) and *after* complexing (boronate anion) them with model diols. The latter compounds were selected such that they caused no interference in the analytical wavelength region. Results in Table I indicate the addition of a *cis*-diol compound, *e.g.* mRib, to a 3aPBA solution significantly lowered the pK_a value of the complex by as much as one pH unit. Moreover, the addition of a *trans*.-diol, *e.g.* mGlc, had little effect on the ionization of the PBA derivative. The PBA ionization was also influenced with the presence of other *cis*-diol

TABLE I

IONIZATION CONSTANTS OF PHENYLBORONIC ACID DERIVATIVES AND *cis*-DIOL COMPLEXES DETERMINED BY SPECTROPHOTOMETRY

Phenylboronates (and with *cis*-diol derivatives)	pK_a values (± 0.02)
3-(Aminophenyl)boronic acid	8.75[a]
Complexed with α-O-methylglucopyranoside	8.60
Complexed with β-methylribofuranoside	7.85
Phenylboronic acid	8.8[b]
Complexed with β-methylribofuranoside	8.1
Complexed with catechol[c]	8.5
Complexed with L-dopa[d]	8.4
Complexed with dopamine[e]	7.9 (±0.47)
2-(Nitrophenyl)boronic acid	9.17[f] (±0.06)
Complexed with β-methylribofuranoside	8.95
3-(Nitrophenyl)boronic acid	7.15[g]
Complexed with β-methylribofuranoside	6.98
Complexed with L-dopa[d]	6.75
4-(Nitrophenyl)boronic acid	7.00[h]
Complexed with α-O-methylglucopyranoside	7.00 (±0.09)
Complexed with β-methylribofuranoside	6.71 (±0.09)
Complexed with L-dopa[d]	6.74
Complexed with dopamine[e]	6.92
N-(4-Nitro-3-dihydroxyborylphenyl)succinamic acid	8.45[i](±0.05)
Complexed with β-methylribofuranoside	8.25
N-(6-Nitro-3-dihydroxyborylphenyl)succinamic acid	7.15 (±0.05)
N-(5-Nitro-3-dihydroxyborylphenyl)succinamic acid	7.30

[a] The pK_{a_1} and pK_{a_2} of 3aPBA are reported as 4.47 and *8.81*, respectively [61,62].

[b] The pK_a value of PBA is reported as 8.86 [61,63].

[c] The pK_a value of catechol is reported to be 9.48 [64].

[d] The pK_a values of L-dopa [3(3,4-dihydroxyphenyl)alanine)] are reported as 2.32, *8.68*, and 9.88, respectively [65].

[e] The pK_a values of dopamine (3,4-dihydroxyphenethylamine) are reported as *8.68*, and 9.88, respectively [65] and also as 8.9 (amine) and 10.5 (hydroxyls), respectively, elsewhere [66].

[f] The pK_a value of 2nPBA [2(nitrophenyl)boronic acid] is reported as 9.2 [67]. This apparently high pK_a of this compound is apparently due to internal cyclization of the *ortho* nitro group with the vicinyl boronic acid [68].

[g] The pK_a value of 3nPBA [3(nitrophenyl)boronic acid is reported as 7.3 [5].

[h] The pK_a value of 4nPBA [4(nitrophenyl)boronic acid is reported as 7.15 [69].

[i] This apparently high pK_a of this compound is apparently due to internal cyclization of the *ortho* nitro group with the vicinyl boronic acid [68].

derivatives. For example, the pK_a value of PBA was lowered by 0.3, 0.4, and 0.9 pH units when mixed respectively with catechols, L-dopa and dopamine. A similar decrease in pK_a values of nitro-PBA derivatives was noted when the latter were complexed with *cis*-diols (Table I).

The ionization and complex-formation properties of two ligands (3aPBA and the other with a nitro substitution, 4nPBA) with mRib and mGlc were examined at

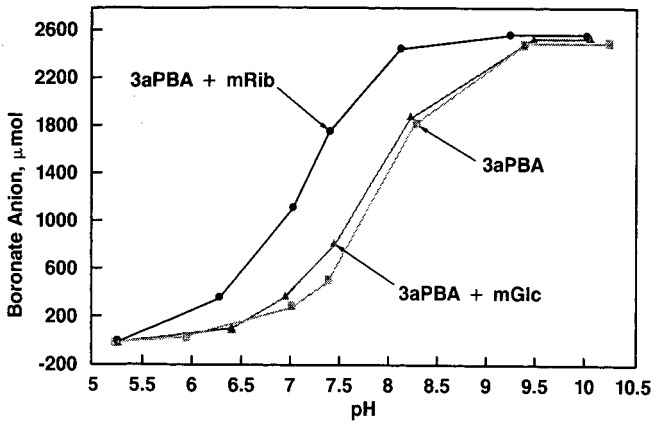

Fig. 2. Boronate complex formation studied by absorption spectroscopy (without ligand immobilization) between a boronate ligand (3aPBA = 3-aminophenylboronic acid) and polyalcohols affinity molecules (mRib = β-methylribofuranoside; mGlc = α-methylglucopyranoside).

different pH values. The boronate-*cis*-diol complex formation with mRib occurred approximately one pH unit below the pK_a of 3aPBA, but 1.8 pH units below the pK_a value of 4nPBA (Figs. 2 and 3). However, the pK_a values of the two ligands remained *unaffected* by the presence of a non-*cis*-diol sugar (mGlc). Thus, the substitution of a nitro group in the phenyl ring significantly lowers the pK_a value of the PBA derivative, and furthermore, it allows the complex formation with a *cis*-diol at one pH unit below the pK_a value of the nitro derivative.

Studied by ^{11}B *NMR*

Chemical shifts of ^{11}B NMR of boronates ligands were expected to change as a result of complexation with *cis*-diols because of differential electronic shielding in the

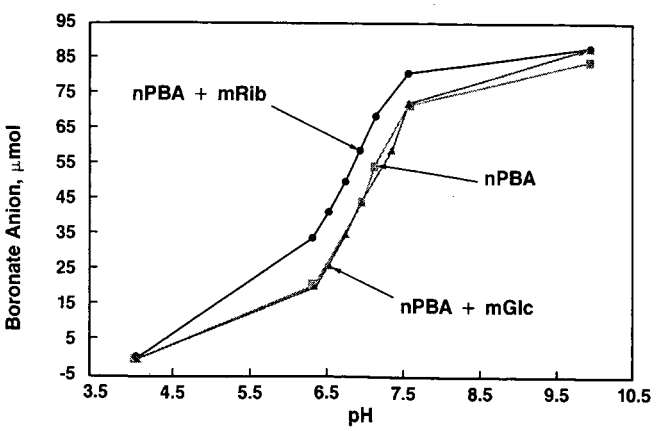

Fig. 3. The ionization of 4-nitrophenylboronic acid (4nPBA) studied at different pH values by using a spectrophotometric method and in buffered solutions. Note boronate complex formation with β-methylribofuranoside (mRib), but none with α-methylglucopyranoside (mGlc).

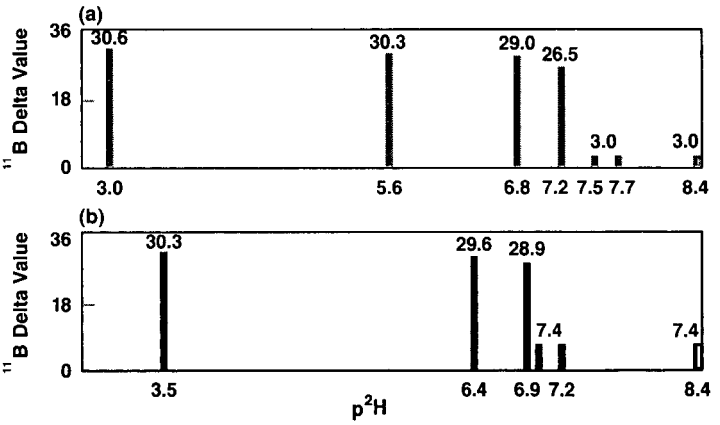

Fig. 4. ^{11}B NMR spectroscopy of ionization of a boronate ligand, (a) phenylboronic acid (PBA); and (b) boronate–*cis*-diol complex in solution. Chemical shifts: (a) 8.2 m*M* PBA; (b) 8.2 m*M* PBA mixed with 50 m*M* β-methylribofuranoside (mRib).

^{11}B atom. Thus, specific signals can be distinguished between the complexed-boronate anions (Bc) and the neutral (B^0) species. With this technique, we wanted to compare the complex formation in solution to that observed with the ligand linked to the matrix, *i.e.* in actual chromatography conditions.

In Fig. 4a, the bars represent chemical shifts (δ values) of a ^{11}B NMR spectrum of PBA analyzed at several p^{2}H values. The neutral molecule, such as that at p^{2}H 3.0, displayed a single peak at δ 30.6. However, as the solution turned basic by NaO^{2}H addition, the peak position gradually shifted to a lower δ value. PBA gave chemical shifts of δ 29 and δ 26.5 at p^{2}H values of 6.8 and 7.2, respectively. Thus, the lower δ value (between 0 and 3) was characteristic of the anionic species and the higher δ value (*ca.* 30) was specific for the neutral species. This was further confirmed by returning the p^{2}H of the solution from the alkaline back to the acidic medium, which produced a characteristic peak at δ 30. In the presence of mRib and under acidic conditions (p^{2}H 3.5 to 6.4), PBA produced the usual shift at δ 30, but two peaks at δ 28.9 and δ 7.3 were observed as the solution p^{2}H was raised to p^{2}H 6.85. Moreover, the first peak (δ 28.9) disappeared as soon as the solution p^{2}H was further raised to 7.0. At this and higher p^{2}H values, the chemical shift only at δ 7 was observed (Fig. 4b). The results indicate that the addition of mRib to PBA causes: (a) a rapid loss of signal due to neutral species, (b) the presence of two distinct signals, one specific for the neutral and the other for the anionic species, at a p^{2}H value consistent with the start of boronate–*cis*-diol complex formation, and (c) absence of the chemical shift specific for pure PBA anion (δ 3), but the presence of a new signal (δ 7.4) characteristic of the boronate–*cis*-diol anionic complex. These observations were further confirmed by regaining the δ 30 signal after acidification of the basic PBA-mRib solution.

To confirm these conclusions, complexation of different PBA derivatives was examined at various p^{2}H values. Results with 3aPBA (Fig. 5a) indicate a gradual downfield shift of δ 29 peak (p^{2}H 4.9) to a lower δ value with an increase in the p^{2}H of the solution. Above p^{2}H 8.2, only a signal (δ 0 to δ 3), indicative of the pure anions, was observed. The downfield peak is typical of the neutral boronic acid molecule and

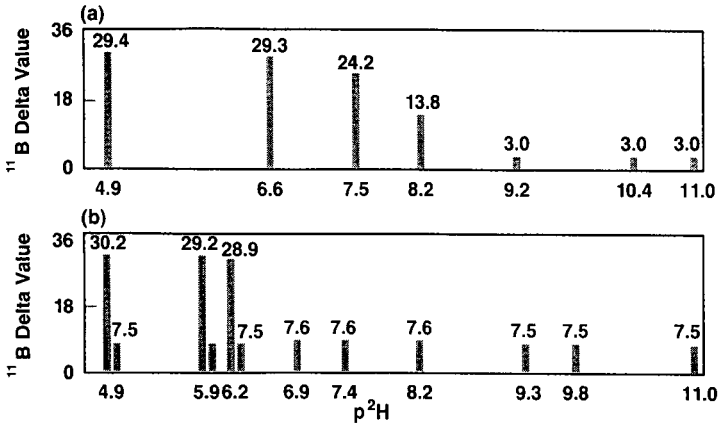

Fig. 5. ^{11}B NMR spectroscopy of ionization of (a) 3-aminophenylboronic acid, 3aPBA; and (b) boronate–*cis*-diol complex. Chemical shifts: (a) 50m*M* 3aPBA; (b) this 3aPBA mixed with 250 m*M* β-methylribofuranoside (mRib).

the upfield peak characteristic of the boronate anion. In the presence of mRib, 3aPBA spectrum gave two peaks (δ 30 and δ 7.5) under acidic conditions (p^{2}H 4.9–6.2), but only one peak (δ 7.5) at p^{2}H 7 and above (Fig. 5b). Thus, a chemical shift of δ 3 is specific of the *pure* boronate anion (p^{2}H > 8.2, Fig. 5a), while that at δ 7.0–7.6 is due to the *complexed* boronate anion (with mRib at p^{2}H < 7, Fig. 5b). These results were further confirmed by substituting ribonucleosides, *e.g.* uridine and cytidine for ribose in the reaction mixture. Each nucleoside in the 3aPBA solution produced two peaks (δ 28.42 and δ 7.21) at p^{2}H 6.4, but only one (δ 8) at p^{2}H 6.8 and above (results not shown). Thus, the complex formation with the nucleosides occurs at a p^{2}H value very close to that of ribose (p^{2}H 6.8 *versus* 7), but at a pH significantly *less* than the ionization (pK_a) of the free 3aPBA.

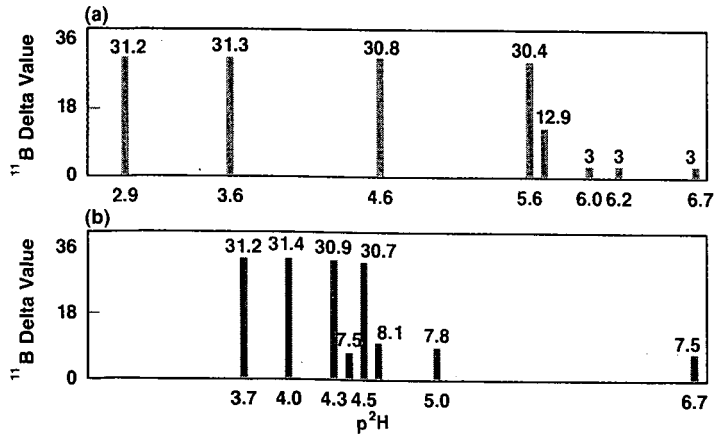

Fig. 6. Ionization of 2-nitrophenylboronic acid (2nPBA) studied by ^{11}B NMR in the presence and absence of a *cis*-diol at different p^{2}H values. Chemical shifts: (a) 8.2 m*M* 2nPBA and (b) this 2nPBA mixed with 10 m*M* β-methylribofuranoside (mRib).

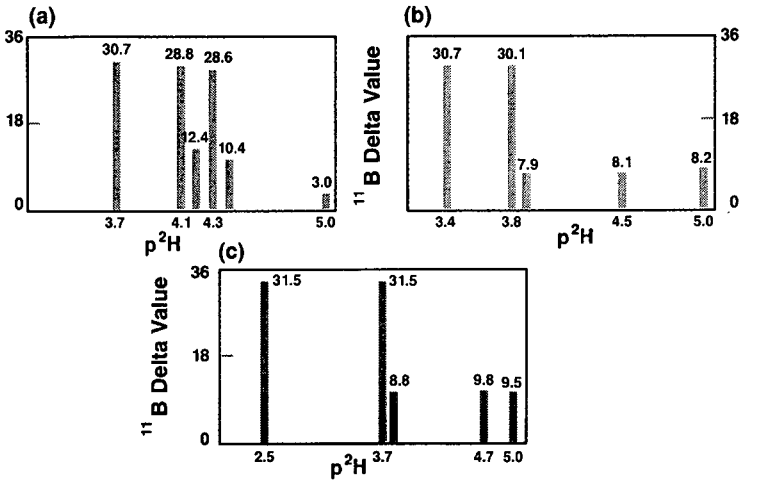

Fig. 7. Ionization of N-(4-nitro-3-dihydroxyborylphenyl)succinamic acid (4nsPBA) observed by ^{11}B NMR in the presence and absence of a *cis*-diol at different p^{2}H values. Chemical shifts: (a) 50 m*M* 4nsPBA, (b) this 4nsPBA mixed with 250 m*M* β-methylribofuranoside (mRib) and (c) 4nsPBA also mixed with 250 m*M* with dopamine.

The effect of a nitro group, especially one in the *ortho* position of PBA, on the boronate complex formation is shown in Fig. 6. The ionization of free 2nPBA occurred at only p^{2}H 6, but those of PBA and 3aPBA took place at higher p^{2}H values (7.2 and 8.2). This effect was more pronounced in spectra determined in the presence of ribose. For example, in the presence of ribose, 2nPBA gave a single peak at p^{2}H 5 (Fig. 6b), while PBA and 3aPBA produced this chemical shift of the boronate complex at p^{2}H 7.2 and 6.9, respectively (Figs. 4b and 5b). Similar to the other two ligands, the boronate complex with ribose also occurred at one pH unit (pH 4.98) less than the ionization of free 2nPBA (p^{2}H 6.0).

The ^{11}B NMR spectrum of an affinity ligand with a five-atom spacer arm, 4nsPBA, at different p^{2}H values was examined. Transformation of free 4nsPBAcid to its anionic form, as shown in Fig. 7a, occurs between p^{2}H 4.3 and p^{2}H 5.0. Furthermore, its complex with ribose or an aromatic *cis*-diol, *i.e.* dopamine (3,4-dihydroxyphenethylamine), is observed at approximately p^{2}H 4.5 (Fig. 7b and c). Thus, this ligand can form the boronate complex under fairly acid conditions as determined by ^{11}B NMR spectroscopy (see Discussion).

Evaluation of boronate affinity matrices

Two boronate affinity column matrices were examined for their binding capacity and apparent dissociation constant. Each column was then evaluated for retention (k') of affinity molecules of different structures, such as alkyl and aryl *cis*-diols. An example of frontal analysis of 4nsPBA column is shown in Fig. 8 and the results from the two matrices are compared in Table II. Though a smaller concentration of the 4nsPBA ligand (27% less) had been used for immobilization, the matrix containing the nitro functionality exhibited a binding capacity almost two times that of the matrix having no such group (sPBA). The apparent dissociation constant of the

TABLE II

CHARACTERISTICS OF BORONATE AFFINITY COLUMNS

Column properties	Boronate ligands	
	sPBA	4nsPBA
Amount of boronate ligand reacted[a] with each ml of the matrix[b] to immobilize (mmol)	220	160
Column bed volume (V_t), ml	2.37	1.42
Frontal volume (V_f), ml	11.01	13.07
Binding capacity: mmol of adenosine[c] bound to each ml of matrix	0.74	1.47
Apparent dissociation constant (K_d), mM	21.4	10.7

[a] A 1-mmol amount of the carbodiimide coupling reagent (EDAC) was used for each immobilization.

[b] The amount of amine present in the matrix (Amino-Toyopearl 650, TosoHaas, Japan) was 100 mmol/ml of the gel.

[c] A 0.16 mM solution of adenosine [A] was used in the feed solution.

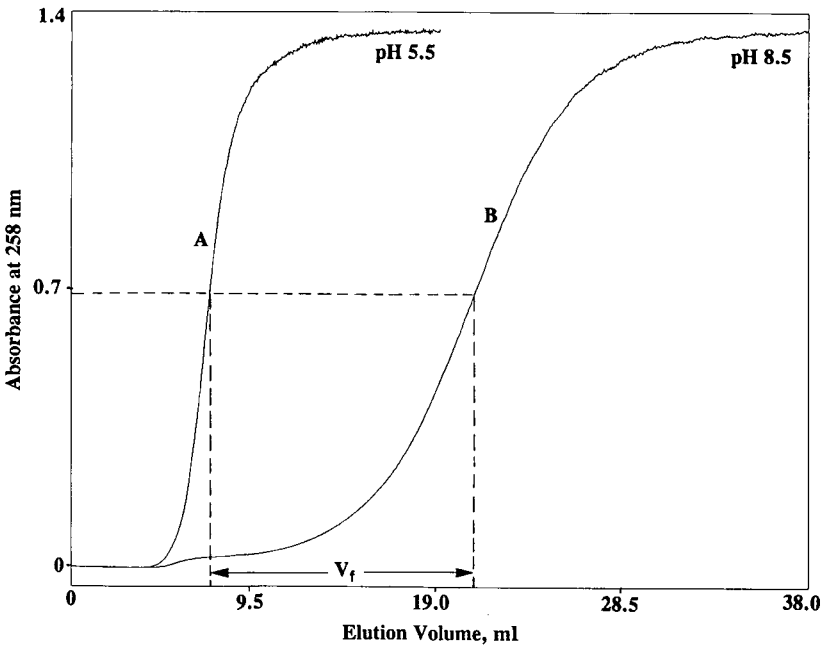

Fig. 8. Binding capacity of a boronate affinity (4nsPBA) column determined by frontal uptake of the affinity molecule (adenosine) by the matrix. The curve A was obtained by passing a 0.16 mM adenosine solution made in a 50 mM phosphate buffer (pH 5.5), *i.e.* in a non-complexing environment. The curve B was similarly obtained using adenosine under complexing conditions (pH 8.5). The frontal volume (V_f), 13.1 ml, was derived from the volume difference between the 50% saturation points (mid-points) of the two curves.

4nsPBA matrix was 50% of the sPBA matrix. Thus, in the nitrophenylboronate matrix, the affinity molecule binds with the matrix to a much greater degree and the boronate complex also breaks down with the same spontaneity.

The retention of adenosine (A) and cytidine (C) is compared in Fig. 9. Though both ribonucleosides have the same sugar, A is a purine while C is a pyrimidine derivative. However, this structural difference should not influence the complex formation. Nevertheless, A is retained three times more than C as evident from their k' values on the two columns. The two matrices also yield appreciably different results. For example, A is retained more strongly on the 4nsPBA matrix than on the sPBA matrix in buffers of pH > 7. However, at pH less than 7, the retention is poor and the difference in their retention is less obvious. Thus, the retention capacity is greatly influenced by both the *nature* of the affinity molecule and also by the *structure* of the boronate ligand.

The two boronate matrices were examined for complexation of aromatic *cis*-diols. Dopamine, in addition to the catechol structure, contains an ethylamine substitution. The results in Fig. 10 clearly indicate that both molecules are retained to approximately the same extent by each boronate matrix. However, the sPBA matrix exhibits a very low retention for both catechol and dopamine. In fact, catechol in buffers of less than pH 7 and dopamine in less than pH 6.5 exhibit very little retention on the sPBA matrix. The 4nsPBA matrix consistently shows high capacity factors, but relatively more for catechol than dopamine. The two aryl molecules exhibit different pK_a values for their hydroxyl groups (catechol, pK_a 9.5; dopamine, pK_a 10.5), dopamine in addition has a cationic charge due to the primary amine group (pK_a 8.9). Though diols exhibit different ionization constants, they make no difference to the structures since they remain unionized under the chromatography conditions. Steric hindrance, possibly caused by the presence of ethylamine substitution, and the cation-

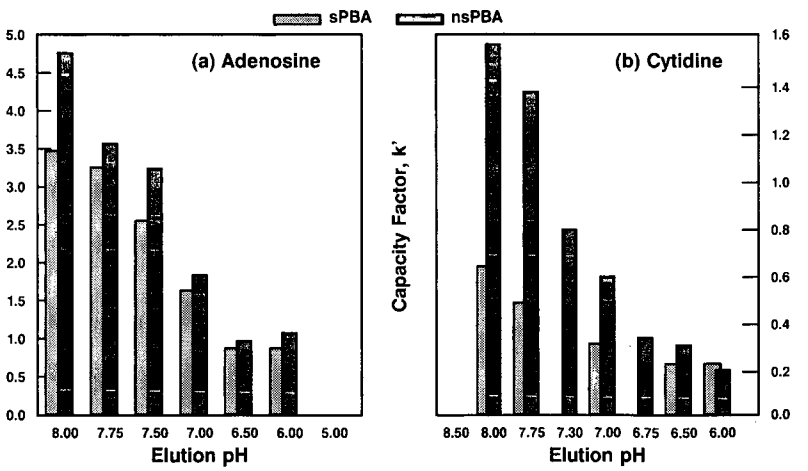

Fig. 9. A comparison of capacity factors of ribonucleosides on two boronate affinity matrices [sPBA = N-(3-dihydroxyborylphenyl)succinamic acid-matrix; nsPBA = N-(6-nitro-3-dihydroxyborylphenyl)succinamic acid-matrix]. Note different scales are used for the k' values. Binding and desorption of the two nucleosides were carried out in identical conditions. (For details, see the Experimental section.)

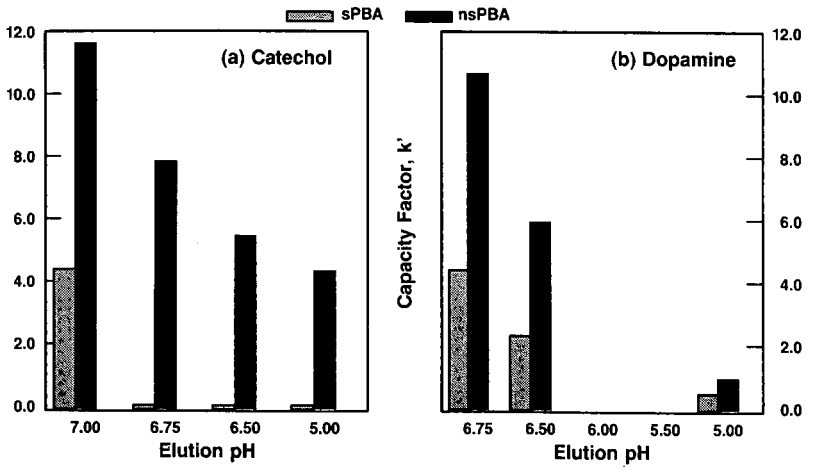

Fig. 10. A comparison of capacity factors of two aryl-*cis*-diols on boronate affinity matrices. Note very little binding of catechol to the sPBA affinity column (see legend to Fig. 9 for details).

ic charge on dopamine are perhaps responsible for the loss of retention on the sPBA matrix.

The separation of three important bioamines was compared on the two boronate matrices (Fig.11). Epinephrine and norepinephrine, with a secondary amine (pK_a 9.9) and a primary amine (pK_a 8.6) respectively, exhibit very similar retentions on each boronate matrix. However, L-dopa (L-3,4-dihydroxyphenylalanine), also

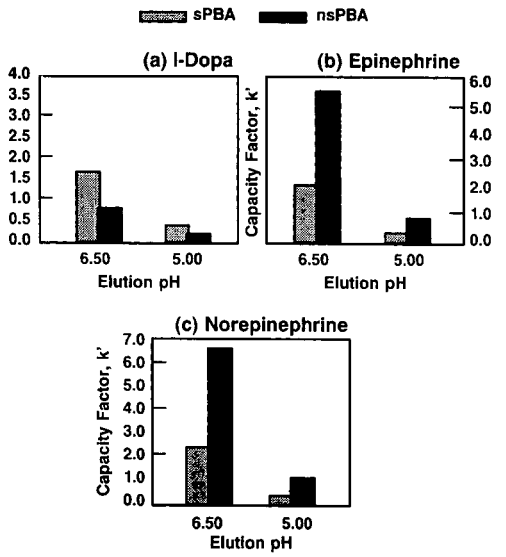

Fig. 11. The retention of three structurally similar compounds at pH 5.0 and 6.5 on two different boronate matrices. Note different scales are used to express the k' values (see legend to Fig. 9 for details).

having a primary amine group (pK_a 8.7), shows very little retention in the pH range examined. This loss of affinity for L-dopa is perhaps caused by the carboxylic group in the structure, although it is not ionized under these conditions.

DISCUSSION

The results indicate that the complex formation of boronate ligands can be studied by absorption spectrophotometry and ^{11}B NMR spectroscopy techniques, without their immobilization to solid supports. The results obtained by the two procedures are in fairly good agreement. For example, the complex formation with *cis*-diols occurs approximately one pH unit below the pK_a value of the boronic acid ligands (compare Table I data with results in Figs. 2–11). The boronate ligands clearly demonstrate the effect of nitro functionality in phenylboronates. The introduction of this electron-withdrawing group to the ring stabilizes the tetrahedral boronate anion in the interaction of the ligand with *cis*-diols, even at lower pH values . For example, a nitro group introduced into the phenyl ring causes boronate to be more acidic [43,53] (Table I). The *ortho*-nitro derivative, 4nsPBA, appears to be the best among the different isomers studied. The nitrophenylboronate ligand forms a complex with *cis*-diols at a much lower pH value than does the phenylboronate (compare Fig. 2 *versus* Fig. 3 and Fig. 4 *versus* Fig. 6). Small differences in the ligand structure apparently cause important differences in complex formation (compare Fig. 3 *versus* Fig. 7a).

The mechanism of boronate complex formation. A typical reaction of phenylboronate with 1,2-diol and 1,3-diol compounds involves cyclic ester formation. One of the proposed mechanisms involves a change of the *trigonal* boron structure in boronic acid into a *tetrahedral* boronate anion upon ionization of the acid and subsequent reaction with 1,2-diols or 1,3-diols to yield a complex [54]. Another proposed mechanism involves the sequential nucleophilic attack of the diol oxygen atoms on the boron atom of the free acid, thus yielding an anionic or neutral complex [55,56]. Our results summarized in Fig. 12 indicate: (1) The ^{11}B resonance frequency gradually shifts from δ 30 to δ 3 with an increase in the pH of the PBA solution. The signal

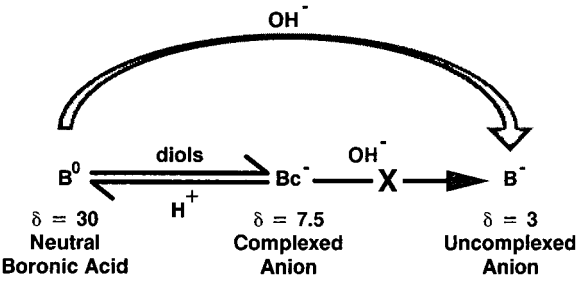

Fig. 12. A reaction mechanism proposed on the basis of ionization and complex formation of ligands studied by ^{11}B NMR and spectroscopic methods. Neutral boronic acid (B^0) undergoes a facile complex formation in the presence of *cis*-diols, yielding a complexed anion (Bc^-). The complex is stable and fails to dissociate even under alkaline conditions though the neutral boronic acid ionizes under such basic conditions.

shows an upfield shift with an increase in pH of the solution; the peak is assigned to the equilibrium state, [$B^0 \leftrightarrow B^-$], between the B^0 and B^- species [57]. *The conversion of neutral to anionic species occurs at a very fast rate*, consequently escaping detection of the signal on the ^{11}B NMR time scale. Thus, the change of B^0 to B^- is so rapid that only the average signal of the two species can be recognized. At a higher pH value, *e.g.* pH 9, the δ value of B^- lies between 0 and 3, since this peak remains unresolved from the external standard peak due to broadening of the boron signals. Similar broadening of the ^{11}B NMR signal has also been observed by others while working with phenylboronate compounds [58]. (2) An addition of a *cis*-diol compound to the PBA solution results in different chemical shifts. Specific signals of the complexed-boronate anion (Bc) and the neutral (B^0) molecules can be distinguished. For example, while the complexed species exhibit a characteristic δ of 7.5, the neutral ones exhibit a chemical shift of approximately δ 30. The results indicate all the boronic acid molecules are complexed (δ 7.5) without exhibiting δ 3 signals. From this we conclude that *the forward reaction resulting in complex formation is favored.* (3) *The boronate–cis-diol complex (Bc-) is stable* and fails to break down in free boronate anion, even when the pH of the solution is raised appreciably. In fact, the boronate complex of alkali-unstable compounds, *e.g.* catechols, exhibit their original spectrum upon lowering the pH of the complex from a fairly basic to an acidic pH.

The complex formation of a phenylboronate having a nitro group with *cis*-diols is shown in Fig. 13. The presence of an electron-withdrawing group in the immediate vicinity of boron lowers the ionization constant of phenylboronic acid. For example, phenylboronic acid exhibits a pK_a value of 8.8, but the introduction of a nitro group

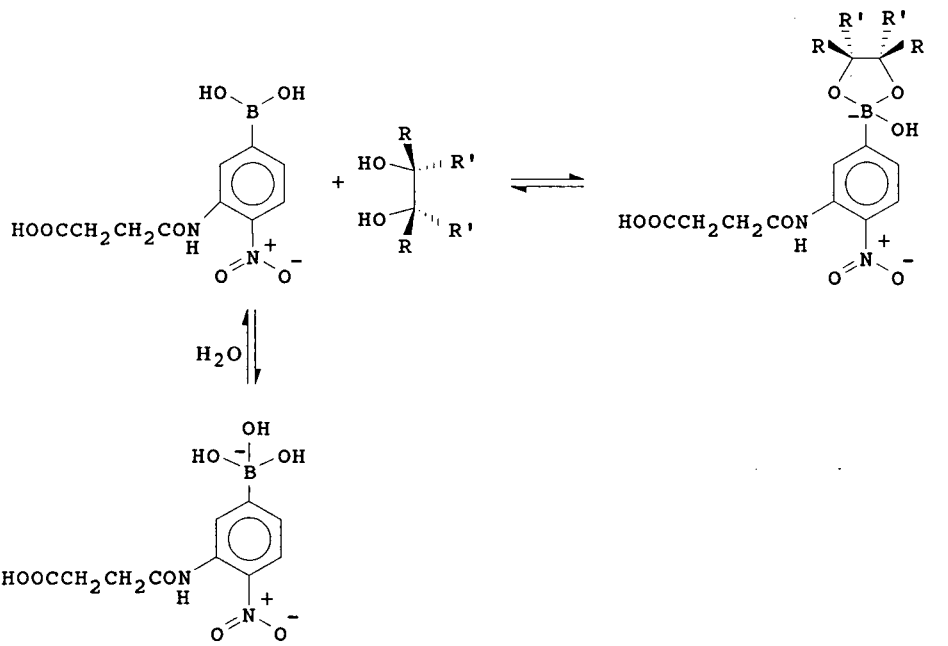

Fig. 13. The mechanism of complex formation between N-(6-nitro-3-dihydroxyborylphenyl)succinamic acid and *cis*-diols. Note the electron-withdrawing effect on the boron atom.

in the *meta-* or *para*-positions of the boron atom lowers the pK_a value to 7.15 and 7.00, respectively. The nitro group in the *ortho-* position causes an internal cyclization with vicinal boronic acid [53].

Discrepancy between NMR data and UV data. In the NMR spectrum of 4nsPBA, the peak of δ 12.4 is apparently due to an internal nucleophilic attack by the electron from the oxygen atom of the nitro group on the boron atom. The pK_a of 2nPBA was found to be 9.17 and that of 4nsPBA as 8.45 by the spectrophotometric method, but boronate anion signals were observed at a more acidic p^{2}H (p^{2}H 6.0). We believe this difference is due to intramolecular nucleophilic attack, resulting in an internal cyclic and tetragonal boron structure. Its existence tends to decrease the strength of the acid because of the negative charge imposed on the boron atom [59]. This structure, however, easily makes a complex with the *cis*-diols at an acidic p^{2}H, as evident from the NMR and spectrophotometric data. However, in the pK_a determination by UV, as the pH is raised, the OH^- ions of the medium attack the cyclic structure causing it to change to boronate anion; hence a higher pK_a value by this procedure. For this reason, we did not observe a higher pK_a in the NMR experiments for the *ortho* derivatives. Since the complex forms at approximately one p^{2}H unit below the pK_a of the ligand, this *apparent* high pK_a should not interfere with its application to affinity chromatography. Moreover, 6nsPBA (unlike 4nsPBA), having no such internal cyclization and a pK_a of 7.1, should form complex with *cis*-diols under acidic conditions.

Interaction of cis-diols with different boronate matrices. Frontal analysis of two matrices, containing sPBA ligand and 4nsPBA ligand, indicate significant differences in binding capacities and apparent dissociation constants between the two matrices (Table II). The complex formation and also the breakdown of the complex are greatly enhanced due to the presence of the electron-withdrawing group in the boronate ligand. A greater amount of 4nsPBA is immobilized to a hydrophilic matrix than that of sPBA, perhaps because of greater solubility and reactivity associated with the nitro group in the 4nsPBA structure. The binding capacities determined for the two matrices clearly indicate that although affinity molecules can bind to the matrix under the same acidic conditions as those observed by ^{11}B NMR spectroscopy, the binding is very weak ($k' < 1$). Effective binding can be observed at a slightly higher pH value, approaching a neutral pH. This difference in complex formation can perhaps be caused by greater accessibility of the affinity ligand in the solution than in the solid (immobilized) medium. The results further demonstrate that small structural differences in the affinity molecule —which may not even influence the net charge of the molecule— have significant influence on the binding capacities (compare retention of adenosine *versus* cytidine in Fig. 9). A comparison of binding between alkyl-*cis*-diols and aryl-*cis*-diols to the boronate matrices indicates that the aryl affinity molecules not only form a complex but they do so very effectively (compare results in Fig. 9 to those in Fig. 10). The nervous system amines, such as L-dopa, epinephrine and norepinephrine, form a stable complex at pH 5.0. This complex has a far greater binding capacity at pH 5.5 than at pH 5.0 (Fig. 11). Again, the binding capacity of these molecules on sPBA matrix is far less than observed on 4nsPBA (except for L-dopa for some unknown reason). The results with immobilized matrices are in good agreement with those observed derived from studies in solution by ^{11}B NMR spectroscopy (compare Fig. 7 with Fig. 11).

Boronate ligand synthesis. Synthesis and recovery of the nitro isomers are influenced by the reaction conditions. Though the net yield of nitro derivatives remains approximately constant (26 mol% of the starting material, sPBA), three isomers are formed in different proportions, depending on the reaction method used. A preferential substitution of the nitro group in the *ortho* position of the boronic acid is apparently caused by coordination with a pair of electrons of the oxygen atom (acetic anhydride) to the electron-deficient boron atom (boronic acid), thus resulting in an enhanced electrophilicity of the *ortho* carbon [60]. [The ionization constant of the *para*-nitro derivative (pK_a 7.2) is slightly less than that of the *ortho*-nitro derivative (pK_a 7.4–7.6).]

Significance. The significance of this work lies in the demonstration that the best environment for the ligand–solute interaction can be determined by studies in solution, without prior immobilization of the ligand. The results derived from in-solution studies and those from the affinity columns are in very good agreement. The new nitrophenylboronate matrix offers enhanced binding of most affinity molecules over those examined with phenylboronate matrix. In addition, the new matrix offers chromatographic separations of alkali-unstable biomolecules. The results further demonstrate that significant differences in capacity factors can be caused by small differences in the structure of the affinity molecules.

ACKNOWLEDGEMENT

This research was supported by a grant from the Wesley Foundation, Wichita, KS, U.S.A. (No. T8707011).

REFERENCES

1 J. K. Inman and H. M. Dintzis, *Biochemistry*, 8 (1969) 4074.
2 H. L. Weith, J. L. Wiebers and P. T. Gilham, *Biochemistry*, 9 (1970) 4396.
3 M. Rosenberg, J. L. Wiebergs and P. T. Gilham, *Biochemistry*, 11 (1972) 3623.
4 E. A. Ivanova, I. E. Kolodkina and A. M. Yurkevich, *J. Gen. Chem. USSR (Engl. Transl.)*, 44 (1974) 409.
5 A. M. Yurkevich, I. I. Kolodkina, E. A. Ivanova and E. I. Pichuzhkina, *Carbohydr. Res.*, 43 (1975) 215.
6 M. Uziel, L. H. Smith and S. A. Taylor, *Clinical Chem. (Winston-Salem, N.C.)*, 22 (1976) 1451.
7 R. G. Moran and W. C. Werkheiser, *Anal. Biochem.*, 88 (1978) 668.
8 E. H. Pfadenhauser and S. Tong, *J. Chromatogr.*, 162 (1979) 585.
9 B. Pace and N. R. Pace, *Anal. Biochem.*, 107 (1980) 128.
10 N. W. Y. Ho, R. E. Duncan and P. T. Gilham, *Biochemistry*, 20 (1981) 64.
11 R. P. Singhal, R. K. Bajaj, C. M. Buess, D. B. Smoll and V. N. Vakharia, *Anal. Biochem.*, 109 (1980) 1.
12 J. H. Hageman and G. D. Kuehn, *Anal. Biochem.*, 77 (1977) 547.
13 D. Pruess-Schwartz, S. M. Sebti, P. T. Gilham, and W. M. Baird, *Cancer Res.*, 44 (1984) 4104.
14 A. E. Annamalai, P. K. Pal and R. F. Colman, *Anal. Biochem.*, 99 (1979) 85.
15 M. Sugumaran and H. Lipke, *Anal. Biochem.*, 121 (1982) 251.
16 S. Hiza, T. Suzuki, A. Hayashi, T. Tsuze and Y. Yamamura, *Anal. Biochem.*, 77 (1977) 18.
17 A. Gasion, T. Wood and L. Chiltemerere, *Anal. Biochem.*, 118 (1981) 4.
18 R. E. Duncan and P. T. Gilham, *Anal. Biochem.*, 66 (1975) 532.
19 T. F. McCutchan, P. T. Gilham and D. Soll, *Nucleic Acids Res.*, 2 (1975) 853.
20 R. P. Singhal, *J. Chromatogr.*, 266 (1983) 359.
21 H. E. Wilk, N. Kerskemethio and K. N. Schajer, *Nucleic Acids Res.*, 10 (1982) 7621.
22 H. Okayama, K. Ulda and O. Hayaishi, *Proc. Natl. Acad. Sci. U.S.A.*, 75 (1978) 1111.
23 G. T. Williams, A. P. Johnstone and P. D. G. Dean. *Biochem. J.*, 205 (1982) 167.

24 G. T. Williams, A. P. Johnstone, V. Bouriotis and P. D. G. Dean, *Biochem. Soc. Trans.*, 9 (1981) 137.
25 F. A. Middle, A. Bannister, A. J. Bellingham and P. D. G. Dean, *Biochem. J.*, 209 (1983) 771.
26 V. K. H. Akparov and V. M. Stepanov, *J. Chromatogr.*, 155 (1978) 329.
27 H. F. Bunn, *Am. J. Med.*, 70 (1981) 325.
28 D. C. Klenk, G. T. Hermanson, R. I. Krohn, E. K. Fujimoto, A. K. Malia, P. K. Smith, J. D. England, H. M. Wiedmeyer, R. R. Little and D. E. Goldstein, *Clin. Chem. (Winston-Salem, N.C.)*, 28 (1982) 2088.
29 B. J. Gould, P. M. Hall and G. H. Cook, *Clin. Chim. Acta*, 125 (1982) 41.
30 R. Kluckiger, T. Woodtli and W. Berger, *Diabetes*, 33 (1984) 73.
31 K. Nakano, K. Shindo, T. Yaraka and H. Yamamoto, *J. Chromatogr.*, 332 (1985) 21.
32 K. Nakano, K. Shindo, T. Yaraka and H. Yamamoto, *J. Chromatogr.*, 332 (1985) 127.
33 S. Mubarak, J. B. Stanford and K. K. Sugden, *Drug Dev. Ind. Pharm.*, 10 (1984) 1131.
34 W. Seaman and J. R. Johnson, *J. Am. Chem. Soc.*, 53 (1931) 711.
35 A. Albert and E. P. Sergeant, *Ionization Constants of Acids and Bases*, Chapman & Hall, New York, 1984, p. 70.
36 C. L. Coon, W. G. Bucher and M. E. Hill, *J. Org. Chem.*, 38 (1973) 4243.
37 F. Effenberger and J. Geke, *Synthesis*, (1975) 40.
38 R. P. Singhal and D. B. Smoll, *J. Liq. Chromatogr.*, 9 (1986) 2660.
39 R. P. Singhal and D. B. Smoll, *J. Liq. Chromatogr.*, 9 (1986) 2719.
40 R. P. Singhal and J. P. Landes, *J. Chromatogr.*, 458 (1988) 117.
41 S. Peterson and E. Muller, *Chem. Ber.*, 81 (1948) 31.
42 C. Lowe and P. Dean, in *Affinity Chromatography*, Wiley, New York, 1974.
43 B. Johnson, *Biochemistry*, 20, (1981) 6103.
44 L. Nichol, A. Ogsten, D. Winzor and W. Sawyer, *Biochem. J.*, 143 (1974).
45 A. D. Ainley and F. Challenger, *J. Chem. Soc.*, (1930) 2171.
46 J. R. Johnson, M. G. van Campen, Jr. and O. Grummitt, *J. Am. Chem. Soc.*, 60 (1938) 111.
47 H. R. Snyder, J. A. Kuck and J. R. Johnson, *J. Am. Chem. Soc.*, 60 (1938) 105.
48 D. S. Matteson and K. Peacock, *J. Am. Chem. Soc.*, 82 (1960) 5759.
49 A. J. Weinheimer and W. E. Marcio, *J. Org. Chem.*, 27 (1964) 1926.
50 J. J. Tufariello, L. T. C. Lee and C. Wojtkowski, *J. Am. Chem. Soc.*, 89 (1967) 6804.
51 G. A. Olah and H. C. Lin, *Synthesis*, (1974) 444.
52 G. A. Olah, S. C. Narang, J. A. Jolah and K. Lammertsma, *Proc. Natl. Acad. Sci. U.S.A.*, 79 (1982) 4487.
53 R. P. Singhal, S. S. M. DeSilva, and Y. Sarwar, presented at the *14th International Symposium on Column Liquid Chromatography, Boston, MA, May 20–25, 1990.*
54 J. P. Lornand and J. O. Edwards, *J. Org. Chem.*, 24 (1959) 769.
55 S. A. Barker, A. K. Chopra, B. W. Hatt and P. J. Somers, *Carbohydr. Res.*, 26 (1973) 33.
56 A. Bergold and W. M. Scouten, *Boronate Chromatography*, [(*Chemical Analysis (New York)*, Vol. 66], Wiley, New York, 1983, p. 149.
57 M. van Duin, J. A. Peters, A. P. G. Kieboom and H. van Bekkum, *Tetrahedron*, 40 (1984) 2901.
58 P. Diehl, E. Fluck and R. Kosfeld, *NMR Series*, 14 (1978).
59 B. Bettman, G. E. K. Branch and D. L. Yabroff, *J. Am. Chem. Soc.*, 56 (1934) 1865.
60 D. R. Harvey and R. O. C. Norman, *J. Chem. Soc.*, (1962) 3822.
61 K. Smith (Editor), *Organometallic Compounds of Boron*, Chapman and Hall, London, 1985, p. 80.
62 Bean *et al.*, *J. Am. Chem. Soc.*, 54 (1932) 4415.
63 Reltig *et al.*, *Can. J. Chem.*, 55 (1977) 3071.
64 H. A. Sober (Editor), *Handbook of Biochemical Molecular Biology*, CRC Press, Cleveland, OH, 2nd ed., 1970, p. J-195.
65 H. A. Sober (Editor), *Handbook of Biochemical Molecular Biology*, CRC Press, Cleveland, OH, 1970, p. B-17.
66 D. W. Newton and R. B. Kluza, in Foye (Editor), *Principles of Medicinal Chemistry, Lippincotte*, p. 821.
67 J. A. Settepani, J. B. Stokes and A. B. Borkovek, *J. Med. Chem.*, 13 (1970) 128.
68 B. Bettman, G. E. K. Branch and D. L. Yabroff, *J. Am. Chem. Soc.*, 56 (1934) 1865.
69 K. Torssel, J. H. McLendol and G. F. Somers, *Acta Chem. Scand.*, 12 (1958) 1373.

Journal of Chromatography, 543 (1991) 39–47
Elsevier Science Publishers B.V., Amsterdam

CHROM. 23 079

Use of 1-[*p*-(2,3-dihydroxypropoxy)phenyl]-1-alkanones as retention index standards in the identification of trichothecenes by liquid chromatography–thermospray and dynamic fast atom bombardment mass spectrometry

R. KOSTIAINEN*
Food and Environmental Laboratory of Helsinki, Helsinginkatu 24, 00530 Helsinki (Finland)
and
P. KURONEN
Department of Chemistry, Division of Organic Chemistry, University of Helsinki, Vuorikatu 20, 00100 Helsinki (Finland)

(First received October 18th, 1990; revised manuscript received December 27th, 1990)

ABSTRACT

A homologous series of 1-[*p*-(2,3-dihydroxypropoxy)phenyl]-1-alkanones (D-standards) were used as retention index standards in the detection of trichothecenes by reversed-phase (RP) gradient elution liquid chromatography–mass spectrometry (LC–MS). Thermospray (TSP) and dynamic fast atom bombardment (dynamic FAB) were used as LC–MS interfaces. The retention indices provide independent identification of compounds, improving the reliability of the identification by LC–MS. The TSP and dynamic FAB mass spectra of the D-standards and trichothecenes are presented.

INTRODUCTION

Retention indices have been widely used in gas chromatography (GC) but seldom in liquid chromatography (LC). Baker and Ma [1] made the first proposal for a retention index series suitable for reversed-phase (RP) LC, studying 2-alkanones as reference standards. However, 2-alkanones have only a weak chromophore and they are of only limited use as reference compounds in UV detection. Smith [2] and Kuronen [3] later introduced the 1-phenyl-1-alkanones as retention index standards for RP-LC, Smith [2] in an isocratic solvent system and Kuronen [3] under gradient elution conditions. The use of retention indices in RP gradient elution LC has been applied to chemical warfare agents [3–8] and mycotoxins [9–11]. Chromatographic parameters with the greatest effect on the reliability of the gradient-programmed retention indices have been carefully studied and the long-term reproducibilities of the indices were found to be at least adequate (the average relative standard deviation was 0.3%) [8] under specified chromatographic conditions, allowing tentative identifications on an interlaboratory basis [5,8].

0021-9673/91/$03.50

Although the reliability of identifications can be improved by the use of retention indices, LC has some serious limitations owing to the lack of a specific and sensitive detector. Mass spectrometry, which combines high sensitivity and selectivity, has long been utilized with gas chromatography, but it is more difficult to interface a mass spectrometer to LC than GC systems. However, many interfacing techniques have been developed during the last few years and some of them, especially thermospray (TSP) and dynamic fast atom bombardment (dynamic FAB), are already routinely used in several laboratories.

We describe here the use of 1-[*p*-(2,3-dihydroxypropoxy)phenyl]-1-alkanones (D-standards) as retention index standards in the detection of the trichothecenes DON, MAS, DAS, TAS, HT-2 and T-2 (Table I) by RP gradient elution LC–TSP- and dynamic FAB-MS. The TSP and FAB mass spectra of the trichothecenes and D-standards are presented.

EXPERIMENTAL

Reagents

The D-standards (Table I) were synthesized according to the method presented by Kuronen [8]. All the trichothecenes (Table I) were obtained from Sigma. The D-standards and the trichothecenes were dissolved in methanol.

Equipment and conditions

The two different experimental instrumental set-ups for LC–MS measurements are summarized in Table II. The mass spectrometers were operated in low-resolution (resolution = 1000) modes. In the dynamic FAB the matrix (glycerol, 4%) in methanol was added by means of a post-column tee-connection at a flow-rate of 250 μl/min. The eluent was split (1:200) before the mass spectrometer by a JEOL pneumatic splitter. Xenon was used in the bombardment (particle energy 5 keV). A liquid nitrogen trap was installed in the JEOL SX102 (used in FAB experiments) to increase the evacuation speed of the ion source.

RESULTS AND DISCUSSION

All the TSP mass spectra of the D-standards exhibit only a protonated molecule and the TSP mass spectra of the trichothecenes only an ammonium adduct ion, except the spectrum of DON, which exhibits peaks for both a protonated molecule and an ammonium adduct ion (Table III). The TSP mass spectra of the trichothecenes are very similar to those recorded in earlier studies [12–14]. The lack of fragmentation is due to the low exothermicity of the ionization process in the ammonium acetate-buffered TSP, owing to the high proton affinity of ammonia (858 kJ/mol) [15]. Since only one ion (ammonium adduct ion) can be used for detection, the reliability of detection of the trichothecenes is not good.

The dynamic FAB mass spectra of trichothecenes exhibit an abundant protonated molecule, a glycerol adduct ion and fragment ions formed by the losses of functional groups as neutral species in various combinations (Table IV). The spectra have been discussed in more detail in earlier studies [12,16].

The dynamic FAB mass spectra of the D-standards exhibit an abundant pro-

TABLE I

D-STANDARDS (D_1–D_6) AND TRICHOTHECENES STUDIED

D-Standards[a]

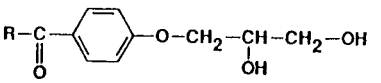

Trichothecenes[b]

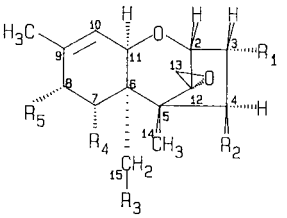

	R_1	R_2	R_3	R_4	R_5
T-2 toxin (T-2)	OH	OAc	OAc	H	$OCOCH_2CH(CH_3)_2$
HT-2 toxin (HT-2)	OH	OH	OAc	H	$OCOCH_2CH(CH_3)_2$
Triacetoxyscirpenol (TAS)	OAc	OAc	OAc	H	H
Diacetoxyscirpenol (DAS)	OH	OAc	OAc	H	H
Monoacetoxyscirpenol (MAS)	OH	OH	OAc	H	H
Deoxynivalenol (DON)	OH	H	OH	OH	=O

[a] $R = CH_3(CH_2)_{n-1}$; n = 1–6.
[b] OAc = Acetyl.

TABLE II

DESCRIPTIONS OF SYSTEMS

Component/parameter	LC–TSP-MS	LC–dynamic FAB-MS
Liquid chromatograph	LKB 2249	HP 1090 LC
Column	Spherisorb ODS-18, 3 μm, 15 cm × 4.6 mm I.D. (Phase Separations, Queensferry, U.K.)	ODS-18, 3 μm, 15 cm × 4.6 mm I.D. (Nomura Kagaku, Tokyo, Japan)
Column temperature	Ambient	Ambient
Mobile phase A	H_2O + 0.1 *M* CH_3COONH_4	H_2O
Mobile phase B	CH_3OH + 0.1 *M* CH_3COONH_4	CH_3OH
Elution programme	B; 30–80% for 0–15 min	B; 30–80% for 0–15 min
LC flow-rate	1 ml/min	1 ml/min
Injection volume	20 μl	20 μl
Splitting ratio	–	1:200
Flow-rate to MS	1 ml/min	5 μl/min
Mass spectrometer	VG TRIBRID	JEOL JMS-SX102
Interface	VG Plasmaspray	JEOL Frit Fab
Ion source temperature	220°C	50°C
Vaporizer temperature	200°C	–

TABLE III

TSP MASS SPECTRA OF D-STANDARDS AND TRICHOTHECENES

Compound	*m/z* (relative intensity, %)		
	$[M + H]^+$	$[M + NH_4]^+$	Other ions
D_1	211 (100)	–	–
D_2	225 (100)	–	–
D_3	239 (100)	–	–
D_4	253 (100)	–	–
D_5	267 (100)	–	–
D_6	281 (100)	–	–
T-2	–	484 (100)	–
HT-2	–	442 (100)	–
TAS	–	426 (100)	–
DAS	–	384 (100)	–
MAS	–	342 (100)	–
DON	297 (46)	314 (100)	–

tonated molecule and a fragment ion $[RCOC_6H_4OH]^+$, which is formed by the loss of $CH_2CH(OH)CH_2OH$ after protonation of the ether oxygen. The more extensive fragmentation in FAB than in TSP indicates a more energetic ionization process with FAB. The formation of abundant fragment ions in FAB allows reliable detection of the trichothecenes by selected ion monitoring. However, the energetic ionization process in FAB may lead to decreased selectivity in the detection of trichothecenes in

TABLE IV

DYNAMIC FAB MASS SPECTRA OF D-STANDARDS AND TRICHOTHECENES

Compound	*m/z* (relative intensity, %)		
	$[M + H]^+$	$[M + H + 92]^+$	Other ions
D_1	211 (100)	–	137 (11)
D_2	225 (100)	–	151 (9)
D_3	239 (100)	–	165 (11)
D_4	253 (100)	–	179 (13)
D_5	267 (100)	–	193 (12)
D_6	281 (100)	–	207 (11)
T-2	467 (33)	559 (12)	449 (12), 407 (5), 365 (96), 323 (10), 305 (100), 275 (18), 263 (15), 257 (18), 245 (59), 233 (21), 215 (65), 203 (22), 197 (19)
HT-2	425 (67)	517 (19)	407 (21), 365 (15), 323 (69), 305 (12), 263 (100), 245 (25), 233 (26), 215 (42), 203 (28)
TAS	409 (100)	501 (20)	391 (17), 367 (13), 349 (37), 307 (15), 289 (23), 247 (26), 229 (35), 201 (13), 199 (14)
DAS	367 (97)	459 (39)	349 (34), 307 (100), 289 (9), 265 (10), 247 (30), 229 (28), 201 (13), 199 (12)
MAS	325 (17)	417 (25)	307 (46), 265 (100), 247 (10), 229 (8)
DON	297 (100)	389 (32)	215 (68)

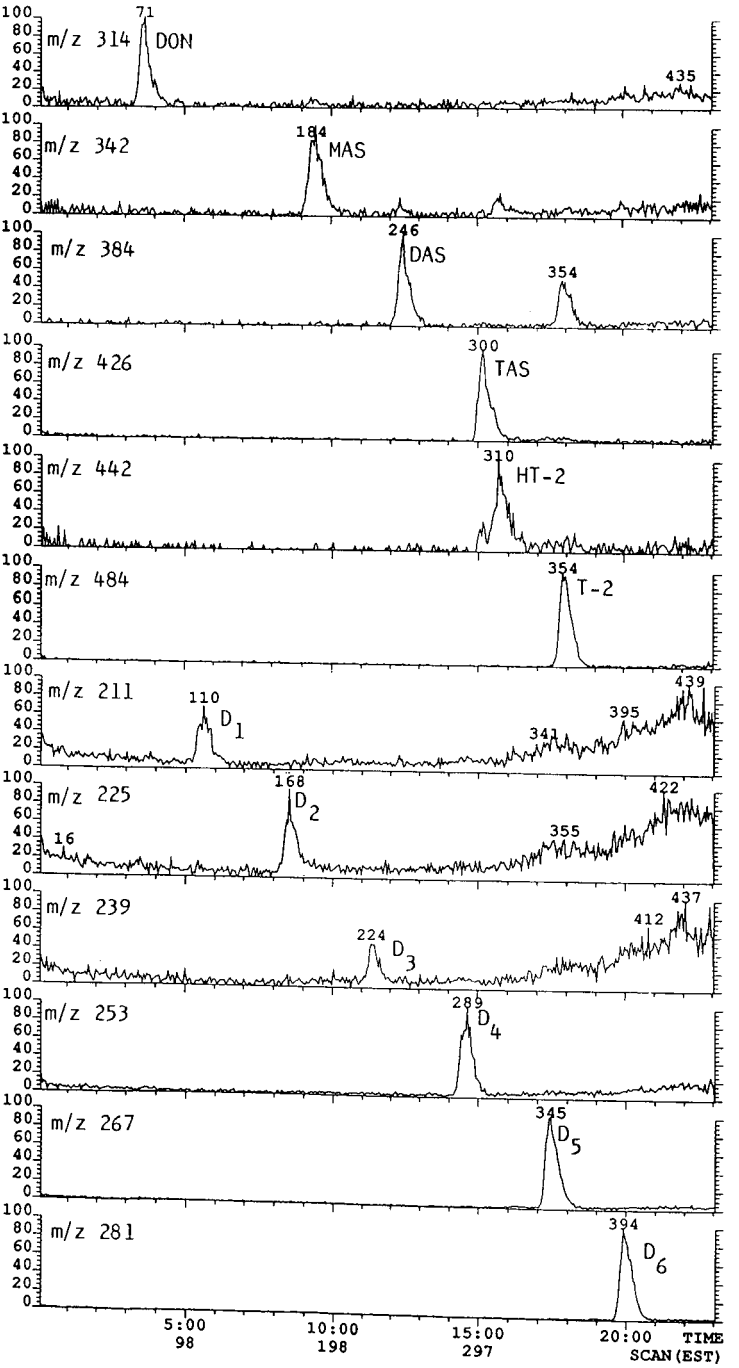

Fig. 1. Mass chromatograms of ammonium adduct ions of the trichothecenes and protonated molecules of the D-standards recorded by LC–TSP-MS. The scan range was 200–600 u. The amount introduced on-column was 200 ng for trichothecenes and 100 ng for D-standards (5 ng/μl, 20-μl injections). For conditions, see Table II. Time scale in min.

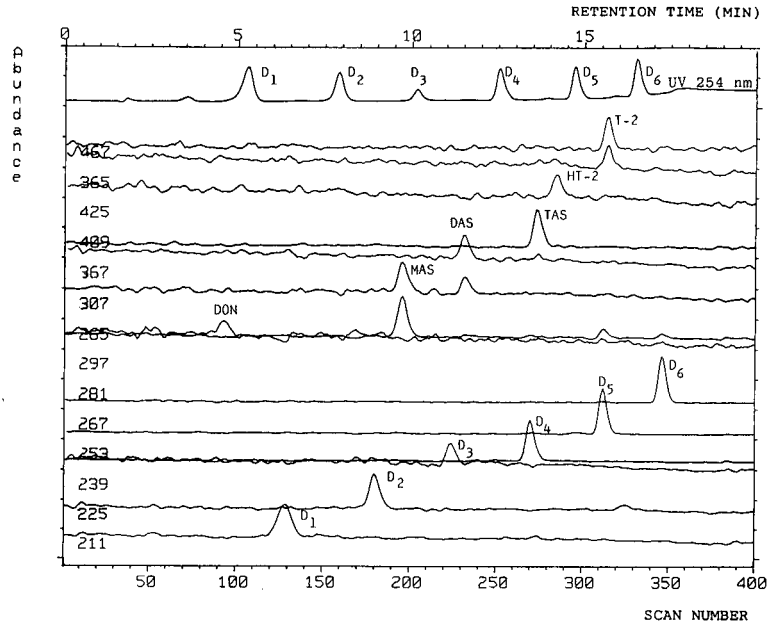

Fig. 2. Mass chromatograms of protonated molecules of the trichothecenes and D-standards recorded by LC–dynamic FAB-MS. The scan range was 200–600 u. The amount introduced on-column was 1 μg for trichothecenes and 1 μg for D-standards (50 ng/μl, 20-μl injections). For conditions, see Table II.

complex matrices, where the number of interfering ions from background compounds is increased.

The reliability of the detection of the trichothecenes can be greatly improved by the use of retention indices, which offer an independent identification parameter, in addition to the TSP or dynamic FAB mass spectra, from the same LC run. Figs. 1 and 2 illustrate the detection of trichothecenes by LC–TSP- and dynamic FAB-MS where the D-standards are used as retention index standards. The mass chromatograms show that the trichothecenes and the D-standards are eluted with sufficiently symmetrical and narrow peaks under the chosen LC–MS conditions. The noisier peaks in the TSP than in the dynamic FAB mass chromatograms are due to background noise rather than instability of the LC or TSP conditions, as the sample used in the TSP measurements was of lower concentration than that used in the dynamic FAB measurements (5 ng/μl *vs.* 50 ng/μl per trichothecene, 20-μl injections). The post-column addition of glycerol in LC–FAB-MS has no significant effect on the retention times, but causes peak broadening.

Fig. 3 presents plots of the absolute retention time against number of carbon atoms in the alkyl group of the D-standards recorded by LC–TSP- and dynamic FAB-MS. Under the chosen LC conditions, the curves are non-linear. This non-linearity shows up more clearly when more than six D-standard components are used [8]. In the non-linear situation, the retention indices can be calculated by the polygonal technique [17] or by the more accurate [8] cubic spline interpolation method [18].

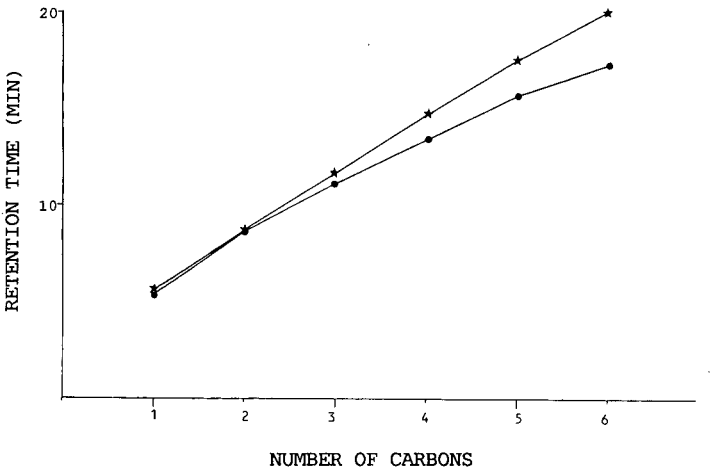

Fig. 3. Plot of retention times of the D-standards against number of carbons in the alkyl chain under linear gradient conditions recorded by (*) LC–TSP-MS and (●) LC–dynamic FAB-MS. For conditions, see Table II.

Table V reports the retention indices of the trichothecenes calculated by the cubic spline interpolation method. DON eluted before the first standard and its retention indices were calculated by extrapolation. The variations in the retention indices obtained with the TSP and dynamic FAB methods are due to the different instrumentation, the use of the buffer solution (ammonium acetate) in TSP and the different columns used (Table II). It has been shown earlier that the retention indexes with C_{18} columns vary with the manufacturer [8]. Slight asymmetry and noise in the LC peaks obtained using TSP due to low concentration (5 ng/μl) may lead to reduced repeatability of the retention indices. The concentrations of the retention standards therefore need to be sufficiently high. In our experiments, the concentration of the D-

TABLE V

RETENTION INDICES (RI_D) OF THE TRICHOTHECENES RECORDED BY LC–TSP-MS AND LC–DYNAMIC FAB-MS CALCULATED BY THE CUBIC SPLINE METHOD

The LC and MS conditions are presented in Table II.

Compound	RI_D	
	TSP	Dynamic FAB
T-2	517.8	508.2
HT-2	435.2	433.4
TAS	418.0	408.8
DAS	334.7	317.8
MAS	229.1	235.7
DON[a]	34.2	40.4

[a] The value of RI_D was calculated by extrapolation, as DON elutes before the first retention index standard.

standards should be tens of nanograms per microlitre for reliable detection of the standards with whole mass range scanning, and a few nanograms with selected ion monitoring (SIM).

The problem with SIM is that several ions must be selected, as trichothecenes and D-standards do not form common ions with either TSP or dynamic FAB, leading to reduced sensitivity. The number of simultaneously monitored ions can be reduced by using a multi-grouping technique in which the monitored mass values are programmed to change during the SIM run. However, this technique also makes the runs more difficult.

CONCLUSIONS

A homologous series of 1-[*p*-(2,3-dihydroxypropoxy)phenyl]-1-alkanones (D-standards) used as retention index standards in RP gradient elution LC–MS where TSP or dynamic FAB provides the interface improves the reliability of identifications made by LC–MS. The D-standards are efficiently ionized by both the TSP and dynamic FAB techniques. The retention indices provide a second level of identification for the compounds of interest, in addition to the MS data, from the same LC run. In general, retention indices can provide a useful means of indentifying peaks of interest in analytical work where the primary analysis is carried out by LC with UV detection and further information is sought by LC–MS.

ACKNOWLEDGEMENTS

Financial support from the Magnus Ehrnrooth and Ella and Georg Ehrnrooth Foundations is gratefully acknowledged.

REFERENCES

1 J. K. Baker and C.-Y. Ma, *J. Chromatogr.*, 169 (1979) 107.
2 R. M. Smith, *J. Chromatogr.*, 236 (1982) 313.
3 P. Kuronen, in J. Enqvist and A. Manninen (Editors), *Systematic Identification of Chemical Warfare Agents, B.3, Identification of Non-Phosphorus Warfare Agents*, Ministry for Foreign Affairs of Finland, Helsinki, 1982, p. 43.
4 P. Kuronen, in J. Enqvist and A. Manninen (Editors), *Systematic Identification of Chemical Warfare Agents, B.4, Identification of Precursors of Warfare Agents, Degradation Products of Non-Phosphorus Agents, and Some Potential Agents*, Ministry for Foreign Affairs of Finland, Helsinki, 1983, p. 51.
5 P. Kuronen, in M. Rautio (Editor), *Air Monitoring as a Means for Verification of Chemical Disarmament, C.2, Development and Evaluation of Basic Techniques*, Ministry for Foreign Affairs of Finland, Helsinki, 1985, p. 162.
6 P. Kuronen, in M. Rautio (Editor), *Air Monitoring as a Means for Verification of Chemical Disarmament, C.4, Further Development and Testing of Methods, Part III*, Ministry for Foreign Affairs of Finland, Helsinki, 1987, p. 44.
7 P. Kuronen, *Proceedings of the 2nd International Symposium on Protection against Chemical Warfare Agents, Stockholm 1986*, National Defence Research Institute, NBS Research Dept., Umeå, 1986, p. 261.
8 P. Kuronen, *Ph. D. Thesis*, University of Helsinki, Helsinki, 1990.
9 D. W. Hill, T. R. Kelley, K. J. Langner and K. W. Miller, *Anal. Chem.*, 56 (1984) 2576.
10 J. C. Frisvad and U. Thrane, *J. Chromatogr.*, 404 (1987) 195.
11 P. Kuronen, *Arch. Environ. Contam. Toxicol.*, 18 (1989) 336.
12 R. Kostiainen, *J. Chromatogr.*, 562 (1991) 555.

13 P. Sakkers, E. Rajakylä and K. Laasasenaho, *J. Chromatogr.*, 384 (1987) 391.
14 R. D. Voyksner, W. M. Hagler, Jr. and S. W. Swanson, *J. Chromatogr.*, 394, (1987) 183.
15 D. H. Aue and M. T. Bowers, in M. Bowers (Editor), *Gas Phase Ion Chemistry*, Vol. 2, Academic Press, New York, 1979, p. 1.
16 R. Kostiainen, K. Matsuura and K. Nojima, *J. Chromatogr.*, 538 (1991) 323.
17 H. van den Dool and P. Dec. Kratz, *J. Chromatogr.*, 11 (1963) 463.
18 W. A Halang, R. Langlais and E. Kugler *Anal. Chem.*, 50 (1978) 1829.

Journal of Chromatography, 543 (1991) 49–58
Elsevier Science Publishers B.V., Amsterdam

CHROM. 23 115

Dual-column high-performance liquid chromatographic cleanup procedure for the determination of polychlorinated dibenzo-*p*-dioxins and dibenzofurans in fish tissue

T. S. THOMPSON*[a], T. M. KOLIC and K. A. MacPHERSON
Ministry of the Environment, Dioxin Laboratory, Laboratory Services Branch, 125 Resources Road, P.O. Box 213, Rexdale, Ontario M9W 5L1 (Canada)
(First received October 9th, 1990; revised manuscript received January 11th, 1991)

ABSTRACT

A high-performance liquid chromatographic cleanup procedure employing normal-phase alumina and carbon–silica separations was developed for isolating polychlorinated dibenzo-*p*-dioxins (PCDDs) and dibenzofurans (PCDFs) from other polychlorinated pollutants present in fish tissue. The method utilizes a column-switching step where the dioxins and furans are trace enriched onto a carbon–silica column as they are eluted from the alumina column. Interfering components such as polychlorinated biphenyls and chlorinated diphenyl ethers elute through the carbon–silica column. The PCDDs and PCDFs are subsequently recovered by backflushing the carbon–silica column using toluene.

INTRODUCTION

The determination of low parts-per-trillion (ppt)[b] concentrations of chlorinated dioxins and furans in fish tissue is complicated by the presence of relatively large amounts of other polychlorinated pollutants. Compounds such as polychlorinated biphenyls (PCBs), organochlorine pesticides (OCs), and other chlorinated aromatic hydrocarbons are widespread in the environment. Like dioxins and furans, PCBs and OCs tend to accumulate in biota, however, they are generally found at concentrations several orders of magnitude higher than the polychlorinated dibenzo-*p*-dioxins (PCDDs) and dibenzofurans (PCDFs). Polychlorinated naphthalenes and diphenyl ethers (PCNs and PCDPEs, respectively) may also be present at levels much higher than either the dioxins or furans.

The presence of PCDPEs poses a major problem in the determination of PCDFs by gas chromatography (GC)–mass spectrometry (MS) techniques since these compounds rearrange under electron impact ionization conditions to yield ions corresponding to PCDF molecular ions. Therefore PCDPEs will interfere in the determination of PCDFs regardless of whether the analysis is carried out using

[a] Present address: Saskatchewan Health, Laboratory and Disease Control Services Branch, H. E. Robertson Laboratory, 3211 Albert Street, Regina, Saskatchewan S4S 5W6, Canada.

[b] Throughout the article the American trillion (10^{12}) is meant.

0021-9673/91/$03.50

low-resolution, high-resolution, or tandem mass spectrometry (LRMS, HRMS or MS–MS). PCBs strongly interfere in the determination of PCDDs by LRMS and even HRMS if they are present at several orders of magnitude higher in concentration than the dioxins. While MS–MS very successfully eliminates the interference due to PCBs by selectively monitoring the loss of a COCl group from the PCDD molecular ion, it is still desirable to remove the bulk of the PCBs present in the sample extract. It should also be noted that high concentrations of PCBs and other components may affect response factors involved in the quantitation of PCDDs and PCDFs using either LRMS or HRMS.

In order to unambiguously identify and quantitate low ppt levels of PCDDs and PCDFs in fish tissue, highly efficient sample cleanup procedures must be employed. Alumina has been identified as the most frequently used adsorbent in sample preparation procedures for the determination of dioxins and furans in various sample matrices [1]. PCDDs and PCDFs may be separated from other closely related polychlorinated pollutants using alumina liquid–solid chromatography [2–5]. Activated carbon is also frequently used in the isolation of dioxins and furans. Careful selection of mobile phase composition permits fused ring aromatic compounds such as PCDDs, PCDFs, and PCNs to be retained while non-planar compounds such as PCBs and polychlorinated diphenyl ethers are eluted [6,7].

Since early work by Baughman and Meselson [8], numerous cleanup techniques have been employed by various groups. Many of the sample preparation procedures reported in the literature are variations of the method initially devised by Lamparski *et al.* [9]. Acid-, base- and silver nitrate-modified silica gel packing materials and alumina were used to remove the bulk of the chemical interferences from 2,3,7,8-tetrachlorodibenzo-*p*-dioxin (TCDD). Final isolation of 2,3,7,8-TCDD was accomplished using reversed-phase high-performance liquid chromatography (HPLC).

HPLC is increasingly being used as a sample preparation technique in environmental analysis [10–12]. Despite the frequent use of alumina in open column liquid–solid chromatographic separations, relatively little work has been done utilizing alumina as an HPLC stationary phase. The major reason behind the lack of success in employing alumina normal-phase HPLC as a cleanup technique is the difficulty in obtaining a constant and reproducible activity. Dolphin initially demonstrated that dioxins could be separated from PCBs, PCNs, 2,2-bis-(4-chlorophenyl)-1,1-dichloroethene (*p,p'*-DDE) and 2,2-bis-(4-chlorophenyl)-1,1,1-trichloroethane (*p,p'*-DDT) [13]. However in this study and a subsequent one [14], the separation of PCDDs from the other polychlorinated pollutants was demonstrated using only standard solutions. It was not until recently that a practical application of alumina HPLC for the cleanup of environmental samples was demonstrated [15]. Thompson devised a method for isolating 2,3,7,8-TCDD from compounds co-extracted from fish tissue using two HPLC separation procedures, first on silica and finally on alumina. The use of C_{18} reversed-phase and alumina normal-phase HPLC fractionation procedures for the isolation of PCDDs and PCDFs from co-extracted compounds was also demonstrated [16].

O'Keefe *et al.* [17] developed a semi-automated cleanup method for the determination of PCDDs and PCDFs in environmental samples. Sample extracts are fractionated on acidic alumina, Amoco PX-21 carbon dispersed on Celite 545, and neutral alumina in a serial process. By using a combination of switching valves, solvent

reservoirs, and a low-pressure pump the system was semi-automated. Donnelly reported the use of AX-21 carbon dispersed on silica as an HPLC stationary phase for the cleanup of environmental samples [18]. This carbon HPLC cleanup step was performed after initial cleanup using multi-phase silica and alumina columns.

In the work presented herein, the liquid chromatographic fractionation steps are carried out using a single HPLC separation procedure employing both alumina and carbon stationary phases. A series of eighteen fish tissue samples were processed using the HPLC cleanup procedure.

EXPERIMENTAL

Initial preparation of fish tissue samples

Each tissue sample consists of a homogenized composite sample of whole small fish. Approximately 20 g of ground fish is weighed into a 250-ml erlenmeyer flask. Each sample is spiked with a standard solution containing five $^{13}C_{12}$-labelled dioxin isomers (one per congener group for each of tetra- through octachlorodioxin). The levels of the individual isotopically labelled internal standards are given in Table III. Approximately 75 ml of hydrochloric acid, previously extracted with dichloromethane followed by hexane, is added to each flask. The acid digestion is allowed to proceed overnight (about 16 h).

The acid digest is extracted with three 70-ml portions of hexane using a 250-ml separatory funnel. Each hexane extract is passed through a cylindrical funnel (14 × 3.5 cm I.D.) which contains a 2-cm layer of anhydrous sodium sulphate over a 4-cm layer of a 44% (w/w) mixture of sulphuric acid and silica gel. By passing the hexane extracts through this column, residual water and oily co-extracted material are removed. After all three hexane portions have been collected, the separatory funnel is rinsed with a fresh aliquot of hexane and the rinsing is passed through the sodium sulphate/acid–silica column. The extracts are concentrated by rotary evaporation under vacuum with the aid of a warm water bath. Each extract is quantitatively transferred to a 100-μl conical glass vial and concentrated just to dryness under a gentle stream of ultrahigh purity nitrogen gas. The final residue is reconstituted with 30 μl of hexane prior to injection on the HPLC system.

High-performance liquid chromatography cleanup

All HPLC separations are performed using a Waters high-performance liquid chromatography system. This system consists of three Model 510 dual piston pumps (only two are required) and a Waters 481 Lambda Max variable-wavelength ultraviolet detector. The pumps and detector are controlled by an NEC APCIV personal computer to which they are linked via the Waters System Interface Module. This permits complete computerized control of the system in addition to data storage and manipulation. Sample extracts are introduced into the HPLC using a Rheodyne 7125 injector system equipped with a 50-μl sample loop. All initial separations are achieved using a normal-phase alumina column (0.46 cm I.D. × 25; Spherisorb 5-μm particulates from Phenomenex, Torrance, CA, U.S.A.). Secondary separations are performed using a carbon–silica column prepared in our laboratory. A mixture of 10% (w/w) of Amoco PX-21 carbon and silica gel (70–230 mesh) was prepared and packed into a empty Waters guard column (3 × 0.46 cm I.D.). The silica does not provide any additional separation but rather it serves as a solid support for the carbon. The

carbon–silica mixture was activated at 130°C overnight prior to being packed into the guard column. Once packed into the column, the carbon–silica mixture was washed with approximately 1 l of toluene before being used.

Two four-port pneumatically actuated valves (Valco, Houston, TX, U.S.A.) are used to permit the column-switching and backflushing steps. A Tracor 955 LC pump is used to backflush the carbon–silica column with toluene. A general schematic diagram of the entire HPLC system is illustrated in Fig. 1. The gradient elution program and valve switching are described in Table I.

After trace enriching the dioxins and furans onto the carbon–silica column, the PCDDs and PCDFs are eluted by backflushing with 75 ml of toluene. The toluene extracts are concentrated by rotary evaporation and transferred to conical vials where they are taken just to dryness by nitrogen gas blowdown. Prior to being analyzed by GC–MS, the residues are reconstituted in 20 μl of toluene.

Once a run has been completed, the system must be returned to its initial state. The column-switching valve (1 in Fig. 1) is switched to position 2 and dichloromethane followed by hexane are pumped through both the alumina and carbon–silica columns for approximately 20 min each. When the absorbance reading on the UV detector returns to zero, the toluene and any other UV adsorbing material have been completely flushed from the carbon–silica column and the system is ready for the next sample injection.

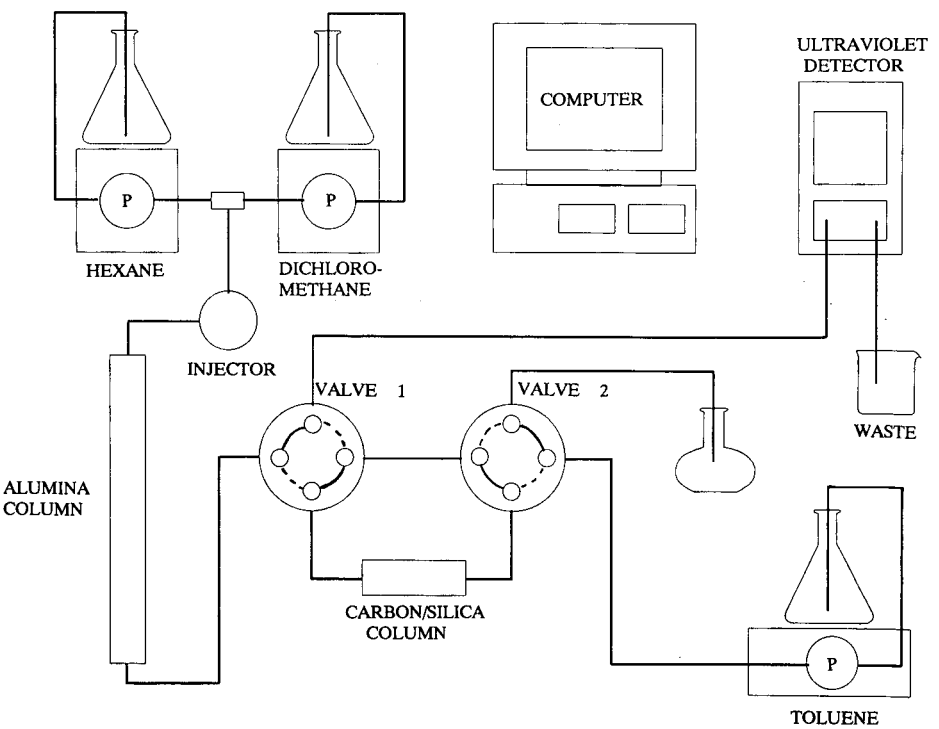

Fig. 1. Schematic diagram of HPLC system used for cleanup of fish tissue extracts. P = HPLC pump; ——— = valve position 1; — — — = valve position 2.

TABLE I

HPLC GRADIENT ELUTION PROGRAM AND VALVE CONFIGURATION

V1 = valve 1 in Fig. 1 (1 = position 1, 2 = position 2); V2 = valve 2 in Fig. 1 (1 = position 1, 2 = position 2); B.F. pump = secondary pump used for backflushing carbon column.

Time (min)	Primary pumping system			V1	V2	B.F. pump flow-rate (ml/min)
	Flow-rate (ml/min)	% Hexane	% Dichloromethane			
0	2.0	100	0	1	1	0
10	2.0	100	0	1	1	0
12	2.0	90	10	2	1	0
15	2.0	75	25	2	1	0
35	2.0	75	25	1	2	0
36	2.0	60	40	1	2	5
40	2.0	0	100	1	2	5
51	2.0	0	100	1	1	5
52	2.0	0	100	1	1	0

GC–MS determination of PCDDs and PCDFs

All GC–MS analyses are carried out using a Finnigan 4500 gas chromatograph–mass spectrometer. The GC system is linked to the low-resolution quadrupole mass spectrometer by a direct capillary interface. A cool on-column injection system and 30-m DB-5 fused-silica capillary column (0.25 mm I.D. with 0.25 μm film thickness; J & W Scientific, Folsom, CA, U.S.A.) are employed in all analyses. The oven

TABLE II

GC–MS SIM PARAMETERS

Compound[a]	Ions monitored	Group No.	Compound[a]	Ions monitored	Group No.
TCDFs	304, 306, 308	1	H_7CDFs	406, 408, 410	4
TCDDs	320, 322, 324	1	H_7CDDs	422, 424, 426	4
$^{13}C_{12}$-TCDD	332, 334	1	$^{13}C_{12}$-H_7CDD	436, 438	4
P_5CDPE	340	1	OCDPE	442	4
H_6CDPE	374	1	N_9CDPE	476	4
P_5CDFs	338, 340, 342	2	OCDF	442, 444, 446	5
P_5CDDs	354, 356, 358	2	OCDD	458, 460, 462	5
$^{13}C_{12}$-P_5CDD	368, 370	2	$^{13}C_{12}$-OCDD	470, 472	5
H_6CDPE	374	2			
H_7CDPE	408	2			
H_6CDFs	372, 374, 376	3			
H_6CDDs	388, 390, 392	3			
$^{13}C_{12}$-H_6CDD	402, 404	3			
H_7CDPE	408	3			
OCDPE	442	3			

[a] T = tetra, P_5 = penta, H_6 = hexa, H_7 = hepta, O = octa, N_9 = nona.

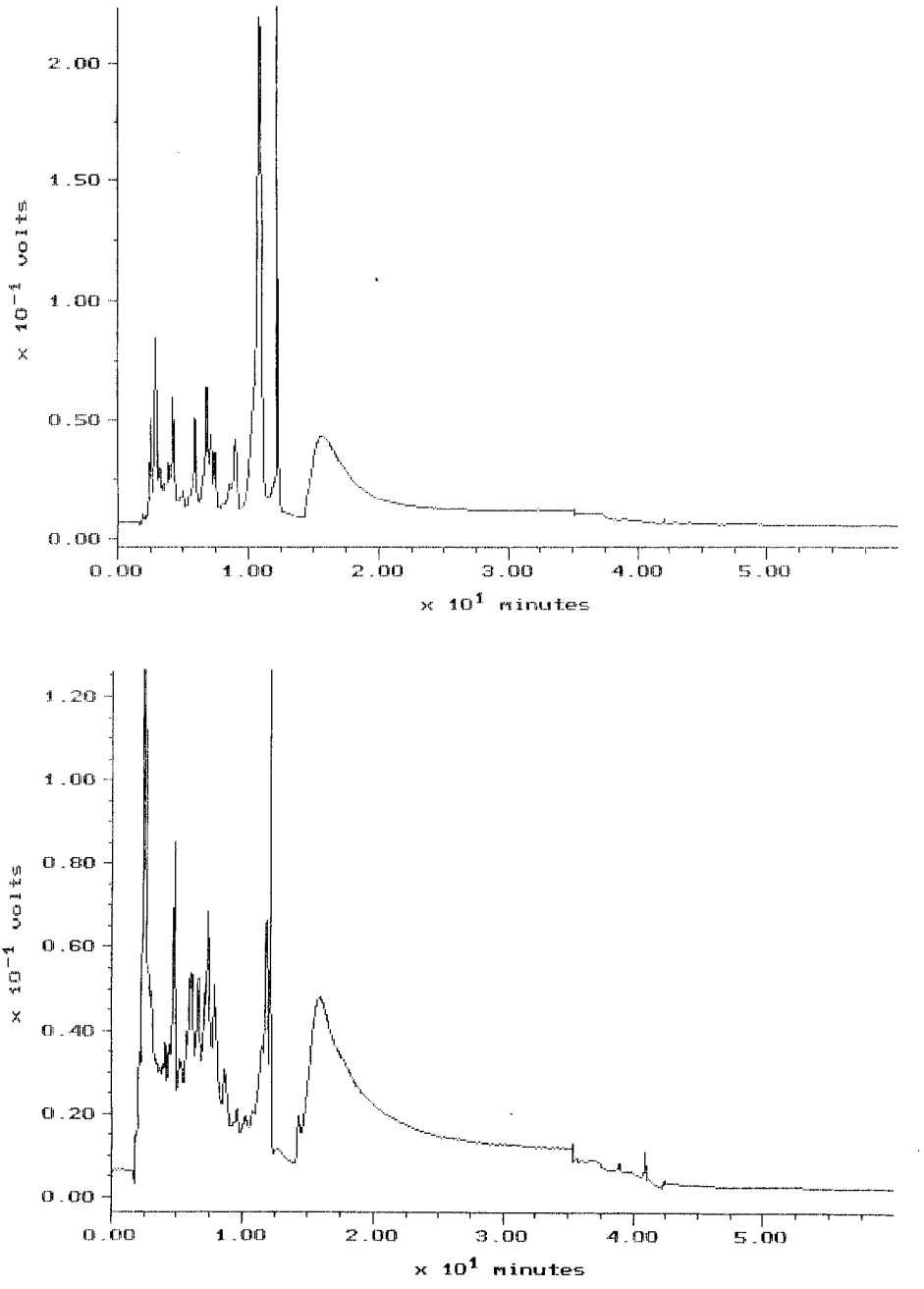

Fig. 2. HPLC chromatograms (UV detection at 254 nm) for fish tissue extracts.

temperature program is: initial oven temperature held for 2 min at 110°C, ramped to 250°C at 15°C/min, ramped to 300°C at 5°C/min and held for 5 min. Helium is used as the GC carrier gas with a column head pressure of 16 p.s.i.

The determination of PCDDs and PCDFs is typically accomplished using selected ion monitoring (SIM) techniques. Three molecular ions are monitored for each congener group in addition to two ions for each $^{13}C_{12}$-labelled internal standard. Two additional ions corresponding to chlorinated diphenyl ethers are also monitored for each congener group (except octachloro) to ensure that no PCDPE interferences are observed. The ions monitored are summarized in Table II. All GC–MS analyses are performed using an electron energy of 35 eV and an electron multiplier voltage of 1200 V.

RESULTS AND DISCUSSION

A series of eighteen fish tissue samples were prepared using the extraction and cleanup procedure described in the experimental section. Fig. 2 shows the HPLC chromatograms (UV detection at 254 nm) which were obtained for two of the fish samples. In both chromatograms, which were typical of most of the samples analyzed, there appears to be a significant amount of material which elutes in the first twelve minutes of the run. These components were most likely PCBs which have been found to largely elute between 3 and 15 minutes on the alumina column using this particular gradient elution program. The later eluting components may have included some

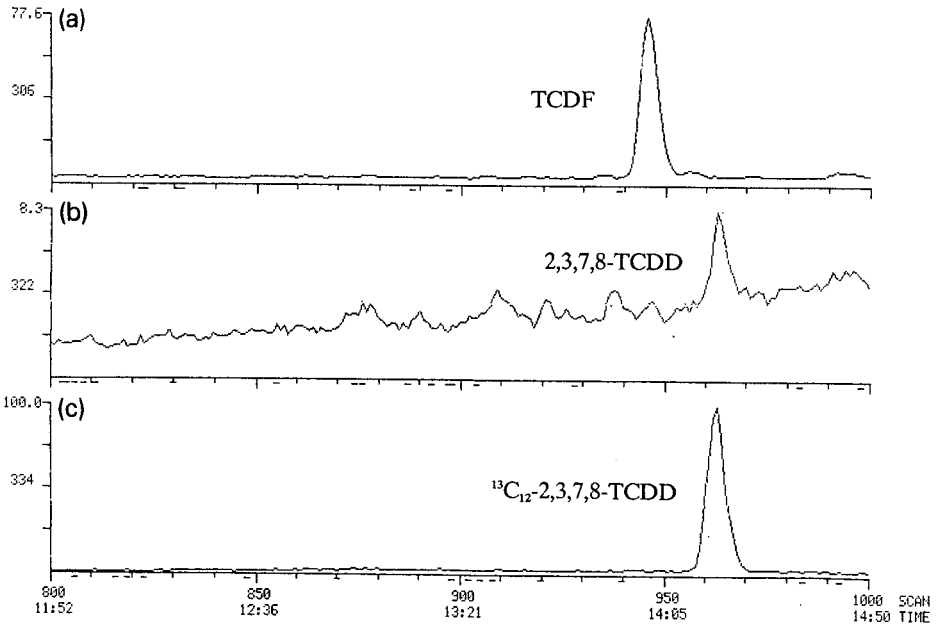

Fig. 3. Reconstructed ion chromatograms for (a) 160 ppt TCDF and (b) 10 ppt 2,3,7,8-TCDD in fish tissue. (c) Reconstructed ion chromatogram for $^{13}C_{12}$-2,3,7,8-TCDD internal standard. Time in min:s. The *y*-axes show the *m/z* values and the intensities (%).

PCDPEs, compounds that are frequently encountered in fish tissue samples collected in or around the Great Lakes.

The reconstructed ion chromatograms obtained for the samples processed using the HPLC cleanup scheme were found to be free of interferences. This permitted the unambiguous identification and quantitation of dioxins and furans at the low ppt level. No PCDPE interferences were observed for any of the samples analyzed. PCBs also appear to have been effectively removed using the dual column HPLC cleanup procedure. Figs. 3 and 4 show the reconstructed ion chromatograms obtained for the determination of TCDDs and TCDFs in two of the tissue samples analyzed. The concentrations of 2,3,7,8-TCDD in the two samples were 10 and 14 ppt (Figs. 3 and 4, respectively) while the concentrations of the TCDF were 160 and 91 ppt. No carry over was observed in any of the samples cleaned using the HPLC method. Both samples run after the samples containing 91 and 160 ppt of TCDF were found to have nondetectable levels of TCDF.

In order to investigate the reproducibility of the extraction and HPLC cleanup, the mean and standard deviation for the recovery of the individual isotopically labelled internal standards were calculated. The mean recoveries along with their respective standard deviations and relative standard deviations are given in Table III. The mean recoveries were found to range from 48 to 63% with typical relative standard deviations (R.S.D.) being approximately 28%.

Table IV shows the concentration ranges of the dioxins and furans found in the fish tissue samples. Mean detection limits were calculated based on those samples for which no dioxins or furans were detected. It should be noted that the results for two of

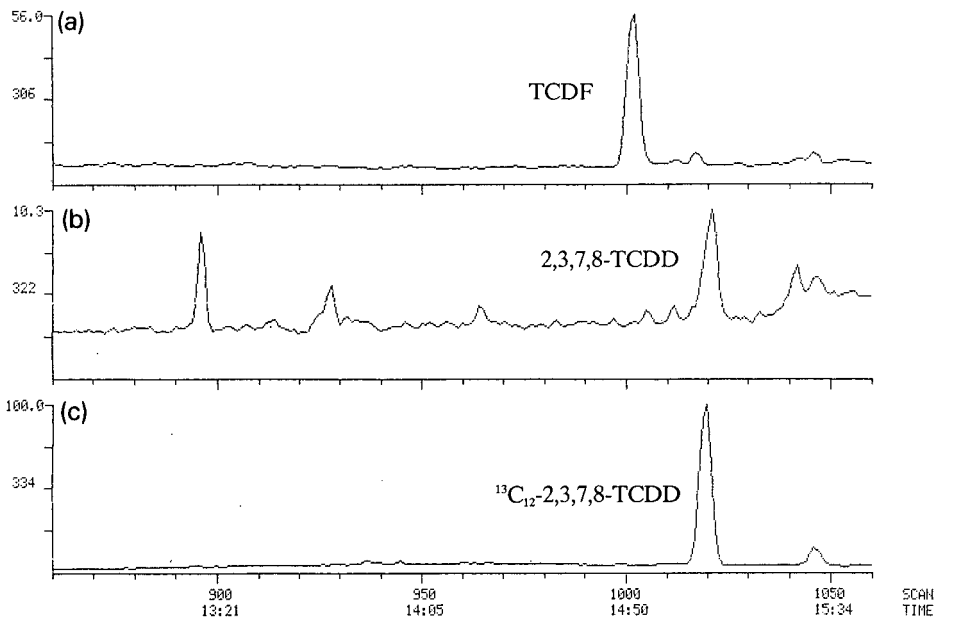

Fig. 4. Reconstructed ion chromatograms for (a) 91 ppt TCDF and (b) 14 ppt 2,3,7,8-TCDD in fish tissue. (c) Reconstructed ion chromatogram for $^{13}C_{12}$-2,3,7,8-TCDD internal standard. Time in minutes. The *y*-axes show the *m/z* values and the intensities (%).

TABLE III

RECOVERY OF ISOTOPICALLY LABELLED INTERNAL STANDARDS

Calculations based on results obtained from eighteen fish tissue samples.

Isomer	Level of spike (ng)	Mean recovery ± S.D. (%)	% R.S.D.
$^{13}C_{12}$-2,3,7,8-TCDD	4.9	48 ± 14	29
$^{13}C_{12}$-1,2,3,7,8-P_5CDD	5.5	63 ± 17	27
$^{13}C_{12}$-1,2,3,4,7,8-H_6CDD	4.1	56 ± 15	26
$^{13}C_{12}$-1,2,3,4,6,7,8-H_7CDD	18.8	57 ± 18	31
$^{13}C_{12}$-OCDD	9.2	62 ± 15	25

the fish tissue samples were not included in these calculations. The sample weights (3 to 4 grams) were much smaller than the 20 grams used for the majority of the samples which resulted in considerably higher detection limits.

CONCLUSIONS

The HPLC cleanup method devised in this study was found to be very effective in removing interferences such as PCBs and PCDPEs. The recovery of internal standards was found to be acceptable and quite consistent (average relative standard deviations of 28%). This procedure permitted the final analysis to be performed using a LRMS system. More selective techniques such as HRMS or MS–MS were not required because no interferences were encountered, however the increased sensitivity of such instrumentation would result in much lower detection limits.

TABLE IV

SUMMARY OF PCDD AND PCDF RESULTS

Based on results from sixteen fish tissue samples (two samples with only 3 to 4 g total weight were omitted in this summary). Superscripts indicate the number of isomers detected for each congener group. ND = Not detected. DL = Detection limit.

Congener group	Number of samples with positives	Concentrations (ppt)	Number of NDs	Mean DL (ppt)
2,3,7,8-TCDD	4	10, 14, 15, 27	12	4
TCDD	4	10^1, 14^1, 23^2, 66^2	12	4
P_5CDD	1	3^1	15	6
H_6CDD	1	22^2	15	8
H_7CDD	1	130^2	15	7
OCDD	2	15, 380	14	7
TCDF	5	7^1, 25^1, 60^1, 91^1, 160^1	11	4
P_5CDF	0		16	4
H_6CDF	1	36^2	15	6
H_7CDF	1	55^2	15	8
OCDF	1	44	15	6

This cleanup procedure should be easily automated and at this time we are currently setting up a fully automated HPLC system complete with autosampler, fraction collector, and automated switching valves. With such an arrangement we hope to be able to process a set of 10 tissue samples (and associated quality assurance/quality control (QA/QC) samples) through the HPLC cleanup in about 20 h.

In future work, we will be evaluating the useful lifetime of the carbon–silica column. No deterioration of performance was observed during the injection of numerous standard solutions, QA/QC samples, and the 18 tissue sample extracts. By using the column-switching step, the bulk of the pollutants are not introduced onto this column which presumably extends its useful lifetime.

REFERENCES

1 R. E. Clement and S. A. Lennox, *Chemosphere*, 15 (1986) 1941.
2 D. T. Williams and B. J. Blanchfield, *J. Assoc. Off. Anal. Chem.*, 54 (1971) 1429.
3 M. L. Porter and J. A. Burke, *J. Assoc. Off. Anal. Chem.*, 54 (1971) 1426.
4 P. W. Albro and C. E. Parker, *J. Chromatogr.*, 197 (1980) 155.
5 H. Steinwandter, *Fresenius' Z. Anal. Chem.*, 321 (1985) 600.
6 D. L. Stalling, L. M. Smith, J. D. Petty, J. W. Hogan, J. L. Johnson, C. Rappe and H. R. Buser, in R. E. Tucker, A. L. Young and A. P. Gray (Editors), *Human and Environmental Risks of Chlorinated Dioxins and Related Compounds*, Plenum Press, New York, 1983, p. 221.
7 L. M. Smith, D. L. Stalling and J. L. Johnson, *Anal. Chem.*, 56 (1984) 1830.
8 R. Baughman and M. Meselson, *Environ. Health Perspect.*, 5 (1973) 27.
9 L. L. Lamparski, T. J. Nestrick and R. H. Stehl, *Anal. Chem.*, 51 (1979) 1453.
10 T. J. Nestrick, L. L. Lamparski and R. H. Stehl, *Anal. Chem.*, 51 (1979) 2273.
11 J. J. Ryan and J. C. Pilon, *J. Chromatogr.*, 197 (1980) 171.
12 H. Y. Tong, D. L. Shore and F. W. Karasek, *Anal. Chem.*, 56(13), 2442, 1984.
13 R. J. Dolphin and F. W. Willmott, *J. Chromatogr.*, 149 (1978) 161.
14 F. W. Willmott, I. Mackenzie and R. J. Dolphin, *J. Chromatogr.*, 167 (1978) 31.
15 T. S. Thompson, D. H. Schellenberg, K. P. Naikwadi and F. W. Karasek, *Chemosphere*, 19 (1989) 45.
16 T. S. Thompson, *Ph.D. Thesis*, University of Waterloo, Waterloo, 1989.
17 P. W. O'Keefe, R. M. Smith, D. R. Hilker, K. M. Aldous and W. Gilday, in L. H. Keith, C. Rappe and G. Choudhary (Editors), *Chlorinated Dioxins and Dibenzofurans in the Total Environment II*, Butterworth, Boston, MA, 1985, p. 111.
18 J. R. Donnelly, W. D. Munslow, N. J. Nunn, A. H. Grange, T. L. Vonnahme, J. F. Fisk and G. W. Sovocool, *Chemosphere*, 20 (1990) 123.

Journal of Chromatography, 543 (1991) 59–67
Elsevier Science Publishers B.V., Amsterdam

CHROM. 23 076

Application of an anhydrotrypsin-immobilized precolumn for selective separation of peptides having arginine or lysine at their C-termini by column-switching high-performance liquid chromatography

TAKAFUMI OHTA*, TAKASHI INOUE and SHOJI TAKITANI
Faculty of Pharmaceutical Sciences, Science University of Tokyo, 12 Ichigaya-Funagawara-Machi, Shinjuku-Ku, Tokyo 162 (Japan)

(First received October 1st, 1990; revised manuscript received December 20th, 1990)

ABSTRACT

A column-switching high-performance liquid chromatographic (CS-HPLC) system which consisted of an anhydrotrypsin (AHT)-immobilized diol–silica precolumn and a reversed-phase analytical column was developed for the selective separation of peptides having Arg or Lys at their C-termini. Tuftsin (Thr-Lys-Pro-Arg) could be enriched almost quantitatively on the precolumn when loaded with water as a carrier solvent and the precolumn was washed with 10–30 m*M* acetate buffer (pH 5.0). An investigation of the affinity characteristics of 55 peptides to the AHT precolumn showed that among twelve peptides having Arg or $ArgNH_2$ at their C-termini and more than four amino acid residues, ten were retained almost quantitatively on the precolumn, and eight out of nine peptides having Lys at their C-termini were less retained. The peptide having D-Arg at its C-termini was not retained. However, twelve out of thirty peptides having no Arg or Lys at their C-termini were also retained, but the retention was greatly decreased, in contrast to the Arg peptides, when the precolumn was washed with 20 m*M* calcium chloride solution. The results indicate that the CS-HPLC system equipped with an AHT precolumn offers new selectivity in the HPLC separation of peptides.

INTRODUCTION

Column switching (CS) is a powerful technique in high-performance liquid chromatography (HPLC) for the separation of compounds of interest in multi-component samples. For the analysis of peptides that have a large number of isomers, the technique is an especially good candidate to give better resolution. Reversed-phase and immunoaffinity precolumns have so far been used for the CS-HPLC analysis of peptides [1–5]. The immunoaffinity method offers highly selective retention, but the preparation of antibody is time consuming. Methods based on other bioaffinities such as enzyme–inhibitor or –substrate seem rational, but have not been used in the CS-HPLC analysis of peptides.

Anhydrotrypsin (AHT), a catalytically inert derivative of trypsin in which the active site Ser residue is converted into a dehydroalanine, is known to exhibit affinity

0021-9673/91/$03.50

toward peptides having Arg or Lys at their C-termini, and AHT-immobilized agarose has been used as a selective adsorbent for the isolation of the C-terminal peptides from tryptic or chymotryptic digests of proteins [6–10].

Recently, we have developed an AHT-immobilized diol–silica for the high-performance affinity chromatographic separation of peptides having Arg or Lys at their C-termini from the other [11]. The excellent characteristics of the AHT column with regard to separation speed and stability prompted us to investigate the possibility that it might be used as a precolumn in CS-HPLC.

In this study, we developed a CS-HPLC system in which peptides retained on an AHT-immobilized diol–silica precolumn were selectively transferred to and separated on a reversed-phase analytical column, and affinity characteristics of various peptides with respect to the AHT column were examined by using the system.

EXPERIMENTAL

Materials

Peptides were purchased from the Peptide Institute (Osaka, Japan) and Sigma (St. Louis, MO, U.S.A.). Diol–silica was prepared from LiChrospher Si 300 (10 μm) (E. Merck, Darmstadt, Germany) as described previously [11]. Other chemicals were of analytical-reagent grade. Deionized water (obtained with a Millipore RO-Q system) was used throughout.

Preparation of an AHT-immobilized precolumn

An AHT-immobilized precolumn (10 × 4.6 mm I.D.) was prepared as described previously [11]. In brief, diol–silica, prepared by silanization of LiChrospher Si 300 (10 μm) with 3-glycidoxypropyltrimethoxysilane under anhydrous conditions followed by hydrolysis of the epoxy groups with 0.01 *M* hydrochloric acid, was activated with 2,2,2-trifluoroethanesulphonyl chloride, and AHT was immobilized onto the diol–silica by shaking the activated gel in phosphate buffer (pH 8.0) containing AHT. The amount of AHT immobilized onto the diol–silica was 10 mg/g. The column was stored in water at 4°C when not in use.

CS-HPLC

The set-up of the CS-HPLC system used is shown schematically in Fig. 1. A Model LC-6A pump (P1) (Shimadzu, Kyoto, Japan) was used for sample loading at a flow-rate of 0.5 ml/min with ice-cold water (S1) as the eluent. Peptide solution was

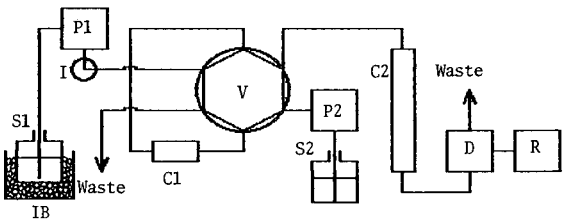

Fig. 1. Schematic diagram of the CS-HPLC system. P1, P2 = Pumps; C1 = precolumn; C2 = analytical column; I = injector; S1, S2 = eluents; IB = ice-bath; V = column-switching valve; D = detector; R = integrator.

injected onto the AHT precolumn (C1) through a Model NVI-3002 injector (Nihon Seimitsu Kagaku, Tokyo, Japan) equipped with a 1- or 5-ml loop. After removal of the sample from the loop, 1 ml of 10 m*M* acetate buffer (pH 5.0) was injected to eliminate non-specific adsorption of peptides, and the precolumn was further washed with the eluent for 5–10 min depending on the loop volume. The switching valve, a Model NHV-7000-6M (Nihon Seimitsu Kagaku), was then changed from "load" to "inject". A Model LC-5A pump (P2) (Shimadzu) was used for back-flushing the retained peptide from the precolumn onto an analytical column (C2) (Asahipak ODP-50; 250 × 4.6 mm I.D.) at a flow-rate of 0.7 ml/min with 0.1 *M* $NaClO_4$–[CH_3CN–0.14% H_3PO_4 (1–30:99–70, v/v)] (S2) as eluents. The column eluent was monitored at 214 nm with a Jasco Model 870-UV detector (Japan Spectroscopic, Tokyo, Japan) connected to a Chromatopac CR-1B integrator (Shimadzu).

The percentage retention of each peptide on the AHT precolumn was calculated by dividing the peak height obtained with the precolumn by that obtained by injecting a 50 μl of solution containing the corresponding amount of the peptide directly onto the analytical column.

RESULTS AND DISCUSSION

Optimization of the CS-HPLC system

A preliminary study using non-immobilized diol–silica in the precolumn showed that certain peptides were non-specifically retained. In order to eliminate such non-specific binding, washing of the precolumn with acetate buffer (pH 5.0) after loading a sample was examined. Fig. 2 shows the retention of a peptide, No. 14 (tuftsin), on the AHT and the diol–silica precolumns after washing with various concentrations of the acetate buffers. The non-specific binding of tuftsin to the diol–silica precolumn was eliminated completely by washing with 1 m*M* acetate buffer. On the other hand, almost quantitative retention was obtained at least up to 30 m*M* when the AHT precolumn was used, indicating that tuftsin was retained on the precolumn by its affinity to immobilized AHT.

Fig. 3 shows the effect of the flow-rate of S1 on the retention of tuftsin on the AHT precolumn. Almost quantitative retention was observed at flow-rates of 0.5–1.5 ml/min. As ligand–ligate interaction is generally decreased in affinity chromatogra-

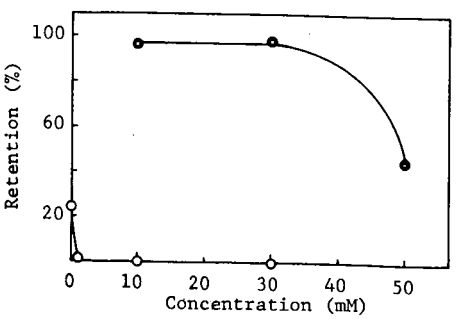

Fig. 2. Effect of concentration of acetate buffer (pH 5.0) on the retention of tuftsin on (○) diol–silica and (●) AHT precolumns. Tuftsin: 2 nmol in 400 μl.

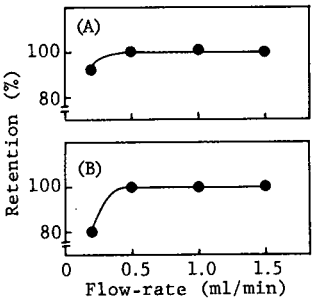

Fig. 3. Effect of flow-rate on retention of tuftsin on the AHT precolumn. Tuftsin: (A) 0.2 nmol in 400 μl; (B) 0.2 nmol in 1.6 ml.

phy with an increase in flow-rate, the lower retention at a flow-rate less than 0.5 ml/min seems strange. However, no further studies were carried out to clarify the phenomenon. In this study, a flow-rate of 0.5 ml/min was used.

Using the defined flow-rate and concentration of washing buffer, calibration graphs for tuftsin were constructed using various sample sizes. Linear relationships between the peak height and tuftsin concentration were observed at any sample size, but good reproducibility was obtained for sample sizes up to 1.6 ml (Table I). The detection limit (signal-to-noise ratio = 2) was 5 ng for a 1.6-ml injection (6.25 n*M*).

Affinity characteristics of various peptides

As tuftsin could be enriched and determined using the present CS-HPLC system, the retentions of various peptides on the AHT precolumn after washing with 10 or 30 m*M* acetate buffer (pH 5.0) were also examined. As shown in Table II, peptides that had Arg at their C-termini and more than four amino acid residues, except Nos. 14 and 16, were retained almost quantitatively on the AHT precolumn after washing with 10 m*M* acetate buffer. These peptides, except No. 7, were also retained in good yield after washing with 30 m*M* acetate buffer. No. 11, which had C-terminal D-Arg was not retained at all, whereas No. 5, which had C-terminal $ArgNH_2$, was retained almost quantitatively. The peptides that had Lys at their C-termini showed less affinity to the AHT precolumn, especially after washing with 30 m*M* acetate buffer.

TABLE I

CALIBRATION GRAPH FOR TUFTSIN

Sample volume (ml)	Regression equation[a]	Relative standard deviation (%)[b]
0.1	$y = 2.91x - 0.36$ ($r = 0.9999$)	1.6
0.4	$y = 2.53x + 0.12$ ($r = 0.9998$)	4.9
0.8	$y = 2.09x + 0.45$ ($r = 0.9997$)	2.4
1.6	$y = 2.28x - 0.02$ ($r = 0.9998$)	7.6
3.2	$y = 2.10x - 0.10$ ($r = 0.9998$)	14.2

[a] 0.1–20 nmol per injection. y = peak height (cm); x = injected amount (nmol).

[b] 0.2 nmol per injection ($n = 4$).

TABLE II

EFFECT OF WASHING WITH ACETATE BUFFER ON THE RETENTION OF PEPTIDES ON THE AHT AND DIOL–SILICA PRECOLUMNS

No.	Peptides[a]	Retention (%)			
		AHT precolumn		Diol–silica precolumn	
		10 mM^b	30 mM^b	10 mM^b	30 mM^b
1	Tyr-Arg	4	0	0	–[c]
2	Bz-Gly-Arg	0	–	0	–
3	Gly-Gly-Arg	0	–	–	–
4	Thr-Lys-Pro-Arg	97	101	0	–
5	Tyr-Ile-Gly-Ser-ArgNH_2	90	92	0	–
6	His-Leu-Gly-Leu-Ala-Arg	97	92	0	–
7	Tyr-Gly-Gly-Phe-Leu-Arg	105	21	0	–
8	Tyr-Gly-Gly-Phe-Leu-Arg-Arg	99	96	1	1
9	Tyr-Gly-Gly-Phe-Leu-Arg-Lys-Arg	91	97	7	4
10	Gly-Arg-Gly-Leu-Ser-Leu-Ser-Arg	80	89	0	–
11	Dnp-Gln-Gly-Ile-Ala-Gly-Gln-D-Arg	0	–	0	–
12	Arg-Pro-Pro-Gly-Phe-Ser-Pro-Phe-Arg	97	100	3	2
13	Tyr-Gly-Gly-Phe-Leu-Arg-Arg-Ile-Arg	93	99	10	5
14	Phe-Ser-Trp-Gly-Ala-Glu-Gly-Gln-Arg	17	7	0	–
15	Tyr-Arg-Pro-Pro-Gly-Phe-Ser-Pro-Phe-Arg	89	88	3	2
16	Ala-Asp-Ser-Gly-Glu-Gly-Asp-Phe-Leu-Ala-Glu-Gly-Gly-Gly-Val-Arg	0	–	0	–
17	Bz-Gly-Lys	0	–	0	–
18	Lys-Trp-Lys	96	105	2	2
19	Thr-Pro-Arg-Lys	87	103	0	–
20	Pro-Phe-Gly-Lys	44	0	0	–
21	Tyr-Gly-Gly-Phe-Met-Lys	68	4	1	–
22	Tyr-Gly-Gly-Phe-Leu-Lys	55	4	1	–
23	Ser-Ile-Gly-Ser-Leu-Ala-Lys	20	0	0	–
24	Val-His-Leu-Thr-Pro-Val-Glu-Lys	89	84	0	–
25	Tyr-Gly-Gly-Phe-Leu-Arg-Lys-Tyr-Pro-Lys	52	61	7	4
26	Gly-Gly-Gly	0	–	–	–
27	Tyr-Pro-Phe	0	–	0	–
28	Tyr-Tyr-Phe	0	–	0	–
29	Glu-Val-Phe	0	–	0	–
30	Met-Leu-Phe	0	–	0	–
31	Val-Ala-Ala-Phe	0	–	0	–
32	Ala-Ala-Ala-Ala	0	–	–	–
33	Arg-Gly-Asp-Ser	0	–	–	–
34	Gly-Arg-Gly-Asp	0	–	0	–
35	Arg-Pro-Lys-Pro	87	87	0	–
36	Phe-Gly-Gly-Phe	0	–	0	–
37	Phe-Leu-Glu-Glu-Val	0	–	0	–
38	Tyr-Pro-Phe-Pro-Gly	0	–	0	–
39	Tyr-Gly-Gly-Phe-Leu	0	–	0	–
40	Tyr-Gly-Gly-Phe-Met	0	–	0	–
41	Arg-Ser-Arg-His-Phe	52	62	19	6
42	Arg-Lys-Asp-Val-Tyr	109	20	0	–
43	Lys-Val-Ile-Leu-Phe	78	32	0	–
44	Arg-Val-Tyr-Ile-His-Pro-Phe	86	86	2	1

(Continued on p. 64)

TABLE II *(continued)*

No.	Peptides[a]	Retention (%)			
		AHT precolumn		Diol–silica precolumn	
		10 m*M*[b]	30 m*M*[b]	10 m*M*[b]	30 m*M*[b]
45	Arg-Val-Tyr-Ile-His-Pro-Ile	92	91	0	–
46	Tyr-Pro-Phe-Pro-Gly-Pro-Ile	1	0	0	–
47	Tyr-Gly-Gly-Phe-Met-Arg-Phe	73	71	0	–
48	Ser-Met-Glu-Val-Arg-Gly-Trp	0	–	0	–
49	Asp-Arg-Val-Tyr-Ile-His-Pro-Phe	60	58	1	–
50	Arg-Pro-Pro-Gly-Phe-Ser-Pro-Phe	78	77	1	1
51	Arg-Pro-Pro-Gly-Phe-Ser-Pro-Leu	97	97	0	–
52	Ala-Ser-Thr-Thr-Thr-Asp-Tyr-Thr	0	–	0	–
53	Tyr-Gly-Gly-Phe-Leu-Arg-Lys-Tyr-Pro	71	69	3	2
54	Trp-Ala-Gly-Gly-Asp-Ala-Ser-Gly-Glu	0	–	0	–
55	Arg-Arg-Leu-Ile-Glu-Asn-Ala-Glu-Tyr-Ala-Ala-Arg-Gly	100	100	0	–

[a] 1 nmol per 50-μl injection (5 nmol for Nos. 3, 26 and 32).
[b] Concentration of acetate buffer (pH 5.0).
[c] Not determined.

Among thirty peptides that had no Arg or Lys at their C-termini, twelve were retained considerably on the AHT precolumn, as opposed to our expectations. On the other hand, almost all the peptides examined showed no affinity to the diol–silica precolumn, indicating that the retained peptides were recognized with the immobilized AHT.

Ishii and co-workers [6–10] investigated the chromatographic behaviour of twenty peptides (twelve C-terminal Arg peptides, six C-terminal Lys peptides and two other peptides) on an AHT–agarose column, and reported that Arg or Lys peptides having more than three amino acid residues, except those having D-Arg or $ArgNH_2$, were retained on the column, and that the Lys peptides showed less affinity to the column. These characteristics generally coincided with our results, but there are several discrepancies. Peptides Nos. 2 and 16, which showed a strong affinity to the AHT–agarose column, were not retained on the AHT precolumn in this study. In order to assess the possibility that these were retained but not eluted from the precolumn, the eluates from the precolumn were collected and analysed by HPLC. The eluates contained 90% (No. 2) and 94% (No. 16) of the loaded peptides, indicating that these were not retained on the AHT precolumn. Because the eluent used in this study (water and 10–30 m*M* acetate buffer, pH 5.0) was different from that in previous studies (20 m*M* calcium chloride–50 m*M* acetate buffer, pH 5.0), the retention behaviour of these peptides on the AHT precolumn pre-equilibrated with 20 m*M* calcium chloride or 20 m*M* calcium chloride–10–50 m*M* acetate buffer (pH 5.0) was also investigated. However, none of them were retained on the precolumn at all. Therefore, the discrepancy in retention between our study and previous studies is likely to be attributable to differences in the chromatographic supports and the method of immobilization of AHT.

The retention of $ArgNH_2$ peptide No. 5 also seems to conflict with the results of the previous investigation in which Bz-$ArgNH_2$, in contrast to Bz-Arg, is not retained on the AHT–agarose column. However, the number of $ArgNH_2$ peptides examined in both studies seems too small to draw conclusions.

Another serious problem is the retention of some of the peptides that have no Arg or Lys at their C-termini on the AHT precolumn. However, it should be noted that only two such peptides were examined previously, and that the recovery of C-terminal peptides having no Arg or Lys at their C-termini from the AHT–agarose column loaded with tryptic digests of proteins was reported sometimes to be low [8]. Therefore, the retention of these peptides observed in our study seems not to conflict necessarily with the previous observations. In order to clarify whether these peptides are recognized at the same site of immobilized AHT as the peptides having Arg or Lys at their C-termini, the retentions of No. 50 on the AHT precolumn and that presaturated with tuftsin were compared. No difference in retention between the two columns was observed, as shown in Fig. 4, indicating the presence of multiple sites on the immobilized AHT for affinity of peptides. However, it still remains uncertain what factor governs the retention of some of the peptides having no Arg or Lys at their C-termini.

Reinvestigation of the washing solvents

The above results indicated that the selectivity of the AHT precolumn was not necessarily satisfactory because of the retention of some of the peptides having no Arg or Lys at their C-termini. Therefore, other washing solvents were investigated. As trypsin had a calcium binding site and was stabilized with the ion [12], washing with 20 m*M* calcium chloride was compared with that with 60 m*M* sodium chloride, which had the same ionic strength. The effect of these washings on retention of the selected peptides is shown in Fig. 5. The retention of some of the Arg peptides, Nos. 7 and 10, and most of the Lys peptides, Nos. 20–24, was decreased greatly by using 60 m*M* sodium chloride, which had a higher ionic strength than 10 and 30 m*M* acetate

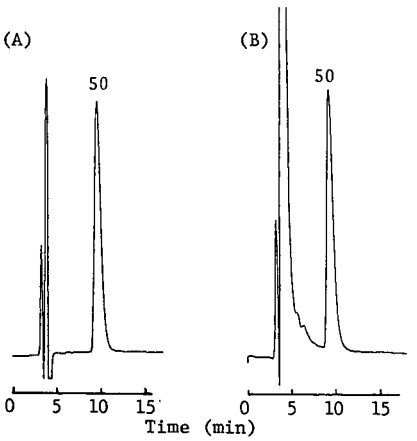

Fig. 4. Effect of presaturation of the AHT precolumn with tuftsin on the retention of peptide No. 50. (A) AHT precolumn; (B) AHT-precolumn presaturated with tuftsin (0.5 μmol). No. 50: 1 nmol in 50 μl. Mobile phase: 0.1 *M* $NaClO_4$–[CH_3CN–0.14% H_3PO_4 (30:70, v/v)].

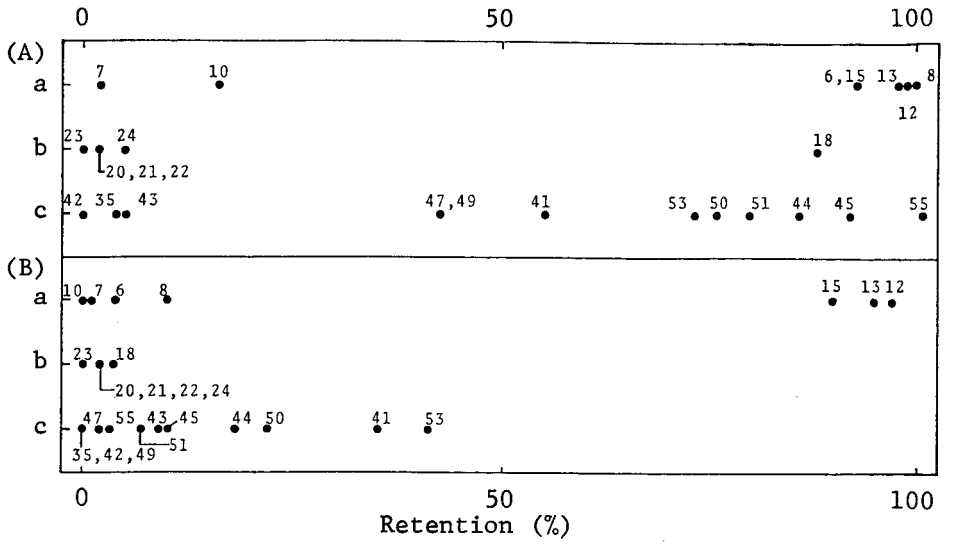

Fig. 5. Effect of washing solvents on retention of peptides on the AHT precolumn. (A) 60 m*M* NaCl; (B) 20 m*M* $CaCl_2$. (a) Peptides having Arg at their C-termini; (b) peptides having Lys at their C-termini; (c) peptides having no Arg or Lys at their C-termini. Peptide numbers as in Table II.

buffers. The retention of many of the peptides having no Arg or Lys at the C-termini, however, was not changed or changed only slightly. On the other hand, the retention of all of these peptides with no Arg or Lys was decreased greatly by using 20 m*M* calcium chloride, while some Arg peptides, Nos. 12, 13 and 15, remained unchanged. These results indicated that the selectivity of the AHT precolumn was enhanced by the use of 20 m*M* calcium chloride although some of the Arg peptides became unretained. The difference in retention between the Arg peptides and peptides with no Arg or Lys supports the notion that multiple sites on the immobilized AHT are responsible for peptide affinity.

Selective separation of peptides by CS-HPLC

The above results indicate that the selectivity of the AHT precolumn can be changed by changing the washing solvent. Fig. 6 shows the HPLC of a model peptide mixture after washing with various solvents. No. 28, which had Phe at the C-termini, was removed by washing with 10 m*M* acetate buffer (B) and, in addition, No. 22, which had Lys at the C-termini, was removed by washing with 30 m*M* acetate buffer (C). When the precolumn was washed with 20 m*M* calcium chloride, all of the peptides that had no Arg at C-termini were removed (D). Therefore, changing the concentration and/or type of washing solvent is useful for controlling the selectivity of the precolumn.

Stability of the AHT precolumn

We determined the stability of the AHT precolumn by measuring the retention of tuftsin after various periods of operation. The AHT precolumn showed no decrease in retention after exposure for about 800 cycles to acidic eluents containing

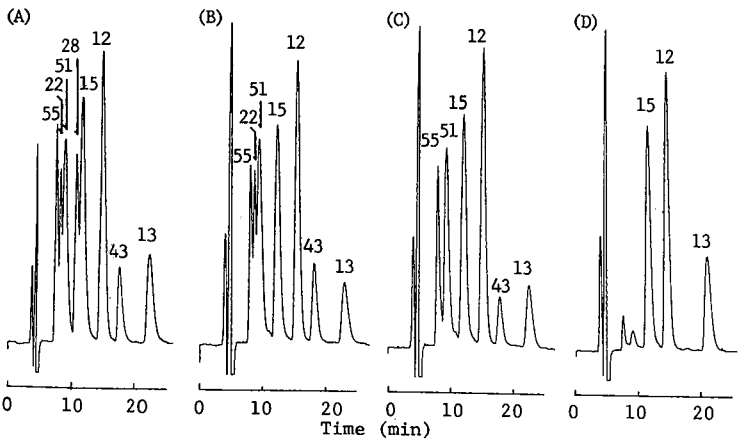

Fig. 6. HPLC of a model peptide mixture after washing the AHT precolumn with various solvents. (A) The mixture (50 μl) containing 1 nmol each of peptides was chromatographed without the AHT precolumn (B)–(D) the mixture (400 μl) containing 1 nmol each of peptides was chromatographed with the AHT precolumn [washing solvent: B, 10 m*M* acetate buffer (pH 5.0); C, 50 m*M* acetate buffer (pH 5.0); D, 20 m*M* $CaCl_2$]. Mobile phase: 0.1 *M* $NaClO_4$–[CH_3CN–0.14% H_3PO_4 (30:70, v/v)].

acetonitrile during 1 year: the retention (2 nmol per 400-μl injection) at 2, 5, 8 and 12 months after the preparation of the column were 96, 104, 105 and 93%, respectively.

CONCLUSIONS

Reversed-phase and immunoaffinity precolumns have been used for the CS-HPLC separation of peptides [1–5]. The use of the AHT precolumn offers new selectivity in the CS-HPLC separation of peptides. The AHT precolumn may be useful for on-line sample pretreatment in the HPLC determination of peptides having Arg or Lys at their C-termini in biological fluids because of its high stability.

REFERENCES

1 T. Hayashi, S. Sakamoto, T. Fuwa, I. Morita and H. Yoshida, *Anal. Sci.*, 3 (1987) 445.
2 T. Hayashi, S. Sakamoto, T. Fuwa, I. Wada and H. Yoshida, *Anal. Sci.*, 4 (1988) 313.
3 T. Hayashi, S. Sakamoto, I. Wada and H. Yoshida, *Chromatographia*, 27 (1989) 574.
4 T. T. Nguyen, A. D. Lean and H. Ong. *Anal. Biochem.*, 179 (1989) 24.
5 A. Foucault, H. Pinochet, R. Rosset and D. Tome, *Chromatographia*, 25 (1988) 822.
6 S. Ishii, H. Yokosawa, T. Kumazaki and I. Nakamura, *Methods Enzymol.*, 91 (1983) 378.
7 H. Yokosawa and S. Ishii, *Biochem. Biophys. Res. Commun.*, 72 (1976) 1443.
8 T. Kumazaki, T. Nakano, F. Arisaka and S. Ishii, *Proteins Struct. Funct. Genet.*, 1 (1986) 100.
9 T. Kumazaki, K. Terasawa and S. Ishii, *J. Biochem.*, 102 (1987) 1539.
10 S. Ishii, H. Yokosawa, S. Shiba and K. Kasai, *Adv. Exp. Med. Biol.*, 120A (1989) 15.
11 T. Ohta, T. Inoue, Y. Fukumoto and S. Takitani, *Chromatographia*, 30 (1990) 410.
12 M. Delaage and M. Lazdunski, *Biochem. Biophys. Res. Commun.*, 28 (1967) 390.

Journal of Chromatography, 543 (1991) 69–80
Elsevier Science Publishers B.V., Amsterdam

CHROM. 23 072

Determination of sorbic acid in margarine and butter by high-performance liquid chromatography with fluorescence detection

GIOVANNI BURINI* and PIETRO DAMIANI

Istituto di Chimica Bromatologica, Facoltà di Farmacia, Università degli Studi di Perugia, 06100 Perugia (Italy)

(First received April 17th, 1990; revised manuscript received December 20th, 1990)

ABSTRACT

A procedure is reported for the separation and determination of sorbic acid, as a derivative of 4-bromomethyl-6,7-dimethoxycoumarin, by reversed-phase high-performance liquid chromatography with fluorescence detection using enanthic acid as an internal standard. Sorbic acid, separated from samples of commercial margarine and butter by steam distillation, was evaluated using the proposed procedure and by UV absorption and visible spectrophotometric methods (AOAC). The preparation of the calibration graph and the determination of sorbic acid with the visible spectrophotometric method was improved. The sorbic acid content determined using UV and visible spectrophotometric methods was higher than that obtained with the reversed-phase high-performance liquid chromatographic method owing to the presence of interfering substances in the samples. The range of recovery and the precision of the proposed method and the reference methods are also reported.

INTRODUCTION

Sorbic acid, isolated for the first time from the berries of mountain ash (*Sorbus aucuparia* L.) is a particular unsaturated fatty acid (2,4-hexadienoic acid) which, in the lactone state (parasorbic acid), is also found in berries of some other genera of the Rosaceae family. Sorbic acid and its sodium, potassium and calcium salts are food preservative additives which counteract microbiological alterations by inhibiting the action of moulds and yeasts. Gooding [1] was the first to confirm its fungistatic properties and proposed its use to prevent the growth of moulds in foods and packaging materials. Today sorbic acid is one of the most widely used additives. It is allowed (Italian regulations [2]) at various concentrations (50–2000 mg/kg) in a wide range of foods.

Extraction followed by determination is the procedure generally reported in the literature to determine the sorbic acid content in foods. It can easily be isolated from complex food matrices by steam distillation [3–5], diethyl ether extraction of the food mixed with sand [6] and extraction with an aqueous solution of metaphosphoric acid followed by partitioning into a diethyl ether–light petroleum mixture [7,8].

0021-9673/91/$03.50

Leuenberger *et al.* [9] and Coelho and Nelson [10] used an Extrelut prepacked column (Merck, Darmstadt, Germany) containing silica with a large-pore granular structure which permits the extraction of lipophilic substances from an aqueous phase by liquid–liquid partition chromatography. Extraction by ion-pair formation with tertiary amines and their salts was used by Puttemans *et al.* [11] and Terada *et al.* [12].

For determination the first methods used UV and visible spectrophotometry. The former is based on absorption at *ca.* 260 nm due to an extensive conjugated system of three double bonds, one of which originated from a carboxyl group. The second (oxidation method) is based on absorption at 532 nm due to a red pigment derived from the reaction of malonaldehyde, a product of the oxidation of sorbic acid, with 2-thiobarbituric acid [13]. Some spectrophotometric procedures [3–5,8] were adopted as AOAC methods [14] for the determination of sorbic acid in cheeses, wine and dairy products.

The usefulness of thin-layer chromatography (TLC) should be noted with respect to qualitative and semi-quantitative research [15,16]; it can also permit a quantitative evaluation if a reflectance spectrophotometric determination is performed [17–19]. High-performance TLC with fluorescence detection [20,21], used to determine propionic, sorbic and benzoic acids, requires a derivatization procedure with dansylsemipiperazide in the presence of N,N′-dicyclohexylcarbodiimide. Determination of the fluorescent amidic derivatives of the acids is performed using a TLC plate scanner ($\lambda_{ex.}$ = 366 nm).

Determination of sorbic acid in foods by gas chromatography [6,22–25] can be achieved directly by injecting the extract obtained from the sample or after its derivatization.

In recent years, high-performance liquid chromatography (HPLC) has been used for the determination of sorbic acid in a number of different food systems. Some workers employed anion-exchange chromatography [26–28] and others reversed-phase (RP) HPLC [12,29–36], including ion-pair chromatography [11,37]. Most of these methods were also used for the determination of other preservatives in the eluted sample and detection was always performed by means of UV spectrophotometry.

This present paper describes an RP-HPLC procedure with fluorimetric detection which offers high sensitivity and specificity in the detection of sorbic acid as a derivative of 4-bromomethyl-6,7-dimethoxycoumarin. This procedure allows the identification, separation and determination of sorbic acid isolated from commercial samples of margarine and butter by steam distillation. The derivatization with 4-bromomethyl-6,7-dimethoxycoumarin [38], which converts sorbic acid into a fluorophore, and the chromatographic parameters were optimized. The method was compared with the AOAC UV and visible spectrophotometric procedures [14].

EXPERIMENTAL

Apparatus

The separation of the sorbic acid from the samples was achieved with a steam distillation apparatus similar to that reported [14]. A Varian (Palo Alto, CA, U.S.A.) Model 5000 liquid chromatograph equipped with a Varian Fluorichrom fluorescence detector was used at the following settings: gain and lamp, LO; attenuator, × 20; excitation filters, CS 7-60/CS 7-54 (maximum wavelength transmission at 355 nm); emission filters, CS 3-73/CS 4-76 (wavelength emission >420 nm).

Separation was performed by RP-HPLC on a Spherisorb ODS-2 (5 μm) column (250 × 4.6 mm I.D.) (Custom LC, Houston, TX, U.S.A.). The system was interfaced with a Varian 4270 computing integrator: attenuation × 2, chart speed 0.25 cm/min.

The spectrophotometric analyses were performed on a Varian DMS Model 200 UV–visible spectrophotometer.

Reagents

Potassium sorbate (99%), analytical-reagent grade magnesium sulphate heptahydrate, enanthic acid, 2-thiobarbituric acid (TBA), potassium dichromate, sulphuric acid, hydrochloric acid and all the solvents for HPLC, such as acetone, water and methanol, were purchased from Carlo Erba (Milan, Italy). 4-Bromomethyl-6,7-dimethoxycoumarin (4-Brmdmc) and 18-crown-6 were purchased from Sigma (St. Louis, MO, U.S.A.).

A 2 *M* methanolic potassium hydroxide solution was prepared by dissolving 5.6 g of potassium hydroxide in 50 ml of methanol. Acetone solutions of 4-Brmdmc (0.7 mg/ml) and 18-crown-6 (0.63 mg/ml) were prepared.

Samples

Commercial samples of margarine and butter were used.

Preparation of standard solutions

A solution was prepared by dissolving 134 mg of potassium sorbate (equivalent to 100 mg of sorbic acid) in 100 ml of distilled water. The internal standard solution was prepared by adding 0.4 ml of 2 *M* methanolic potassium hydroxide solution to 100 mg of enanthic acid in a 100-ml volumetric flask and diluting to volume with distilled water. Stock solutions (100 μg/ml) were obtained diluting these two solutions 1:10 with distilled water. Aliquots of 0.5–4 ml of sorbic acid stock solution were mixed with 1 ml of internal standard stock solution in separate 100-ml volumetric flasks, containing 50 μl of 2 *M* methanolic potassium hydroxide solution, and diluted to volume with distilled water. These standard solutions, containing 0.5–4 μg/ml of sorbic acid and 1 μg/ml of the internal standard, were then derivatized and used to obtain the calibration graph by HPLC analysis. When refrigerated, the standard solutions were stable for several days.

Derivatization and calibration

The derivatization is based on the reaction between fatty acid potassium salts and 4-Brmdmc in the presence of 18-crown-6, which yields a fluorescent derivative as shown in Fig. 1.

After preliminary studies the following derivatization procedure was adopted throughout. A 0.5-ml volume of each standard solution was pipetted into a 10-ml emery-cap test-tube and evaporated using a Rotavapor at 50–55°C under reduced pressure. The dry residue was treated with 100 μl of the 4-Brmdmc solution, 100 μl of 18-crown-6 solution and 300 μl of acetone. The test-tube was closed and placed in a water-bath at 80°C for 15 min, then cooled to room temperature. The relative response factors (RRF) of sorbic acid were obtained from separate injections (10 μl) of their derivatized standard solutions at various concentrations [mean RRF = 1.26, relative standard deviation (R.S.D.) = 3.5%]. The calibration graph was obtained by

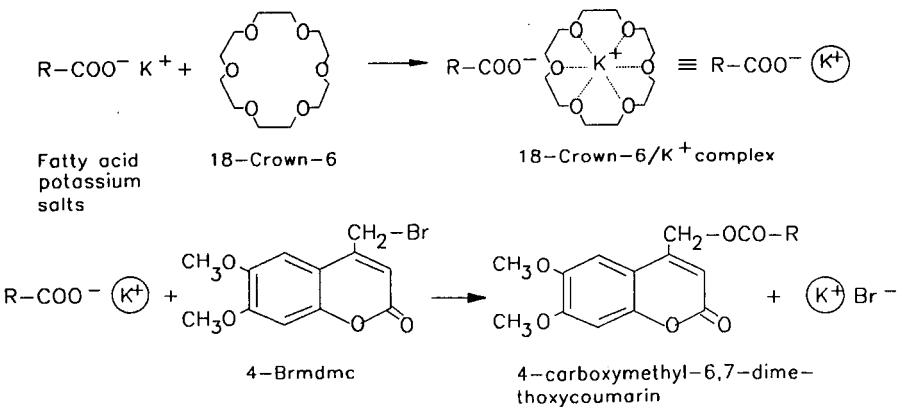

Fig. 1. Derivatization reaction.

plotting the concentration of sorbic acid *versus* the peak-area ratio of sorbic acid to the internal standard. Fig. 2 shows a chromatogram of the derivatized standard solution containing 1 μg/ml of sorbic acid and 1 μg/ml of enanthic acid. The derivatized solutions remain stable for several days if stored in the dark.

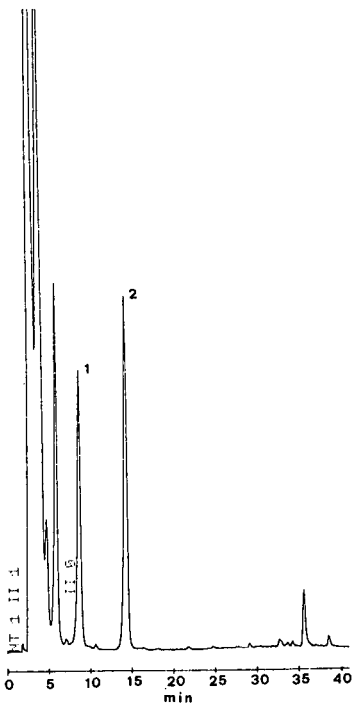

Fig. 2. Standard chromatogram of (1) sorbic and (2) enanthic acid derivatives (10 ng of each). Retention times: (1) 8.23 min; (2) 13.54 min.

Chromatographic conditions

The chromatographic conditions used were as follows: solvent A, water; solvent B, methanol; elution gradient programme, starting composition 30% of A and 70% of B, linear gradient from 70 to 100% of B in 25 min (1.2%/min), isocratic flow of 100% B for 15 min, return of the system to 30% of A and 70% B in 5 min; flow-rate, 1 ml/min; column pressure, initial 152 bar, final 65 bar; column, Spherisorb ODS-2 (5 μm) (250 × 4.6 mm I.D.); fluorimetric detection.

Preparation of samples and standards

A 1-g amount of margarine or butter, 10 ml of 1 *M* sulphuric acid, 10 g of magnesium sulphate heptahydrate and 2 ml of a 100 μg/ml aqueous solution of internal standard were placed in a 250-ml flask. Steam distillation afforded 130 ml, which were collected into a 200-ml volumetric flask containing 0.5 ml of 0.1 *M* hydrochloric acid. The condenser was washed with distilled water and the distillate was diluted to volume and mixed. Aliquots of 1, 2 and 4 ml of 100 μg/ml stock solution of sorbic acid were similarly distilled.

Determination by RP-HPLC

A 50-μl volume of 2 *M* methanolic potassium hydroxide solution were added to 50 ml of the distillates obtained from pure standards and from samples and 0.5-ml aliquots were then derivatized as described for the standard solutions (see *Derivatization and calibration*). A 10-μl volume of each solution was then injected in duplicate into the LC apparatus and the peak-area ratio of sorbic acid to internal standard was integrated on the calibration graph in order to obtain the sorbic acid concentration in samples and in pure standards. Fig. 3 shows typical chromatograms of commercial samples of margarine and butter.

Determination by UV and visible spectrophotometric methods

The distillate was treated according to the AOAC methods [14]. The preparation of the calibration graph and the determination of sorbic acid with the spectrophotometric method was simplified as follows: 2 ml of each solution containing 0, 1, 2 and 3 μg/ml of sorbic acid were pipetted into a 15-ml test-tube, 1 ml of 0.15 *M* sulphuric acid, 1 ml 0.15% potassium dichromate solution and 2 ml of 0.5% TBA solution were added and the tube was placed in a boiling water-bath for exactly 10 min. The solution was then cooled to room temperature and the absorbance was measured at 532 nm against the reagent blank. Fig. 4 shows the calibration graphs obtained plotting absorbance at 260 and 532 nm against sorbic acid concentration; the correlation coefficients were 0.9992 and 0.9995, respectively.

RESULTS AND DISCUSSION

After various trials, the RP-HPLC procedure proposed for the determination of sorbic acid in margarine and butter was adjusted so as to establish the optimum derivatization conditions for the internal standard to be used and to determine the chromatographic parameters that would provide the best separation results and reproducibility.

The concentrations of 4-Brmdmc and 18-crown-6 in the derivatization reaction

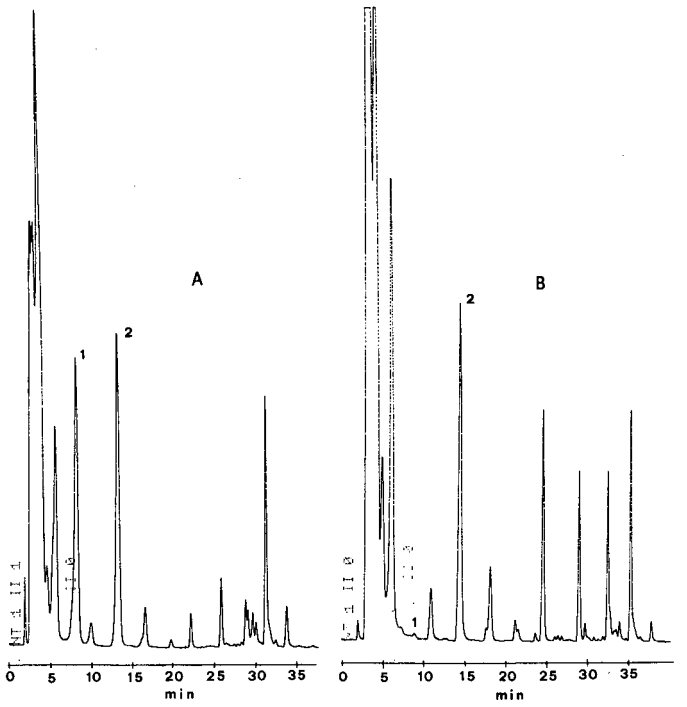

Fig. 3. Typical chromatograms of commercial samples of (A) margarine and (B) butter. Amount of sorbic acid (1) found: in margarine, 12.16 ng; in butter, not detected. Amount of enanthic acid (2) taken: 10 ng in both margarine and butter.

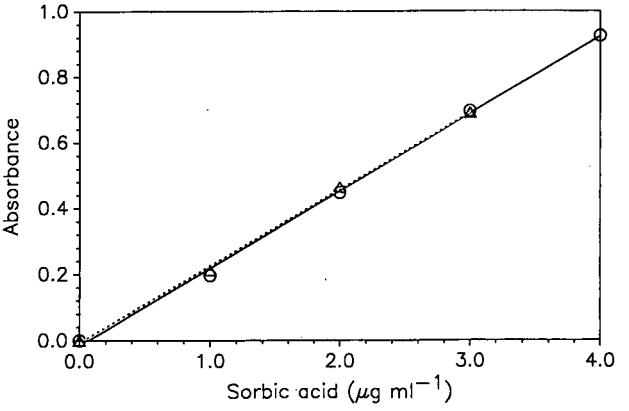

Fig. 4. Calibration graphs for (○) UV (260 nm) and (△) visible (532 nm) spectrophotometric determination of sorbic acid.

were equimolar. When the concentration of the sorbic acid in the sample was 500 mg/kg (the maximum amount permitted by Italian law) and the concentrations of the sorbic acid added and the enanthic acid, used as the internal standard, were 400 and 200 mg/kg, respectively, the concentrations of 4-Brmdmc and 18-crown-6 were ten times greater than the total concentration of sorbic and enanthic acids.

The use of a catalytic amount of 18-crown-6 in the derivatization reaction did not lead to the formation of fluorophores of the acids. Enanthic acid, a C_7 saturated fatty acid, was chosen as the internal standard because it was absent from or present in only trace amounts in the samples. The addition of the internal standard before steam distillation eliminates many causes of error during the separation of the sorbic acid and the subsequent derivatization and does not invalidate determinations which use UV and visible spectrophotometric procedures. The calibration graph obtained by plotting sorbic acid concentrations *versus* the peak-area ratio of sorbic acid to internal standard showed good linearity with a correlation coefficient of 0.9994 and an R.S.D. of 3.5%. The linearity was verified for sorbic acid concentrations up to four times greater than the internal standard concentration (200 mg/kg). This allowed the stringent requirement of employing an internal standard with a concentration similar to that of the peak of interest to be avoided. Therefore, 200 mg/kg of internal standard were added to the sample.

Using water–methanol as eluent, the carboxylic acids showed a considerable increase in retention time which paralleled the increase in the number of carbon atoms; as a consequence, it was necessary to use an elution gradient. As can be seen, the other carboxylic acids were clearly separated and therefore did not cause interference (Fig. 3).

By examining the mean values (bold numbers) in Tables I–III, a comparison can be made between the three different procedures used to determine the sorbic acid contents in the margarine and butter samples. It can be seen that the UV and visible spectrophotometric methods gave considerable differences in the mean values for all the samples examined when compared with RP-HPLC. In butter, the data obtained with UV and visible spectrophotometric procedures (Tables II and III) show average values of 9 and 5 mg/kg of sorbic acid, respectively, although sorbic acid was absent. In order to study this problem, experiments were carried out on pure standard solutions of sorbic acid. These solutions were distilled as described under *Preparation of samples and standards* and analysed by RP-HPLC and UV and visible spectrophotometry. The results obtained showed good agreement between the mean values and standard deviations in the three different methods used (Table IV). The reliability suggests that the real source of the discrepancies mentioned above can be explained by the presence of interfering substances in margarine and butter.

The precision of the methods was assessed by submitting each sample of five runs; in addition, the percentage recovery of sorbic acid was verified by adding different amounts of sorbic acid to three samples of margarine and butter (Tables I–III). The R.S.D. values show reliability regarding the reproducibility of the methods; the R.S.D. values were below 5.6% in each instance except for the values (Tables II and III) for the butter samples without the addition of sorbic acid.

The validity of the procedures is demonstrated by the recovery of sorbic acid from margarine and butter samples spiked with known amounts. The recovery using the proposed procedure ranged from 93.5 to 103.5% and using the UV and visible

TABLE I

RESULTS OF FIVE REPLICATE ANALYSES ON FIVE COMMERCIAL MARGARINE AND BUTTER SAMPLES USING THE PROPOSED RP-HPLC METHOD

For bold values, see text.

Sample No.	Sorbic acid (mg/kg)										
	Added	Margarine					Butter				
		Range	Mean	S.D.	R.S.D. (%)	Recovery (%)	Range	Mean	S.D.	R.S.D. (%)	Recovery (%)
1	0	90.6–101.3	**96.2**	4.6	4.8	–	n.d.[a]	–	–	–	–
	100	193.0–200.5	198.0	2.7	1.4	98.8–103.5	94.5–99.5	96.9	2.1	2.2	94.5–99.5
	200	276.1–297.4	285.3	7.1	2.5	94.8–98.7	193.4–200.2	196.7	2.7	1.4	96.7–100.1
	400	488.0–503.2	498.6	5.5	1.1	99.5–101.8	380.0–394.6	387.7	4.9	1.3	95.0–98.7
2	0	124.4–130.9	**127.8**	2.2	1.7	–	n.d.	–	–	–	–
	100	212.6–233.4	224.7	6.8	3.0	94.7–101.1	93.5–100.1	97.7	2.3	2.4	93.5–100.1
	200	312.1–330.5	321.0	6.9	2.1	96.2–98.7	192.0–201.5	197.2	3.9	2.0	96.0–100.8
	400	510.6–520.5	515.9	3.2	0.6	97.0–98.2	378.5–396.5	387.6	7.0	1.8	94.6–99.1
3	0	226.0–243.2	**233.8**	6.8	2.9	–	n.d.	–	–	–	–
	100	315.6–340.5	326.2	8.7	2.7	96.1–99.4	93.6–98.5	96.4	1.7	1.8	93.6–98.5
	200	422.7–430.5	426.0	3.4	0.8	97.0–99.4	185.0–197.2	190.0	4.0	2.1	92.5–98.6
	400	625.5–644.3	634.6	8.1	1.3	97.7–102.1	385.2–400.1	390.4	5.2	1.3	96.3–100.0
4	0	175.5–195.5	**180.9**	8.7	4.8	–	n.d.	–	–	–	–
5	0	108.2–120.5	**113.2**	5.1	4.5	–	n.d.	–	–	–	–

[a] n.d. = Not detected.

TABLE II

RESULTS OF FIVE REPLICATE ANALYSES ON FIVE COMMERCIAL MARGARINE AND BUTTER SAMPLES USING THE UV SPECTROPHOTOMETRIC METHOD

Sample No.	Sorbic acid (mg/kg)										
	Added	Margarine					Butter				
		Range	Mean	S.D.	R.S.D. (%)	Recovery (%)	Range	Mean	S.D.	R.S.D. (%)	Recovery (%)
1	0	114.0–129.0	**122.0**	5.6	4.6	–	7.8–10.6	**9.1**	1.2	13.2	–
	100	202.0–224.2	214.5	9.8	4.6	93.6–99.8	103.3–112.7	107.3	3.6	3.4	94.2–102.2
	200	297.4–304.2	302.0	2.4	0.8	92.5–95.5	191.6–215.7	203.1	8.5	4.2	92.2–102.4
	400	488.0–516.0	497.9	9.9	2.0	93.5–98.4	376.3–392.5	386.3	6.1	1.6	92.2–95.6
2	0	152.7–166.3	**161.7**	6.4	4.0	–	8.5–10.5	**9.2**	0.7	7.6	–
	100	239.5–264.0	251.6	8.3	3.3	93.2–100.2	102.2–106.0	104.3	1.5	1.4	93.5–97.7
	200	338.8–352.0	347.4	5.4	1.6	92.5–99.8	194.2–215.3	203.7	7.4	3.6	93.1–102.5
	400	530.7–542.5	535.0	4.4	0.8	93.0–97.2	397.0–402.1	391.2	9.4	2.4	92.8–98.0
3	0	234.3–253.1	**245.0**	7.4	3.0	–	7.1–11.5	**8.9**	1.5	16.9	–
	100	338.2–360.3	348.9	8.5	2.4	99.6–102.0	98.8–109.9	104.1	3.5	3.4	93.2–98.6
	200	438.0–459.1	446.7	7.5	1.7	99.0–101.3	192.8–210.0	202.6	6.6	3.3	95.3–100.2
	400	634.4–645.3	638.5	4.0	0.6	97.4–100.3	390.1–410.5	399.4	7.9	2.0	95.8–99.8
4	0	190.2–215.6	**201.7**	9.0	4.5	–	6.8–10.8	**8.6**	1.5	17.4	–
5	0	132.5–145.6	**136.8**	4.5	3.3	–	7.5–10.9	**9.2**	1.3	14.1	–

TABLE III

RESULTS OF FIVE REPLICATE ANALYSES ON FIVE COMMERCIAL MARGARINE AND BUTTER SAMPLES USING THE VISIBLE SPECTROPHOTOMETRIC METHOD

Sample No.	Sorbic acid (mg/kg)										
	Added	Margarine					Butter				
		Range	Mean	S.D.	R.S.D. (%)	Recovery (%)	Range	Mean	S.D.	R.S.D. (%)	Recovery (%)
1	0	114.0–128.2	**119.9**	4.7	3.9	–	0.0–13.0	**5.8**	5.3	91.4	–
	100	197.0–218.4	207.5	6.8	3.3	92.1–95.9	92.9–106.0	101.6	5.4	5.3	92.9–99.6
	200	293.5–312.5	302.8	6.6	2.2	93.5–96.6	185.0–204.0	195.2	6.8	3.5	92.5–98.8
	400	489.6–510.0	497.3	7.5	1.5	94.6–96.7	378.0–396.9	387.3	6.9	1.8	93.9–97.6
2	0	135.1–155.3	**143.5**	7.3	5.1	–	0.0–12.5	**5.1**	4.7	92.2	–
	100	228.8–247.0	236.1	6.3	2.7	94.8–99.4	93.5–110.0	102.6	5.7	5.6	93.5–99.1
	200	324.5–343.5	331.8	6.5	2.0	93.2–98.0	188.2–205.6	196.6	6.3	3.2	94.1–97.1
	400	522.7–540.1	534.3	6.4	1.2	96.8–100.2	375.0–400.0	389.8	9.1	2.3	93.8–98.5
3	0	230.0–247.8	**240.2**	6.2	2.6	–	0.0–10.9	**4.7**	4.2	89.4	–
	100	328.8–346.1	338.6	6.0	1.8	97.1–100.8	93.0–104.2	100.0	4.9	4.9	93.0–99.2
	200	425.3–444.6	436.8	8.3	1.9	97.1–100.5	190.3–207.8	197.5	6.0	3.0	95.2–100.9
	400	620.8–639.4	628.6	6.2	1.0	96.5–99.9	380.3–410.5	397.0	9.8	2.5	95.1–99.9
4	0	181.0–195.5	**187.4**	5.2	2.8	–	0.0–9.8	**5.1**	4.2	82.4	–
5	0	118.5–130.0	**123.7**	4.5	3.6	–	0.0–12.0	**4.4**	4.4	100.0	–

TABLE IV

RESULTS OF FIVE REPLICATE ANALYSES ON THREE PURE STANDARD SOLUTIONS OF SORBIC ACID

Sorbic acid (mg/kg)

Given	RP-HPLC method			UV spectrometric method			Visible spectrophotometric method		
	Found	Mean	S.D.	Found	Mean	S.D.	Found	Mean	S.D.
100	94.7–99.1	97.0	1.7	93.5–98.2	96.3	2.1	93.2–99.1	96.2	2.2
200	190.0–202.5	196.1	5.1	187.5–202.1	195.3	5.3	186.1–199.3	193.7	4.9
400	380.5–399.2	390.8	7.0	375.0–390.9	386.2	7.5	378.5–396.8	388.9	6.9

spectrophotometric methods from 92.2 to 102.5% and from 92.1 to 100.5%, respectively.

The determination of sorbic acid as the 4-Brmdmc derivative by HPLC with fluorescence detection offers some advantages over earlier HPLC determinations with UV detection: fluorescence is a more selective means of detection than absorption and, further, it is far more sensitive, allowing the detection of very low levels of sorbic acid.

The results of the proposed procedure for the determination of sorbic acid in margarine and butter samples, on comparison with those of UV and visible spectrophotometric methods, show that the most accurate data are obtained by steam distillation of the samples followed by RP-HPLC determination with fluorescence detection.

Research is in progress on benzoic acid, another preservative added to foods and beverages to prevent or inhibit microbial growth. Preliminary investigations show that benzoic acid reacts with 4-Brmdmc, under the derivatization conditions described, to produce a fluorescent derivative that can be separated by HPLC.

REFERENCES

1 C. M. Gooding, *U.S. Pat.*, 2 379 294 (1945).
2 Ministerial Decree, March 31, 1965, *Italian Official Journal (G.U.)*, n. 101, April 22, 1965; updated: July 28, 1967; July 10, 1969; August 12, 1969; May 3, 1971; July 30, 1971; March 7, 1980.
3 G. Wilamowski, *J. Assoc. Off. Anal. Chem.*, 54 (1971) 663.
4 A. Caputi, Jr., M. Ueda and B. Trombella, *J. Assoc. Off. Anal. Chem.*, 57 (1974) 951.
5 A. Caputi, Jr. and K. Slinkard, *J. Assoc. Off. Anal. Chem.*, 58 (1975) 133.
6 J. A. W. Gossele, *J. Chromatogr.*, 62 (1971) 429.
7 J. J. Maxstadt and A. B. Karasz, *J. Assoc. Off. Anal. Chem.*, 55 (1972) 7.
8 G. Wilamowski, *J. Assoc. Off. Anal. Chem.*, 57 (1974) 675.
9 U. Leuenberger, R. Gauch and E. Baumgartner, *J. Chromatogr.*, 173 (1979) 343.
10 R. G. Coelho and D. L. Nelson, *J. Assoc. Off. Anal. Chem.*, 66 (1983) 209.
11 M. L. Puttemans, C. Branders, L. Dryon and D. L. Massart, *J. Assoc. Off. Anal. Chem.*, 68 (1985) 80.
12 H. Terada, K. Hisada, Y. Maruyama and Y. Sakabe, *Eisei Kagaku*, 29 (1983) 297.
13 H. Schmidt, *Fresenius' Z. Anal. Chem.*, 178 (1960) 173.
14 *Official Methods of Analysis of the Association of Official Analytical Chemists*, AOAC, Arlington, VA, 14th ed., 1984, Secs. 11075–11078; 11079, 11080; 20115–20118; 20119–20121.
15 G. H. Tjan and J. Th. A. Jansen, *J. Assoc. Off. Anal. Chem.*, 54 (1971) 1150.
16 A. Venturini and G. Angiuli, *Boll. Lab. Chim. Prov.*, 24 (1973) 27.

17 V. M. Rios, *Z. Lebensm.-Unters.-Forsch.*, 147 (1972) 331.
18 B. Mandrou and F. Bressolle. *Ann. Falsif. Expert. Toxicol.*, 72 (1979) 619.
19 B. Mandrou and F. Bressolle, *J. Assoc. Off. Anal. Chem.*, 63 (1980) 675.
20 W. Haensel and R. Stroemmer, *Dtsch. Lebensm.-Rundsch.*, 83 (1987) 315.
21 W. Haensel and R. Stroemmer, *GIT, Suppl.*, No. 3 (1987) 21-2, 25-5.
22 A. Graveland, *J. Assoc. Off. Anal. Chem.*, 55 (1972) 1024.
23 M. Iwaida, Y. Ito, M. Toyoda and T. Kanamori, *Eisei Shikensho Hokoku*, 94 (1976) 62.
24 M. Toyoda, T. Kanamori, Y. Ito and M. Iwaida, *Eisei Kagaku*, 23 (1977) 100.
25 A. E. Stafford and D. R. Black, *J. Agric. Food Chem.*, 26 (1978) 1442.
26 M. A. McCalla, F. G. Mark and W. H. Kipp, *J. Assoc. Off. Anal. Chem.*, 60 (1977) 71.
27 M. C. Bennett and D. R. Petrus, *J. Food Sci.*, 42 (1977) 1220.
28 S. Kubota, *Yamanashi-kenritsu Eisei Kogai Kenkyusho Nempo*, 23 (1980) 39.
29 F. Eisenbeiss, M. Weber and S. Ehlerding, *Chromatographia*, 10 (1977) 262.
30 J. Hild and C. Gertz, *Z. Lebensm.-Unters.-Forsch.*, 170 (1980) 110.
31 A. W. Archer, *Analyst (London)*, 105 (1980) 407.
32 G. L. Park and D. B. Nelson, *J. Food Sci.*, 46 (1981) 1629.
33 C. Gertz and K. Herrmann, *Dtsch. Lebensm.-Rundsch.*, 79 (1983) 331.
34 S. Hyoung Lee, L. Russell Rouseff and F. James Fisher, *J. Food Sci.*, 51 (1986) 568.
35 M. L. Williams, *Food Chem.*, 22 (1986) 235.
36 V. Lap Bui and C. Cooper, *J. Assoc. Off. Anal. Chem.*, 70 (1987) 892.
37 I. Saito, H. Oshima, N. Kawamura, K. Uno and M. Yamada, *J. Assoc. Off. Anal. Chem.*, 70 (1987) 507.
38 R. Farinotti, Ph. Siard, J. Bourson, S. Kirkiacharian, B. Valeur and G. Mahuzier, *J. Chromatogr.*, 269 (1983) 81.

Journal of Chromatography, 543 (1991) 81–103
Elsevier Science Publishers B.V., Amsterdam

CHROM. 23 087

Determination of bovine butterfat triacylglycerols by reversed-phase liquid chromatography and gas chromatography

CLOTAIRE MANIONGUI, JOSEPH GRESTI, MAURICE BUGAUT[a], STEPHANE GAUTHIER and JEAN BEZARD*

Laboratoire de Physiologie Animale et de la Nutrition, Faculté des Sciences Mirande, BP 138, 21004 Dijon cedex (France)

(First received July 23rd, 1990; revised manuscript received December 28th, 1990)

ABSTRACT

Triacylglycerols (TGs) from a sample of summer butterfat (bovine milk) were analysed and fractionated by reversed-phase liquid chromatography (RPLC). Fatty acid and TG compositions of each of the 47 RPLC fractions ranging from 0.1 tot 6.9% were determined by capillary gas chromatography. The data were used together to determine the quantitative composition of the molecular species of TGs. A large number of TG species, accounting for 80% of the total, could be unequivocally identified and individually determined. The combination of the chromatographic methods used proved to be a powerful and accurate approach for the determination of molecular species of TGs in a complex fat, but also a difficult and time-consuming task.

INTRODUCTION

Butterfat from bovine milk represents one of the most complex mixtures of natural triacylglycerols (TGs). The component fatty acids range from C_2 to C_{26}, including even and odd carbon numbers, straight and branched chains, numbers of double bonds from zero to six and *cis* and *trans* isomers. The fourteen even-carbon number, straight-chain fatty acids studied in this work, and commonly reported in a number of publications, comprise a total of 95 mol% [1]. About 40 minor fatty acids at levels ranging from 0.01 to 0.5%, except 15:0 (1.5%), are also present in butterfat [1–5].

Without considering the possible positional isomers of the three acyl chains within the molecular TG species the only $n = 14$ fatty acids distinguished in this present work can yield $(n + 3n + 2n)/6 = 560$ different TGs [6]. In the past, butterfat TGs have been resolved on the basis of carbon number and double bond number by packed [7] and capillary [8–12] gas chromatography (GC) and reversed-phase liquid

[a] Present address: Laboratoire de Biologie Moléculaire et Cellulaire, Faculté des Sciences Mirande, BP 138, 21004 Dijon cedex, France.

0021-9673/91/$03.50

chromatography (RPLC) [13–19] into a wide range of peaks from C_{22} to C_{54}. However, most of the peaks contained several molecular species of TGs when total butterfat TGs were chromatographed, preventing the exact identification and determination of any TG species. A combination of two or more analytical techniques is therefore necessary.

Kalo *et al.* [11] fractionated butterfat TGs on the basis of degree of unsaturation by thin-layer chromatography (TLC) and analysed the fatty acids and TGs of each fraction by GC. However, they were not able to achieve the determination of any TG species. Myher *et al.* [1] combined silver nitrate TLC, capillary GC and mass spectrometry to analyse a volatile molecular distillate of butteroil, containing acetyldiacylglycerols, and obtained the identities and amounts of many major TG species in the TLC fractions. By silver nitrate TLC, TGs are resolved according to chain length, number of double bonds and geometric configuration. As a result, overlapping between several bands is generally observed, and a complete extraction (without oxidation) of all the polyunsaturated TGs from the gel of minor bands is difficult.

An alternative method is the fractionation of total TGs by RPLC and analysis of the fatty acids and TGs of each fraction. Using the data obtained in this way, Weber *et al.* [20,21] could determine the proportions of 116 different molecular TG species in two butterfat samples, but the fatty acid and TG compositions of the RPLC fractions were not published. Barron *et al.* [22] also identified 116 molecular species of TGs in a sample of bovine butterfat by a combination of RPLC analysis of total TGs and GC analysis of fatty acids from each collected RPLC fraction and on the basis of a random TG composition calculated from the molar percentages of eleven main fatty acids present in the total milk fat. They considered *a priori* that the most probable molecular species were those with $>0.1\%$ random values. The way in which they combined experimental and theoretical data seemed to us open to criticism, because it is known that significant differences occur between experimental and random values in natural fats [23–25] and also that butyric acid in bovine butterfat TGs is specifically esterified at the *sn*-3 position [26] and not distributed randomly over the whole glycerol skeleton.

In this study, started before the publication of Weber *et al.*'s work, butterfat TGs were first analysed and fractionated by RPLC and each fraction was analysed for the fatty acid composition. The data were used for the identification and quantitative distribution of TG species, as has been done successfully for a natural long-chain TG mixture, namely peanut oil [27]. However, the fatty acid composition of TGs in most of the RPLC fractions appeared so complex, and the theoretical number of possible TG species so large, that extra data were required. Analysis of TGs by capillary GC was thought to provide sufficient data to determine the composition of the major TG species in butterfat. Some of the results are reported in this paper.

EXPERIMENTAL

Materials

The summer butterfat (bovine milk) was a sample from Union Laitière Normande (Condé-sur-Vire, France). Total lipids were extracted according to Delsal [28]. The pure TG fraction was isolated by silicic acid column chromatography [29] and its purity was checked by thin-layer chromatography. Synthetic TGs in an individual form and quantitative mixtures were obtained from Nu-Chek-Prep (Elysian, MN, U.S.A.).

All the solvents were of pure grade and provided by SDS (Peypin, France), except *n*-butanol, obtained from Aldrich-France (Strasbourg, France).

Reversed-phase liquid chromatography of triacylglycerols

A Model 6000A solvent delivery system and a Model R401 differential refractometer (Waters Assoc., Milford, MA, U.S.A.) were used. The 250 × 4 mm I.D. LiChroCART column packed with LiChrospher 100 RP-18 (4-μm particles), protected by a LiChrosorb RP-18 precolumn, was purchased from Merck (Darmstadt, Germany). The column was maintained at a constant temperature using a thermostat described previously [30], which permitted reproducible analyses.

Analysis and fractionation of butterfat TGs were carried out on samples of 4 mg of TGs dissolved in 40 μl of acetone under isocratic conditions in two steps. In the first step the column and injector were maintained at 40°C, avoiding possible precipitation of saturated long-chain compounds, and the mobile phase was acetone–acetonitrile (55:45, v/v) at 1 ml min^{-1}. The chromatographic profile showed 47 peaks but the first 27 peaks were poorly separated. The first 27 RPLC fractions were collected together and the next 20 RPLC fractions were collected individually at the outlet of the detector. In the second step, the first 27 RPLC fractions collected together were analysed at 30°C using acetone–acetonitrile (50:50, v/v) at 1 ml min^{-1} and individually collected. The fractionation of butterfat TGs was repeated five times and the RPLC fractions collected were added. Each of the 47 collected RPLC fractions was purified by rechromatography under its own elution conditions to eliminate the contaminating adjacent RPLC fractions (essentially the preceding major peaks). The purified TG fractions were divided into two parts for GC of fatty acid butyl esters and TGs. During RPLC analyses of butterfat TGs, peak areas were measured by means of an ENICA 21 (Delsi, France) integrator–calculator.

Mixtures of standard saturated simple TGs were analysed under the same conditions to determine the theoretical partition number of the butterfat TGs in some RPLC fractions. The partition number (*PN*) of a TG is calculated from the total carbon number (*CN*) and total double-bond number (*DB*) of the three constituent acyl moieties using the equation $PN = CN - 2DB$, according to Litchfield [31].

Gas chromatography of fatty acids

Fatty acid methyl esters were prepared by instantaneous reaction by adding 0.1 ml of 0.5 *M* sodium methoxide to a 7-ml tube containing *ca.* 1 mg of a TG mixture dissolved in 1.8 ml of hexane at room temperature [3,32,33]. After centrifugation, the upper hexane phase containing methyl esters was not evaporated before injection so as to avoid any loss of short-chain fatty acids.

Fatty acid butyl esters were prepared in a 3-ml tube with a Teflon-lined screw-cap by heating *ca.* 1 mg of a TG mixture in the presence of 0.2 ml of acidic (2%, w/w, sulphuric acid) *n*-butanol at 100°C for 2.5 h. To the chilled mixture were added 1 ml of 5% (w/w) potassium carbonate in water and 1 ml of hexane and the tube was vigorously shaken. The clear butanol–hexane upper phase containing butyl esters was ready for injection. When the amounts of the collected RPLC fractions of butterfat TGs were less than 0.1 mg, butylation was carried out in 0.3-ml reaction vials (Reacti-Vials, Pierce, Rotterdam, The Netherlands) in the presence of 10-μl of acidic *n*-butanol at 80°C for 2 h. Then 30 μl of aqueous potassium carbonate and 90 μl of hexane were added to the chilled mixture. The clear upper phase was injected directly.

Methyl or butyl esters were analysed using a Packard Model 438A chromatograph including a cold on-column injector, a 30 m × 0.32 mm I.D. fused-silica column coated with Carbowax 20M (AML Chromato, Limoges, France) and a flame ionization detector maintained at 240°C. The carrier gas was hydrogen at a flow-rate of 1 ml min^{-1}. When methyl esters were analysed the oven temperature was programmed as follows: 35°C for 1.5 min after injection, then increased to 155°C at 30°C min^{-1} and finally to 220°C at 4°C min^{-1}. When butyl esters were injected, the temperature was initially maintained at 35°C for 4.5 min instead of 1.5 min. Approximately 0.4 μl of fatty acid ester solution (0.5–1 $\mu g\ \mu l^{-1}$ of total esters) was injected. Peak areas were measured by means of a Shimadzu C-R3A integrator–calculator.

In preliminary experiments, methyl and butyl esters of a wide range of fatty acids (saturated and unsaturated, even fatty acids from C_4 to C_{18}) were prepared from a quantitative mixture of synthetic simple TGs approximating the composition of butterfat TGs. Methyl and butyl esters were used for comparison in the determination of fatty acids by GC and for the determination of calibration factors (Table I).

The possible loss of short-chain compounds during the preparation of butter fatty acid esters, especially methyl esters, was thoroughly examined. First, the response factors determined for methyl esters were found to vary little, from 1.15 (8:0) to 0.93 (unsaturated long chains), except for 6:0 (1.34) and 4:0 (1.67). When standard quantitative mixtures of methyl esters (Nu-Chek-Prep) were injected directly into the chromatograph, the calibration factors (results not shown) were not different from those obtained for the methyl esters prepared from the mixture of simple TGs. This

TABLE I

MOLAR RESPONSE FACTORS[a] FOR ACID METHYL AND BUTYL ESTERS DETERMINED FROM A STANDARD TG MIXTURE AND COMPOSITION (mol%)[a] OF MAJOR FATTY ACIDS OF TOTAL BUTTERFAT TGs ANALYSED AS BUTYL ESTERS

Fatty acid	Response factor		Total butterfat TGs
	Methyl esters	Butyl esters	
4:0	1.669 ± 0.018	1.116 ± 0.010	9.61 ± 0.05
6:0	1.341 ± 0.017	1.155 ± 0.018	4.85 ± 0.04
8:0	1.147 ± 0.013	1.061 ± 0.012	2.17 ± 0.01
10:0	1.052 ± 0.011	1.031 ± 0.005	3.87 ± 0.01
12:0	0.998 ± 0.004	0.994 ± 0.003	3.71 ± 0.01
14:0	0.973 ± 0.006	0.984 ± 0.003	11.37 ± 0.02
14:1	0.985 ± 0.004	1.007 ± 0.004	1.08 ± 0.01
16:0	0.952 ± 0.008	0.969 ± 0.004	24.78 ± 0.03
16:1	0.966 ± 0.002	0.996 ± 0.002	1.51 ± 0.02
18:0	0.988 ± 0.011	1.028 ± 0.007	11.36 ± 0.02
18:1	0.929 ± 0.008	0.960 ± 0.006	23.02 ± 0.03
18:2	0.919 ± 0.007	0.949 ± 0.002	1.70 ± 0.04
18:3	0.942 ± 0.015	0.970 ± 0.010	0.83 ± 0.01
20:0	1.015 ± 0.014	1.050 ± 0.012	0.14 ± 0.01

[a] The values are means ± standard errors of the means (S.E.M.) of six GC analyses.

demonstrated the absence of losses of short-chain compounds during the preparation of methyl esters. The correction factors for short-chain fatty acid butyl esters determined from the known mixture of TGs were lower than those of the corresponding methyl esters (Table I) because of the large differences in molecular weights. When methyl and butyl esters were prepared from the same sample of butterfat TGs and analysed by GC, and when the appropriate response factors were applied, the same quantitative results were obtained. However, butyl esters were preferred to methyl esters for the following reasons. A loss of short-chain methyl esters was still possible for the smallest butterfat RPLC fractions. Moreover, the determination of short-chain methyl esters was less accurate than that of the corresponding butyl esters because of the higher response factors and the varying amounts of an impurity with a retention time very close to that of butyric acid methyl ester (shouldering). This impurity could not be entirely removed by distillation of methanol and the other solvents.

The composition of fatty acid butyl esters of each RPLC fraction was determined more accurately by subtracting a blank obtained under the same experimental conditions.

Gas chromatography of triacylglycerols

TGs of the butterfat RPLC fractions and standard mixtures (Nu-Chek-Prep) were analysed by GC using a Packard Model 419 chromatograph equipped with a Ros injector maintained at 330°C, a laboratory-made 10 m × 0.3 mm I.D. glass capillary column coated with SE-30 silicone phase and a flame ionization detector at 330°C. The chromatograph was connected to an ENICA 21 integrator–calculator. The column temperature was programmed from 200 to 300°C at 6°C min^{-1}. The carrier gas was hydrogen at a flow-rate of 3 ml min^{-1}.

RESULTS AND DISCUSSION

RPLC resolution of butterfat triacylglycerols

Among animal fats, bovine butterfat shows one of the broadest TG and fatty acid spectra. Gaining good resolution of a wide range of TG species in an RPLC run under isocratic conditions is a particularly difficult task. One possibility is the use of a temperature programme for the column and Fig. 1 shows a chromatogram obtained when temperature was programmed from 10 to 55°C at 1°C min^{-1}. More than 50 peaks were eluted within 70 min but some were only partially separated. Such an RPLC analysis of butterfat TGs using temperature programming was also reported by Weber *et al.* [20] under similar conditions. However, the chromatographic profile obtained in this work does not resemble theirs.

Fig. 2 gives the chromatograms obtained during the two-step RPLC resolution of the same sample of butterfat TGs without temperature programming under slightly different conditions. The first 27 peaks, which were not sufficiently separated in the first step at 40°C (Fig. 2A) were collected together and rerun at 30°C (Fig. 2B). The elution pattern of the 47 peaks is very similar to that obtained by Weber *et al.* [20] with temperature programming and by other workers [14,17,19] at constant temperature. The RPLC profile of butterfat TGs is generally characterized by a series of four-peak groups (quartets), such as the groups 28–31, 32–35, 36–39, 40–43 and 44–47 in Fig. 2A.

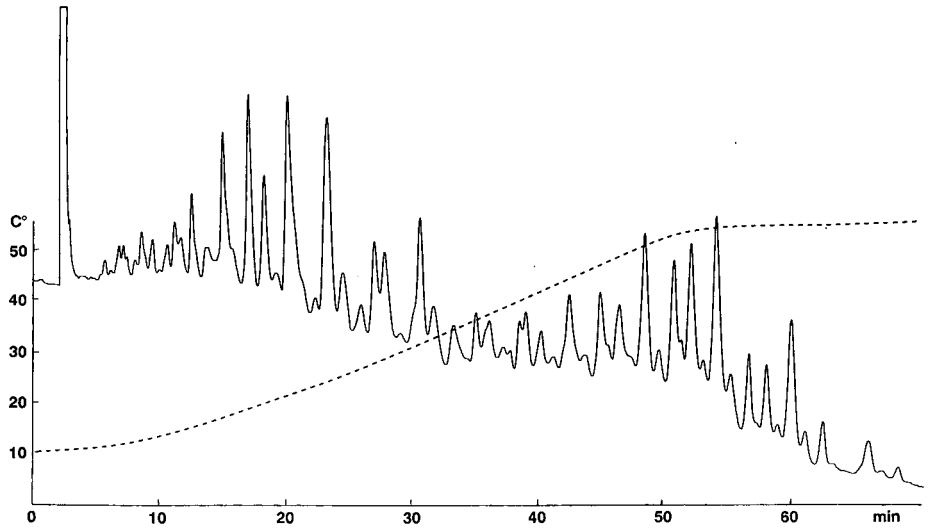

Fig. 1. RPLC profile of total butterfat TGs using temperature programming. RPLC conditions: column, 250 × 4 mm I.D. LiChrospher 100 RP-18 (Merck); eluent, acetone–acetonitrile (50:50, v/v) at 1 ml min^{-1}; column temperature, programmed (– – – –) at 1°C min^{-1} from 10 to 55°C; injection, 4 mg of TGs in 40 μl of acetone.

Butterfat TGs have also been eluted with a solvent gradient and then detected by means of either a light-scattering detector [13,15,16], or a UV detector at 220 nm [22], or a flame ionization detector [34]. However, the chromatographic profile characterized by quartets was not always found under such RPLC conditions [13,15,16, 18,22].

Although TGs seemed to be less well resolved at constant temperature (Fig. 2) than using a temperature programme (Fig. 1), the two-step procedure was preferred in this study for the following reasons. The present results can be easily compared with those of other authors [14,17, 19–21] who obtained a similar RPLC profile of butterfat TGs. Further, when a run was started at low temperature (10°C), the risk of making long-chain saturated TGs insoluble could not be entirely ruled out.

A mixture of standard simple TGs made up of saturated or unsaturated even-carbon number fatty acids (C_{24} to C_{56}) was injected along with total butterfat TGs and their retention times were determined. As expected, the caption in Fig. 2 indicates that the standard saturated TGs were resolved on the basis of their increasing total carbon number and eluted later than the corresponding unsaturated TGs, according to the general rules of RPLC resolution of TGs [35,36]. Further, TGs were partially resolved on the basis of the chain length of each of the three constituent acyl moieties. Fig. 3 clearly shows that TGs containing one or two butyric acids were eluted later than long-chain TGs. In contrast, the two TGs 12:0, 12:0, 16:0 and 12:0, 14:0, 14:0 having the same carbon number ($CN=40$) and double bond number ($DB=0$) were not resolved under our chromatographic conditions.

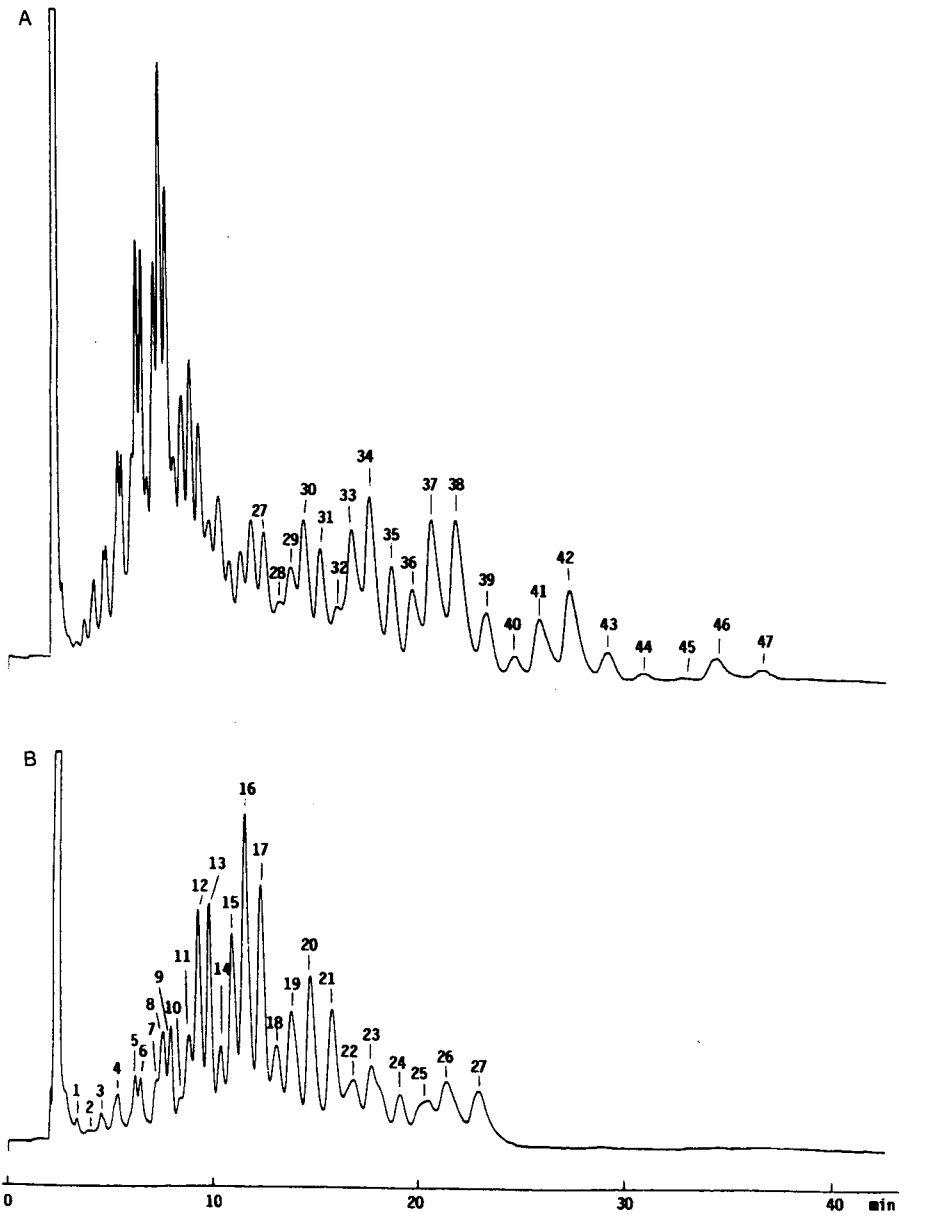

Fig. 2. Two-step RPLC analysis of butterfat TGs: (A) analysis at 40°C using acetone–acetonitrile (55:45, v/v); (B) analysis at 30°C of the first 27 peaks collected in (A) using acetone–acetonitrile (50:50, v/v). Other conditions as in Fig. 1. The retention time of trioctanoylglycerol was identical with that of peak 2. Such an identity of retention times was also observed for the following TGs and RPLC peaks: tridecanoylglycerol (peak 5), trilinolenoylglycerol (peak 12), trilauroylglycerol (peak 15), trilinoleoylgycerol (peak 23), tripalmitoleoylglycerol (peak 24), trimyristoylglycerol (peak 27), trioleoylglycerol (peak 36), tripalmitoylglycerol (peak 39).

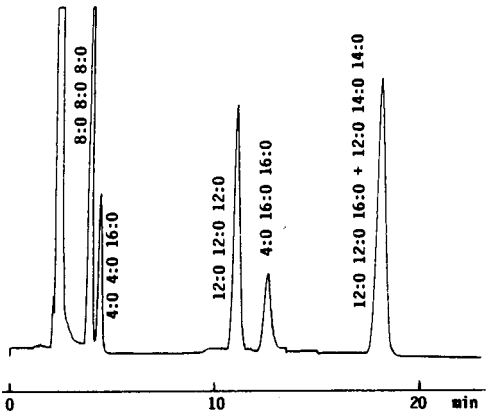

Fig. 3. RPLC analysis of a mixture of standard saturated TGs. RPLC conditions as in Fig. 2B. The retention times of 8:0 8:0 8:0 + 4:0 4:0 16:0, 12:0 12:0 12:0, 4:0 16:0 16:0 and 12:0 12:0 16:0 + 12:0 14:0 14:0 correspond to those of peaks 2, 15, 17 and 23 in Fig. 2B, respectively.

RPLC determination of butterfat triacylglycerols

The measurement of peak areas and the calculation of the relative proportions of peaks were performed automatically during the two analysis steps. The results given in Table I were established on the basis of peak 27 common to both chromatograms. Because of the complexity of the TG mixture in each RPLC fraction, it was not possible to determine useful response factors using standard simple TGs and assuming that the response factors of the constituent fatty acids are additive, as proposed by Goiffon *et al.* [37]. The molar percentage of a peak was therefore calculated directly from the peak area and the average molecular weight of TGs in the peak, calculated from $MW = 134 + 14CN - 2DB$. The average number of double bonds of TGs was calculated from the fatty acid composition of the RPLC fraction concerned (see Table II). The average carbon number of TGs was calculated not from the fatty acid composition but from the TG composition of the RPLC fraction (see Table III). The CN data in Table III were more accurate than those in Table II because they were calculated from all the TGs, *i.e.*, even- and odd-carbon number TGs, whereas in Table II only the distribution of the listed even-carbon number fatty acids was used for calculation.

As most of the RPLC peaks were not completely separated (no return to the baseline), the reproducibility of peak-area measurements was checked. The relative standard deviation ranged from 1.7 to 13.6% (5.6% on average) when considering the peaks $\geqslant 1\%$.

Tabel I shows that only two peaks represented slightly more than 5%, namely peaks 16 (6.9%) and 17 (5.6%). The percentages of most of the peaks (34 peaks) ranged from 1.0 to 5.0% and amounted to 80% of the total. Our results are similar to those of Weber *et al.* [20,21], although the bovine butterfat samples studied were different. In the butterfat there is, therefore, no really major TG species that could be made up of three major fatty acids, such as butyric, palmitic and oleic acids. In other words, the numerous short- and long-chain fatty acids in butterfat are largely interesterified.

TABLE II

QUANTITATIVE DISTRIBUTION[a] OF 47 FRACTIONS OF BUTTERFAT TRIACYLGLYCEROLS OBTAINED BY RPLC AND FATTY ACID COMPOSITIONS (mol %) OF THE RPLC FRACTIONS ANALYSED BY GC

Fatty acids[b]	RPLC fraction No. and mol %												
	1	2	3	4	5	6	7	8	9	10	11	12	13
	0.13 ±0.02	0.11 ±0.01	0.46 ±0.03	1.13 ±0.03	1.02 ±0.03	1.05 ±0.03	0.90 ±0.02	1.64 ±0.04	1.71 ±0.04	0.67 ±0.03	1.65 ±0.04	4.15 ±0.10	3.97 ±0.10
4:0	22.5	24.7	26.0	23.6	16.7	25.1	15.1	24.0	27.6	12.6	15.2	25.0	27.7
6:0	5.9	13.4	16.5	11.3	14.5	4.4	12.9	9.5	1.5	9.6	11.7	7.5	1.0
8:0	2.9	7.6	9.9	12.5	7.3	4.3	7.2	3.1	0.6	5.0	4.3	1.2	0.2
10:0	3.7	5.9	9.8	12.2	14.2	17.0	14.7	6.1	3.5	8.1	7.6	1.6	0.4
12:0	3.3	8.6	7.9	5.5	6.1	9.6	9.3	13.0	15.8	7.7	7.8	3.6	3.1
14:0	16.0	10.0	9.2	10.9	9.5	10.5	8.6	9.7	21.4	17.5	11.1	19.8	28.7
14:1	1.2	1.0	1.0	1.1	2.1	1.3	4.0	3.4	1.5	4.0	2.5	0.6	0.4
16:0	21.3	9.5	7.6	8.6	6.3	16.8	6.2	9.5	18.9	10.6	6.4	12.9	27.3
16:1	2.1	1.6	0.7	0.9	1.7	0.6	2.7	1.9	1.0	3.1	4.3	3.4	1.4
18:0	2.7	2.7	0.8	2.1	3.1	4.1	1.6	1.0	3.9	2.3	0.4	1.8	3.5
18:1	13.5	10.9	8.6	8.8	13.0	4.3	10.2	12.6	2.9	11.4	19.0	19.2	5.7
18:2	3.5	1.8	1.0	1.1	2.4	0.6	3.2	2.5	0.4	3.7	7.2	3.4	0.4
18:3	1.4	2.3	1.0	1.4	3.1	1.3	4.3	3.5	1.0	4.2	2.3	–	0.2
20:0	–	–	–	–	–	0.1	–	0.2	–	0.2	0.2	–	–
CN[c]	36.60	31.57	28.67	30.34	32.20	32.32	33.61	33.52	34.06	37.14	36.62	35.98	36.08
DB[d]	0.84	0.72	0.46	0.52	0.83	0.34	1.09	1.00	0.28	1.16	1.41	0.90	0.27
PN[e]	34.92	30.13	27.73	29.30	30.54	31.64	31.43	31.52	33.50	34.82	33.80	34.18	35.54
	14	15	16	17	18	19	20	21	22	23	24	25	26
	1.54 ±0.02	4.11 ±0.06	6.86 ±0.17	5.61 ±0.16	2.31 ±0.11	3.65 ±0.06	4.05 ±0.04	3.42 ±0.06	2.10 ±0.04	3.01 ±0.03	1.42 ±0.09	1.87 ±0.13	2.71 ±0.14
4:0	17.0	15.3	21.5	30.2	8.3	3.1	9.7	20.0	2.7	0.2	–	9.5	0.8
6:0	9.0	11.9	7.9	1.9	12.6	18.6	15.8	2.2	1.9	6.0	22.8	1.2	0.3
8:0	4.4	3.2	0.6	0.6	6.2	5.5	1.1	2.5	9.3	8.3	2.2	1.0	2.3
10:0	6.3	4.9	0.4	0.8	6.5	5.5	0.7	2.7	13.7	11.7	4.4	11.9	16.5
12:0	4.6	3.8	1.0	0.6	4.1	3.9	0.5	1.6	5.2	5.7	1.8	4.3	2.8
14:0	11.3	12.3	7.5	8.2	7.7	9.2	5.6	1.8	12.7	15.6	3.2	7.9	13.1
14:1	0.7	0.6	–	0.4	1.4	0.2	0.2	1.1	2.3	–	1.6	3.8	3.9
16:0	17.4	10.6	28.2	42.3	15.4	27.0	28.8	28.2	18.1	27.5	27.3	7.1	22.6
16:1	3.3	1.7	1.0	0.4	1.7	0.9	0.2	0.9	2.1	–	0.9	2.1	2.1

(Continued on p. 90)

TABLE II (*continued*)

Fatty acids[b]	RPLC fraction No. and mol %												
	14	15	16	17	18	19	20	21	22	23	24	25	26
	1.54 ±0.02	4.11 ±0.06	6.86 ±0.17	5.61 ±0.16	2.31 ±0.11	3.65 ±0.06	4.05 ±0.04	3.42 ±0.06	2.10 ±0.04	3.01 ±0.03	1.42 ±0.09	1.87 ±0.13	2.71 ±0.14
18:0	1.9	1.1	2.9	8.0	4.8	4.8	20.4	27.4	6.3	14.0	27.7	18.8	6.9
18:1	18.6	32.6	28.4	5.8	28.8	20.6	15.9	9.7	23.2	11.0	6.0	25.6	25.9
18:2	4.0	1.5	0.6	0.6	1.4	0.7	0.5	1.1	1.4	–	1.2	4.0	1.5
18:3	1.3	0.4	–	0.2	1.1	–	0.2	0.7	0.9	–	0.9	2.6	1.3
20:0	0.2	0.1	–	–	–	–	0.4	0.1	0.2	–	–	0.2	–
CN[c]	37.19	38.13	39.02	36.56	39.70	39.53	41.24	41.03	42.17	41.91	41.48	43.70	44.88
DB[d]	1.04	1.17	0.88	0.25	1.14	0.69	0.54	0.48	0.99	0.33	0.41	1.42	1.16
PN[e]	35.11	35.79	37.26	36.06	37.42	38.15	40.16	40.07	40.19	41.25	40.66	40.86	42.56
	27	28	29	30	31	32	33	34	35	36	37	38	39
	2.59 ±0.18	0.93 ±0.07	1.85 ±0.02	2.92 ±0.02	2.18 ±0.03	0.74 ±0.01	3.41 ±0.05	4.01 ±0.06	2.08 ±0.02	1.79 ±0.05	3.97 ±0.03	4.24 ±0.03	1.51 ±0.02
4:0	–	–	–	–	–	–	–	–	–	–	–	–	–
6:0	–	3.8	1.5	–	–	–	–	–	–	–	–	–	–
8:0	2.3	4.3	–	–	0.4	–	–	–	–	–	–	–	–
10:0	17.9	5.3	1.8	4.1	7.0	2.4	–	–	1.5	–	–	–	–
12:0	11.0	4.8	8.7	10.9	10.8	3.5	–	3.1	5.6	–	–	–	–
14:0	17.6	7.6	12.8	19.0	21.2	10.7	15.9	22.3	23.0	5.4	1.6	9.4	17.3
14:1	0.7	3.8	5.5	3.8	–	–	–	1.1	–	1.5	–	–	–
16:0	34.8	15.8	15.8	23.1	32.7	15.4	17.5	29.6	37.9	14.2	28.0	38.1	41.4
16:1	0.7	3.0	3.9	2.6	0.1	6.0	4.9	2.6	–	–	1.6	1.3	–
18:0	8.9	16.9	5.7	7.1	13.0	8.3	4.9	7.9	14.3	5.8	7.0	16.4	26.9
18:1	5.4	24.0	33.0	24.9	11.5	39.5	46.9	30.3	17.7	69.8	58.4	34.8	14.4
18:2	0.5	7.1	7.4	3.0	3.0	11.0	6.7	3.1	–	3.3	3.4	–	–
18:3	0.2	3.3	3.9	1.5	0.3	3.2	3.2	–	–	–	–	–	–
20:0	–	0.3	–		–	–	–	–	–	–	–	–	–
CN[c]	42.71	46.72	48.01	46.00	46.37	50.22	50.75	48.70	47.60	52.32	52.03	50.54	49.44
DB[d]	0.25	1.65	2.07	1.25	0.56	2.31	2.24	1.21	0.53	2.34	2.00	1.06	0.43
PN[e]	42.21	43.42	43.87	43.50	45.25	45.60	46.27	46.28	46.54	47.64	48.03	48.42	48.58

	40 0.34 ±0.01	41 1.44 ±0.02	42 2.29 ±0.08	43 0.63 ±0.06	44 0.19 ±0.02	45 0.14 ±0.02	46 0.88 ±0.05	47 0.47 ±0.04	Total TGs[f]
4:0	–	–	–	–	–	–	–	–	10.07
6:0	–	–	–	–	–	–	–	–	4.93
8:0	–	–	–	–	–	–	–	–	2.02
10:0	–	–	–	–	–	–	–	–	4.16
12:0	–	–	–	–	–	–	–	–	3.71
14:0	4.9	0.8	0.6	9.2	–	4.7	–		11.72
14:1	–	–	–	–	–	–	–	–	1.05
16:0	32.7	5.4	32.0	40.4	23.6	22.2	3.1	34.3	24.05
16:1	–	–	0.6	–	–	–	–	–	1.52
18:0	31.6	34.5	34.6	42.9	57.8	42.3	63.6	49.7	10.66
18:1	30.8	57.6	32.2	7.0	18.6	24.7	32.7	12.8	23.33
18:2	–	1.7	–	–	–	–	–	–	1.93
18:3	–	–	–	–	–	–	–	–	0.77
20:0	–	–	–	0.5	–	6.1	0.6	3.2	0.08
CN[c]	51.45	53.26	51.97	50.50	52.58	82.47	53.79	52.13	43.87
DB[d]	0.92	1.83	0.98	0.21	0.56	0.74	0.98	0.38	0.96
PN[e]	49.61	49.60	50.01	50.08	51.46	50.99	51.83	51.37	41.95

[a] The values (mol%) are the means ± S.E.M. of five RPLC analyses. Two minor fractions (48, 0.10% and 51, 0.05%) were eluted later than fraction 47, but their acid composition was not determined.

[b] Isomers *n*-7 and *n*-9 were added for 16:1 and 18:1. 18:2 included 18:2 *n*-6 and 18:2 conjugated. 18:3 was the isomer 18:3 *n*-3.

[c] *CN* = average total acyl carbon number of TGs calculated from the constituent fatty acids.

[d] *DB* = average total number of double bonds of TGs calculated from the fatty acid compositions.

[e] *PN* = partition number of TGs ($PN = CN - 2DB$).

[f] The values (mol%) are calculated from the proportions of the RPLC fractions in total butter TGs and the fatty acid compositions of the RPLC fractions.

TABLE III

TG COMPOSITIONS (mol %) OF 46 BUTTERFAT FRACTIONS OBTAINED BY RPLC AND ANALYSED BY CAPILLARY GC

Carbon number	RPLC fraction No.												
	2	3	4	5	6	7	8	9	10	11	12	13	14
24	62.4	1.4	–	–	–	–	–	–	–	–	–	–	–
26	27.9	58.7	2.1	–	–	–	–	–	–	–	–	–	–
27	–	–	2.1	–	–	–	–	–	–	–	–	–	–
28	6.4	32.6	54.8	3.5	–	–	–	–	–	–	–	–	–
29	–	–	1.6	5.3	–	–	–	–	–	–	–	–	–
30	3.3	4.0	28.5	24.6	75.2	3.7	–	–	–	–	–	–	
31	–	–	–	–	3.2	11.7	–	–	–	–	–	–	
32	–	3.3	7.4	43.4	16.5	11.3	23.1	75.6	10.9	–	–	–	–
33	–	–	–	–	1.4	3.2	–	1.2	32.3	12.1	1.0	–	–
34	–	–	2.5	11.5	0.8	29.9	43.5	15.5	1.4	10.5	19.4	71.5	6.5
35	–	–	–	–	–	–	–	1.0	13.3	3.4	–	2.3	31.1
36	–	–	0.6	8.4	1.5	15.1	18.0	1.9	9.4	28.2	54.5	14.1	0.8
37	–	–	–	–	–	0.9	–	1.3	4.9	1.6	–	6.4	23.1
38	–	–	0.2	1.8	0.8	9.1	9.4	1.8	12.4	18.5	18.9	2.7	13.2
39	–	–	–	–	–	–	–	0.5	–	–	–	2.2	2.0
40	–	–	0.2	1.5	0.5	13.4	5.7	0.2	6.4	22.7	5.9	0.3	11.4
42	–	–	–	–	0.1	1.5	0.3	1.0	8.4	2.7	0.1	0.2	11.0
44	–	–	–	–	–	0.2	–	–	0.6	0.3	0.2	0.3	0.9
CN[a]	25.01	26.98	29.06	32.00	30.65	34.88	34.64	32.75	35.52	36.87	36.22	34.78	37.30
PN[b]	23.57	26.06	28.02	30.34	29.97	32.70	32.64	32.19	33.20	34.07	34.42	34.24	35.22

	15	16	17	18	19	20	21	22	23	24	25	26	27
35	11.6	1.1	–	–	–	–	–	–	–	–	–	–	–
36	11.9	22.2	71.2	3.4	–	–	–	–	–	–	–	–	–
37	3.1	0.4	3.3	29.0	8.6	–	–	–	–	–	–	–	–
38	30.1	62.7	11.6	0.8	24.9	52.9	67.7	2.9	–	–	–	–	–
39	–	1.0	6.1	8.0	0.9	1.9	6.4	11.1	2.8	0.6	–	–	–
40	40.6	10.8	0.6	25.6	57.7	39.4	6.3	1.6	54.9	78.5	28.6	1.9	–
41	–	1.7	0.5	–	–	4.8	3.5	1.3	0.6	4.6	14.6	2.2	1.1
42	2.7	0.1	4.7	31.0	7.9	–	–	60.4	38.3	1.8	–	2.1	81.1
43	–	–	–	–	–	1.0	–	–	–	10.9	4.6	–	–
44	–	–	1.5	2.2	–	–	10.5	18.8	1.8	–	–	75.3	10.6
45	–	–	–	–	–	–	–	–	1.4	0.9	–	–	4.7
46	–	–	0.5	–	–	–	4.6	3.7	–	–	40.7	14.8	0.5
47	–	–	–	–	–	–	–	–	0.2	–	–	–	2.0
48	–	–	–	–	–	–	1.0	0.2	–	1.3	7.6	3.7	–
50	–	–	–	–	–	–	–	–	–	0.7	3.9	–	–
52	–	–	–	–	–	–	–	–	–	0.7	–	–	–
CN[a]	38.30	37.80	36.81	39.61	39.39	39.00	39.53	42.04	40.86	40.79	43.72	44.26	42.46
PN[b]	35.96	36.04	36.30	37.33	38.01	37.92	38.57	40.06	40.20	39.97	40.88	41.94	41.96

(Continued on p. 94)

TABLE III (*continued*)

Carbon number	RPLC fraction No.												
	28	29	30	31	32	33	34	35	36	37	38	39	40
42	49.2	3.6	–	–	–	–	–	–	–	–	–	–	–
43	–	11.1	1.4	1.7	–	–	–	–	–	–	–	–	–
44	1.8	–	1.8	65.8	16.2	0.7	–	–	–	–	–	–	–
45	15.3	4.3	0.7	–	20.2	7.4	0.6	–	–	–	–	–	–
46	–	2.5	67.8	10.4	–	–	1.4	67.4	2.4	–	–	–	–
47	2.3	–	–	8.1	26.2	5.9	0.6	–	13.3	4.5	1.3	2.9	–
48	–	41.4	22.9	2.3	–	–	68.5	6.9	1.0	–	–	66.4	1.7
49	0.5	–	–	5.4	8.2	0.3	–	14.4	23.9	2.2	1.0	–	32.5
50	17.0	24.0	5.4	–	–	51.4	24.5	–	–	2.3	79.9	6.9	4.0
51	–	–	–	1.2	–	–	–	11.3	4.5	–	–	16.0	58.8
52	6.3	10.4	–	–	13.8	28.3	4.4	–	–	76.4	17.5	0.6	–
53	–	–	–	–	–	–	–	–	–	–	–	–	3.0
54	7.6	2.7	–	5.1	15.4	6.0	–	–	54.9	14.6	0.3	7.2	–
CN[a]	45.55	48.11	46.59	45.39	47.90	50.21	48.61	47.14	51.49	51.96	50.31	49.05	50.32
PN[b]	42.25	43.97	44.09	44.27	43.28	45.73	46.20	46.08	46.81	47.96	48.19	48.22	48.48

	41	42	43	44	45	46	47
48	1.2	–	–	–	–	–	–
49	7.5	–	8.4	–	–	–	–
50	–	1.0	76.7	2.5	11.2	0.6	–
51	2.3	3.3	–	41.3	72.8	–	–
52	2.6	91.9	12.8	4.2	–	1.7	95.8
53	2.3	–	–	49.9	7.9	5.1	–
54	84.1	3.8	2.1	2.1	8.1	92.6	4.2
CN[a]	53.41	52.02	50.26	52.08	51.29	53.89	52.08
PN[b]	49.75	50.06	49.84	50.96	49.81	51.93	51.32

[a] *CN* = average total acyl carbon number of TGs calculated from the constituent TGs.
[b] *PN* = Partition number of TGs calculated from CN (data in this table) and from *DB* determined from the constituent fatty acids (Table II).

Fatty acid compositions of RPLC fractions

Table I shows that butterfat contained a high proportion of short- and long-chain fatty acids, mainly butyric (10%), myristic (12%), palmitic (24%), stearic (10%) and oleic (23%) acids, in agreement with the data generally published. In addition to the even-carbon number saturated and unsaturated long-chain fatty acids and the saturated short-chain fatty acids listed in Table I, minor amounts of odd-carbon number saturated and monounsaturated acids and branched-chain acids were also seen but not reported here. In the whole butterfat TGs, odd-carbon fatty acids totalled 4.5%, and even-carbon number branched acids and monounsaturated medium acyl chains reached 0.5%. These percentages are not different from those reported elsewhere [1].

Butterfat TGs were fractionated by RPLC, and TGs of each RPLC fraction were purified by RPLC and analysed as butyl esters. Table II gives the fatty acid compositions determined for TGs of 47 RPLC fractions. As could be expected, the short-chain fatty acids were mainly found in the RPLC fractions eluted first (Fig. 2B), for example 4:0 in fractions 1–25 and 6:0 and 8:0 in fractions 1–28. However, saturated and unsaturated long-chain fatty acids, especially palmitic and oleic acids, were present in all the fractions. The fatty acid complexity of almost all the RPLC fractions confirms the large interesterification of fatty acids in butterfat.

Table II also shows that *CN* and *PN* roughly increased in order of increasing retention times. When the values for *CN*, *DB* and *PN* are examined within a four-peak group, such as the quartet 32–35 or 36–39, it can be seen that *PN* was fairly constant as a result of a simultaneous decrease in *CN* and *DB* in the four peaks of the quartet in order of increasing retention times. *CN* increased by 2 units on average from a quartet (*e.g.*, *CN* = 46.17 in group 32–35) to the following one (*CN* = 48.17 in group 36–39). TGs in the last peak of a quartet (peaks 27, 31, 35, 39, 43 and 47 in Fig. 2B) were mainly made up of saturated fatty acids. Indeed, the retention times of the standard saturated simple TGs in Fig. 2 correspond to these peaks (trimyristoylglycerol to peak 27 and tripalmitoylglycerol to peak 39). All these observations agree with the general rules of the resolution of TGs by RPLC according to their degree of unsaturation and chain length [35,36]. In the first two minor RPLC fractions 1 and 2, the values of *CN* and *PN* seem too high, and the fatty acid compositions are probably wrong, as a result of an insufficient subtraction of long-chain compounds via the blank. In fact, on the basis of the RPLC resolution of long-chain TGs, a theoretical *PN* can be assigned to TGs of the RPLC fractions showing a retention time identical with that of at least one known standard TG. Thus, the retention time of peak 2 corresponds to that of trioctanoylglycerol (Figs. 2 and 3), *i.e.*, *PN* = 24, whereas the experimental value was 31.6. In the same way, the theoretical *PN* of TGs in RPLC fractions 5, 15, 24, 27, 36, 39 and 51 are 30, 36, 42, 42, 48, 48 and 54, respectively. The experimental values (Table II) are generally close to the theoretical values (the difference is 1.1% on average), except in RPLC fractions 24 and 25 where the experimental *PN* values (40.7 and 40.9, respectively) are lower than the theoretical *PN* (42). In this instance, the TG species 6:0 16:0 18:0 and 4:0 18:0 18:0 (theoretical *PN* = 40) were probably eluted not in fraction 23 as expected but later in fractions 24 and 25, respectively, because of the presence of a short-chain fatty acid (6:0 and 4:0) in the molecule, as demonstrated for 4:0 in Fig. 3.

To check the accuracy of the relative proportions and fatty acid compositions of the 47 RPLC fractions, these results were used to calculate a fatty acid composition of

the total butterfat TGs. Table II shows that the calculated values are in close correlation with the experimental values (Table I) for all the fatty acids except for 20:0 because the minor RPLC fractions eluted later than fraction 47 were not studied.

GC resolution of triacyglycerols

Total butterfat TGs and aliquots of each RPLC-purified fraction were analysed directly by GC. Fig. 4 illustrates the GC profile of total butterfat TGs, which were essentially resolved on the basis of carbon number. Carbon numbers were identified by addition of the standard TGs already used for RPLC (see Figs. 2 and 3). Between the major even-carbon number peaks are seen minor peaks, which are due to odd-carbon number TGs arising from the substitution of one of the three-component even-carbon acyl moieties by an odd-carbon fatty acid, mainly 15:0 or 17:0. Identification of TGs in each RPLC fraction according to carbon number was realized by comparison of their relative retention times with those of the total butterfat TGs. Although GC analyses were performed using a relatively short capillary column (10 m) and a non-polar stationary phase (SE-30), the peaks did not appear homogeneous and parent TGs were partially resolved into several peaks within each carbon number, on the basis of the carbon and double bond numbers of each of the three acyl moieties.

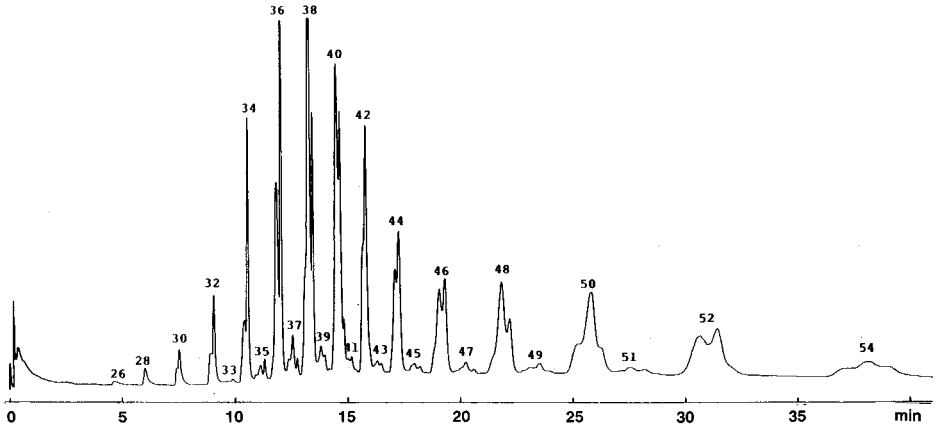

Fig. 4. Capillary GC profile of total butterfat TGs. Peaks are identified by their carbon number (*CN*). GC conditions: instrument, Packard Model 419; column, 10 m × 0.3 mm I.D. coated with SE-30; carrier gas, hydrogen at 3 ml min^{-1}; oven temperature, programmed from 200 to 300°C at 6°C min^{-1}.

Fig. 5 shows the segregation of some standard TGs under the same chromatographic conditions. It is seen clearly that butyrates (4 *X X*) were eluted later than the longer chain-length species of TGs within the range C_{24}–C_{36}. Such chain-length separations beyond the carbon number have also been observed by Myher *et al.* [1] on a polar capillary column. They demonstrated that within a given carbon number butyrates were preceded by caproates (6 *X X*), caprylates (8 *X X*) and mixtures of TGs containing exclusively longer chain-length fatty acids. They also found that for TG species within the same total carbon number, the shifts in equivalent carbon number decreased as the minimum chain length increased. As a result, the saturated TG species

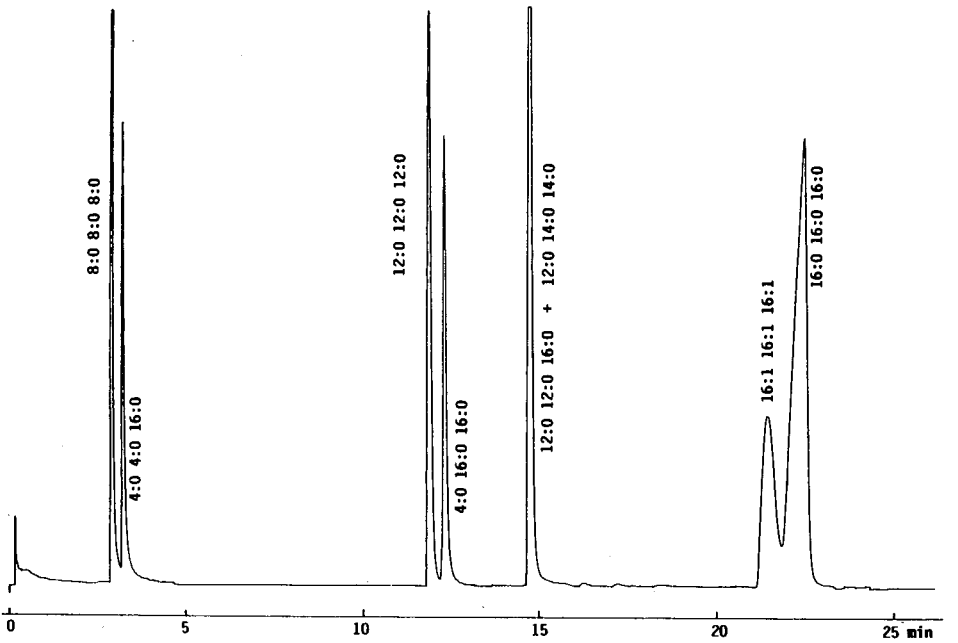

Fig. 5. Capillary GC profile of a mixture of standard TGs. GC conditions as in Fig. 4.

containing capric and longer fatty acids within a carbon number (*e.g.*, 10 16 18, 12 14 18, 12 16 16 and 14 14 16 in C_{44}) were not resolved, although Myher *et al.* used a 25-m capillary column. The non-resolution of 12 12 16 and 12 14 14 within carbon number C_{40}, as shown in Fig. 5, is in agreement with their findings. Thus, in the present study the resolution factors observed in GC for the saturated TGs within a carbon number are similar to those found in RPLC (see Fig. 3).

A partial resolution of TGs on the basis of double bound number was also obtained as tripalmitoleoylglycerol was separated from tripalmitoylglycerol (Fig. 5). However, unsaturated TGs were eluted ahead on our apolar capillary column, whereas saturated TGs preceded unsaturated TGs when using a polar capillary column [1]. It is possible that the actual segregations in our GC profiles of TGs were more complex and other factors, such as the presence of small amounts of acetates (2 *X X*) and *trans* and branched isomers or the positional placement of the fatty acids on the glycerol skeleton, could intervene, as described in detail by Myher *et al.* [1]. Under our experimental conditions, the GC resolution of TGs within a carbon number was generally too poor to be useful for identification and determination of the parent species. Further, fractionation of butterfat TGs by RPLC yielded a complete separation of butyrates, caproates and longer chain length TGs within the same carbon number (see above). As a result, GC was no longer useful for separation of these three groups of parent TG species.

Triacylglycerol compositions of RPLC fractions

TG compositons of each RPLC fraction and total butterfat according to the total *CN* distribution are given in Tables III and IV, respectively. Molar percentages

TABLE IV

TG COMPOSITION OF TOTAL BUTTERFAT TGs ANALYSED BY CAPILLARY GC

Carbon number	Experimental[a]	Calculated[b]	Carbon number	Experimental[a]	Calculated[b]
24	0.03 ± 0.004	0.08	40	10.80 ± 0.21	11.46
26	0.17 ± 0.04	0.33	41	1.06 ± 0.02	0.93
27	0.03 ± 0.01	0.02	42	6.39 ± 0.11	6.85
28	0.70 ± 0.04	0.81	43	1.10 ± 0.02	0.57
29	0.03 ± 0.01	0.07	44	5.31 ± 0.07	4.96
30	1.07 ± 0.03	1.42	45	1.19 ± 0.02	0.85
31	0.03 ± 0.01	0.14	46	5.44 ± 0.06	5.21
32	2.17 ± 0.06	2.57	47	1.62 ± 0.06	1.19
33	0.37 ± 0.02	0.52	48	6.21 ± 0.02	5.73
34	4.91 ± 0.11	5.34	49	2.15 ± 0.12	1.33
35	1.09 ± 0.05	1.29	50	7.80 ± 0.08	7.73
36	9.98 ± 0.02	10.04	51	2.08 ± 0.14	1.08
37	1.90 ± 0.02	2.03	52	7.69 ± 0.15	8.01
38	12.61 ± 0.26	13.45	53	0.74 ± 0.19	0.20
39	1.67 ± 0.02	1.38	54	3.66 ± 0.21	4.41

[a] Means (mol%) ± S.E.M. from five GC analyses.

[b] Calculated from the relative proportions (Table II) and TG compositions (Table III) of the 46 RPLC fractions of butterfat.

were calculated from chromatographic peak areas without applying any correction factors according to chain length or/and degree of unsaturation. Some correction factors were determined from standard TGs in the C_{24}–C_{54} range (results not shown), but remained low enough to be included in the range of measurement errors. Blanks were not subtracted as for fatty acid compositions because blanks performed and analysed under the same GC conditions contained no traces of TGs in the range C_{24}–C_{54}. No RPLC fraction appeared to be made up of only one TG species as several GC peaks were found for each fraction, even if 31 fractions exhibited one major even-carbon number peak (50–96%). TGs with the same *CN* were found to be present in a higher number of RPLC fractions (*e.g.*, TG C_{40} in the 23 RPLC fractions 4–26) than would have been otherwise expected. This results from extensive interesterification of the short- and longer-chain fatty acids in butterfat.

The odd-carbon number peaks were in low proportions, except in some minor RPLC fractions (fractions 10, 14, 32, 40 and 45) where their proportions exceeded those of the even-carbon number peaks. The odd-carbon number TGs accounted for 15.1% of the butterfat TGs when determined from the profile of the total butterfat (Fig. 4 and Table IV) or 11.6% when calculated from the distribution of the odd-carbon number peaks in each RPLC fraction (Table III) and from the proportions of the RPLC fractions in the total butterfat (Table II). They would make up 13.5% if this percentage was calculated from the proportion of the odd-carbon number fatty acids in the total fatty acids (*ca.* 4.5%), admitting that the odd-carbon number TGs occur with a stoichiometry of only one odd-carbon number fatty acid per TG molecule [1].

As expected, the mean *CN* values calculated from the data given in Table III are

consistent with those calculated from the fatty acid compositions and shown in Table II. However, differences exceeding one unit were observed for eighteen RPLC fractions. The fact that the odd-carbon number fatty acids were not taken into account in Table II could account for the differences, especially in some minor RPLC fractions (fractions 10, 32, 40 and 45) rich in odd-carbon number fatty acids. However, no explanation could be given when differences reached major (>3%) RPLC fractions (fractions 13, 16, 20 and 21) where the odd-carbon number TGs were in low proportions. The same differences were observed for the *PN* because in Table III *PN* values were calculated using the *DB* values given in Table I. When the TG composition of the total butterfat on the basis of *CN* was calculated from the TG compositions of the RPLC fractions (Table III) and the proportions of each RPLC fraction in the butterfat (Table II), the results were in good agreement with the experimental data (Table IV). These TG compositions are close to that determined by Amer *et al.* [10] under similar conditions.

Identification and elution order of triacylglycerol species in the RPLC fractions

The identity of a molecular species of TG is defined here by that of its component fatty acids, but the positioning of fatty acids is not determined. The fourteen different fatty acids listed in Table I could theoretically yield 560 different TG species in total (*PN* = 12–60) and 541 species in the studied RPLC fractions 1–47 (*PN* = 22–52). The identities of molecular species of TG present in an RPLC fraction often could not be assigned only by the examination of the chemical compositions of the fraction, as given in Tables II and III, because of their evident complexity. An RPLC fraction can gather together up to 26 different TG species distributed among nine classes (fraction 5). The identities of TG species, therefore, were also based on the general rules of elution order in RPLC, consistent with chromatographic data, such as relative retention times of standard TGs, and comparison with results obtained by other workers for mixtures of natural or synthetic TGs. Table V gives an example of the determination of the identities of TG species. There is not much point in calculating the equivalent carbon numbers (*ECN*) for each molecular species of TG, based on the retention times of the homologous series of standard simple TGs, because they would not be of any help in the determination of identities in this work, in contrast to the case with less complex fats [27].

First, we observed that TGs containing caprylic or longer chain saturated and monounsaturated fatty acids were resolved within a *PN* into four RPLC peaks corresponding to TG classes 111, 011, 001 and 000 in order of increasing retention times, as generally described [38]. Within a class, no apparent resolution of parent TGs was observed on the basis of the chain length of acyl moieties in the range C_8–C_{20}, even if a certain segregation within an RPLC peak was probable. Indeed, Nurmela and Satama [34] using two LiChrospher 100 CH-18 (5 μm) columns connected in series and a non-linear acetonitrile–acetone gradient elution programme showed that 10 10 10 and 8 8 14, and also 10 10 14 and 8 8 18, could be partially resolved with longer retention times for caprylates. When TGs contained a caproic or butyric residue in combination with two longer chain fatty acids, the retention time was lengthened with a time equivalent to one or two more RPLC peaks as follows: *X*:1 *X*:1 *X*:1, *X X*:1 *X*:1, *X X X*:1 + 6 *X*:1 *X*:1, *X X X* + 6 *X X*:1 + 4 *X*:1 *X*:1, *X*:1 *X*:1 *X*:1 (*PN* + 2) + 6 *X X* + 4 *X X*:1, *X X*:1 *X*:1 (*PN* + 2) + 4 *X X*. This sequence was complete only in

TABLE V

DISTRIBUTION OF MOLECULAR SPECIES OF TRIACYLGLYCEROLS IN RPLC FRACTION 12[a]

CN[b]	Class[c]	*PN*[d]	Molecular species[e]	Content (mol%)	
				In the RPLC fraction	In the total butterfat TGs
34	000	34	6 12 16	11	0.456
			6 14 14	4	0.166
			6 10 18	4	0.166
36	001	34	4 14 18:1	43	1.783
			4 16 16:1	10	0.415
			4 18 14:1	2	0.083
38	002	34	4 16 18:2	10	0.415
42	111	36	14:1 14:1 14:1	0.1	0.004
44	013	36	8 18:1 18:3 + 10 16:1 18:3 + 12 14:1 18:3	0.2	0.008

[a] 4.15% in total butterfat TGs (see Table II).
[b] *CN* = carbon number of the TG species in a TG class.
[c] Each digit represents the number of double bonds (*DB*) of each of the three acyl chains.
[d] *PN* = partition number (*PN* = *CN* – 2*DB*) of the TG species in a TG class.
[e] The position of the three acyl chains on the glycerol skeleton is not determined.

the series of RPLC fractions 12–17 where *PN* = 36. The same sequence, except for some butyrates, was found by Weber *et al.* [20,21], who analysed butterfat TGs on a Shandon ODS Hypersil (5 μm) column (250 × 4 mm I.D.). In contrast to our findings, they assigned the TG 4 12 14 to RPLC fraction 5, which preceded fraction 6 containing 4 10 16 as expected, although both TGs have same carbon number. In the same way, they found an earlier elution time for 4 16 14:1 than for 4 12 18:1, and for 4 14 14 than for 4 12 16 + 4 10 18. Baron *et al.* [22] reported that not only some butyrates (4 *X X*) were separated according to the chain length of the other two acyl moieties but TGs *X X X* and *X X X*:1 with *X* in the range C_8–C_{18} were also resolved. For example, 18 14 8 + 12 16 12 + 14 12 14, 16 8 16 and 18 12 10 belonged to three different RPLC peaks in increasing elution order. In their work [22], ascribing the molecular species of TGs to a given RPLC fraction did not seem to follow clear elution rules. According to our results obtained with standard mixed TGs (Fig. 3) it is hardly likely that such complete separations can occur under the RPLC conditions used by other workers [20,21,22], even if the RPLC columns used appeared to give slightly better separations.

The order of resolution of the TGs containing linoleic acid was consistent with that determined by Semporé and Bézard [27], who analysed peanut oil TGs using the same RPLC column. Their chromatogram indicated that 16 18:1 18:1, 16 18 18:2 and 16 16 18:1 were separated and eluted in order of increasing retention time, but 16 18 18:2 and 16 16 18:1 were only partially separated and eluted clearly later than 16 18:1 18:1. In this work, TGs of classes 001 and 002 within a *PN* were found in the same RPLC fraction, probably because class 002 was always present in a much smaller proportion than class 001 as a result of the relative proportions of 18:1 (22.2%) and

18:2 (2.1%) in butterfat. TG classes within a *PN* were separated as follows: 222 + 122 + 112 + 111, 022 + 012 + 011, 002 + 001 and 000 in increasing elution order. This elution order was still apparently valid when within such a series of TGs one of the three saturated acyl residues was a short-chain fatty acid. In contrast, Weber *et al.* [20,21] found that 16:0 16:0 18:2 was associated with 14:0 18:1 18:1 in an RPLC fraction and that both these TGs were retained for a longer time than 16:0 18:1 18:2 but a shorter time than 14:0 16:0 18:1. According to Barron *et al.* [22], long-chain TGs within a *PN* were eluted in increasing order as follows: 012, 011, 002 and 001.

Concerning the TG species containing linolenic acid, the elution order was more difficult to establish because of the very small proportions of most of these TG species and a lack of comparative chromatographic data from other workers. TGs containing odd-carbon number fatty acids were not studied in this work.

Determination of triacylglycerol species in butterfat

The proportions of the TG species in each RPLC fraction were obtained as follows. The proportions of fatty acids and TGs in an RPLC fraction (Tables II and III) were first recalculated to eliminate the residual contaminations from the preceding and succeeding major fractions when these contaminations were obvious and easy to remove. For instance, GC peak C_{38} (2.9%) in fraction 22 (see Table III) probably resulted from tailing of fraction 21 because there was no known TG C_{38} in fraction 22 (see Table III) and the proportion of TGs C_{38} in fraction 21 was high (67.7%). Further, the fatty acid compositions of both fractions were consistent with this contamination because a small amount of butyric acid (2.7%) was detected in fraction 22, which was expected to contain no butyrate, whereas GC peak C_{38} in fraction 21 was identified as being made up of 4 16 18.

The proportions of the TG species in an RPLC fraction were then calculated as described by Bézard *et al.* [23]. The proportions had to be consistent first with those of the GC peaks of TGs (Table III), which were more accurate than the corresponding fatty acid composition because of even-carbon number fatty acids provided by odd-carbon number TGs, especially when these TGs were present in high proportions in RPLC fractions. As the odd-carbon number TG species were not identified in RPLC fractions even-carbon number fatty acids supplied in this way could not be subtracted. Further, subtracting a blank from each fatty acid distribution introduced some errors, especially for minor unsaturated fatty acids.

In a second step, the distribution of the parent TG species in an RPLC fraction was such that the fatty acid composition recalculated from the TGs species distribution was as close to the experimental fatty acid composition as possible. Sometimes, the capillary GC resolution of the TGs of an RPLC fraction clearly yielded more than one peak within a *CN*. The chromatographic data (not given in Table III) were then used for subtraction of contaminations or the determination of different TG classes within a *CN*. The total proportion of all the TG species within a *CN* in an RPLC fraction was sometimes lower than the experimental percentage of the corresponding GC peak of TGs (Table III). The difference resulted from the subtraction of contaminations from another RPLC fraction or an unidentified TG, as explained for fraction 12 (see Table V). In the GC peak C_{38} (18.9%) of fraction 12, 4 16 18:2 could not exceed 10% because linoleic acid accounted for 3.4% in this fraction. The remaining 9% could be made up of a contamination from fraction 11 (TGs with $CN=38$) and/or an unknown TG. In

the same way, no TG C_{40} was given in Table V although a GC peak of corresponding TGs (5.9%) was detected experimentally (Table III) because no known molecular species of TG C_{40} was identified in fraction 12.

Calculation of the proportions of TG species in an RPLC fraction was relatively easy in the fractions where the number of species did not exceed 5 (*e.g.*, fractions 16, 20, 31, 32 and 37–47) and remained smaller than the number of available data (fatty acid and TG percentages). However, many RPLC fractions contained a large number of TG species, and the proportions of all the species could not then be determined accurately, especially when a class made up of several (from two to six) parent TGs was in a low proportion, as is the case for fraction 12 (Table V). As a result, 181 minor TG species were identified but not individually quantified, and they accounted for only 4.1%. In contrast, 223 individual TG species distributed among 45 RPLC fractions were recognized, and accounted for a large proportion (79.3%) in the butterfat sample studied. The detailed results will be published elsewhere [39].

In conclusion, the methodology choosen in this work, namely fractionation by RPLC and GC analysis of fatty acids and TGs in each RPLC fraction, appears to provide sufficient data to determine a large number of TG species in a complex fat.

ACKNOWLEDGEMENTS

These studies were supported in part by funds from Union Laitière Normande, Condé-sur-Vire, France.

REFERENCES

1 J. J. Myher, A. Kuksis, L. Marai and P. Sandra, *J. Chromatogr.*, 452 (1988) 93–118.
2 A. M. Massart-Len, H. De Pooter, M. Decloedt and N. Schamp, *Lipids*, 16 (1981) 286–292.
3 H. T. Badings and C. Dejonc, *J. Chromatogr.*, 279 (1983) 493–506.
4 S. Kuzdzal-Savoie, *Tech. Lait.*, (1984) 43–47.
5 J. L. Iverson and A. J. Sheppard, *Food Chem.*, 21 (1986) 223–234.
6 B. F. Daubert, *J. Am. Oil Chem. Soc.*, 26 (1949) 556–558.
7 A. Kuksis, L. Marai and J. J. Myher, *J. Am. Oil Chem. Soc.*, 50 (1973) 193–201.
8 K. Grob, Jr., H. P. Neukom and R. Battaglia, *J. Am. Oil Chem. Soc.*, 57 (1980) 282–286.
9 H. Traitler, *Rev. Fr. Corps Gras*, 28 (1981) 263–268.
10 M. A. Amer, D. B. Kuprancycz and B. E. Baker, *J. Am. Oil Chem. Soc.*, 62 (1985) 1551–1557.
11 P. Kalo, K. Vaara and M. Antila, *J. Chromatogr.*, 368 (1986) 145–151.
12 E. Geeraert and P. Sandra, *J. Am. Oil Chem. Soc.*, 64 (1987) 100–105.
13 A. Stolyhwo, H. Colin and G. Guiochon, *J. Chromatogr.*, 265 (1983) 1–18.
14 E. Deffense, *Rev. Fr. Corps Gras*, 31 (1984) 123–129.
15 J. L. Robinson and R. Macrae, *J. Chromatogr.*, 303 (1984) 386–390.
16 A. Stolyhwo, H. Colin and G. Guiochon, *J. Chromatogr.*, 288 (1985) 253–275.
17 B. Herslof and G. Kindmark, *Lipids*, 20 (1985) 783–790.
18 A. Stolyhwo, H. Colin and G. Guiochon, *Anal. Chem.*, 57 (1985) 1342–1354.
19 E. Frede and H. Thiele, *J. Am. Oil Chem. Soc.*, 64 (1987) 521–528.
20 K. Weber, E. Schulte and H.-P. Thier, *Fat Sci. Technol.*, 9 (1988) 341–344.
21 K. Weber, E. Schulte and H.-P. Thier, *Fat Sci. Technol.*, 10 (1988) 389–395.
22 L. J. R. Barron, T. G. Hierro and G. Santa Maria, *J. Dairy Sci.*, 57 (1990) 517–526.
23 J. Bézard, M. Bugaut and G. Clément, *J. Am. Oil Chem. Soc.*, 48 (1971) 134–139.
24 M. Bugaut and J. Bézard, *Oléagineux*, 34 (1979) 77–87.
25 M. Bugaut, *Lipids*, 24 (1989) 193–203.
26 R. E. Pitas, J. Sampugna and R. G. Jensen, *J. Dairy Sci.*, 50 (1967) 1332–1336.
27 G. Semporé and J. Bézard, *J. Chromatogr.*, 366 (1986) 261–282.

28 J. L. Delsal, *Bull. Soc. Chim. Biol.*, 26 (1944) 99–105.
29 D. L. Fillerup and J. F. Mead, *Proc. Soc. Exp. Biol. Med.*, 83 (1953) 574–577.
30 M. Narce, J. Gresti and J. Bézard, *J. Chromatogr.*, 448 (1988) 249–264.
31 C. Litchfield, *Analysis of Triglycerides*, Academic Press, New York, London, 1972.
32 W. W. Christie, *J. Lipid Res.*, 23 (1982) 1072–1075.
33 C. D. Bannon, J. D. Craske and A. E. Hilliker, *J. Am. Oil Chem. Soc.*, 62 (1985) 1501–1507.
34 K. V. Nurmela and L. T. Satama, *J. Chromatogr.*, 435 (1988) 139–148.
35 R. D. Plattner, G. F. Spencer and R. Kleiman, *J. Am. Oil Chem. Soc.*, 54 (1977) 511–515.
36 A. H. El-Hamdy and E. G. Perkins, *J. Am. Oil Chem. Soc.*, 50 (1981) 867–872.
37 J.-P. Goiffon, C. Reminac and D. Furon, *Rev. Fr. Corps Gras*, 28 (1981) 199–207.
38 M. W. Dong and J. L. Dicesare, *J. Am. Oil Chem. Soc.*, 60 (1983) 788–791.
39 J. Gresti, M. Bugaut, C. Maniongui, S. Gautier and J. Bézard, in preparation.

Journal of Chromatography, 543 (1991) 105–112
Elsevier Science Publishers B.V., Amsterdam

CHROM. 23 136

Liquid chromatographic separation of the enantiomers of dinitrophenyl amino acids using a β-cyclodextrin-bonded stationary phase

SONG LI and WILLIAM C. PURDY*

Department of Chemistry, McGill University, 801 Sherbrooke St. West, Montreal, Quebec H3A 2K6 (Canada)

(First received November 9th, 1990; revised manuscript received January 22nd, 1991)

ABSTRACT

A β-cyclodextrin-bonded chiral stationary phase was used for the liquid chromatographic resolution of racemic amino acid derivatives. Ten pairs of dinitrophenyl amino acid enantiomers were separated by this technique. Methanol–triethylammonium buffer solutions were used as the mobile phases. The effects of pH, methanol and triethylammonium acetate buffer concentration in the mobile phase, and the structural features of the solutes on the retention and enantio-selectivity were examined and discussed in terms of the overall retention mechanism.

INTRODUCTION

Enantiomeric separation of amino acids is important in many fields, such as peptide synthesis, asymmetric syntheses in organic chemistry, amino acid biochemistry, the studies of food processing and protein degradation processes in humans [1–3] and the dating of archaeological materials [4]. For the last several years, there existed two general approaches to the high-performance liquid chromatographic separations of the enantiomers of amino acids. One is ligand-exchange chromatography using a chiral ligand immobilized on a solid support as the stationary phase. The other technique employs active chelates in the mobile phase. Recently, cyclodextrin-bonded stationary phases developed by Armstrong and co-workers [5,6] were also successfully used for the enantiomeric resolution of amino acids.

Cyclodextrins (CDs) are oligosaccharides in which glucose units are joined together to form a toroidal structure with a hydrophobic cavity and hydrophilic exterior faces. The main property of CDs which allows them to affect chiral separation is their ability to form enantio-selective inclusion complexes with guest molecules. It is believed that chiral recognition is caused by inclusion complex formation between the cavity of CD and the hydrophobic moiety of the solute, and by hydrogen bonding between the polar functional groups of the solute in the vicinity of its chiral center and the hydroxyl groups of the CD [5]. The enantiomers of tryptophan, phenylalanine, tyrosine and analogues have been separated on an α-CD bonded phase column [6]. The

0021-9673/91/$03.50

separation of some racemic 5-dimethylamino-1-nahthalenesulphonyl (dansyl) amino acids using a β-CD bonded phase column have also been reported [5]. To date, however, there has been no report on the enantiomeric separation of any 2,4-dinitrophenyl (DNP) amino acids on any CD-bonded stationary phase.

In this paper we describe a method for separating D- and L-DNP-amino acids using a β-CD bonded stationary phase with traditional aqueous-organic mobile phases. The effects of pH, the mobile phase composition, buffer concentration and the structural features of solutes on the retention time and enantiomeric resolution will be discussed in terms of the retention mechanism.

EXPERIMENTAL

Apparatus

Chromatography was performed using a liquid chromatographic system which consisted of a Model 590 pump (Waters Assoc., Milford, MA, U.S.A.), a Model 7125 injector containing a 10-μl loop (Rheodyne, Cotati, CA, U.S.A.) and a Model 440 UV detector (Waters). The chromatograms were recorded on a Model SE120 strip chart recorder (Goerz Electro, Austria). The column temperature was controlled through a HETO 623 water bath (Bach-Simpson, London, Canada).

A Cyclobond I, 250 × 4.6 mm I.D. column was purchased from Advanced Separation Technologies (Whippany, NJ, U.S.A.). The Cyclobond I column is β-CD molecules chemically bonded to spherical silica gel through a five-atom, non-nitrogen-containing spacer. When not in use, the column was stored in 100% methanol.

Chemicals

All D- and L-DNP-amino acids were obtained from Sigma (St. Louis, MO, U.S.A.). HPLC-grade methanol and triethylamine were purchased from Fisher (Fair Lawn, NJ, U.S.A.). Glacial acetic aid was obtained from Allied Chemical (Pointe Claire, Canada). Water was deionized by passing distilled water through a Barnstead water-purification system.

Procedures

Mobile phase was prepared by mixing methanol with triethylammonium acetate (TEAA) buffer. The mobile phase was degassed by bubbling helium into it for about 10 min before use. Sample solutions were prepared by dissolving each raceme in methanol to give a concentration of about 1 mg/ml. Typically, 2 μl of sample solution were injected. The chromatography was performed at a flow-rate of 1.0 ml/min. Absorbance of the column effluent was monitored at a wavelength of 254 nm.

All data points on graphs were obtained by averaging at least three separate determinations. A careful reproducibility study involving five injections revealed a relative standard deviation of less than 2% in capacity factors, and of less than 6% in resolution factors.

RESULTS AND DISCUSSION

In this investigation, the optical separations of ten DNP-amino acids were examined using a β-CD bonded phase column. Table I lists the optical separation data

TABLE I

OPTICAL RESOLUTION OF THE ENANTIOMERS OF DNP-AMINO ACIDS

The separation was done on a 250 × 4.6 mm I.D. β-cyclodextrin-bonded phase column. In the structures, *R* represents 2,4-dinitrophenyl. k' = Capacity factor of the first eluted enantiomers; α = enantioselectivity; R_s = resolution.

No.	Solutes	Structure	k'	α	R_s	Mobile phase[a]
1	DNP-DL-α-Amino-*n*-butyric acid	CH_3CH_2–CHCOOH NHR	3.00	1.04	0.60	20:80
2	DNP-DL-Norvaline	$CH_3CH_2CH_2$–CHCOOH NHR	4.0	1.06	0.80	10:90
3	DNP-DL-Norleucine	$CH_3(CH_2)_3$–CHCOOH NHR	2.67	1.28	2.45	25:75
4	DNP-DL-α-Amino-*n*-caprylic acid	$CH_3(CH_2)_5$–CHCOOH NHR	11.3	1.30	3.40	25:75
5	DNP-DL-Methionine sulphoxide	$CH_3SOCH_2CH_2$–CHCOOH NHR	6.67	1.05	0.8	5:95
6	DNP-DL-Methionine sulphone	$CH_3SO_2CH_2CH_2$–CHCOOH NHR	1.32	1.05	0.9	5:95
7	DNP-DL-Methionine	$CH_3SCH_2CH_2$–CHCOOH NHR	1.88	1.14	1.50	25:75
8	DNP-DL-Ethionine	$CH_3CH_2SCH_2CH_2$–CHCOOH NHR	5.00	1.18	2.50	25:75
9	DNP-DL-Citrulline	$H_2NCONH(CH_2)_3$–CHCOOH NHR	1.90	1.05	0.80	5:95
10	DNP-DL-Glutamic acid	$HOOCCH_2CH_2$–CHCOOH NHR	3.60	1.06	0.90	10:90

[a] The numbers represents the volume ratio of methanol to TEAA buffer (0.5% TEAA, pH 6.20).

obtained, together with the structures of these amino acid derivatives. The L-isomers are eluted first for all the DNP-derivatized amino acids. The same elution order has been reported for dansyl-amino acids [5]. Some typical chromatograms are shown in Fig. 1. As can be seen, the β-CD column exhibits high enantioselectivity toward the DNP-amino acids. The enantiomers of these DNP-amino acids could be separated on a 250 × 4.6 mm I.D. β-CD bonded phase column with resolution factors from 0.6 up to 3.40.

Effect of structural features on enantioselectivity

From our experience of working with a β-CD bonded phase column and to the best of our knowledge, no enantiomers of underivatized amino acids can be separated with the β-CD column. It is believed that the size of unsubstituted amino acids is too small to bind tightly with the CD cavity to form a strong inclusion complex [7,8], a prerequisite for the chiral recognition. The results of this study show that the DNP substituent of the amino acids plays an important role in chiral recognition. This is not

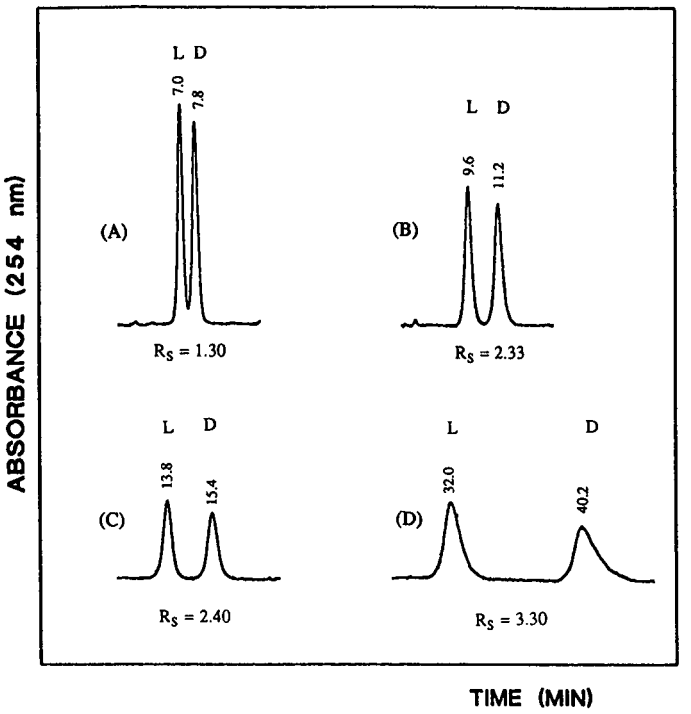

Fig. 1. Chromatograms showing the resolutions of DNP-D,L-amino acids. (A) DNP-DL-Methionine; (B) DNP-DL-norleucine; (C) DNP-DL-ethionine; (D) DNP-DL-α-amino-*n*-caprylic acid. Column, 250 × 4.6 mm I.D. Cyclobond I; mobile phase, 30:70 methanol–TEAA buffer (0.5%, pH 6.2) (30:70); temperature, 20°C; flow-rate, 1 ml/min.

surprising since it had been previously reported that the nitrophenyl group could tightly bind to the β-CD cavity to form a strong inclusion complex [9,10]. The introduction of a DNP substituent into the amino acid molecules provides the strong binding site required for the chiral recognition.

A comparison of the α values obtained for these DNP-amino acids indicates that the enantioselectivity is also affected by the size of the alkyl substituents around the chiral center. As can be seen from Table I, the enantioselectivities (α) for α-amino-*n*-butyric acid, norvaline, norleucine and α-amino-*n*-caprylic acid are 1.04, 1.06, 1.28 and 1.30, respectively. The only difference between the structures of these solutes is the size of the alkyl substituent on the chiral center. The results obtained in this study show that the enantioselectivity increases with the size of alkyl substituent. This is true for the enantioselectivities of DNP-DL-methionine ($\alpha = 1.14$) and DNP-DL-ethionine ($\alpha = 1.18$) as well. It seems that the alkyl substituent plays an important role of steric hindrance, which weakens the strength of inclusion complexation and/or hydrogen bonding for one of the enantiomers.

Effect of methanol content

The effects of the methanol content on the retention and resolution were investigated by changing the methanol-water ratio in the mobile phase. Fig. 2 shows

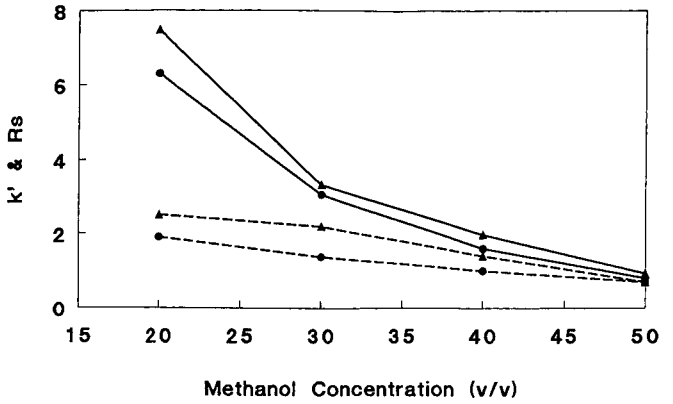

Fig. 2. Effect of methanol concentration in the mobile phase on the retention (solid lines: capacity factors of the first eluted enantiomers, k') and resolution (broken lines: R_s) of (▲) DNP-DL-ethionine and (●) DNP-DL-norleucine. Column, 250 × 4.6 mm I.D. Cyclobond I; mobile phase, 0.5% TEAA and pH 5.0; temperature, 20°C; flow-rate, 1 ml/min. k' is the capacity factor of the first eluted enantiomer.

the typical plots of capacity factors and resolution factors *versus* the methanol contents. The TEAA buffer concentration is 0.5%, and the pH of the mobile phase is 5.0 in this set of experiments.

It is found that the effect of methanol content on retention and optical resolution of DNP-amino acids gives almost the same tendencies as those observed with dansyl-amino acids [5], that is, an increase in the methanol content results in both a decreased retention and a decreased enantioselectivity or resolution factor. For some of these DNP-amino acids, the optical separation can be achieved only at very low methanol content (< 10%). It is not surprising since it is known from the CD-binding studies that an increase in organic content in the solvent will weaken the strength of inclusion complexation between guest molecules and β-CD [11]. In this case, the increase of methanol content in the mobile phase diminishes the extent of inclusion complexation between the DNP substituent and β-CD, resulting in a decreased retention and a decreased optical resolution factor.

Effect of TEAA buffer concentration

Fig. 3 shows the influence of TEAA buffer concentration in the mobile phase on the retention and resolution. It is found that an increase in the TEAA concentration in the mobile phase results in a decreased retention of both enantiomers in all instances. However, the effect of TEAA concentration on the optical resolution is somewhat more complex. As the TEAA concentration in the mobile phase varies from 0.1% to 1.0%, two types of behavior can be observed. The resolution increases with the increasing TEAA concentration and then decreases when TEAA is greater than 0.5%. Resolution maxima are observed at TEAA concentrations of about 0.5%.

These facts can be explained by considering the effect of TEAA on both the column separation efficiency (N) and the enantioselectivity (α) of β-CD column. It has been found that the addition of TEAA buffer in the mobile phase substantially increased the separation efficiency of a β-CD bonded phase column. A TEAA buffer

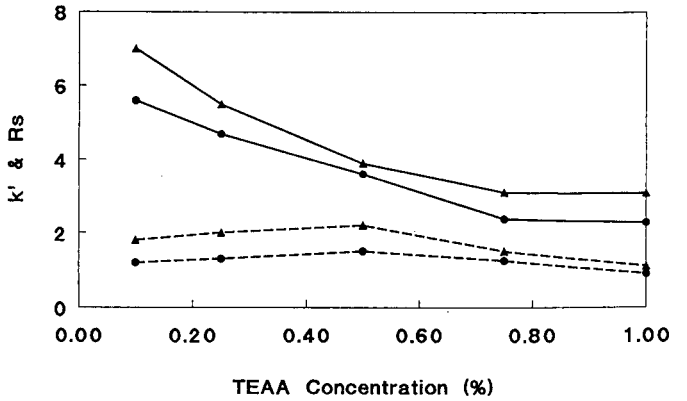

Fig. 3. Effect of TEAA concentration in the mobile phase on the retention and resolution of (▲) DNP-DL-ethionine and (●) DNP-DL-norleucine. Conditions: column, 250 × 4.6 mm I.D. Cyclobond I; mobile phase, methanol–TEAA buffer solution (30:70); pH 5.0; temperature, 20°C; flow-rate, 1 ml/min. Solid and broken line as in Fig. 2.

(0.02 *M* and pH 5.0) substituted for water in a methanol–water (40:60) system can produce a three- to four-fold increase in the column efficiency for the separation of phenothiazine derivatives [12]. The increasing separation efficiency will result in an increase in the resolution. On the other hand, the TEAA molecule, as an organic modifier, can include in the β-CD cavity and there it competes with solute. The addition of TEAA in the mobile phase will weaken the strength of inclusion complexation between the DNP substituent and the β-CD cavity, resulting in a decrease in the enantioselectivity. The results obtained in this study indicate that at low TEAA concentrations the separation efficiency is the limiting factor for the resolution. An increase in TEAA concentration increases the column efficiency, thus increasing the optical resolution. As the TEAA concentration increases in the mobile phase, the enantioselectivity (α) becomes the limiting factor, and the resolution decreases with the increasing TEAA concentration. When the TEAA concentration increases to 1.5%, no optical separation can be observed for most of these amino acid derivatives.

Effect of pH

The influence of pH on the retention and resolution of DNP-DL-amino acids was investigated by changing the pH of the mobile phase from 4.5 to 7.0 using 0.5% TEAA buffer. Some typical plots of the capacity factor and resolution *versus* pH values are shown in Fig. 4. The retention timse of all the DNP-amino acids decreased with increasing pH. This fact can be explained by considering the effect of pH on the form of the amino acids and on the bonding strength of the carboxylic acid function to the hydroxyl group of β-CD.

By N-substitution, the DNP-amino acids have lost the dipolar ion character of the parent amino acids, and hence can be considered as carboxylic acids with a –NHDNP substituent mostly at α-position. Since the –NHDNP group is a strong electron-withdrawing group, the pK_a values of DNP-amino acids should be much

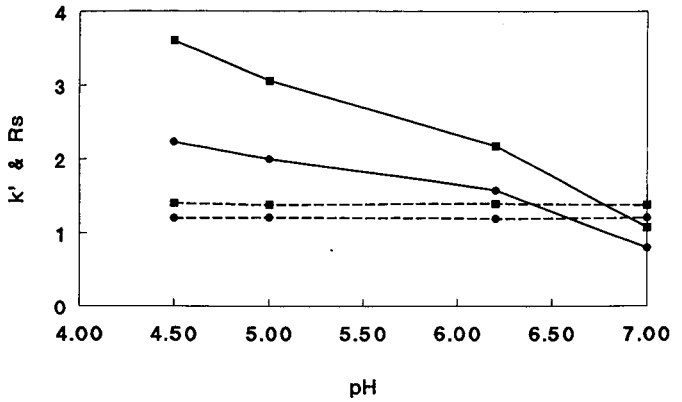

Fig. 4. Effect of pH on the retention and resolution of (■) DNP-DL-ethionine and (●) DNP-DL-methionine. Conditions: column, 250 × 4.6 mm I.D. Cyclobond I; mobile phase, methanol–TEAA buffer (0.5% TEAA) (30:70); temperature, 20°C; flow-rate, 1 ml/min. Solid and broken lines as in Fig. 2.

lower than that of carboxylic acids, even much lower than the pK_a value (3.71) of N-acetylglycine ($CH_3CONHCH_2COOH$) [13]. Therefore, it can be expected that the DNP-amino acids exist mainly in the form of anions in the pH range of 4.5 to 7.0. Thus, the strength of the inclusion complexation between the DNP substituent and the cavity of cyclodextrin should not be affected by changing pH. However, it had been reported that the OH^- ion had a high hydrogen bonding ability to the hydroxyl groups of ROH molecules [14,15]. The existence of OH^- in the mobile phase will compete with the carboxylate group of DNP-amino acids to interact with the hydroxyl group of cyclodextrin. With the increase of OH^- concentrations in the mobile phase, caused by the increasing pH, the bonding strength between the carboxylate group of the solute and the hydroxyl group of the cyclodextrin, and thus the overall interaction of solute with β-CD, will be weakened. Therefore, a decreased retention time with the increase of pH is observed.

Fig. 4 also shows that the optical resolutions are not affected by changing pH. This suggests that the interaction between the polar groups of solute and the hydroxyl groups of CD is not the main factor for the chiral recognition.

CONCLUSIONS

It has been demonstrated that the β-CD bonded phase column exhibits a high enantioselectivity for the DNP-amino acid derivatives. The effects of methanol and TEAA concentration in the mobile phase, pH, and the structural features on the retention and resolution suggest that the inclusion complex formation between the cavity of CD and the DNP substituent, and the steric hindrance of alkyl substituents around the chiral center of the solutes are the important factors in the chiral recognition.

ACKNOWLEDGEMENT

The authors are indebted to the Natural Science and Engineering Research Council of Canada for the financial support of this work.

REFERENCES

1 E. Bayer, E. Gil-Av, W. A. Konig, S. Nakaparksin, J. Oro and W. Parr, *J. Am. Chem. Soc.*, 92 (1970) 1738.
2 G. C. Barret (Editor), *Chemistry and Biochemistry of Amino Acids*, Chapman & Hall, New York, 1985, p. 8.
3 E. H. Man, M. E. Sandhouse, J. Burg and G. H. Fisher, *Science (Washington, DC)*, 220 (1983) 1407.
4 R. Hardial and C. F. Simpson, *Anal. Proc.*, 26 (1989) 57.
5 W. L. Hinze, T. E. Riehl, D. W. Armstrong, W. DeMond, A. Alak and T. Ward, *Anal. Chem.*, 57 (1985) 237.
6 D. W. Armstrong, X. Yang, S. M. Hand and R. A. Menges, *Anal. Chem.*, 59 (1987) 2594.
7 A. Cooper and D. D. MacNicol, *J. Chem. Soc., Perkin. Trans.*, II (1978) 760.
8 C. D. Tran and J. H. Fendler, *J. Phys. Chem.*, 88 (1984) 2167.
9 Y. Inoue, H. Hoshi, M. Sakurai and R. Chujo, *J. Am. Chem. Soc.*, 107 (1985) 2319.
10 R. L. VanEtten, J. F. Sebastian, G. A. Clowes and M. L. Bender, *J. Am. Chem. Soc.*, 87 (1967) 3240.
11 M. L. Bender and M. Komiyama, *Cyclodextrin Chemistry*, Springer, New York, 1978.
12 S. Li and W. C. Purdy, *J. Pharm. Biomed. Anal.*, in press.
13 G. Kortum, W. Vogel and K. Andrusson, *Dissociation Constants of Organic Acids in Aqueous Solution*, Butterworths, London, 1961, p. 320.
14 M. M. Davis, *Acid–Base Behavior in Aprotic Organic Solvents*, National Bureau of Standards, Washington, DC, 1968, p. 89.
15 B. R. Agarwal and R. M. Diamond, *J. Phys. Chem.*, 67 (1963) 2785.

Journal of Chromatography, 543 (1991) 113–121
Elsevier Science Publishers B.V., Amsterdam

CHROM. 23 121

Synthesis of esters of acetyloxycaffeic acids and their occurrence in poplar bud exudates

W. GREENAWAY* and F. R. WHATLEY
Department of Plant Sciences, University of Oxford, South Parks Road, Oxford OX1 3RB (U.K.)
(First received October 30th, 1990; revised manuscript received January 16th, 1991)

ABSTRACT

The novel 3-methyl-3-butenyl, 2-methyl-2-butenyl, 3-methyl-2-butenyl, benzyl and 2-phenylethyl esters of 3-acetyloxycaffeic acid and 4-acetyloxycaffeic acid were synthesised on a micro scale and characterised by gas chromatography–mass spectrometry. These compounds are identified for the first time in poplar bud exudates.

INTRODUCTION

Poplar bud exudate is a complex mixture which may contain flavonoids, substituted benzyl and phenylpropenoic acids and their esters, terpenoids and hydrocarbons. The composition of bud exudate is characteristic of a species, or even clone [1] and there can be considerable differences in bud exudate composition between species. Thus in *Populus balsamifera* L. (section *Tacamahaca*) the principal components of the bud exudate are dihydrochalcones and terpenoids [2], whereas in bud exudate of *P. fremontii* S. Wats. (section *Aigeiros*) these compounds are entirely lacking, the principal components being flavanonols and chalcones [3].

In some Asiatic poplars, such as *P. ciliata* Wall. and *P. simonii* Carr. (both currently classified in section *Tacamahaca*), the bud exudate is distinctive in that caffeic acid and other acids, together with their esters, form a major part of the bud exudate (75% in *P. ciliata* and 45% in *P. simonii*). Preliminary study of mass spectra of these other unidentified acids suggested that they might be trimethylsilyl derivatives of acetyloxycaffeic acids and their esters. We here describe the synthesis of several series of acetyloxycaffeates and indicate how they may easily be located in complex chromatograms of poplar bud exudate by single ion reconstructions of gas chromatography–mass spectrometric (GC–MS) data, thus confirming our view of their identity. These acetyloxycaffeic acids and their esters have not been previously identified in poplar bud exudate.

0021-9673/91/$03.50

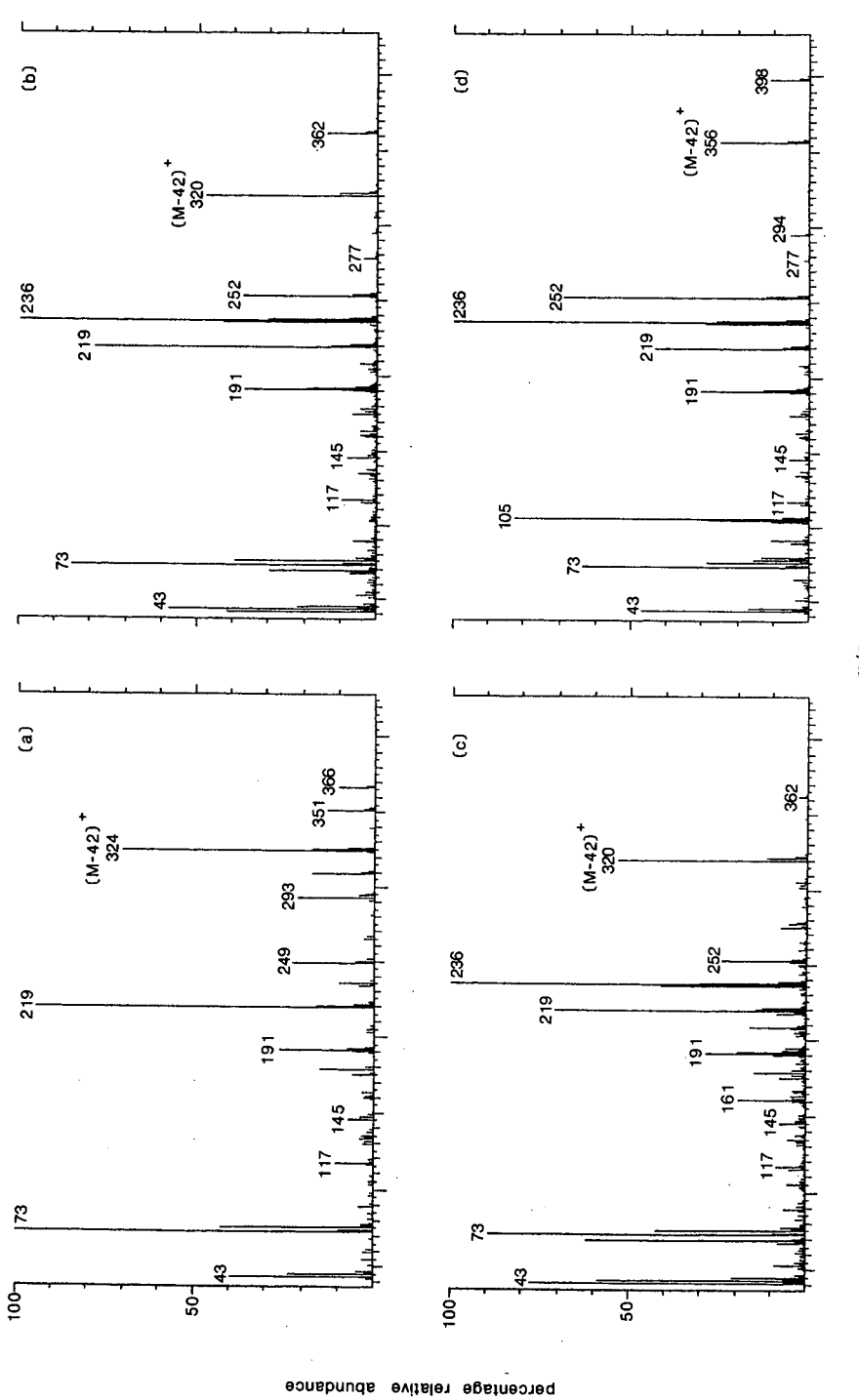

Fig. 1. Mass spectra recorded at 70 eV of (a) *trans*-3-acetyloxycaffeic acid bis-TMS, $[M]^+$ $m/z = 366$; (b) 3-methyl-3-butenyl *trans*-3-acetyloxycaffeate mono-TMS, $[M]^+$ $m/z = 362$; (c) 3-methyl-2-butenyl *trans*-3-acetyloxycaffeate mono-TMS, $[M]^+$ $m/z = 362$; (d) 2-phenylethyl *trans*-3-acetyloxycaffeate mono-TMS, $[M]^+$ $m/z = 398$. Spectra a–c are from *P. simonii*, spectrum d is from *P. ciliata*. The 4-acetyloxy-compounds have mass spectra very similar to those of the corresponding 3-acetyloxy-compounds.

EXPERIMENTAL

Reagents and materials

Acetic anhydride (Analar) was purchased from BDH (Dorset, U.K.), bis(trimethylsilyl)trifluoroacetamide (BSTFA) including 1% trimethylchlorosilane (TMCS) from Sigma (Dorset, U.K.), N,N-dimethylformamide dineopentylacetal (DMF acetal) from Lancaster Synthesis (Lancashire, U.K.). Other chemicals were purchased from Aldrich (Dorset, U.K.) and Lancaster Synthesis, or provided by gift from Shell Research (Sittingbourne, U.K.).

Sample preparation

Bud exudate was obtained from buds of *P. ciliata*, clone ref D (originating from Dehra Dun, India) at the Forestry Commission Research Station (Alice Holt Lodge, Farnham, U.K.) and *P. simonii* (originating from Luozhenying, Shanxi, China) at the Poplar Bureau of Shanxi Province (Datong, Shanxi, China).

Exudate was collected by dipping five buds in 3 ml ethyl acetate for 10 s at room temperature. The ethyl acetate was evaporated in a screw-top conical glass tube under a stream of N_2 and the extract freeze dried for 10 min to remove residual water. After addition of 50 μl pyridine and 100 μl BSTFA containing 1% TMCS the tube was sealed and heated for 30 min at 100°C to produce trimethylsilyl (TMS) derivatives for GC.

GC–MS

The derivatised samples were separated and analysed in a Finnigan 1020 automated GC–MS system (incorporating a Data General Nova 3 computer). The GC–MS system was fitted with a 25 m × 0.32 mm I.D. Thames Chromatography (Maidenhead, U.K.) silica column coated with 0.5 μm of immobilized polydimethylsiloxane, and had a splitless injector with a flush 30 s after sample injection to remove residual gases. The end of the GC column was introduced directly into the mass spectrometer analyser chamber. The GC system was operated under the following conditions: He pressure, 13 p.s.i.; injector temperature, 310°C; GC temperature, 75–310°C at 3°C/min. The mass spectrometer was set to scan 40–650 a.m.u. per nominal second with an ionizing voltage of 70 eV. The filament was switched on 250 s after the injection of the sample (0.5–1 μl) into the GC.

Identification of compounds in bud exudate

This was by comparison with GC retention times in methylene units (MU; as defined by Dalgliesh *et al.* [4]) and mass spectra of trimethylsilyl (TMS) derivatives of reference compounds. The synthesis as reference compounds of acetyloxyferulic acid, acetyloxyisoferulic acid, the three acetyloxycaffeic acids and a number of esters of these acetyloxycaffeic acids is described in the Appendix.

RESULTS AND DISCUSSION

Preliminary studies of mass spectra suggested that a series of unidentified peaks in GC–MS analyses of bud exudate of *P. ciliata* and *P. simonii* were likely to be TMS derivatives of acetyloxycaffeic acids and their esters. The presence in these mass spectra of prominent m/z 43 and $[M - 42]^+$ ions (Fig. 1) representing CH_3CO and the

loss of CH_2CO from the mass ion, respectively, indicated the presence of an acetyl group.

The mass ions of the unidentified compounds added up to that expected for the TMS derivatives of 3- or 4-acetylated caffeic acids or their esters with benzyl alcohol, the methylbutenols or phenylethanol, all of which alcohols have previously been found in poplar bud exudates in the form of esters of caffeic acid.

Synthesis of acetyloxycaffeic acids and their esters enabled the methylene unit (MU) retention times and mass spectral patterns of several series of these compounds to be recorded (see Appendix). The two acetyloxy-derivatives produced from each parent compound, representing the 3-acetyloxy- and 4-acetyloxy-derivatives, had closely similar mass spectra but differed in MU retention times (Table I).

Caffeic acid, 3(3,4-dihydroxyphenyl)-2-propenoic acid, has two adjacent hydroxyl groups on the phenyl ring and the selective acetylation of only one of these groups presents difficulties. Ferulic acid, 3(3-methoxy-4-hydroxyphenyl)-2-propenoic acid,

TABLE I

CAFFEIC ACID, CAFFEATE ESTERS AND THEIR ACETYLOXY-DERIVATIVES IDENTIFIED IN POPLAR BUD EXUDATES BY GC–MS

Peak numbers correspond to those given in chromatograms shown in Figs. 3 and 4. GC retention times in methylene units (MU; defined by Dalgliesh *et al.* [4]) are given to two decimal places to indicate the elution sequence of peaks which chromatograph closely. Factors such as concentration of the compound concerned, together with the characteristics of a particular GC column, are liable to affect the chromatography and for general purposes the MU figures are probably reliable to only a single decimal place only.

Peak[a] no.	Compound[b]	MU	Number of TMS groups	Distinctive ion	Composition
1	*trans*-4-Acetyloxycaffeic acid[c] (*trans*-3(3-hydroxy-4-acetyloxyphenyl)-2-propenoic acid)	21.42	2	366	$[M]^+$
2	*trans*-Caffeic acid	21.44	3	396	$[M]^+$
3	*trans*-3-Acetyloxycaffeic acid[c]	22.10	2	366	$[M]^+$
4	3-Methyl-3-butenyl *trans*-caffeate	23.47	2	392	$[M]^+$
5	3-Methyl-3-butenyl *trans*-4-acetyloxycaffeate[c]	23.52	1	320	$[M - 42]^+$
6	2-Methyl-2-butenyl *trans*-caffeate	23.83	2	392	$[M]^+$
7	2-Methyl-2-butenyl *trans*-4-acetyloxycaffeate[c]	23.88	1	320	$[M - 42]^+$
8	3-Methyl-2-butenyl *trans*-caffeate (prenylcaffeate)	23.96	2	392	$[M]^+$
9	3-Methyl-2-butenyl *trans*-4-acetyloxycaffeate[c]	23.98	1	320	$[M - 42]^+$
10	3-Methyl-3-butenyl *trans*-3-acetyloxycaffeate[c]	24.17	1	320	$[M - 42]^+$
11	2-Methyl-2-butenyl *trans*-3-acetyloxycaffeate[c]	24.49	1	320	$[M - 42]^+$
12	3-Methyl-2-butenyl *trans*-3-acetyloxycaffeate[c]	24.58	1	320	$[M - 42]^+$
13	Benzyl *trans*-caffeate	26.79	2	414	$[M]^+$
14	Benzyl *trans*-4-acetyloxycaffeate[c]	26.80	1	342	$[M - 42]^+$
16	2-Phenylethyl *trans*-caffeate	27.80	2	428	$[M]^+$
17	Benzyl *trans*-3-acetyloxycaffeate[c]	27.83	1	342	$[M - 42]^+$
18	2-Phenylethyl *trans*-4-acetyloxycaffeate[c]	27.85	1	356	$[M - 42]^+$
19	2-Phenylethyl *trans*-3-acetyloxycaffeate[c]	28.44	1	356	$[M - 42]^+$

[a] Location of peaks nos. 1–12 are shown in bud exudate of *P. simonii* (Fig. 3) and of peaks 13–19 in bud exudate of *P. ciliata* (Fig. 4).

[b] The names given do not include the TMS substituents.

[c] We are not aware of previous identifications of these compounds.

and isoferulic acid, 3(3-hydroxy-4-methoxyphenyl)-2-propenoic acid, differ from caffeic acid only in that one of the hydroxyls on the phenyl ring is methylated, leaving a single hydroxyl group available for acetylation (Fig. 2). With these as starting compounds it is possible to produce an acetylated derivative with the acetyl group in a defined position. Separate synthesis of acetyloxyferulic acid [3(3-methoxy-4-acetyloxyphenyl)-2-propenoic acid] and acetyloxyisoferulic acid [3(3-acetyloxy-4-methoxyphenyl)-2-propenoic acid] as described in the Appendix showed that, as trimethylsilyl derivatives, the 4-acetyloxy-compound (acetyloxyferulic acid), MU 20.73, chromatographed close to ferulic acid, MU 20.78, whereas the 3-acetyloxy-compound (acetyloxyisoferulic acid), MU 21.07, chromatographed much later than isoferulic acid, MU 20.65.

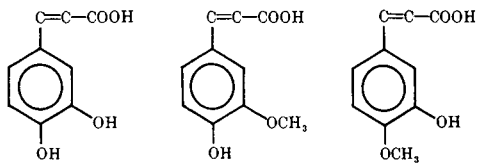

caffeic acid ferulic acid isoferulic acid

Fig. 2. Structures of caffeic acid, 3(3,4-dihydroxyphenyl)-2-propenoic acid; ferulic acid, 3(3-methoxy-4-hydroxyphenyl)-2-propenoic acid and isoferulic acid, 3(3-hydroxy-4-methoxyphenyl)-2-propenoic acid.

We believe that the differences in chromatographic retention time of acetyloxyferulic acid and acetyloxyisoferulic acid are likely to apply to the acetyloxycaffeates. We therefore assign the first of a pair of TMS–acetyloxycaffeates, *i.e.* that which chromatographs closely with the unacetylated parent compound, as the 4-acetyloxy-derivative and the second, which chromatographs later than the parental compound, as the 3-acetyloxy-derivative (see Table I, Figs. 3–5).

The 3-acetyloxy- and 4-acetyloxy-derivatives of caffeic acid, benzyl caffeate, 3-methyl-3-butenyl caffeate, 2-methyl-2-butenyl caffeate, 3-methyl-2-butenyl caffeate and 2-phenylethyl caffeate are identified in poplar bud exudate (Table I, Figs. 3, 4 show results from *P. simonii* and *P. ciliata*). The mass spectra of 3-acetyloxycaffeic acid bis-TMS, 3-methyl-3-butenyl 3-acetyloxycaffeate mono-TMS, 3-methyl-2-butenyl 3-acetyloxycaffeate mono-TMS and 2-phenylethyl 3-acetyloxycaffeate mono-TMS are shown in Fig. 1. Previous results have shown that the mass spectra of the different methylbutenyl esters of caffeic acid are very similar, and that the methylbutenyl esters are best differentiated by their characteristic MU retention times [5]. A similar, but more complex, situation occurs with the methylbutenyl esters of acetyloxycaffeate, in which the various methylbutenyl esters of both the 3-acetyloxy- and 4-acetyloxy-caffeates have very similar spectra. Here also the MU retention times provide the best means of identification (Table I). Although the 3,4-diacetyloxy-derivatives of caffeic acid and its esters were produced in the synthetic mixtures (see Appendix, Fig. 5), they appear not to occur in poplar bud exudates.

The acetyloxycaffeic acids and their esters occur primarily in those Asiatic poplars, such as *P. ciliata* [6], in which caffeic acid and its esters form the bulk of the

bud exudate. In such poplars the methylbutenyl acetyloxycaffeates may be major components: in one specimen of *P. ciliata* they formed *in toto* 26% of the bud exudate TIC, with 3-methyl-3-butenyl 4-acetyloxycaffeate present as both the *cis* (1%) and *trans* (12%) isomers [6].

We have previously demonstrated the potential of single ion reconstructions (SIR) of GC–MS data in resolving and identifying the components of complex mixtures [7,8] and of microsynthesis (as in the Appendix) and identification of reference compounds by GC–MS of the reaction mixture [5,9,10]. The work reported here confirms the potential of these methods.

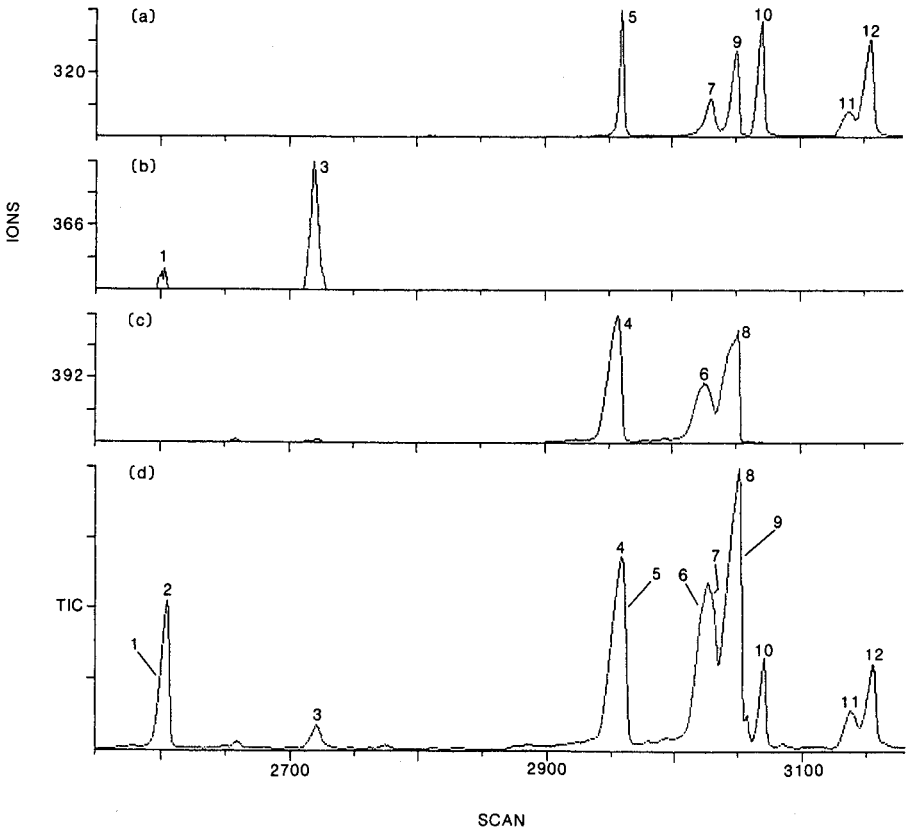

Fig. 3. Acetyloxycaffeic acids, methylbutenyl caffeates and methylbutenyl acetyloxycaffeates identified in bud exudate of *P. simonii*. (a) Single ion reconstruction (SIR) of m/z = 320 $[M - 42]^+$ locating 3-methyl-3-butenyl *trans*-4-acetyloxycaffeate mono-TMS (peak 5), 2-methyl-2-butenyl *trans*-4-acetyloxycaffeate mono-TMS (7), 3-methyl-2-butenyl *trans*-4-acetyloxycaffeate mono-TMS (9), 3-methyl-3-butenyl *trans*-3-acetyloxycaffeate mono-TMS (10), 2-methyl-2-butenyl *trans*-3-acetyloxycaffeate mono-TMS (11) and 3-methyl-2-butenyl *trans*-3-acetyloxycaffeate mono-TMS (12); (b) SIR of m/z = 366 $[M]^+$ locating *trans*-4-acetyloxycaffeic acid bis-TMS (1) and *trans*-3-acetyloxycaffeic acid bis-TMS (3); (c) SIR of m/z = 392 $[M]^+$ locating 3-methyl-3-butenyl *trans*-caffeate bis-TMS (4), 2-methyl-2-butenyl *trans*-caffeate bis-TMS (6) and 3-methyl-2-butenyl *trans*-caffeate bis-TMS (8); (d) total ion current between 21–25 MU. Peak 2 is *trans*-caffeic acid tris-TMS.

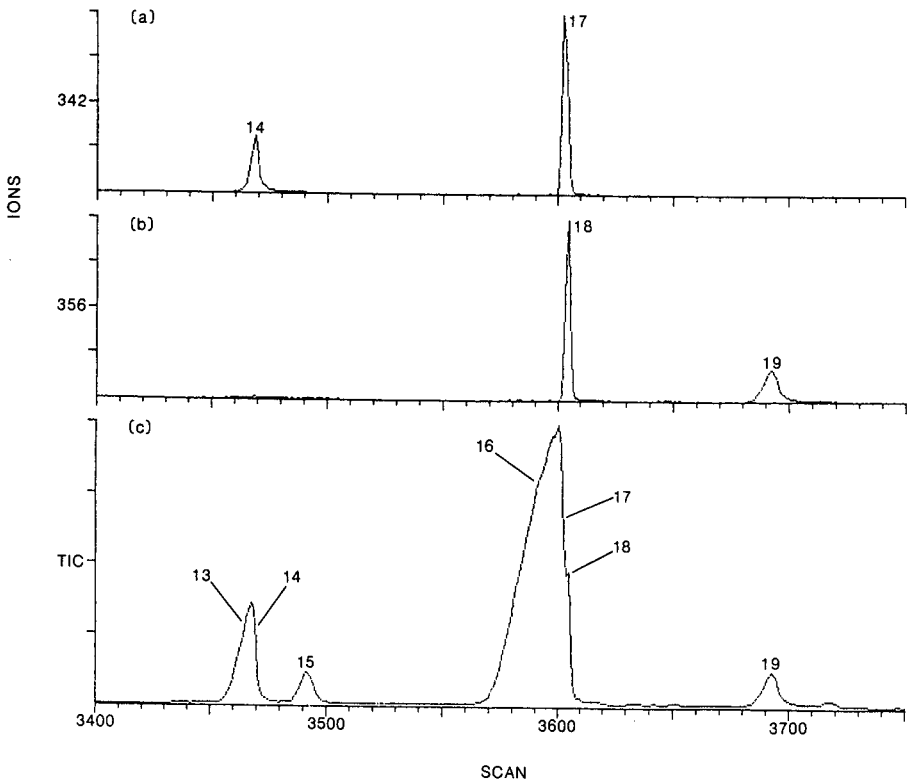

Fig. 4. Benzyl acetyloxycaffeates and phenylethyl acetyloxycaffeates identified in bud exudate of *P. ciliata*. (a) Single ion reconstruction (SIR) of m/z = 342 $[M - 42]^+$ locating benzyl *trans*-4-acetyloxycaffeate mono-TMS (peak 14) and benzyl *trans*-3-acetyloxycaffeate mono-TMS (17); (b) SIR of m/z = 356 $[M - 42]^+$ locating 2-phenylethyl *trans*-4-acetyloxycaffeate mono-TMS (18) and 2-phenylethyl *trans*-3-acetyloxycaffeate mono-TMS (19); (c) total ion current between 26–29 MU. Peak 13 is benzyl caffeate bis-TMS, peak 15 is heptacosane and peak 16 is 2-phenylethyl *trans*-caffeate bis-TMS.

ACKNOWLEDGEMENTS

We thank P. Howard, Forestry Commission, U.K. and Director Yang, Poplar Bureau of Shanxi Province, China for permission to collect plant material from their clonal collections of poplars and P. Jewess of Shell Research for providing a sample of 2-methyl-2-butenol.

APPENDIX

Synthesis of acetyloxyferulic and acetyloxyisoferulic acids

To 1 mg of ferulic acid, *trans*-3(3-methoxy-4-hydroxyphenyl)-2-propenoic acid, in a screw top glass derivatization tube, was added 75 μl pyridine and 25 μl acetic anhydride. The tube was heated at 60°C for 1 h, producing a mixture of unreacted ferulic acid and 4-acetyloxyferulic acid. The solvent was evaporated under a stream of

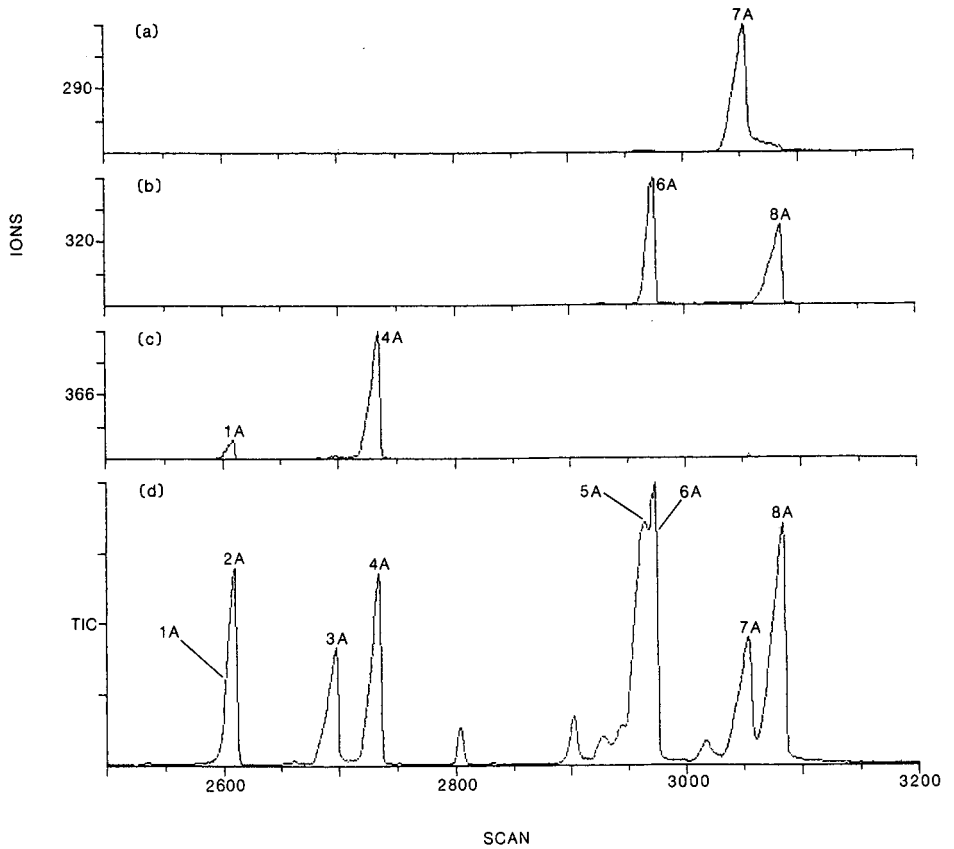

Fig. 5. Single ion reconstructions (SIR) and GC–MS total ion chromatogram (TIC) of caffeic acid derivatives produced by esterification of a mixture of acetyloxycaffeates with 3-methyl-3-butenol. (a) SIR m/z = 290 $[M - 42]^+$, locating 3-methyl-3-butenyl *trans*-3,4-diacetyloxycaffeate (7A), MU = 23.95; (b) SIR m/z = 320 $[M - 42]^+$, locating 3-methyl-3-butenyl *trans*-4-acetyloxycaffeate mono-TMS (6A), MU = 23.52, and 3-methyl-3-butenyl *trans*-3-acetyloxycaffeate mono-TMS (8A), MU = 24.17; (c) SIR m/z = 366 $[M]^+$, locating *trans*-4-acetyloxycaffeic acid bis-TMS (1A), MU = 21.42, and *trans*-3-acetyloxycaffeic acid bis-TMS (4A), MU = 22.10; (d) TIC between 21–25 MU. In addition to peaks identified above the following are present, *trans*-caffeic acid tris-TMS (2A), MU = 21.44; *trans*-3,4-diacetyloxycaffeic acid mono-TMS (3A), MU = 21.88; and 3-methyl-3-butenyl *trans*-caffeate bis-TMS (5A), MU = 23.47.

nitrogen and the residue briefly freeze dried. For gas chromatography 100 μl BSTFA (inc. 1% TMCS) and 50 μl pyridine was added to the mixture of acids and the tube was heated at 100°C for 1 h, to produce trimethylsilyl (TMS) derivatives with any unreacted hydroxyl or carboxyl groups. The same procedure, but using isoferulic acid, *trans*-3(3-hydroxy-4-methoxyphenyl)-2-propenoic acid, resulted in the synthesis of the TMS derivative of 3-acetyloxyisoferulic acid.

Synthesis of esters of acetylcaffeic acid

Caffeic acid, *trans*-3(3,4-dihydroxyphenyl)-2-propenoic acid (1 mg) was heated with pyridine and acetic anhydride as above. This resulted in a mixture of unreacted

caffeic, 3-acetyloxycaffeic, 4-acetyloxycaffeic and 3,4-diacetyloxycaffeic acids. The solvent was evaporated under a stream of nitrogen and the residue of acids briefly freeze dried as above. To this mixture of acids was added 10 μl of the appropriate alcohol (*e.g.*, 2-phenylethyl alcohol for 2-phenylethyl esters, 3-methyl-3-butenol for 3-methyl-3-butenyl esters, etc.), 150 μl of dichloromethane and 10 μl of DMF acetal. This latter compound mediates the esterification of acids with alcohols [11]. The tube was heated at 100°C for 1 h, the solvent evaporated under a stream of nitrogen and the residue briefly freeze dried. The resultant mixture of compounds was derivatized with BSTFA (inc. 1% TMCS) as above.

Whereas this mixture is complex, the various constituents can be located after GC separation by their characteristic ions (Fig. 5 shows the mixture resulting when 3-methyl-3-butenol is used as the alcohol). The appropriate methylene unit (MU) retention times were calculated after the addition of a series of straight chain hydrocarbon standards to the derivatized mixture.

REFERENCES

1 W. Greenaway, J. Jobling and T. Scaysbrook, *Silvae Genet.*, 38 (1989) 28.
2 W. Greenaway, J. May and F. R. Whatley, *J. Chromatogr.*, 472 (1989) 393.
3 W. Greenaway, S. English, E. Wollenweber and F. R. Whatley, *J. Chromatogr.*, 481 (1989) 352.
4 C. E. Dalgliesh, E. C. Horning, M. G. Horning, K. L. Knox and K. Yarger, *Biochem. J.*, 101 (1966) 792.
5 W. Greenaway, E. Wollenweber, T. Scaysbrook and F. R. Whatley, *Z. Naturforsch. C*, 43 (1988) 795.
6 W. Greenaway and F. R. Whatley, *Phytochemistry*, 30 (1991) in press.
7 W. Greenaway and F. R. Whatley, *J. Chromatogr.*, 519 (1990) 145.
8 W. Greenaway, J. May, T. Scaysbrook and F. R. Whatley, *Z. Naturforsch. C*, 46 (1991) 111.
9 W. Greenaway, T. Scaysbrook and F. R. Whatley, *Proc. R. Soc. London, Ser. B*, 232 (1987) 249.
10 W. Greenaway, E. Wollenweber, T. Scaysbrook and F. R. Whatley, *J. Chromatogr.*, 448 (1988) 284.
11 H. Buchi, K. Steen and A. Eschenmoser, *Angew. Chem., Int. Ed. Engl.*, 3 (1964) 62.

Journal of Chromatography, 543 (1991) 123–128
Elsevier Science Publishers B.V., Amsterdam

CHROM. 23 092

Reversed-phase high-performance liquid chromatographic separation of tertiary and quaternary alkaloids from *Chelidonium majus* L.

LIANG-FENG HAN, WASSYL NOWICKY and VIKTOR GUTMANN*
Institute of Inorganic Chemistry, Technical University of Vienna, Getreidemarkt 9, A-1060 Vienna (Austria)
(First received November 6th, 1990; revised manuscript received December 28th, 1990)

ABSTRACT

A reversed-phase high-performance liquid chromatographic procedure is described for the determination of the alkaloids in *Chelidonium majus* L. extracts. For the analysis of tertiary and quaternary alkaloids, replacement of the commonly applied organic amine modifiers with potassium iodide led to a considerable improvement in resolution. By using a gradient elution programme more than twenty peaks were resolved and thirteen tertiary and quaternary alkaloids were identified.

INTRODUCTION

Chelidonium majus L., a medicinal plant of the Papaveraceae family, has stimulated much interest owing to its chemically and pharmacologically interesting alkaloids. By classical methods more than twenty alkaloids have been detected in this plant [1], but no systematic studies have been carried out by high-performance liquid chromatography (HPLC). Three quaternary alkaloids from this plant, sanguinarine, chelerythrine and berberine, and a non-quaternary one, chelidonine, have been separated by normal-phase chromatography [2]. Reversed-phase ion-pair chromatography using different ion-pair agents for the separation of chelidonine, chelerythrine and sanguinarine [3] and for the separation of allocryptopine, protopine and chelidonine [4] have been reported. However, little attention has been paid to the alkaloids present in very small amounts, probably because the available HPLC techniques were unsuitable for their identification.

In this paper, an HPLC method for the separation and identification of tertiary and quaternary alkaloids from *Chelidonium majus* L. is described.

EXPERIMENTAL

Apparatus

A Hewlett-Packard (Palo Alto, CA, U.S.A.) Model 1090 liquid chromatograph was used, equipped with an HP Model DR5 solvent-delivery system and an HP 1090

0021-9673/91/$03.50

option 044 auto-injector. Detection was performed with an HP 1090 option 080 diode-array UV detector.

Chemicals

Acetonitrile (LiChrosolv; Merck, Darmstadt, Germany), methanol (reinst, Merck) and water (Chromasolv für Gradientenelution, Riedel-de Haën, Seelze, Germany) were used. Potassium iodide (Merck) was of analytical-reagent grade.

The following standard alkaloids were kindly supplied: sanguinarine and allocryptopine by L. Jusiak (Lublin, Poland); methoxychelidonine, oxysanguinarine, dihydrosanguinarine, chelerythrine, dihydrochelerythrine, chelilutine, chelirubine, corysamine and (−)-stylopine by J. Slavik and L. Slavikova (Brno, Czechoslovakia); berberine and protopine by W. Debska (Poznan, Poland); and chelidonine, homochelidonine and sparteine by F. Kuffner (Vienna, Austria). Their structures are given in Fig. 1.

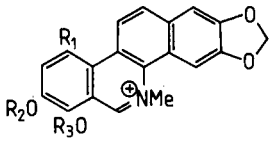

sanguinarine, $R_3+R_2=CH_2$, $R_1=H$
chelerythrine, $R_3=R_2=CH_3$, $R_1=H$
chelilutine, $R_3=R_2=CH_3$, $R_1=OCH_3$
chelirubine, $R_3+R_2=CH_2$, $R_1=OCH_3$

oxisanguinarine, $R_1+R_2=CH_2$, $R_3+R_4=O$
dihydrochelerythrine, $R_3=R_4=H$, $R_1=R_2=CH_3$
dihydrosanguinarine, $R_1+R_2=CH_2$, $R_3=R_4=H$

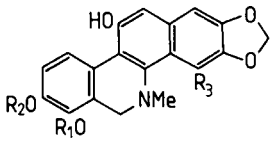

chelidonine, $R_1+R_2=CH_2$, $R_3=H$
homochelidonine, $R_1=R_2=CH_3$, $R_3=H$
methoxychelidonine, $R_1+R_2=CH_2$, $R_3=OCH_3$

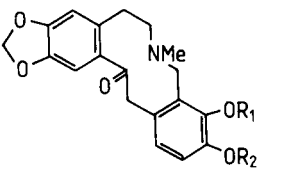

protopine, $R_1+R_2=CH_2$
allocryptopine, $R_1=R_2=CH_3$

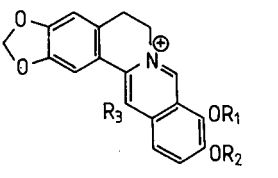

corysamine, $R_1+R_2=CH_2$, $R_3=CH_3$
berberine, $R_1=R_2=CH_3$, $R_3=H$

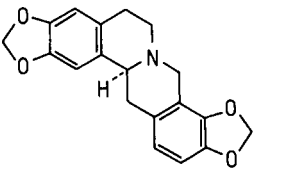

(-)-stylopine

Fig. 1. Structures of alkaloids from *Chelidonium majus* L. Me = Methyl.

All of the standard alkaloids were dissolved in methanol containing 0.1 *M* ammonia and stored in air-tight flasks in the dark. The plants of *Chelidonium majus* L. were collected from fields near Vienna.

Extraction of alkaloids

The plants were dried at room temperature and extracted with ethanol. Ethanol from the extract was distilled off and the residue was transferred into 1% sulphuric acid and filtered. The acidic aqueous filtrate was neutralized with sodium hydroxide and extracted with chloroform. The pH of the solution was then increased to 8 and again extracted with chloroform. The pH was increased again by 1 unit, the solution was extracted, and these procedures were repeated until a pH of 14 was established. The extracts were combined, filtered and evaporated to dryness under vacuum. The residue was dissolved in 1% hydrochloric acid, filtered and the filtrate evaporated to dryness under vacuum. After dissolution in methanol containing 0.1 *M* ammonia, the solution was subjected to HPLC.

Separation and identification method

A Hypersil ODS column (RP C_{18}, Hewlett-Packard) (100 × 4.6 mm I.D., 5 μm particle size) was used. The mobile phase was water–acetonitrile–methanol. The water was adjusted to pH 7.5 with propylamine and the methanol contained 0.15 *M* potassium iodide. Isocratic and gradient elution were used, as given in the captions of Figs. 2 and 4. The column temperature was 30°C. The chromatograms were monitored at 285 nm with a bandwidth of 30 nm. The reference wavelength was 400 nm with a bandwidth of 100 nm. Retention time data were measured directly from chromatograms based on five measurements. Other HPLC conditions are given in the captions of Figs. 2 and 4.

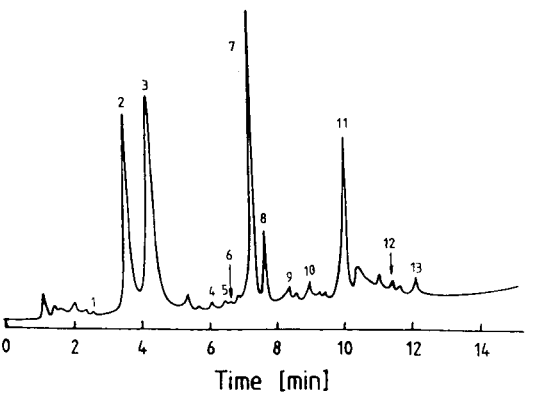

Fig. 2. HPLC of *Chelidonium majus* L. extract using gradient elution. Mobile phase: water–acetonitrile–methanol, from 50:20:30 to 15:55:30 in 15 min. The water was adjusted to pH 7.5 with propylamine and the methanol contained 0.15 m*M* potassium iodide. Flow-rate: increased from 0.8 to 1.5 ml/min in 15 min. Injection volume: 10 μl.

RESULTS AND DISCUSSION

Reversed-phase HPLC is ineffective in many instances for compounds with structures containing basic nitrogen atoms owing to interactions between the basic compounds and the acidic silanol groups on the stationary phase surface [5–10]. Practical experience has shown that in such instances the addition of organic amines to the mobile phase is essential in order to achieve good separations. The general effect of such amines is to decrease retention and improve peak shape in the analysis of basic compounds. Additions of organic amines to the mobile phase have also been reported to alter the selectivity of the stationary phase [11].

In an attempt to obtain improved separations for the crude drug of *Chelidonium majus* L., propylamine and tetrabutylammonium salts were added to the mobile phase with pH < 7.5. However, reversed-phase HPLC with these amines gave unsatisfactory separations. Considerable improvement in the peak shape and resolution of the extract of *Chelidonium majus* L. was achieved by applying potassium iodide as modifier. As shown in Fig. 2, thirteen alkaloids were detected in this way and several

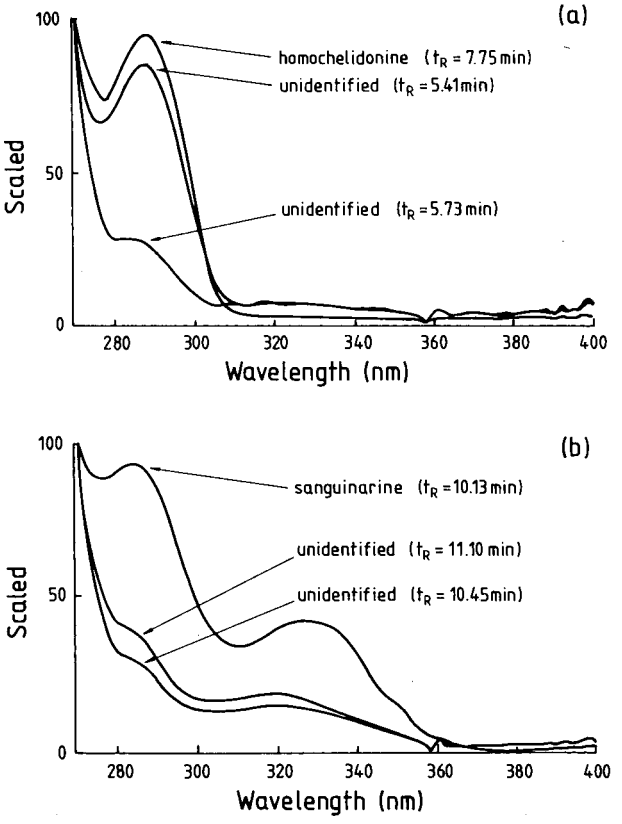

Fig. 3. Examples of spectral comparison between the peaks: (a) spectra of homochelidonine (retention time, t_R = 7.75 min, peak 8 in Fig. 2) and two unknowns at t_R = 5.41 and 5.73 min; (b) spectra of sanguinarine (t_R = 10.13, peak 11 in Fig. 2) and two unknowns at t_R = 10.5 and 11.1 min.

TABLE I

RETENTION TIMES OF THE ALKALOIDS

Chromatographic conditions are given in Fig. 2.

Alkaloid	t_R (min)	Peak No.
Corysamine	2.63	1
Methoxychelidonine	3.61	2
Allocryptopine	4.30	3
Protopine	6.13	4
Chelerythrine	6.52	5
Berberine	6.71	6
Chelidonine	7.34	7
Homochelidonine	7.75	8
Oxysanguinarine	8.28	9
(−)-Stylopine	9.05	10
Sanguinarine (chelitutine, chelirubine)[a]	10.13	11
Dihydrochelerythrine	11.52	12
Dihydrosanguinarine	12.22	13

[a] Alkaloids with the same retention time as Sanguinarine.

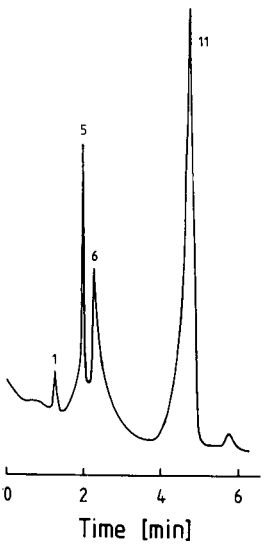

Fig. 4. HPLC of a standard mixture of four quaternary alkaloids. Alkaloids denoted by numbers as in Table I. Mobile phase: water–acetonitrile–methanol (30:40:30); the water was adjusted to pH 7.5 with propylamine and the methanol contained 0.15 *M* potassium iodide. Isocratic elution. Flow-rate: 0.8 ml/min. Injection volume: 10 μl (sample solution concentration about 0.1–0.5 mg/ml of each alkaloid). Other conditions as in Fig. 2.

small peaks were identified by comparing both their retention times and their UV spectra with those of standards. The comparision of the spectra as a second criterion was found useful for the identification, because most of the alkaloids were present in fairly low concentrations. Apart from the identification of thirteen alkaloids (denoted by 1–13 in Fig. 2), several other small peaks may also be due to the presence of alkaloids, because the spectra are typical of them (Fig. 3). In the absence of appropriate standards, their identification has not been possible. It may be noted that according to our results, summarized in Table I, sparteine [12] was not found.

Another difficulty in the separation of quaternary alkaloids arises from their strong interactions with the stationary phase [13]. Our results have shown that these interactions may be weakened by the use of potassium iodide as a modifier. Sharp peaks were achieved for corysamine, chelerythrine and sanguinarine. The separations between corysamine, chelerythrine and sanguinarine are also satisfactory, but berberine has not been resolved clearly from chelerythrine (peaks 5 and 6 in Fig. 2). Better separations with almost symmetrical peaks and good resolution between corysamine, chelerythrine, berberine and sanguinarine were obtained using other gradient conditions, as outlined in legend of Fig. 4. Under these conditions the tertiary alkaloids, especially those present in small amounts, were not well resolved.

Increased interest has recently been shown in the alkaloids from *Chelidonium majus* L. because of the potential use of their derivatives in antitumour therapy [14]. It seems likely that the method described here may be applied in further studies directed towards the isolation and identification of alkaloids of biological and clinical interest.

ACKNOWLEDGEMENTS

This investigation has been carried out under contract of the Bundesministerium für Wissenschaft und Forschung in Österreich. The authors also express their gratitude to Professors L. Jusiak, J. Slavik, L. Slavikova and W. Debska and the late Professor F. Kuffner for the supply of alkaloid standards.

REFERENCES

1 I. W. Southon and J. Buckingham, *Dictionary of Alkaloids*, Chapman & Hall, London and New York, 1989.
2 B. Carlo, C. M. Laura and T. Franca, *J. Chromatogr.*, 393 (1987) 312.
3 W. E. Freytag, *Dtsch. Apoth.-Ztg.*, 126 (1986) 1113.
4 T. Dzido, *J. Chromatogr.*, 439 (1988) 257.
5 I. M. Johansson, K.-G. Wahlund and G. Schill, *J. Chromatogr.*, 149 (1978) 281.
6 K.-G. Wahlund and A. Sokolowski, *J. Chromatogr.*, 151 (1978) 299.
7 A. T. Metin, M. Ljungcrantz and G. Schill, *J. Chromatogr.*, 185 (1979) 225.
8 A. Sokolowski and K.-G. Wahlund, *J. Chromatogr.*, 189 (1980) 299.
9 K. E. Bij, Cs. Horváth, W. R. Melander and A. Nahum, *J. Chromatogr.*, 203 (1981) 65.
10 S. O. Jansson, I. Andersson and B. A. Persson, *J. Chromatogr.*, 203 (1981) 93.
11 C. T. Hung and R. B. Taylor, *J. Chromatogr.*, 240 (1982) 61.
12 E. Späth and F. Kuffner, *Chem. Ber.*, 64 (1931) 1127.
13 F. P. B. Van der Maeden, P. T. Van Rens, F. A. Buytenhuys and E. Buurman, *J. Chromatogr.*, 142 (1977) 715.
14 J. W. Nowicky, M. Greif, F. Hamler, W. Hiesmayr and W. Staub, *J. Tumor Marker Oncol.*, 3 (1988) 463.

Journal of Chromatography, 543 (1991) 129–135
Elsevier Science Publishers B.V., Amsterdam

CHROM. 23 113

On-line determination of the optical purity of nicotine

THOMAS A. PERFETTI

R. J. Reynolds Tobacco, Bowman Gray Technical Center, P.O. Box 2959, Winston-Salem, NC 27102 (U.S.A.)

and

JOEL K. SWADESH*[a]

Polymer Laboratories, Inc., Amherst Fields Research Park, 160 Old Farm Rd., Amherst, MA 01002 (U.S.A.)

(First received November 9th, 1990; revised manuscript received January 3rd, 1991)

ABSTRACT

Nicotine is an alkaloid of medical importance. Precise quantitation of the enantiomeric purity of preparations of nicotine has been difficult. In the present work, a high-performance poly(styrene–divinyl benzene) reversed-phase column was used to separate the enantiomers of nicotine from other components. On-line polarimetric detection with a commercial laser polarimeter permitted sensitive, reproducible quantitation of the relative enantiomeric purity of nicotine. Detection limits of about 12 μg were established, with the range of linearity extending to about 200 μg. It was possible to assign the relative purity of mixtures of nicotine to about ±0.5%. The precision of the on-line polarimeter was comparable to that of a static polarimeter, but the sample requirement was approximately 1000 times less. Optically inactive components were separated, making on-line polarimetry intrinsically more accurate than static polarimetry, and readily adaptable to the analysis of complex mixtures.

INTRODUCTION

Nicotine is a naturally occurring alkaloid existing as a tertiary amine with one chiral carbon located at the 2′ position of the N-methylpyrrolidine ring.

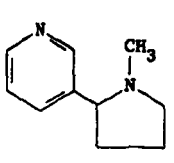

There are two optically active isomers of nicotine, the naturally-occurring (*S*)-(−)-form [1], and the (*R*)-(+)-form [2]. Although 50 species of plants contain nicotine, *Nicotiniana tabacum* and *N. rustica* [3] are the two predominant species containing nicotine. The salt form of (*S*)-nicotine has been used as a natural insecticide [4], while

[a] Address for correspondence: 68 Florence Road, Florence, MA 01060, U.S.A.

0021-9673/91/$03.50

the free base has been used in medicine as an antihelminthic agent [5] and as an experimental drug in the treatment of Parkinson's [6] and Alzheimer's diseases [7]. Both isomers are toxic, exhibiting biological activity in the peripheral and central nervous systems [8]. Toxicity tests have long been performed on both isomers [9]. The (*S*)-form generally exceeds the (*R*)-form in both toxicity and biological activity. However, synergism has been noted for mixtures of (*S*)- and (*R*)-nicotine in studies on rats and guinea pigs [8,10]. There has been sustained interest in (*R*)-nicotine because its toxicity is lower than that of the (*S*)-isomer, while the biological activity is comparable.

The optical purity of (*R*)- of (*S*)-nicotine employed in biomedical studies has been difficult to quantitate. Neither repetitive diastereomeric salt purification techniques [11] nor enantiomerically selective microbial transformation of racemic mixtures [12] are readily capable of providing extremely pure materials. Precise quantitative characterization is similarly difficult. Although conventional polarimetry is suitable for purified samples, these polarimeters require relatively large samples, and are not suitable for analysis of complex mixtures such as serum. The enantiomers of a variety of alkaloids closely related to nicotine have been successfully separated by chiral chromatography, but those of nicotine itself have proved to be difficult to separate, the separation requiring 4 h and a microbore column [13–15].

Numerous chromatographic techniques and detectors have been advanced as means to differentiate and quantitate enantiomeric purity. Among the detectors that have been used in determinations of enantiomeric purity are the Perkin-Elmer 241 LC polarimeter [16–18], and laser polarimeters described by Yeung and co-workers [19,20] and Lloyd *et al.* [21]. The latter has been developed by Applied Chromatography Systems into a commercial instrument known as the ChiraMonitor. The performance characteristics of this on-line polarimeter have been described [21], as have a number of applications [22]. The present work compares static and on-line polarimetry in the analysis of mixtures of nicotine.

EXPERIMENTAL

Reagents

The (*S*)-(−)-isomer of nicotine was from Eastman Kodak (Rochester, NY, U.S.A.). The (*R*)-(+)-isomer was prepared by T.D.C. Research (Blacksburg, VA, U.S.A.) using an established method [11], substituting di-*p*-toluyl tartaric acid for tartaric acid in diastereomer formation. Triethylamine, phosphoric acid, acetonitrile, water, and 2-propanol were high-performance liquid chromatographic grade.

Instrumentation

The mobile phase was mixed and delivered by means of a Model 50 programmer and two Model 364 pumps (Knauer, Berlin, F.R.G.), a Model TCMA 0120113T Visco-Jet Mixer (Lee, Westbrook, CT, U.S.A.) and a Model LP-21 pulse dampener (SSI, State College, PA, U.S.A.). The sample was introduced with a Model 231 autoinjector (Gilson, Middleton, WI, U.S.A.) equipped with a 20-μl fixed-volume sample loop (Rheodyne, Cotati, CA, U.S.A.) onto a 25 × 0.46 cm I.D. 100 Å PLRP-S poly (styrene–divinyl benzene) reversed-phase column (Polymer Labs. Church Stretton, U.K.). The Model 750/14 ChiraMonitor and a Model 87.00 UV detector

(Knauer) were used in series as detectors. Data acquisition and transformation were accomplished by the Roseate data system (Drew Scientific, London, U.K.). The aqueous component of the mobile phase was prepared from 990 ml of 0.2% phosphoric acid, titrated to pH 7.2 with triethylamine and 10 ml 2-propanol. The organic component of the mobile phase was 990 ml acetonitrile and 10 ml 2-propanol. The aqueous and organic components were mixed by the gradient mixer in the proportion 78:22. The flow-rate was 1.0 ml/min. The mobile phase was degassed and left under a positive pressure of helium. The static polarimeter was a SEPA-200 (Horiba, Irvine, CA, U.S.A.) equipped with a sodium lamp and a 10 mm pathlength cell with a volume of 2.5 ml.

Methods

Solutions of *S*-(−)- and *R*-(+)-nicotine were prepared at a concentration of about 10 mg/ml in the mobile phase for on-line polarimetry, and at about 100 mg/ml in ethanol for static polarimetry. Duplicate 20-μl injections of enantiomeric excesses of 99.1, 96.5, 93.0, 86.1 and 73.5% of *S*-(−)-nicotine were used for on-line polarimetric spiking experiments. For static polarimetry, duplicate measurements were made of enantiomeric excesses of 100, 95.2, 85.8, 81.8, 72.4 and 64.4% of *S*-(−)-nicotine.

Calculations

Error analysis was performed by examining polarimetric response as a function of optical purity. The envelope of uncertainty around a regression line was determined by calculation of the standard error, s_Y, estimated from the expression $s_Y = \{s^2_{Y-X}[1/n + (x_i - \bar{x})^2/\Sigma x^2]\}^{1/2}$, where s^2_{Y-X} is the unexplained mean square error about the regression line, n is the number of observations, $\bar{x}$ is the mean value of enantiomeric excess, $\Sigma x^2 = \Sigma x_i^2 - (\Sigma x_i)^2$, and x_i is a particular value of enantiomeric excess [23]. An upper and lower limit for s_Y are obtained when $x_i = 100$ and $x_i = \bar{x}$, respectively. The percent standard error is the standard error expressed as a percentage of the value at the x_i of interest.

RESULTS

Fig. 1 compares the UV and ChiraMonitor traces that are obtained from (*R*)- and (*S*)-nicotine. It can be seen that both contain a small amount of an optically inactive component eluting at about 8.5 min, while the principal component elutes at about 7 min. Additional UV-positive trace components can be seen to elute between 3 and 5 min. The minor components were estimated to comprise about 5% of each sample by UV peak height. These appear to be optically inactive. It is possible to detect a component unresolved from the principal peak by overlay of the UV trace with the normalized polarimetric trace, as has been demonstrated for ephedrine [22]. Assuming that peak broadening is minimal, a pure enantiomer will exhibit a trace that is of the same shape on both the UV and polarimetric detectors. If two components of differing optical rotation or UV absorbance are imcompletely resolved, differences in the polarimetric and UV peak shapes will be observed. No such peak inhomogeneity was noted for nicotine.

Fig. 2 is a graph of the response of the ChiraMonitor to various loadings of (*R*)-

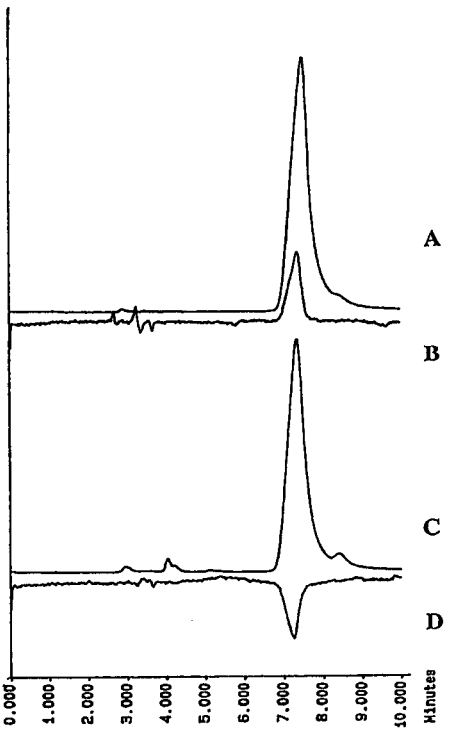

Fig. 1. Comparison of UV and ChiraMonitor response of *R*-(+)- and *S*-(−)-nicotine separated on PLRP-S. Separation was performed on a 5 μm, 25 × 0.46 cm I.D. PLRP-S reversed-phase column using water–acetonitrile–2-propanol (78:22:1) at 1 ml/min as the mobile phase. The water was buffered to pH 7.2 with 0.2% triethylamine phosphate. UV detection was at 276 nm. The upper traces are (A) UV and (B) ChiraMonitor response to *S*-(−)-nicotine. The lower traces are (C) UV and (D) ChiraMonitor responses to *R*-(+)-nicotine. The horizontal axis is retention time in min, while the vertical axis is response in arbitrary units.

and (*S*)-nicotine. Separations were performed as in Fig. 1. Fig. 2 demonstrates that the response of the ChiraMonitor is essentially linear with concentration up to a loading of 200 μg. Above that loading, there are deviations from linearity. The detection limit, defined as four times the peak-to-through amplitude of the noise, was determined to be about 12 μg.

Fig. 3 shows the specific optical rotations of chromatograms of mixtures obtained by the mixture of solutions of *R*-(−)-nicotine and *S*-(+)-nicotine. Separations were performed as in Fig. 1. Loading was about 200 μg. The on-line polarimeter exhibited a coefficient of variation of about 2.1% in the value of the rotation, and analysis of variance indicated that the percent standard error was 0.7% at the mean to 1.0% at the extreme. Therefore, the *purity* of an unknown sample can be determined to ± 0.5% or less by comparison with the calibration curve. The precision, of course, depends on the number of data points used to construct the calibration curve as well as the number of sample replicates, and would be lower if fewer data points were used. For the static polarimeter, an average coefficient of variation in the dupli-

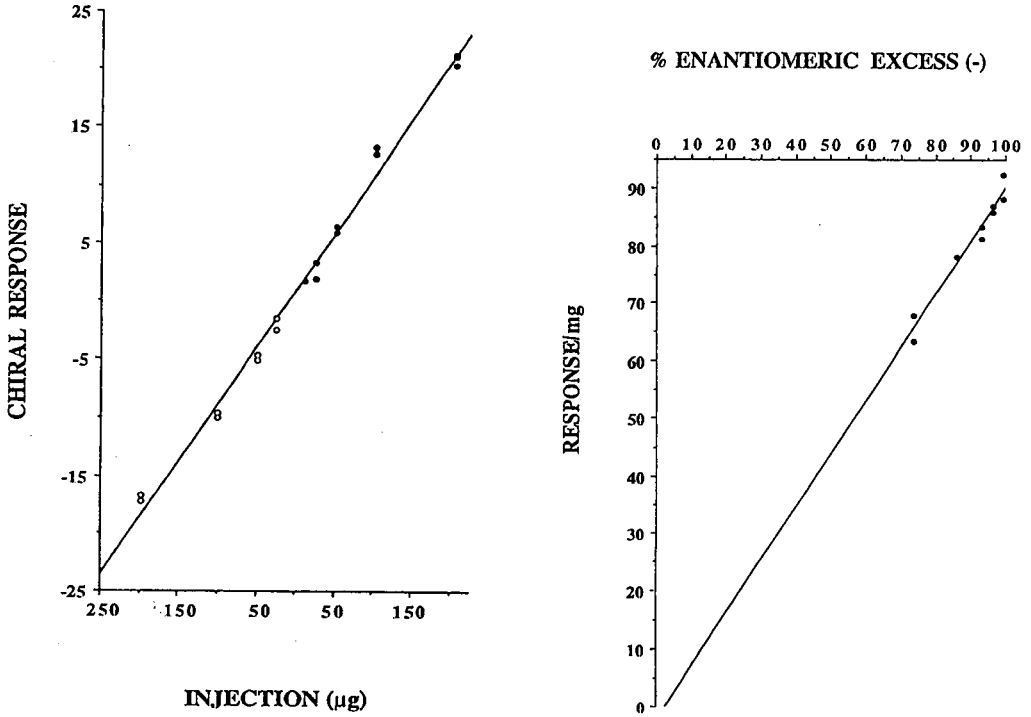

Fig. 2. Linearity of ChiraMonitor response to *R*-(+)- and *S*-(−)-nicotine. Separation conditions are as in Fig. 1. The vertical axis is the chiral peak height in arbitrary units. The horizontal axis to the right of zero is the loading of *S*-(−)-nicotine in units of μg, while the horizontal axis to the left of zero is the loading of *R*-(+)-nicotine in units of μg. ○ = *R*-(+)-nicotine, ● = *S*-(−)-nicotine.

Fig. 3. Spiking of *S*-(−)-nicotine with *R*-(+)-nicotine. Mixtures of *S*-(−)- and *R*-(+)-nicotine were prepared so that the total amount of nicotine was approximately 10 mg/ml. Then, 20 μl of each of these mixtures was injected onto the chromatographic system described in Fig. 1. The ChiraMonitor response divided by the loading is graphed on the vertical axis, while the enantiomeric excess is graphed on the horizontal axis. The mixtures presented on the graph represent duplicate injections of enantiomeric excesses of 99.1, 96.5, 93.0, 86.1 and 73.5% of *S*-(−)-nicotine. Reproduced, with permission from *American Laboratory* [22].

cate values of the observed rotation of 0.4% was observed. Analysis of variance indicated that the percent standard error in rotation increased from 0.2% at the mean to 0.4% at the extreme.

CONCLUSIONS

On-line polarimetry has been shown in the present work to be over 1000 times as sensitive and almost as precise as conventional polarimetry in the determination of the enantiomeric purity of nicotine. Several apparently optically inactive minor components, amounting to about 5% of the total were resolved from the nicotine peak by reversed-phase chromatography. Overlay of the UV chromatogram with a normalized ChiraMonitor trace indicated that no other component co-eluted with nicotine.

On-line polarimetry can be regarded as inherently more accurate than conventional polarimetry because minor components may be resolved chromatographically. Peak inhomogeneity, *i.e.* the presence of an incompletely resolved minor component may be readily detected if either the UV spectrum or the optical rotation differ from the those of the principal component.

It has been difficult to separate the enantiomers of nicotine by chiral chromatography [13–15], requiring the development of alternative means of quantitation. The *R*-(+)- and *S*-(−)-isomers differ in both efficacy and toxicity, making precise determination of optical purity desirable. The sensitivity of the ChiraMonitor was found to be several decades less than would be desired for pharmacological analysis of nicotine in blood and tissue, but adequate for determinations from urine. The greater specificity of polarimetric detection (relative to UV detection) makes it appropriate for complex samples, such as nicotine formulated for administration. On-line polarimetric determination of nicotine was rapid, requiring only about 10 min per run; sensitive, requiring only 200 μg of sample; and precise, permitting quantitation to about ± 0.5% purity.

ACKNOWLEDGEMENTS

Portions of this paper were presented as a poster at the *Western Carolinas Chromatography Discussion Group, Greenville, SC, July 1989* and at the *198th ACS Meeting, Miami Beach, FL, September 1989*. Permission by *American Laboratory* to reprint Fig. 3 is gratefully acknowledged.

REFERENCES

1 A. Pictet and P. Crepieux, *Chem. Ber.*, 28 (1895) 1904.
2 A. Pictet and A. Rotschy, *Chem. Ber.*, 37 (1904) 1225.
3 R. H. F. Manske and H. L. Holmes (Editors), *The Alkaloids: Chemistry and Physiology*, Vol. 1, Academic Press, New York, 1950.
4 N. E. McIndoo, R. C. Roark and R. L. Busbey, *A Bibliography of Nicotine Part II. The Insecticidal Uses of Nicotine and Tobacco (Publication E-392)*, Vol. 2, section 1, U.S. Department of Agriculture, Bureau of Entomology, Washington, D.C., 1936.
5 J. Wilbert, *Tobacco and Shamanism in South America*, Yale University Press, New Haven, CT, 1987, Ch. 4.
6 J. A. Baron, *Neurology*, 36 (1986) 1490.
7 B. Sahakian, G. Jones, R. Levy, J. Gray and D. Warburton, *Brit. J. Psychiatry*, 154 (1989) 797.
8 B. Holmstedt, in M. J. Rand and K. Thuran (Editors), *The Pharmacology of Nicotine*, IRL Press, Washington, D.C., 1988, pp. 61–88.
9 P. Koenig (Editor), *Die Entdeckung des Reinen Nikotins im Jahre 1828 an der Universität Heidelberg durch Reimann und Posselt mit einer Beschreibung ihrer Vorlaufer und mit Abbildungen*, Arthur Geist, Bremen, 1940.
10 D. I. Macht, *Proc. Natl. Acad. Sci., U.S.A.*, 15 (1929) 63.
11 M. D. Aceto, B. R. Martin, I. M. Uwaydah, E. L. May, L. S. Harris, C. Izazola-Conde, W. L. Dewey, T. J. Bradshaw and W. C. Vincek, *J. Med. Chem.*, 22 (1979) 174.
12 W. B. Edwards III and R. McCuen, *J. Org. Chem.*, 48 (1983) 2484.
13 J. I. Seeman, H. V. Secor, D. W. Armstrong, K. D. Timmons and T. J. Ward, *Anal. Chem.*, 60 (1988) 2120.
14 J. I. Seeman, H. V. Secor, D. W. Armstrong, K. D. Ward and T. J. Ward, *J. Chromatogr.*, 483 (1989) 169.
15 D. W. Armstrong, L. A. Spino, S. M. Han, J. I. Seeman and H. V. Secor, *J. Chromatogr.*, 411 (1987) 490.

16 W. Boehme, G. Wagner, U. Oehme and U. Priesnitz, *Anal. Chem.*, 54 (1982) 709.
17 W. Boehme, *Chromatogr. News,* 8 (1980) 38.
18 W. Boehme, H. Stenz and O. Bonsignori, *Int. Lab.*, June (1983) 28.
19 E. S. Yeung, L. E. Steenhoek, S. D. Woodruff and J. C. Kuo, *Anal. Chem.*, 52 (1980) 1399.
20 B. H. Reitsma and E. S. Yeung, *J. Chromatogr.*, 362 (1986) 353.
21 D. K. Lloyd, D. M. Goodall and H. Scrivener, *Anal. Chem.*, 61 (1989) 1238.
22 J. K. Swadesh, *Am. Lab. (Fairfield, Conn.)*, February (1990) 72.
23 R. R. Sokal and F. J. Rohlf, *Biometry*, W. H. Freeman, San Francisco, 1969, Ch. 14.

Journal of Chromatography, 543 (1991) 137–145
Elsevier Science Publishers B.V., Amsterdam

CHROM. 23 093

Resolution of lutein and zeaxanthin using a non-endcapped, lightly carbon-loaded C_{18} high-performance liquid chromatographic column

ADAM M. GILMORE and HARRY Y. YAMAMOTO*

University of Hawaii at Manoa, Department of Plant Molecular Physiology, 3190 Maile Way, St. John 503, Honolulu, HI 96822 (U.S.A.)

(First received July 19th, 1990; revised manuscript received January 3rd, 1991)

ABSTRACT

A new rapid and reproducible high-performance liquid chromatographic method using Spherisorb ODS-1, a non-endcapped, lightly carbon-loaded column material, for the separation of higher-plant chloroplast pigments is described. The method resolves lutein and zeaxanthin, as well as all other major and most minor pigments at or near baseline by either of two solvent programs. Program I is faster and more sensitive than program II while the latter resolves pheophytin *a* and β,ε-carotene slightly better than program I. Both programs use an initial buffered aqueous mixture that appears critical for this application of ODS-1. The method is well suited for analysis of xanthophyll-cycle pigment changes.

INTRODUCTION

Baseline separation of plastid pigments from higher plants in a simple, reproducible, one-step method has yet to be reported. Difficulties arise from the wide-ranging polarities of the comprising pigments and the limited selectivity of the columns. The carotenes are non-polar whereas at the other extreme 9′-*cis*-neoxanthin is polar. Separation of structural isomers such as lutein from zeaxanthin and β,ε-carotene from β,β-carotene is usually incomplete in most reversed-phase high-performance liquid chromatographic (HPLC) procedures. Of several aqueous [1–9] and non-aqueous [10,11] reversed-phase HPLC methods reported for plant and algal pigments, only one method separates lutein from zeaxanthin at the baseline [12]. Rapid quantitative separation of lutein and zeaxanthin has become important for research on photoprotective processes in plants because of the apparent relationship between zeaxanthin and non-photochemical quenching of excess energy in the antennae chlorophylls of photosystem II [13]. Light induces changes in zeaxanthin levels via interconversions with violaxanthin and antheraxanthin in the xanthophyll cycle [14].

Thayer and Björkman [12] obtained baseline separation of lutein and zeaxanthin with a non-endcapped Zorbax-ODS column. Unfortunately this packing material is not presently being manufactured and therefore is not widely available. We sought an alternative solution and here report a new method using ODS-1, a non-endcapped and

0021-9673/91/$03.50

lightly carbon-loaded material. The method separates lutein and zeaxanthin and most other chloroplast pigments at or near baseline. Procedures for analyses of pigment extracts from whole leaves and isolated chloroplasts and the applicability of the method for xanthophyll-cycle studies are detailed.

EXPERIMENTAL

Instrumentation

The chromatographic system was a Beckman/Altex Model 334 gradient liquid chromatograph (Beckman Instruments, Berkeley, CA, U.S.A.) equipped with a Waters 990 photodiode array detector (Millipore, Milford, MA, U.S.A.). All solvents were HPLC grade and obtained from Fisher Scientific, Fair Lawn, NJ, U.S.A. Pigment standards were quantitated spectrophotometrically with a DW-2000 UV–VIS dual-wavelength dual-beam spectrophotometer (SLM Instruments, Urbana, IL, U.S.A.).

Spherisorb ODS-1 columns (5-μm particle size, 250 mm $\times$ 4.6 mm I.D.) were from Alltech, Deerfield, IL, U.S.A. ODS-1 is a non-endcapped, 6% carbon, spherical silica material manufactured by Phase Separations, Clwyd, U.K. The guard column was ODS-1 or Adsorbosphere C_{18} direct-connect cartridge, also from Alltech.

Liquid chromatography

The flow-rate for all separations was 2 ml min^{-1} and all sample injections were 20 μl. Two solvent programs were developed. Program I: solvent A-1 was ran isocratically from 0 to 4 min followed by a 2.5-min linear gradient to 100% solvent B. Program II: solvent A-1 was ran isocratically for 6 min followed by a 10-min linear gradient to 100% solvent C. Solvent A-2 replaced solvent A-1 in some experiments. Solvent mixtures were: A-1, acetonitrile–methanol–Tris · HCl buffer 0.1 *M* pH 8.0 (72:8:3); A-2, acetonitrile–methanol–Tris · HCl buffer 0.1 *M* pH 8.0 (75:12:4); B, methanol–hexane (4:1); C, methanol–ethyl acetate (68:32).

The columns were re-equilibrated between samples for a minimum of 10 min with solvent A-1 for both solvent programs. When changing solvent programs the columns were equilibrated with 60 ml of solvent B or C, and then with 30 ml of solvent A-1. This extensive re-equilibration was necessary when changing programs to remove residual effects of the prior solvents B or C. All runs were at room temperature.

Pigment identification and calibration

β,ε-Carotene and β,β-carotene were obtained from Sigma, St. Louis, MO, U.S.A. Violaxanthin, lutein and zeaxanthin were isolated according to Yamamoto *et al.* [15]. Antheraxanthin, 9′-*cis*-neoxanthin, lactucaxanthin and pheophytins *a* and *b* were identified by absorption spectra.

Chlorophylls *a* and *b* were quantitated according to Vernon [16]. Lutein, violaxanthin and zeaxanthin standards were in ethanol and β,ε-carotene and β,β-carotene were in hexane. Extinction coefficients ($E^{1\%}_{1cm}$) used for quantitation were: lutein and violaxanthin (2550), zeaxanthin (2540), β,ε-carotene (2725) and β,β-carotene (2590) [17]. Linearity of the peak-area (absorbance units $\times$ minutes) calibrations against pigment concentrations was $r^2 \geqslant 0.991$ for all pigment standards. The photodiode-detector wavelength for integration of peak areas was 440 nm.

Conversion factors for peak area to nmol per injection for program I, solvent A-1 were: violaxanthin (20.72); lutein (27.10); zeaxanthin (26.90); chlorophyll *a* (34.94); chlorophyll *b* (38.53); β,ε-carotene (18.51); β,β-carotene (18.94). Antheraxanthin was estimated with the conversion factor for lutein. Lactucaxanthin and 9′-*cis*-neoxanthin concentrations were estimated using the conversion factor for violaxanthin.

Preparation of isolated chloroplast and leaf-disk samples

Leaf disks and isolated chloroplasts with high and low levels of zeaxanthin were prepared to demonstrate the effectiveness of the method for quantitative analysis of the xanthophyll cycle. Chloroplasts were isolated from market lettuce (*Lactuca sativa* L. cv. Romaine) according to Yamamoto *et al.* [18]. Prior to isolation, the leaves were dark-adapted for 12 h to reduce the background level of zeaxanthin. Addition of 10 m*M* sodium ascorbate induced zeaxanthin formation in osmotically shocked chloroplasts suspended in 50 m*M* sodium citrate buffer at pH 5.0. Zeaxanthin formation was stopped after 10 min with 1.5 m*M* DTT. All reactions had a final volume of 3 ml and the chlorophyll concentration was 30 μg total chlorophyll per ml. Chloroplast suspensions were divided into two microcentrifuge tubes, centrifuged for 5 min and the resulting pellet extracted as described under pigment extractions.

Leaf disks (10 cm^2, approximately 0.25 g) were punched from fully developed leaves of shade-grown *Anthurium andraeanum* cv. Brown Tulip. Prior to removal of disks, the plant was dark-adapted for 12 to 15 h to reduce the background level of zeaxanthin. For light-induced zeaxanthin formation, a leaf disk was floated on water in a water-jacketed beaker and exposed to 2000 $\mu E\ m^{-2}\ s^{-1}$ white light for 20 min from a Model 640-HD lamp (Acme Light, Skokie, IL, U.S.A.). The light was filtered through 2.5 cm of refrigerated circulating water to remove heat. Leaf-disk temperature remained between 18 and 25°C.

Pigment extractions

Pigments were extracted at room temperature and under dim laboratory light. Chloroplast pellets (45 μg total chlorophyll) were suspended in 0.25 ml 100% acetone for 5 min at room temperature with occasional vortex mixing, centrifuged for 5 min in a microcentrifuge and the resulting supernatant saved. The acetone-dried pellets were re-extracted as above to ensure complete extraction of β,β-carotene and β,ε-carotene. The supernatants were pooled and then filtered through 0.2 μm nylon-66 microcentrifuge filters (Microfilterfuge; Rainin, Woburn, MA, U.S.A.). Leaf disks were ground in a tissue homogenizer with 25 mg $CaCO_3$ and 2.5 ml 100% acetone. The extract was divided into two microcentrifuge tubes and spun for 5 min. The supernatants were removed and the pellets extracted again with 1.25 ml 100% acetone each at room temperature for 5 min, with occasional vortex mixing before spinning again for 5 min. The supernatants were pooled and filtered as described for chloroplast extracts. The pigment extracts were either analyzed immediately or after 1 to 2 days storage at −20°C under argon. No pigment degradation was observed during this storage period.

RESULTS AND DISCUSSION

Solvent programs

Fig. 1 shows chromatograms of *Anthurium* extracts using solvent program I. The extracts were prepared from dark-adapted (A) and light-treated leaf disks (B). Fig. 1C shows the extract in (B) after acid treatment. The program resolved lutein, zeaxanthin and most of the other plastid pigments at baseline in about 13 min. A low level of zeaxanthin was detectable in the dark-adapted sample. Separation of β,β- and β,ε-carotene was incomplete although adequate for detection and estimation.

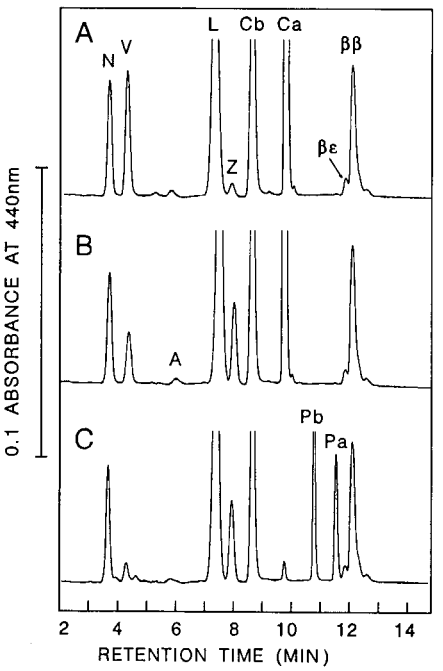

Fig. 1. Chromatograms of anthurium extracts on column 1 with program I, solvent A-1. (A) Before zeaxanthin formation; (B) after zeaxanthin formation; and (C) after acid treatment of the same extract used in B. Abbreviations: N = 9′-*cis*-Neoxanthin; V = violaxanthin; A = antheraxanthin; L = lutein; Z = zeaxanthin; Cb = chlorophyll *b*; Ca = chlorophyll *a*; $\beta\varepsilon$ = β,ε-carotene; $\beta\beta$ = β,β-carotene; Pb = pheophytin *b*; Pa = pheophytin *a*.

Pheophytins *a* and *b* were resolved but the former just barely from β,ε-carotene. Fig. 2 shows that the method also resolves lactucaxanthin in lettuce extracts. Zeaxanthin was undetectable in the dark-adapted lettuce (Fig. 2A). Lettuce also apparently lacks β,ε-carotene.

Increasing the hexane content in solvent B from methanol–hexane (4:1) to (3:1) improved the separation of the pheophytins and carotenes but also introduced a refractive-index change that interfered with the quantitation of the carotenes (data not shown). The proximity of pheophytin *a* to β,ε-carotene with program I is not critical for most applications since pheophytins are not usually detectable at 440 nm in

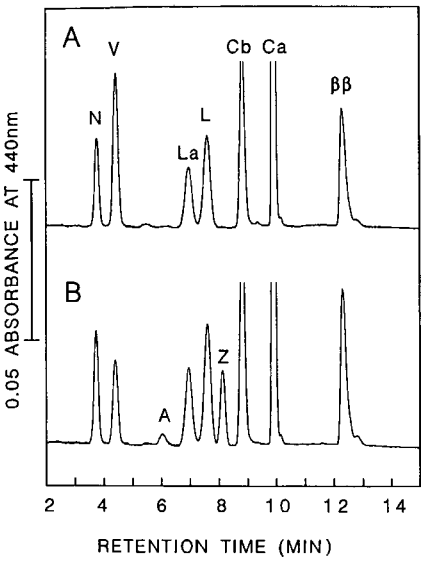

Fig. 2. Chromatograms of lettuce extracts on column 1 with solvent program I, solvent A-1. (A) Before zeaxanthin formation; (B) after zeaxanthin formation. La = lactucaxanthin; other abbreviations as in Fig. 1.

undegraded pigments extracts. When maximum separation of the carotenes and pheophytins is important, program II can be used. Fig. 3 shows that the separations with program II were comparable to program I except that the pheophytins eluted after the carotenes (Fig. 3C) and were more completely resolved from the carotenes. Program II, however, is appreciably longer than program I.

Separation of lutein from zeaxanthin is reportedly less enhanced with endcapped materials [7,12]. Indeed, endcapped column materials such as Lichrosorb RP-18 or ODS-2 did not separate zeaxanthin and lutein satisfactorily with this method (data not shown). Presumably interaction of these pigments with the exposed silanol sites of the non-endcapped ODS-1 material is important. The aqueous condition in solvent A-1 was a key to the successful application of ODS-1 inasmuch as zeaxanthin and chlorophyll *b* were otherwise unresolved. We speculate that water is required for sufficient interaction between the pigments and the lightly carbon-loaded ODS-1 material.

The Tris buffer in solvent A-1 neutralizes the acidity of the ODS-1 columns. Without Tris the chlorophylls and carotenoids degraded. Tris buffer also neutralizes acids inherently present in the acetonitrile solvent [1]. Although chloride ions are known to harm stainless steel we have seen no evidence of corrosion in our system. We flush the system with 20–30 ml of methanol after each days' runs to minimize corrosion and to eliminate residual hexane in the column material. This method demonstrates that non-endcapped column materials, which may have been previously avoided because of their tendency to isomerize and degrade pigments, can be used successfully for pigment separations with proper precautions.

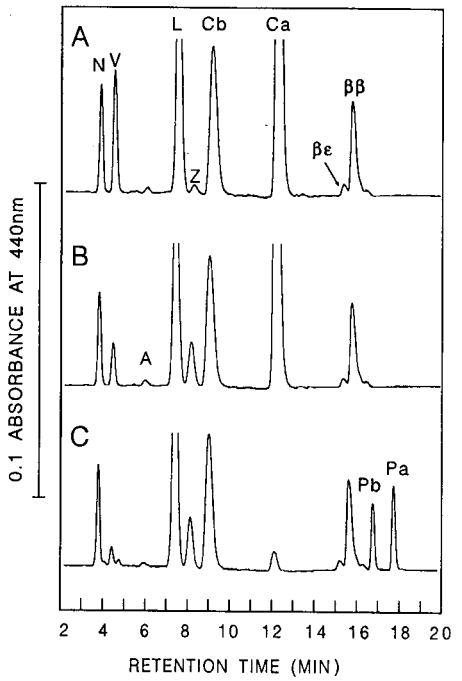

Fig. 3. Chromatograms of the same extracts as in Fig. 1 on column 1 with program II, solvent A-1. Abbreviations as in Fig. 2.

Column variability

Column variability is common in HPLC and may be even greater in non-endcapped materials. We tested three ODS-1 columns designated 1, 2 and 3. Whereas columns 1 and 2 gave similar separations, column 3 performed poorly. As shown in Fig. 4A, the resolution of zeaxanthin and chlorophyll *b* was poor and peak sensitivity

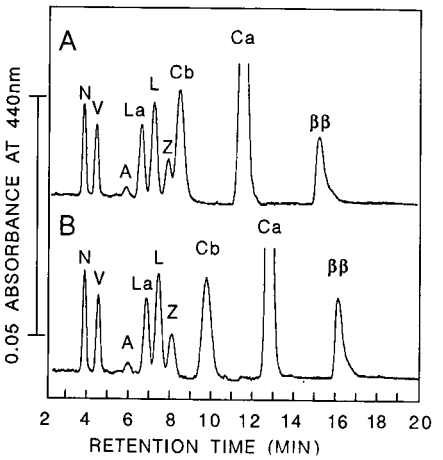

Fig. 4. Chromatograms of lettuce extracts after zeaxanthin formation on column 3 with program II using (A) solvent A-1 and (B) solvent A-2. Abbreviations as in Fig. 2.

was low on column 3 (solvent A-1, program II). We found that the poor resolution of column 3 was improved by further increasing the water and methanol content of the mobile phase. Fig. 4B shows that using the more aqueous A-2 mixture resolved lactucaxanthin, lutein, zeaxanthin and chlorophyll *b* adequately but still not as well as on columns 1 and 2. Apparently, increasing the polarity of the mobile phase by increasing the Tris · HCl buffer and methanol higher than in solvent A-1 caused chlorophyll *b* to interact sufficiently with the stationary phase to separate zeaxanthin. Solvent A-2 also worked satisfactorily with columns 1 and 2, but the resolution and sensitivity for lactucaxanthin, lutein and zeaxanthin was higher with solvent A-1. Thus, we regard solvent A-2 as a second-line solvent to be used only with columns that do not perform satisfactorily with solvent A-1.

The source of the observed column differences is not known. The supplier's test chromatograms for columns 1, 2 and 3 for the separation of ethyl benzene were 75 575, 125 479, and 101 429 plates m^{-1}, respectively. Thus, the reported efficiencies do not explain the performance difference between the columns. Column 3, however, separated N,N-diethyl-*m*-toluamide and toluene by only 0.56 min whereas columns 1 and 2 separated these compounds by 0.91 and 1.22 min, respectively. The separation of these test components appears to correlate with the poorer resolution of chlorophyll *b* and zeaxanthin on column 3 (Fig. 4A). The increased water-content requirement in the mobile phase suggests column 3 may have slightly less carbon loading than the other columns.

Retention time and sensitivity of solvent programs I and II

Table I compares the relative retention times for the major pigments of lettuce on column 1. Retention times varied by less than 0.05 min from the mean in five successive runs for either solvent program. The polar xanthophylls eluted earlier in program II than in program I, whereas the chlorophylls and β,β-carotene eluted later. The peak heights (sensitivity) of the major non-polar pigments were significantly higher in program I than program II, whereas the sensitivities for the polar xanthophylls were similar. For example, chlorophylls *b* and *a* were approximately two- and three-fold higher, respectively, for program I than for program II. Also, β,β-carotene peaks were over 50% higher in program I than in program II. In our studies the rapidity and increased sensitivity of program I outweighed the resolution problem of pheophytin *a* and β,ε-carotene. The detectable limit for individual xanthophyll pigments (V, A or Z) was about 5–7 pmol per 20-μl injection for program I. This is lower sensitivity than that reported by Thayer and Björkman [12] but was more than sufficient for studies involving intact leaf tissue and isolated chloroplasts. The sensitivity can be increased by slowing the flow-rate in both programs to 1 ml per min and proportionally adjusting the changeovers to solvents B or C.

Quantitative analyses of xanthophyll cycle changes with ODS-1

The following data demonstrate the usefulness of this method for quantitative analysis for the violaxanthin-cycle. Table II shows the relative pigment content in lettuce chloroplasts before and after dark ascorbate-induced zeaxanthin formation. Stimulation of violaxanthin de-epoxidation converts violaxanthin to zeaxanthin with virtual mol to mol stoichiometry [14]. The total relative concentrations of the violaxanthin cycle pigments (V + A + Z) were consistent within standard deviation for

TABLE I

RETENTION TIMES (MIN) FOR MAJOR LETTUCE CHLOROPLAST PIGMENTS FOR FIVE SUCCESSIVE SEPARATIONS WITH BOTH SOLVENT PROGRAMS I AND II

Separation	Retention time (min)						
	N	V	La	L	Cb	Ca	ββ
Solvent program I[a]							
1	3.81	4.47	7.00	7.66	8.89	9.96	12.34
2	3.81	4.46	7.02	7.68	8.89	9.96	12.36
3	3.82	4.47	7.03	7.68	8.90	9.99	12.37
4	3.85	4.53	7.11	7.76	8.93	10.00	12.38
5	3.87	4.52	7.11	7.76	8.95	10.00	12.38
Mean	3.83	4.49	7.05	7.71	8.91	9.98	12.37
S.D.	0.03	0.03	0.05	0.05	0.03	0.02	0.02
Solvent program II[b]							
1	3.74	4.40	6.78	7.48	9.13	12.33	15.96
2	3.75	4.41	6.79	7.47	9.11	12.28	15.88
3	3.75	4.41	6.80	7.49	9.11	12.28	15.84
4	3.77	4.43	6.80	7.48	9.17	12.34	15.85
5	3.81	4.47	6.86	7.55	9.24	12.40	15.88
Mean	3.76	4.42	6.81	7.49	9.15	12.33	15.88
S.D.	0.03	0.03	0.03	0.03	0.05	0.05	0.05

[a] Solvent system same as in Fig. 1.
[b] Solvent system same as in Fig. 3.

TABLE II

RELATIVE PIGMENT CONCENTRATION FOR LETTUCE CHLOROPLASTS BEFORE AND AFTER DARK, pH 5.0, ASCORBATE-INDUCED ZEAXANTHIN FORMATION

All values are relative to chlorophyll *a* (mmol mol^{-1} Ca), except Cb/Ca which is (mol/mol). All values are the mean of three individual experiments either before or after zeaxanthin formation. Solvent program I, solvent A-1, and column 1 were used for all runs. Abbreviations same as Fig. 2.

	Pigment concentration								
	N	V	A	Z	V+A+Z	La	L	Cb/Ca	ββ
Pre-zeaxanthin									
Mean	81.89	163.75	0.00	0.00	163.75	93.96	171.98	0.35	134.85
S.D.	0.54	2.11	0.00	0.00	2.11	1.44	0.88	0.01	0.83
C.V. (%)	0.66	1.29	0.00	0.00	1.29	1.53	0.51	2.66	0.62
Post-zeaxanthin									
Mean	81.91	70.64	15.32	77.92	163.88	93.35	173.34	0.36	134.71
S.D.	0.85	1.44	1.32	1.22	2.14	0.11	1.08	0.00	1.64
C.V. (%)	1.04	2.04	8.61	1.57	1.31	0.12	0.62	0.47	1.22

before and after zeaxanthin formation. The variance of the individual violaxanthin cycle components (V, A and Z) in the post-zeaxanthin runs reflected the variance of replicate treatments. All non-violaxanthin cycle pigments remained unchanged. The coefficient of variance for the other major pigments was less than 2.66% for both the before and after runs.

CONCLUDING REMARKS

ODS-1, a currently available high-performance liquid chromatographic column material, with the solvent programs described gives rapid and quantitative separation of all major and most minor chloroplast pigments. The method is well suited for studies on the xanthophyll cycle. Although the method has not been thoroughly tested for separation of more complex pigment compositions such as those found in phytoplankton, we have observed good separation of pigments in undegraded extracts of diatoms and several species of brown algae.

ACKNOWLEDGEMENT

This research was supported in part by a U.S.D.A. CSRS Special Grant No. 88-34135-3606, managed by the Pacific Basin Advisory Group.

NOTE ADDED IN PROOF

The authors of ref. 12 have informed us that non-endcapped Zorbax ODS recently became commercially available again.

REFERENCES

1 D. Siefermann-Harms, *J. Chromatogr.*, 448 (1988) 411.
2 C. A. Bailey and B. H. Chen, *J. Chromatogr.*, 455 (1988) 396.
3 T. Braumann and L. H. Grimme, *J. Chromatogr.*, 170 (1979) 264.
4 T. Braumann and L. H. Grimme, *Biochim. Biophys. Acta.*, 637 (1981) 8.
5 P. Bergweiler and C. Lütz, *Environ. Exp. Bot.*, 26 (1986) 207.
6 K. Eskins and L. Harris, *Photochem. Photobiol.*, 33 (1981) 131.
7 S. W. Wright and J. D. Shearer, *J. Chromatogr.*, 294 (1984) 281.
8 M. Zapata, A. M. Ayala, J. M. Franco and J. L. Garrido, *Chromatographia*, 23 (1987) 26.
9 J. de las Rivas, A. Abadia and J. Ababia, *Plant Physiol.*, 91 (1989) 190.
10 F. Khachik, G. R. Beecher and N. F. Whittaker, *J. Agric. Food Chem.*, 34 (1986) 603.
11 E. A. Landis, J. D. Mikkelsen and B. L. Møller, *Carlsberg Res. Commun.*, 48 (1983) 131.
12 S. S. Thayer and O. Björkman, *Photosynth. Res.*, 23 (1990) 331.
13 B. Demmig-Adams, W. W. III Adams, U. Heber, S. Neimanis, K. Krüger, F.-C. Czygan, *Plant Physiol.*, 92 (1990) 293.
14 H. Y. Yamamoto, *Pure Appl. Chem.*, 51 (1979) 639.
15 H. Y. Yamamoto, E. E. Chenchin and D. K. Yamada, in M. Avron (Editor), *Proceedings of the Third International Congress on Photosynthesis*, Elsevier, Amsterdam, 1974, p. 1999.
16 L. P. Vernon, *Anal. Chem.*, 32 (1960) 1144.
17 B. H. Davies, in T. W. Goodwin (Editor), *Chemistry and Biochemistry of Plant Pigments*, Vol. I, Academic Press, New York, 2nd ed., 1976, Ch. 19, p. 38.
18 H. Y. Yamamoto, L. Kamite and Y. Y. Wang, *Plant Physiol.*, 49 (1972) 224.

Journal of Chromatography, 543 (1991) 147–155
Elsevier Science Publishers B.V., Amsterdam

CHROM. 23 081

Characterization of major carotenoids in water convolvulus (*Ipomoea aquatica*) by open-column, thin-layer and high-performance liquid chromatography

B. H. CHEN*, S. H. YANG and L. H. HAN
Department of Nutrition and Food Science, Fu Jen University, Taipei 24205 (Taiwan)
(First received September 18th, 1990; revised manuscript received December 4th, 1990)

ABSTRACT

The major carotenoids present in water convolvulus (*Ipomoea aquatica*) were characterized by open-column chromatography, thin-layer chromatography (TLC), and high-performance liquid chromatography (HPLC). A 1:1 mixture of activated magnesium oxide and diatomaceous earth was used as the major adsorbent to separate carotenes, monohydroxy, dihydroxy and polyoxy pigments by open-column chromatography. Carotenes and cryptoxanthin were eluted with hexane–acetone at 96:4 and 90:10, respectively. Lutein, violaxanthin and neoxanthin were eluted with hexane–acetone–methanol at 85:15:0.2, 85:15:0.2 and 85:15:1.5, respectively. The elution sequence of lutein and violaxanthin was dependent on the amount of methanol present. A lutein band containing lutein and lutein epoxide was further separated by TLC. An HPLC isocratic solvent system of acetonitrile–methanol–ethyl acetate (75:15:10) was found to be appropriate for determining the reproducibility of retention time with respect to separated bands obtained by open-column chromatography. Each band was identified by comparing the absorption spectra and retention time with reference standards. The major carotenoids present in water convolvulus were β-carotene, lutein, lutein epoxide, violaxanthin and neoxanthin. The amount of each major carotenoid was also determined.

INTRODUCTION

Carotenoids are important biological compounds that are widely distributed in green plants. Carotenoids have been found effective in preventing photosensitization [1,2] and the formation of skin tumours in mice [3,4], and in increasing immune response in rats [5]. Water convolvulus (*Ipomoea aquatica*) is a popular green vegetable grown in Taiwan and China. It has been well documented [6] that increased consumption of water convolvulus is protective against high blood pressure and nosebleeds. As water convolvulus is also a rich source of carotenoids, it has received considerable attention regarding its role in human nutrition and health. However, no information is available as to the major carotenoids present in water convolvulus.

The current AOAC method (1984) [7] uses silica gel as the major adsorbent to separate carotenes, monohydroxy pigments (*e.g.*, zeinoxanthin and cryptoxanthin), dihydroxy pigments (*e.g.*, lutein and zeaxanthin) and polyoxy pigments (*e.g.*, violaxanthin and neoxanthin) by open-column chromatography. It has been reported [8] that losses or degradation of carotenoids could occur on silica columns. Hence it is

0021-9673/91/$03.50

necessary to use magnesium oxide instead of silica gel as the major adsorbent to separate the major carotenoids in water convolvulus. The AOAC method also uses a binary solvent system of hexane–acetone in different proportions to separate polar xanthophylls. However, this solvent system failed to resolve polyoxy pigments such as violaxanthin and neoxanthin. Moreover, it has been established [9–11] that with ternary solvent mixtures it is possible to increase sample resolution by optimizing the mobile phase selectivity while maintaining a constant solvent strength. Therefore, by adding methanol as a modifier to the binary solvent system it is possible to separate some major xanthophylls such as lutein, violaxanthin and neoxanthin.

The objectives of this study were to use open-column chromatography to separate major carotenoids in water convolvulus, to use thin-layer chromatography (TLC) to separate pigments that could not be resolved by open-column chromatography and to use high-performance liquid chromatography (HPLC) to determine the reproducibility of retention time with respect to separated bands for the confirmation of major carotenoids in water convolvulus.

EXPERIMENTAL

Instrumentation

The HPLC instrument consisted of a Hewlett-Packard (Palo Alto, CA, U.S.A.) 1084B liquid chromatograph with a variable-wavelength UV–VIS detector and a Phenomenex (Torrance, CA, U.S.A.) stainless-steel column (25 cm × 4.6 mm I.D.) with an octadecyl (C_{18}) packing of 5 μm particle size. A sensitivity of 0.0064 a.u.f.s was used, and a Hewlett-Packard 79850B integrator was used to record retention times and chromatograms. Spectrophotometric determinations were made with a Hitachi (Tokyo, Japan) Model 220S double-beam spectrophotometer. A solvent system of acetonitrile–methanol–ethyl acetate (75:15:10) pumped at flow-rates of 1.0 and 2.0 ml/min was used.

Marerials

Water convolvulus and yellow corn were purchased from a local supermarket. *trans*-β-Carotene and lutein (75% purity) were purchased from Sigma (St. Louis, MO, U.S.A.). Zeinoxanthin, cryptoxanthin and zeaxanthin standards were prepared from yellow corn according to Quackenbush *et al.* [12]. Lutein epoxide was prepared from water convolvulus by TLC using hexane–acetone–methanol (90:29:1). Violaxanthin and neoxanthin standards were prepared from Bermuda grass according to Chen and Bailey [13].

All solvents were purchased from Merck (Taipei, Taiwan). Acetonitrile, methanol and ethyl acetate were of HPLC grade and hexane, acetone, ethanol and toluene were of ACS grade. HPLC-grade solvents were filtered through a 0.2-μm membrane filter and degassed under vacuum prior to use.

The silica gel, diatomaceous earth and MgO adsorbents were obtained from Merck. The silica gel TLC plates were made with a Camag spreader and activated at 110°C for 2 h before spotting samples.

Purification of lutein standard

Lutein standard purchased from Sigma was found not to be pure by open-

column chromatography, so a further purification step was necessary. A 1-mg amount of lutein dissolved in 1 ml of acetone was pipetted onto a column (30 cm × 12.5 mm I.D.) containing a mixture of activated MgO and diatomaceous earth (1:1). Three bands were observed on the column when employing hexane–acetone–methanol (89:10:1) [12]. One band with the deepest yellow colour was collected with the same solvent system and used as a reference standard of lutein.

Sample preparation and extraction procedure

A 1-kg amount of water convolvulus was freeze-dried to minimize oxidative loss and ground into a fine material, 10 g of which were extracted with 75 ml of hexane–acetone–methanol–toluene (10:7:6:7) in a 250-ml volumetric flask. The solution was saponified by adding 10 ml of 40% methanolic potassium hydroxide solution under nitrogen overnight. Hexane (75 ml) was added to the flask and the mixture was diluted to volume with 10% sodium sulphate solution. After shaking vigorously for 1 min and standing in the dark for 1 h, 5 ml of the upper phase were pipetted onto a column (30 cm × 12.5 mm I.D.) containing a mixture of activated MgO and diatomaceous earth (1:1) for open-column chromatography. All the sample preparations were conducted in the dark and samples were kept under nitrogen whenever possible during the procedure.

Separation and identification of major carotenoids by open-column chromatography and HPLC

Hexane–acetone (96:4 and 90:10) was used to elute the carotene band and monohydroxy pigment band, respectively. As monohydroxy pigments such as cryptoxanthin were not found in water convolvulus, a cryptoxanthin standard prepared from yellow corn was added to the crude extract and pipetted onto the column to determine the ability of this binary solvent system to elute monohydroxy pigments. After carotene and monohydroxy pigment bands had been eluted, dihydroxy pigments such as lutein and polyoxy pigments such as violaxanthin were eluted with hexane–acetone–methanol (85:15:0.2). The other polyoxy pigment, neoxanthin, was the last to be eluted with the same ternary solvent system in the proportions 85:15:1.5. Another ternary solvent system, hexane–acetone–methanol (85:15:1), was also used to compare the elution sequence of lutein and violaxanthin.

Each band eluted from the column was evaporated to dryness and dissolved in an appropriate solvent to determine the absortion spectra. The eluate from each band was also injected into an HPLC system to determine retention times. Reproducibilities of retention time with respect to the separated bands and standards were determined by making a series of five injections. An isocratic solvent system of acetonitrile–methanol–ethyl acetate (75:15:10) pumped at a flow-rate of 1 ml/min for the first 7.5 min and 2 ml/min thereafter. Each band eluted by open-column chromatography was monitored at 450 nm with a sensitivity at 0.0064 a.u.f.s.

The major carotenoids in water convolvulus were identified by comparing the absorption spectra and retention times of the separated bands with those of reference standards. A hypsochromic shift on acidification with hydrochloric acid was used to identify 5,6-epoxy carotenoids such as violaxanthin and neoxanthin.

Separation of carotenoid standards by HPLC

A mixture of neoxanthin, violaxanthin, lutein epoxide, lutein, zeaxanthin, zeinoxanthin, cryptoxanthin and β-carotene standards was dissolved in ethyl acetate and filtered through a 0.2-μm membrane filter before injection into the HPLC system. The HPLC conditions were the same as described above.

Separation of major carotenoids by TLC

A lutein band containing lutein and lutein epoxide eluted by open-column chromatography was further separated on silica gel TLC plates. Some carotenoid standards such as neoxanthin, violaxanthin and lutein epoxide were also separated and prepared from water convolvulus and Bermuda grass with the same procedure.

Development of the TLC plates was carried out in glass tanks lined with filter-paper and equilibrated for 30 min with 150 ml of methanol–acetone–hexane (1:29:90) prior to development. A 10-μl volume of extract was applied to the TLC plate with a syringe. The chromatograms were developed over a distance of 15 cm for *ca.* 25 min in a dark room at ambient temperature. Separated bands were scraped into a small sintered-glass funnel attached to a 25-ml side-arm filtration flask. Pigments were eluted with an appropriate solvent to measure the absorption spectra with a Hitachi 220S double-beam spectrophotometer. An epoxide test [14] was conducted to identify the presence of neoxanthin, violaxanthin and lutein epoxide. The amount of each major carotenoid was determined using Beer's law and the molar absorptivities [14]. The quantitative data were calculated based on averages of duplicate analyses.

RESULTS AND DISCUSSION

Fig. 1 shows the chromatogram of carotenoid standards obtained by employing acetonitrile–methanol–ethyl acetate (75:15:10). This solvent system was chosen based on a similiar system developed by Nelis and De Leenheer [15], who used acetonitrile–methanol–dichloromethane (70:10:20) to separate nine carotenoids within 30 min. Although the nine carotenoids were adequately resolved, the separation time was too long. They also reported that with an isocratic non-aqueous solvent system it was possible to minimize the risk of solute precipitation on the column, increase the sample capacity and chromatographic efficiency and prolong the column lifetime. The total analysis time with this method could be reduced to 18 min by increasing the flow-rate from 1 to 2 ml/min after 7.5 min during a chromatographic run. The reproducibility of the retention times was determined by making a series of five injections of each standard and a mixture of standards. The relative standard deviation (R.S.D.) was less than 3% for all standards except β-carotene (3.38%). This result was expected because of increased sample diffusion at the end of separation.

Table I shows the identification data for major carotenoids in water convolvulus by open-column chromatography and TLC. β-Carotene was first eluted with hexane–acetone (96:4), followed by cryptoxanthin with the same solvent system at 90:10. However, this binary solvent system failed to resolve dihydroxy and polyoxy pigments. Thus, by adding methanol as a modifier to the binary solvent system it was possible to resolve lutein, violaxanthin and neoxanthin. Lutein and violaxanthin were thus eluted with hexane–acetone–methanol (85:15:0.2). Surprisingly, violaxanthin was eluted before lutein. Neoxanthin was the last eluted with the same ternary solvent

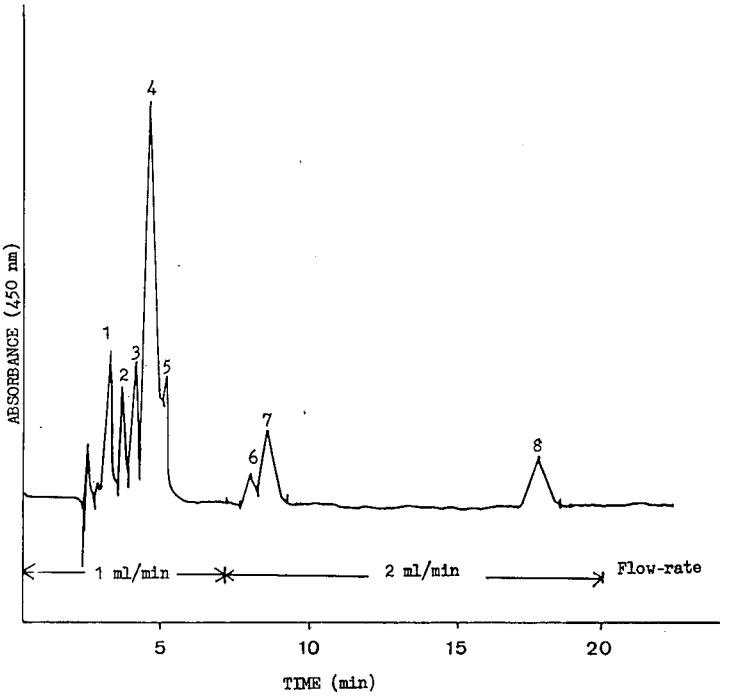

Fig. 1. HPLC of carotenoid standards by employing an isocratic solvent system of acetonitrile–methanol–ethyl acetate (75:15:10). Peaks: 1 = neoxanthin; 2 = violaxanthin; 3 = lutein epoxide; 4 = lutein; 5 = zeaxanthin; 6 = zeinoxanthin; 7 = cryptoxanthin; 8 = β-carotene.

TABLE I

DATA FOR IDENTIFICATION OF PIGMENTS IN WATER CONVOLVULUS BY OPEN-COLUMN CHROMATOGRAPHY AND TLC

Pigment	Visible spectra[a]			Epoxide test	
	λ_{max} found (nm)	Solvent	λ_{max} reported (nm) [14]	Hypsochromic shift	Colour
β-Carotene	429, 451, 477	Ethanol	427, 449, 475	–	–
	436, 462, 488	Choroform	435, 461, 485	–	–
Cryptoxanthin[b]	(427), 448, 471	Ethanol	(428), 449, 473	–	–
	(436), 458, 483	Chloroform	(435), 459, 485	–	–
Lutein[c]	421, 445, 474	Ethanol	422, 445, 474	–	–
	435, 461, 490	Chloroform	435, 458, 485	–	–
Lutein epoxide[c]	417, 440, 471	Ethanol	418, 442, 470	400, 422, 452	Green-blue
	426, 453, 485	Benzene	427, 454, 484	409, 436, 466	Green-blue
Violaxanthin[d]	419, 442, 471	Ethanol	417, 440, 469	381, 403, 431	Blue
	428, 453, 482	Chloroform	426, 449, 478	389, 411, 440	Blue
Neoxanthin[d]	416, 438, 466	Ethanol	415, 438, 467	397, 421, 450	Green-blue
	422, 446, 475	Chloroform	423, 448, 476	416, 430, 457	Green-blue

[a] Values in parentheses represent shoulders on spectral absorption curves.

[b] Cryptoxanthin was not originally present in water convolvulus. It was prepared from yellow corn and added to the crude extract during column chromatography.

[c] Lutein and lutein epoxide which eluted as one band on the column were further separated by TLC to determine absorption spectra.

[d] Both neoxanthin and violaxanthin were separated by open-column chromatography and TLC to determine absorption spectra.

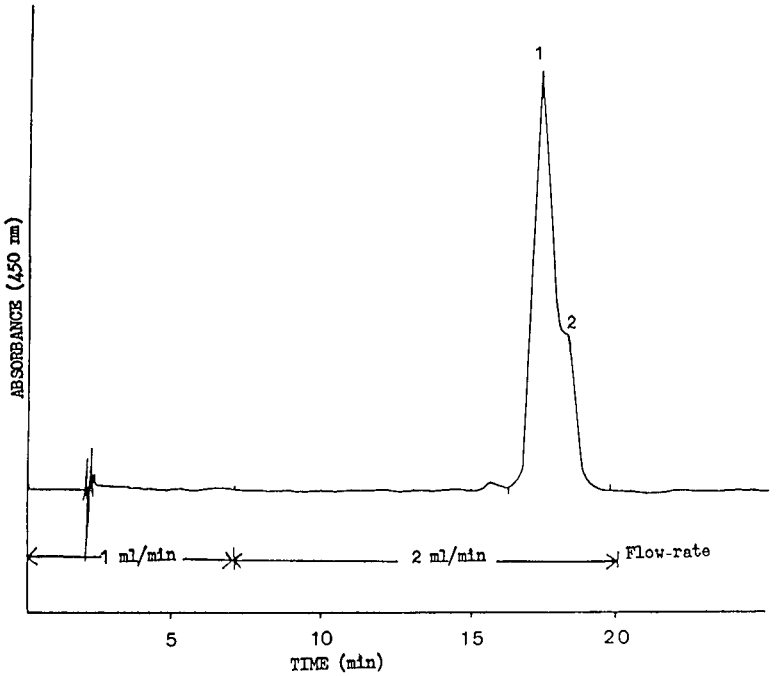

Fig. 2. Chromatogram of a carotene band eluted with hexane–acetone (96:4). Peaks: 1 = β-carotene; 2 = β-carotene isomer.

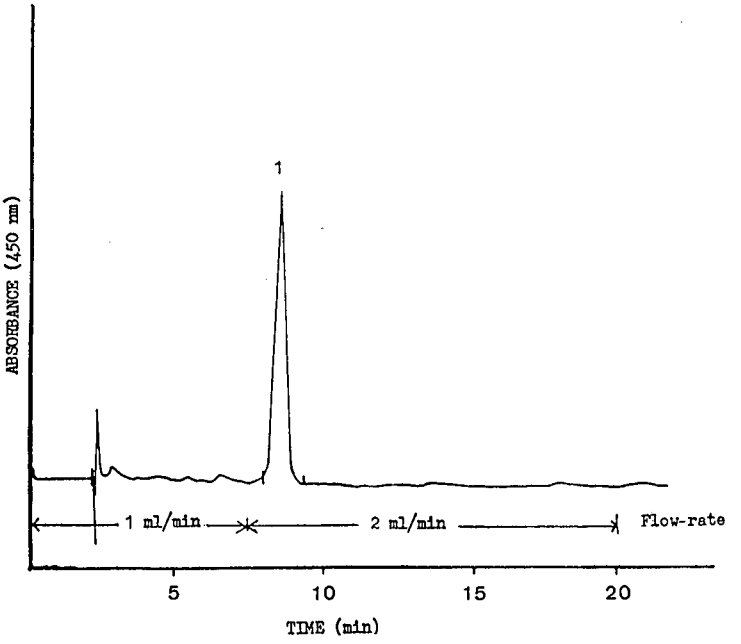

Fig. 3. Chromatogram of a cryptoxanthin band eluted with hexane–acetone (90:10). Peak 1 = cryptoxanthin.

system at 85:15:1.5. In contrast, by using the same ternary solvent system at 85:15:1 it was found that lutein was eluted followed by violaxanthin. This difference in the elution sequence of lutein and violaxanthin should be due to the amount of methanol present in the mobile phase.

Each carotenoid band eluted from the column was injected into the HPLC system to determine retention times. The low R.S.D. (less than 3% with five injections) demonstrates the high reproducibility of this method. Thus the various carotenoids in water convolvulus could be characterized by comparing the absorption spectra and retention times of the separated bands with those of reference standards.

Fig. 2 shows the chromatogram of a carotene band eluted with hexane–acetone (96:4). This band consisted mainly of β-carotene. However, there was a shoulder present, which might be due to the presence of small amount of *cis*-β-carotene.

Fig. 3 shows the chromatogram of a cryptoxanthin band eluted with hexane–acetone (90:10). Although cryptoxanthin was not present in water convolvulus, this result implied that this binary solvent system could adequately elute monohydroxy pigments.

Fig. 4 shows the chromatogram of a violaxanthin band eluted with hexane–acetone–methanol (85:15:0.2).

Fig. 5 shows the chromatogram of a lutein band eluted with hexane–acetone–methanol (85:15:0.2). The lutein band was not pure, as shown by the presence of two major peaks and one minor peak. This band was therefore further separated on silica

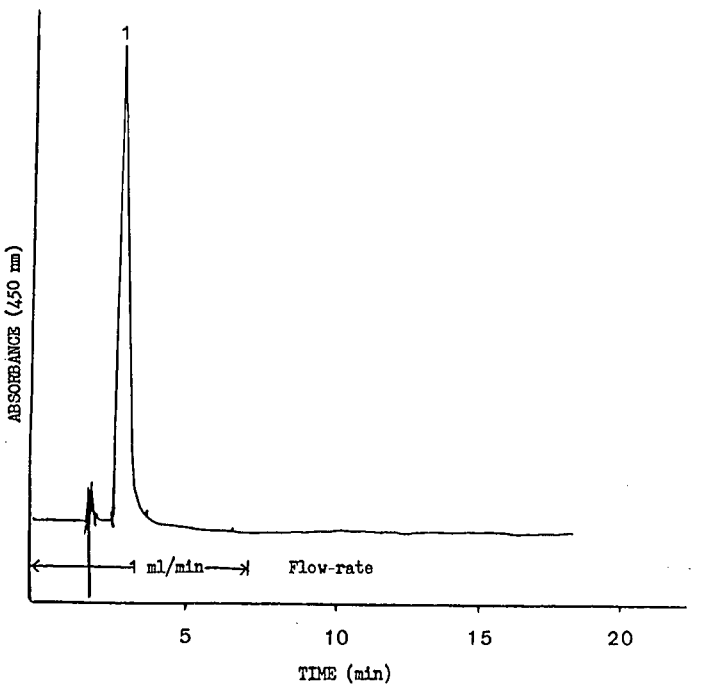

Fig. 4. Chromatogram of a violaxanthin band eluted with hexane–acetone–methanol (85:15:0.2). Peak 1 = violaxanthin.

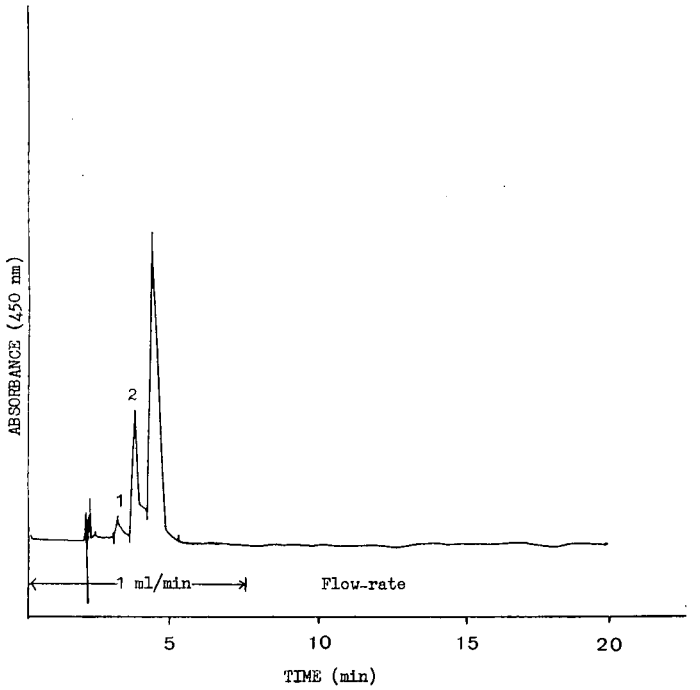

Fig. 5. Chromatogram of a lutein band eluted with hexane–acetone–methanol (85:15:0.2). Peaks: 1 = violaxanthin; 2 = lutein epoxide; 3 = lutein.

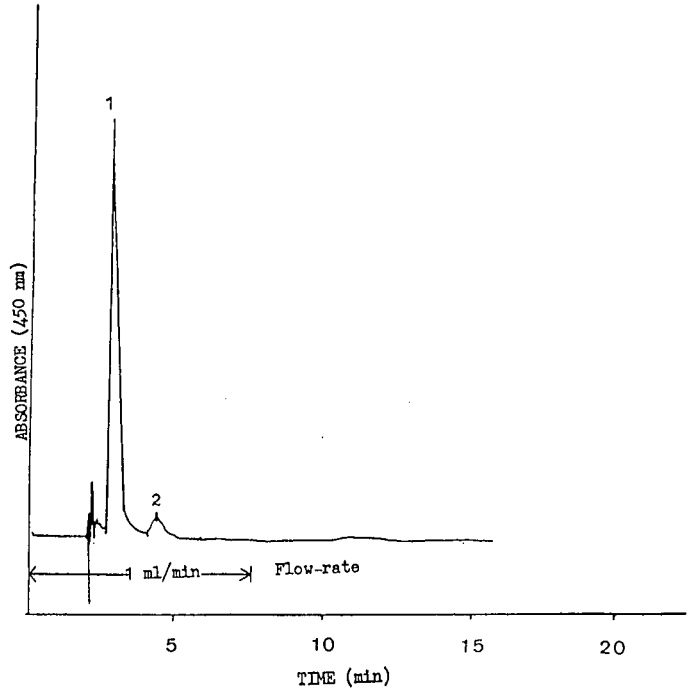

Fig. 6. Chromatogram of a neoxanthin band eluted with hexane–acetone–methanol (85:15:1.5). Peaks: 1 = neoxanthin; 2 = lutein.

gel TLC plates. Two bands were formed and were identified as lutein and lutein epoxide. Lutein epoxide was also confirmed by a hypsochromic shift on acidification with hydrochloric acid. The minor peak should be due to the presence of a violaxanthin residue, according to the retention time.

Fig. 6 shows the chromatogram of a neoxanthin band eluted with hexane–acetone–methanol (85:15:1.5). A minor peak is present, which should be due to the presence of a lutein residue, according to the retention time.

The amounts of neoxanthin, violaxanthin, lutein epoxide, lutein and β-carotene in water convolvulus were 216, 188, 28, 706 and 302 μg/g, respectively.

ACKNOWLEDGEMENT

This study was supported by a grant from the National Science Council, Taiwan.

REFERENCES

1 S. M. Anderson and N. I. Krinsky, *Photochem. Photobiol.*, 18 (1973) 403.
2 M. M. Mathews-Roth, *Nature (London)*, 203 (1964) 1092.
3 M. M. Mathews-Roth, *Oncology*, 39 (1982) 33.
4 M. M. Mathews-Roth, *Pure Appl. Chem.*, 57 (1985) 717.
5 A. Bendich, *J. Nutr.*, 119 (1989) 112.
6 H. M. Li and K. C. Liu, *A Survey of the Medicinal Plants in Taiwan*, National Research Institute of Chinese Medicine, Taiwan, 1973, p. 150.
7 Association of Official Analytical Chemists, *Official Methods of Analysis of the Association of Official Analytical Chemists*, AOAC, Washington, DC, 14th ed., 1984.
8 H. H. Strain, J. Sherma and M. Grandolfo, *Anal. Chem.*, 38 (1967) 926.
9 P. J. Schoenmakers, H. A. H. Billiet and L. de Galan, *J. Chromatogr.*, 218 (1981) 259.
10 S. P. Bakalyar, R. McIlwrick and E. Roggendorf, *J. Chromatogr.*, 142 (1977) 353.
11 E. Roggendorf and R. Spatz, *J. Chromatogr.*, 204 (1981) 263.
12 F. W. Quackenbush, J. G. Firch, W. J. Rabourn, M. McQuistan, E. M. Petzold and T. E. Karl, *J. Agric. Food Chem.*, 9 (1961) 132.
13 B. H. Chen and C. A. Bailey, *J. Chromatogr.*, 393 (1987) 297.
14 B. H. Davies, in T. W. Goodwin (Editor), *Chemistry and Biochemistry of Plant Pigments*, Vol. 2, Academic Press, New York, 2nd ed., 1976, pp. 38–165.
15 H. J. C. F. Nelis and A. P. de Leenheer, *Anal. Chem.*, 55 (1983) 270.

Journal of Chromatography, 543 (1991) 157–169
Elsevier Science Publishers B.V., Amsterdam

CHROM. 23 112

Reversed-phase gradient elution behaviour of polystyrenes in a dichloromethane–methanol solvent system

ROSS ANDREW SHALLIKER* and PETER EDWIN KAVANAGH
Chemical and Analytical Sciences, Deakin University, Waurn Ponds, Victoria 3217 (Australia)
and
IAN MAXWELL RUSSELL
CSIRO, Division of Wool Technology, Belmont, Victoria 3216 (Australia)
(First received October 22nd, 1990; revised manuscript received January 3rd, 1991)

ABSTRACT

A study was made of the gradient elution behaviour of the high-molecular-weight polystyrenes on C_{18} reversed-phase columns in methanol–dichloromethane solvent systems. The polymers were injected into mobile phase compositions which were expected to precipitate the polymer on the column and separation of the polymers was then expected as solvents able to dissolve the various molecular weights entered the column in the solvent gradient. The effects of column pore size, sample load and flow-rate were examined.

Results were determined mainly by polymer molecular weight and its relation to column pore size. When columns were chosen in which polymer had access to the pores, elution occurred after the expected solvent solubility composition indicating that normal adsorption processes were occuring. Polymers which were excluded from the pores underwent unusual elution processes which resulted in their elution at the solvent solubility composition, or before. The extent of this unexpected elution in a solvent of poorer solvating ability was more predominant on columns of small pore size.

The effects of these elution processes was to contribute to band broadening and to reduce selectivity between higher-molecular-weight polymers on small pore size adsorbents. An explanation as to the causes of such elution processes is presented, in which non-equilibrium solvation and precipitation of eluting polymer molecules occurs in the changing solvent gradient mixture.

INTRODUCTION

The molecular weight determination of macromolecules is usually carried out using size-exclusion chromatography (SEC). However, macromolecules have also been separated using reversed-phase high-performance liquid chromatography (RP-HPLC). As far as the chromatography of oligomers and lower molecular weights are concerned the separations achievable are at least as good and at times far exceed any SEC separation [1–6]. The RP-HPLC separation of polymers could become a powerful technique if the separation of the high molecular weights could be improved. Several workers [7–11] have studied separations of molecules with molecular weights in the order of several hundred thousand, however refinement is necessary to obtain separations comparable with those based on SEC.

0021-9673/91/$03.50

A mechanism for the gradient separation of polymers has been described by Glöckner [10], in which the molecules underwent a series of precipitation and redissolution processes along the column until finally eluting at a mobile phase composition equivalent to the solubility of the polymer. Boehm and co-workers [12–14] proposed a mechanism which considered that the polymer eluted at some "critical solution" composition. This mechanism has, however, been criticized by Quarry *et al.* [15] as being redundant and resembling the "on off" model where initially molecules stick to the column and are then eluted by the mobile phase with no reattachment. Snyder and co-workers [16,17] proposed that elution of polymers still obeys the principles of normal chromatographic adsorption and desorption processes. They showed in a study on polystyrene in tetrahydrofuran–water that elution was based on adsorption processes for sample loads less than 30 μg and for molecular weights up to 50 000 dalton. As the sample load was increased the mechanism was shown to change to that of the precipitation and redissolution process described by Glöckner, with corresponding changes in the peak shape. In addition, Lochmüller and McGranaghan [18] have presented evidence to support the adsorption mechanism argued by Snyder.

The improvement in the separation of higher-molecular-weight polymers on small-pore-size columns is hindered by strange behaviour often reported for the larger molecules [11,19,20]. All or part of the polymer may elute in the interstitial volume of the column, or the polymer may appear as a peak eluting within or just after the solvent front. This is largely a result of the necessity to introduce the polymer in a solvent of higher solvating strength than the running solvent. Problems in the separation of these macromolecules caused by the injection solvent are greater than in small-molecule adsorption LC as there is only a small change in polymer solubility for a large change in molecular weight, so that the selectivity which is obtainable in a system which is based largely on solvent–solute interactions is small. Interactions between the stationary phase and the solute play only a minor role as the larger molecules are generally excluded from the pores. Additionally there may be changes in polymer molecular configuration and solvent diffusion effects around the precipitation point [18]. These problems which occur for the higher molecular weights on the small pore size columns are unfortunate as they hinder the separation potential which these columns offer for lower molecular weights. Lochmüller and McGranaghan [18] have overcome some of these problems by recommending a premixing column to make sure the polymer which is dissolved in good solvent is thoroughly mixed with poor solvent before entering the column.

This work is mainly concerned with the elution of high molecular weight ($>50\,000$ dalton) polystyrenes and examines the effect of increasing the solute–stationary phase interactions by increasing the pore size, which provides the larger molecules with a greater surface area. The effects of pore size have previously been examined [1,21], but others have dealt only with molecular weights lower than 50 000 dalton. In this study we describe some unusual chromatographic behaviour that the larger molecules undergo in solvent compositions close to their solubility limit. Small sample loads (0.5 μg) were used to identify factors which contribute to band broadening of the polymer peaks and to a decrease in selectivity as molecular weight increases which may be less apparent at higher sample loads.

EXPERIMENTAL

All chromatographic experiments were performed using two M6000A pumps, a 660 solvent programmer and U6K injector (Waters Assoc., Milford, MA, U.S.A.). The detector was a variable-wavelength UV–VIS set at 262 nm (Activon Scientific, Thornleigh, Australia). Data acquisition and analysis were done with a home-built system. The columns used were a μBondapak C_{18}, 30 cm × 3.9 mm I.D., pore size 120 Å, particle size 10 μm, carbon load 10% (Waters Assoc.), a Serva 300 Å C_{18}, 5 μm particle size, 25 cm × 4.6 mm I.D., pore size 300 Å, carbon load 11.6% (Serva, Heidelberg, Germany) and a self-packed 4000 Å pore size, C_{18}, 10 μm particle size, 25 cm × 4.6 mm I.D. (Merck, LiChrospher SI4000), coated via an *in situ* process [22].

Methanol and dichloromethane (HPLC grade) were obtained from Merck. The monodisperse polystyrene standards used were molecular weights 3600, 110 000, 410 000, 929 000 and $2.7 \cdot 10^6$ dalton (Waters Assoc.) and 9000, 17 500 and 50 000 dalton (Polysciences, Warrington, U.S.A.).

The solvent composition at which each polymer exhibited insolubility, φ_s, was determined by dilution of a stock solution of each polymer (200 mg/l) in 100% dichloromethane. Aliquots of polymer stock solutions were added to various known ratios of methanol–dichloromethane prepared volumetrically in a total volume of 100 ml and these solutions were then shaken for 24 h at 25.0°C and allowed to settle. A 10-μl aliquot of the supernatant solution was then loaded onto a μBondapak C_{18} column and eluted isocratically in 100% dichloromethane to determine the amount of soluble polymer. For solvent compositions in which the polymer remained totally soluble the sample load was equivalent to 0.5 μg. The amount of soluble polymer was plotted against the solvent composition, and the midpoint of the curve between complete insolubility and complete solubility was then chosen as φ_s for each polystyrene standard.

All gradient elutions of polymers were carried out at flow-rates of 0.5 ml/min unless stated otherwise. Gradients were linear with a change of 2%/min, from φ_i to 100% dichloromethane, where φ_i represents the volume fraction of dichloromethane in the initial mobile phase of methanol and dichloromethane. The column was then re-equilibrated with a reverse gradient in 5 min to φ_i and then allowed to flush for a further 20 min. Polymer sample load was 0.5 μg using a 10-μl injection volume. Column temperature was maintained at 25.0°C in a thermostatted waterjacket. All size-exclusion data were recorded at flow-rates of 0.5 ml/min in an isocratic mobile phase of 100% dichloromethane.

To correct for possible pump flow and solvent mixing inaccuracies, gradient profiles at each φ_i composition were obtained by running UV absorbances on mobile phases of methanol, and methanol + benzene (0.012%, v/v) [23]. From these profiles the solvent composition at the time of peak elution (φ_e) for the various molecular weight polymer standards could be obtained.

The reproducibility of φ_e of the system was examined for a series of replicate injections ($n = 7$) of polystyrene molecular weight 410 000 dalton. Elution times for this series had a standard deviation of 0.7%. Performance was examined on a day-to-day basis, also with a standard deviation of 0.7% for the elution times.

Theoretical plate counts were determined by the method of Bristow and Knox [24] using the solute phenetol in water–methanol (60:40) mobile phase at a flow-rate of

0.5 ml/min. The number of theoretical plates on the μBondapak, Serva and 4000 Å columns were 8000, 5000 and 1100 plates/column, respectively.

RESULTS AND DISCUSSION

The elution of the polystyrene via gradient elution RP-HPLC was studied on different columns in order to examine the effects of pore size. The μBondapak column had a nominal average pore size of 120 Å and an exclusion limit of around 35 000 dalton, as shown in Fig. 1, curve A. The Serva column had a nominal average pore size of 300 Å and the exclusion limit was found to be slightly less than 110 000 dalton (Fig. 1, curve B). The 4000 Å column had an exclusion limit greater than $2.7 \cdot 10^6$ dalton thus allowing all the polymers tested access to the pores (Fig. 1, curve C). For each polymer, a range of initial mobile phase compositions (φ_i) was used. The solvent compositions at the times of peak maxima of polymer elution were used as an estimate of φ_e. The graphs in Fig. 2a–c show the relationship between peak elution composition φ_e and polymer molecular weight (curve A) for each column. The bars on the curves of φ_e show the range of the data as detailed in Table I, and curves are drawn through the means of the data. As expected φ_e was independent of φ_i except when φ_i was greater than φ_e. For comparison, the change in polymer solubility compositions φ_s with polymer molecular weight are also shown in Fig. 2 (curve B). The term φ_s refers to the solvent solubility composition for the polymer, the point at which the polymer undergoes a transformation from a soluble state to a solid or a gel phase in 24 h. The midpoint of the φ_s curve as described in the experimental was chosen so as to represent the mean molecular weight of the standard. The curve is typically very steep for the high-molecular-weight polymers changing 1% between complete solubility and insolubility for the 110 000-dalton polystyrene. The midpoint of this curve will vary depending on the concentration of the sample. However, the composition of φ_s was

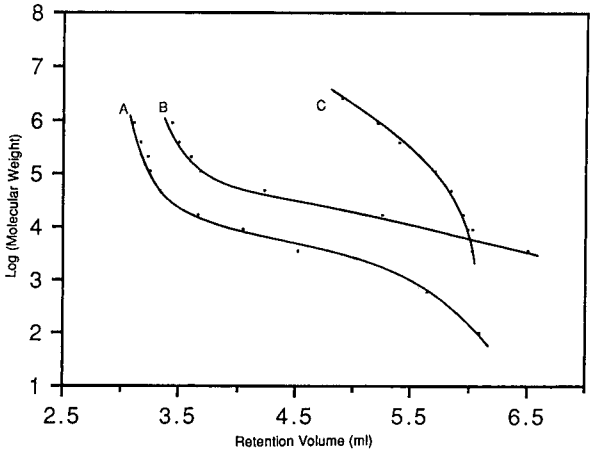

Fig. 1. Plot showing the size exclusion limit of the μBondapak column (A), the Serva 300 Å column (B) and the 4000 Å column (C) in dichloromethane.

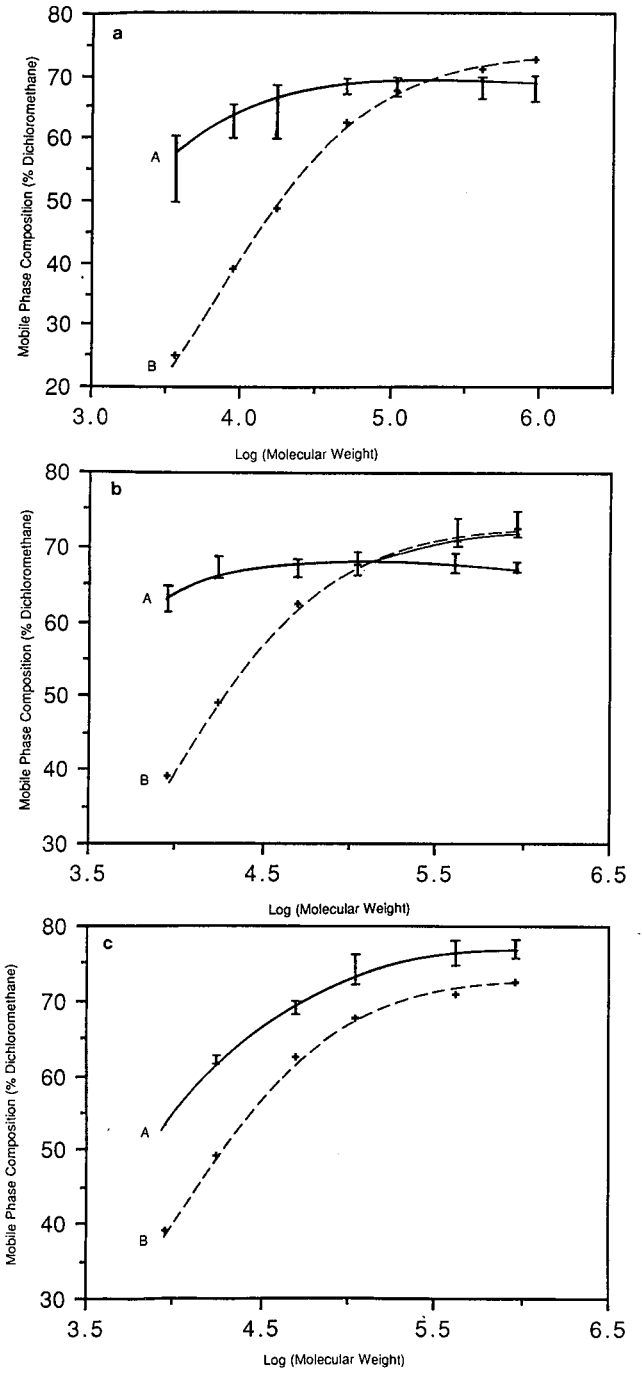

Fig. 2. Plots showing the relationship between elution composition, φ_e, and log molecular weight (A) and the relationship between the critical solubility composition, φ_s, and log molecular weight (B). (a) μBondapak column; (b) Serva 300 Å column; (c) 4000 Å column.

TABLE I

ELUTION COMPOSITION, φ_e, (% DICHLOROMETHANE), AT VARIOUS INITIAL MOBILE PHASE COMPOSITIONS, φ_i, FOR POLYSTYRENE ON THE 120 Å, 300 Å AND 4000 Å COLUMNS

Flow-rate, 0.5 ml/min, gradient 2%/min to 100% dichloromethane (see Experimental for details).

Molecular weight	φ_e (%)					
	φ_i = 60%	φ_i = 50%	φ_i = 40%	φ_i = 30%	φ_i = 20%	φ_i = 10%
120 Å column						
929 000	68.9	69.7	69.3	68.6	66.0	68.4
410 000	68.4	69.1	68.6	68.2	66.2	68.8
110 000	69.0	69.5	69.3	67.7	66.9	69.5
50 000	68.3	69.4	68.8	67.9	67.1	69.2
17 500	60[a]	68.5	67.8	66.2	65.8	67.9
9000	60[a]	64.8	65.2	63.4	63.0	65.0
3600	60[a]	50[a]	56.3	57.3	57.8	58.5
300 Å column						
929 000	71.6	71.9	72.5	72.5	73.3	74.8
929 000[b]	66.6	66.9	67.9	66.9	68.0	71.5
410 000	70.4	70.8	70.4	71.0	72.2	73.7
410 000[b]	66.8	68.1	67.2	67.2	69.0	71.0
110 000	66.8	66.9	66.5	68.7	67.2	69.3
50 000	66.0	66.9	67.5	67.2	66.5	68.2
17 500	66.6	67.3	64.7	67.6	67.2	68.7
9000	[c]	63.8	61.8	61.7	61.5	64.9
4000 Å column						
929 000	78.1	76.6	76.6	75.9	75.7	76.2
410 000	78.2	76.6	77.1	75.7	74.9	77.7
110 000	76.0	73.7	74.2	72.7	72.2	74.2
50 000	69.1	69.8	68.4	69.9	69.4	69.2
17 500	[c]	62.5	61.8	61.7	[c]	[c]
9000	[c]	[c]	[c]	53.5	[c]	[c]

[a] Peak eluted prior to the influence of the gradient.
[b] Elution composition of the pre-eluted polymer.
[c] Peak profile very broad.

determined at a concentration level similiar to that of the chromatographed polystyrenes. If elution of the polystyrene was to obey the precipitation redissolution mechanism then φ_e would be expected to occur at φ_s. In fact, three different types of elution occurred and they are all shown by the 120 Å column, the results for which are now considered in detail and are shown in Fig. 2a.

Elution of the lower-molecular-weight polystyrenes (up to 50 000 dalton) occurred at a higher concentration of dichloromethane than the solvent solubility composition (*i.e.*, $\varphi_e > \varphi_s$), indicating that there was significant adsorption occurring. Elution of the 110 000-dalton polystyrene occurred at the critical solubility composition (*i.e.*, $\varphi_e = \varphi_s$), but, as the molecular weight increased for these higher-molecular-weight polymers, elution occurred at concentrations of dichloromethane lower than the solubility composition (*i.e.*, $\varphi_e < \varphi_s$). The polymer eluted prior to its actual solubility and this unusual behaviour ($\varphi_e < \varphi_s$), shall be termed "pre-elution". This

indicates (1) that elution does not strictly follow a precipitation redissolution process and (2) that adsorption of high-molecular-weight polymers is not significant even given that small amounts of surface interaction may occur through polymer chain dissentanglement snaking into the pores [1] or because of the small surface area available for adsorption outside of the pores [10,25]. As molecular weight increased there was a decrease in the selectivity, to the point where retention times became constant. This decrease in selectivity has also been observed with oligomeric separations on μBondapak columns where the higher oligomers become increasingly difficult to resolve [23]. This was attributed to the limited access available for adsorption for the higher-order oligomers within the pores. Polystyrenes of molecular weight 50 000 dalton and above are all mainly excluded from the pores of the 120 Å column and adsorption effects would be expected to be minimal above this molecular weight limit. As the molecular weight increased beyond 110 000 dalton the peak profile changed from a narrow peak at 110 000 dalton to broad peaks with severe tailing at 410 000 and 929 000 dalton. This tailing extended until, at the extreme end of the peak, a small quantity of polymer eluted near φ_s (Fig. 3).

The 300 Å column had a higher exclusion limit than that of the 120 Å column and adsorption was again observed for polymers of molecular weights below 50 000 dalton.

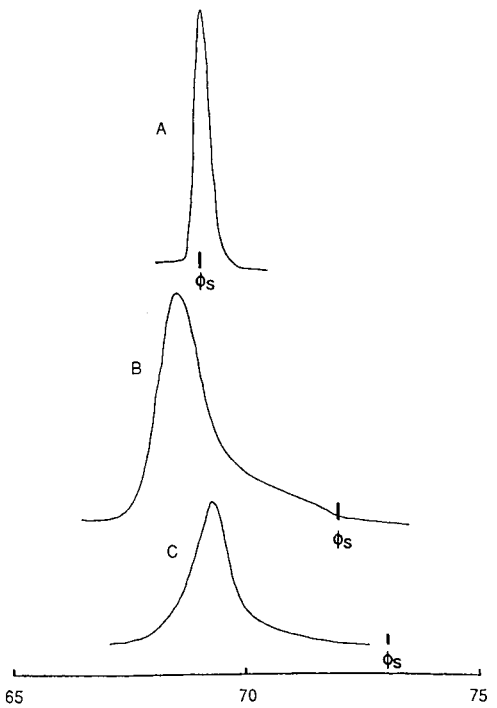

Fig. 3. Elution profiles for polystyrene on the μBondapak column; molecular weight A = $1.1 \cdot 10^5$ dalton, B = $4.1 \cdot 10^5$ dalton and C = $9.29 \cdot 10^5$ dalton. Mobile phase φ_i = dichloromethane–methanol (40:60), gradient elution 2%/min, flow-rate = 0.5 ml/min (note detector sensitivity, A and B = 0.005, C = 0.01 a.u.f.s.).

Elution of the 110 000-dalton polystyrene occurred at the critical solubility composition (*i.e.*, $\varphi_e = \varphi_s$), indicating adsorption processes were insignificant. Elution of the higher-molecular-weight polystyrenes (410 000 and 929 000 dalton) on the 300 Å column produced chromatographic profiles which had two distinct peaks (Fig. 4), as opposed to the tailing observed on the 120 Å column (Fig. 3). The later eluting peak was close to the expected solubility composition ($\varphi_e = \varphi_s$), whilst the other peak eluted with $\varphi_e < \varphi_s$, indicating pre-elution.

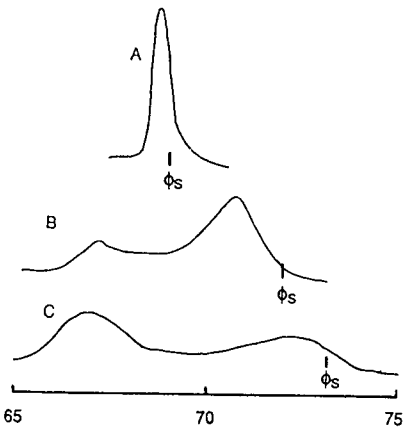

Fig. 4. Elution profiles for polystyrene on the Serva 300 Å column; molecular weight A = $1.1 \cdot 10^5$ dalton, B = $4.1 \cdot 10^5$ dalton and C = $9.29 \cdot 10^5$ dalton. Mobile phase φ_i = dichloromethane–methanol (30:70), gradient elution 2%/min, flow-rate = 0.5 ml/min.

The elution of the higher-molecular-weight polystyrenes was very different on the large-pore-size, 4000 Å C_{18} column. At no stage did the higher molecular weights exhibit pre-elution, and all the polystyrenes eluted with $\varphi_e > \varphi_s$, which indicated adsorption processes were likely to be occurring. The adsorption of these larger molecules is possible due to the larger accessible surface area within the pores. On this column lower-molecular-weight polystyrenes exhibited less adsorption compared with the 120 Å and the 300 Å columns, as the total surface area of the larger pore particles is less than that of the smaller pore size adsorbents.

A possible mechanism for the occurrence of pre-elution may be postulated by considering the behaviour of the high-molecular-weight polymer after it precipitates on the column by interaction with the solvent when it enters the poor mobile phase. If no precipitation occurred then the polymer would elute prior to the solvent front by the usual size-exclusion process. With the addition of the good mobile phase via gradient elution the polymer dissolves at the solvent solubility composition (φ_s), and the polymer begins to elute. While the polymer is in solution and moving down the column, solvent molecules have access to the pores whilst the polymer is excluded. The velocity of the polymer along the column is therefore greater than that of the solvent and the polymer again enters the poorer solvent where precipitation may again occur

as in the original Glöckner [10] model. However, as the molecular weight increases, an increasing time is required for the good solvent to diffuse out of the larger soluble polymer and thus allow precipitation to occur. This diffusion will be especially slow when the solvent composition is similiar to φ_s since the rate of diffusion is proportional to the concentration difference. Two extremes of behaviour can be distinguished. If the kinetics of polymer precipitation and redissolution are rapid the polymer elutes at the solvent solubility composition [10] ($\varphi_e = \varphi_s$). If the reprecipitation process is slow, the polymer may elute from the column in a solvent deficient in the stronger mobile phase by up to one column pore volume when access to the pores is denied ($\varphi_e < \varphi_s$). Hence, elution before φ_s can occur for higher molecular weights in a non-equilibrium process. Lochmüller and McGranaghan [18] also recently reported complications to elution based on a non-equilibrium process within the time domain of the chromatographic system. The consequences of polymer solvation and slow desorption of the solvent from within the larger molecules lead them to discuss non uniform sample distribution of polymer along the column which may lead to varied retention behaviour.

Support for our scheme is provided by the following observations.

(1) Broad tailing peaks were only observed above the column exclusion limit. The elution of the 110 000-dalton polystyrene on the 120 Å column occurred with a narrow peak profile as a result of an apparent adsorption free process and elution appears to be based solely on the solubility of the polymer, indicating a rapid precipitation redissolution process. In comparison, the peak profiles of higher molecular weights were broad with severe tailing (Fig. 3). The peak tailing of the 410 000-dalton polystyrene illustrates that both processes of pre-elution and elution based on the solubility occurred simultaneously. Most of the polymer was subject to pre-elution in the non-equilibrium process but there was peak tailing extending to near φ_s as some of the solvent diffused from within the polymer. Less tailing was observed with the 929 000-dalton polystyrene as more time was required for the good solvent to diffuse out and almost all of the polymer is pre-eluted in the non-equilibrium process.

Similiar effects were observed on the 300 Å column which resulted in the presence of multiple peaks for molecular weights of 410 000 and 929 000 dalton. Fig. 4 illustrates that the proportion of polymer undergoing pre-elution again increased with molecular weight.

(2) For molecular weights greater than the exclusion limit of the column the fraction of polymer eluting via the pre-elution process was dependent upon the pore size of the column. Fig. 5 compares the change in peak profile of polystyrene of molecular weight 410 000 dalton on the three columns again showing that the amount of pre-elution increased as the pore size decreases. For 410 000-dalton polystyrene, relatively more polymer eluted at the solubility composition on the 300 Å column compared with the 120 Å column. This may be a result of the increased surface area available for at least part of the polymer chains, thus increasing the polymer stationary phase interactions which allow a greater rate of diffusion of the solvent from within the polymer.

(3) The extent of pre-elution increased as the flow-rate increased. Fig. 6 illustrates these changes in peak profiles from 0.5 ml/min to 2.0 ml/min for the 410 000-dalton polystyrene on the 300 Å column. The decrease in the amount of polymer eluting at the solubility of the polymer at higher flow-rates indicates that the de-solvation of the polymer which causes pre-elution is a kinetic process. At the lower

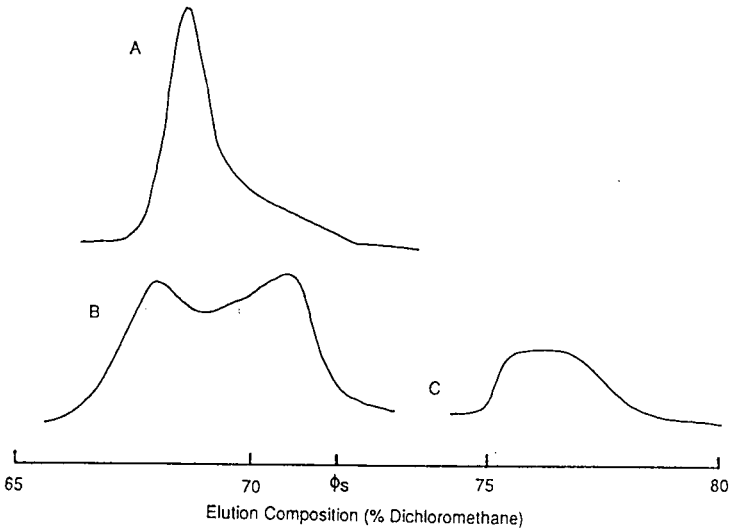

Fig. 5. Elution profiles for polystyrene molecular weight $4.1 \cdot 10^5$ dalton. Mobile phase φ_i = dichloromethane–methanol (50:50), gradient elution 2%/min, flow-rate = 0.5 ml/min. A = μBondapak column; B = Serva 300 Å column; C = 4000 Å column.

flow-rates there was more time for the good solvent to diffuse from the polymer chains.

(4) Pre-elution of the polystyrene always occurred within one column pore volume of φ_s. The maximum amounts of pre-elution calculated for one exclusion volume for the 929 000-dalton polystyrene on the 120 Å column and the 300 Å column correspond to solvent compositions of 6.0% and 8.0%, respectively. These compare to the actual amounts of pre-elution of 4.5% on the 120 Å column and 5.0% on the 300 Å column. The difference between the maximum quantity of pre-elution and that observed is an indication of the rate of diffusion of solvent from within the polymer.

(5) As the sample load was increased (with a constant injection volume of 10 μl) the pre-eluted polymer ceased to be the dominant form of the eluted polystyrene on

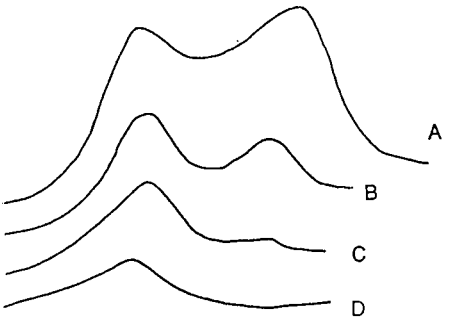

Fig. 6. Elution profiles for polystyrene molecular weight $4.1 \cdot 10^5$ dalton at various flow-rates. Mobile phase φ_i = dichloromethane–methanol (50:50), gradient elution 2%/min. Flow-rates: A = 0.5 ml/min; B = 1.0 ml/min; C = 1.5 ml/min; D = 2.0 ml/min.

both the 120 Å and the 300 Å columns (Fig. 7). At high mass loads the elution occurred predominantly at the solubility of the polymer, but pre-elution was still present (as shown by the assymetry at the front of the peak). The elution profile of the polymer on the 4000 Å column remained constant over the mass loads tested. In a study by Larmann *et al.* [1] it was found that the 50 000-dalton polymer also showed a variation in φ_e with differences in mass load. At low mass loads elution occurred such that adsorption was present and at higher mass loads elution occurred via a precipitation redissolution process. At these higher mass loads peak distortion also became noticeable.

The effect of mass load dependence shows that there was a limited quantity of polymer which could be solvated at any time. On the 120 Å and 300 Å columns this

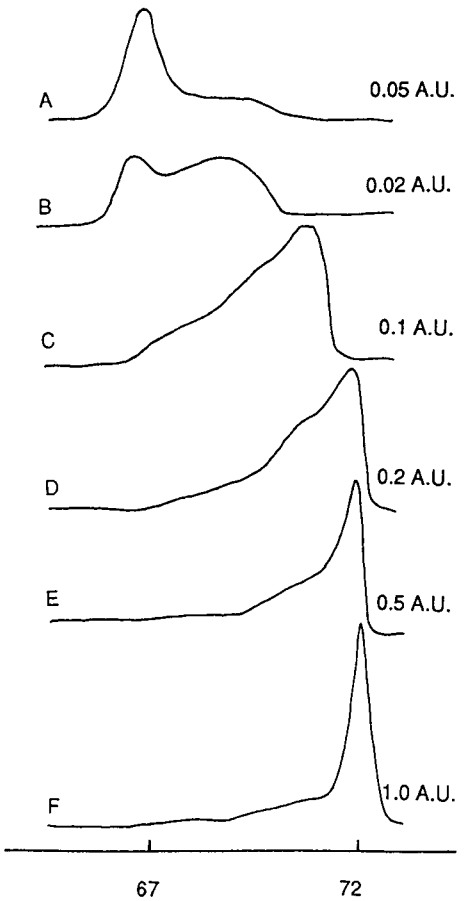

Fig. 7. Elution profiles of polystyrene $4.1 \cdot 10^5$ dalton at various mass loadings on the μBondapak column. A = 0.5 μg; B = 2.5 μg; C = 10.0 μg; D = 20.0 μg; E = 40.0 μg; F = 80.0 μg. Mobile phase φ_i = dichloromethane–methanol (50:50), gradient elution 2%/min, flow-rate = 0.5 ml/min.

amount was less than 0.5 μg. At high sample loads the pre-eluted component was still present, but due to the change in detector sensitivity to correspond with the higher loadings it was often difficult to observe. The band broadening even at the higher mass loads would make the optimization of a separation difficult.

CONCLUSION

This study examines elution behaviour of high-molecular-weight polystyrenes under gradient elution conditions using methanol and dichloromethane solvents on C_{18} reversed-phase columns. The results indicate that the polystyrenes elute from the columns via an adsorption mechanism only when the polymer is enabled access into the pores, as is the case for the 4000 Å pore size column packing or for the low-molecular-weight polystyrenes on the small-pore-size columns. When exclusion of the polymer occurred, two extreme mechanisms of elution were observed. Elution may occur at the solubility of the polymer, or the polymer may elute at a solvent composition below the solubility limit by a process we term pre-elution. Elution at the solvent solubility composition requires rapid reprecipitation of the polymer in the changing solvent gradient. Pre-elution results when diffusion of good solvent from within the polymer is slow relative to the rate of change of the solvent composition. These combined effects contribute to band broadening of the eluting polymer and lead to a decrease in the selectivity to a point where the higher-molecular-weight polymers elute at the same time as the lower-molecular-weight polymers. A greater degree of selectivity was achieved by using the larger-pore-size column, however, band broadening was still a problem especially with the lower molecular weights. These problems indicate that the separation of polystyrenes on reversed-phase columns with a methanol–dichloromethane solvent system is unsuitable and future work will investigate the effects of other solvent systems.

ACKNOWLEDGEMENT

One of the authors (R.A.S.) wishes to acknowledge the support of a Deakin University Postgraduate Award.

REFERENCES

1 J. P. Larmann, J. J. DeStefano, A. P. Goldberg, R. W. Stout, L. R. Snyder and M. A. Stadalius, *J. Chromatogr.*, 255 (1983) 163.
2 P. Jandera and J. Rozkosna, *J. Chromatogr.*, 362 (1986) 325.
3 J. J. Kirkland, *J. Chromatogr.*, 125 (1976) 231.
4 R. R. Lattimer, D. J. Harmon and K. R. Welch, *Anal. Chem.*, 51 (1979) 1293.
5 N. A. Paris, *J. Chromatogr.*, 157 (1978) 161.
6 L. R. Snyder and J. J. Kirkland, *Introduction to Modern Liquid Chromatography*, Wiley, New York, 2nd ed., 1979, p. 679.
7 K. H. Bui, D. W. Armstrong and R. E. Boehm, *J. Chromatogr.*, 288 (1984) 15.
8 D. W. Armstrong and K. H. Bui, *Anal. Chem.*, 54 (1982) 706.
9 D. W. Armstrong and R. E. Boehm, *J. Chromatogr. Sci.*, 22 (1984) 378.
10 G. Glöckner, *Pure Applied Chem.*, 55 (1987) 1553.
11 G. Glöckner, *Chromatographia*, 25 (1988) 854.
12 R. E. Boehm, D. E. Martire, D. W. Armstrong and K. H. Bui, *Macromolecules*, 16 (1983) 466.

13 R. E. Boehm, D. E. Martire, D. W. Armstrong and K. H. Bui, *Macromolecules*, 17 (1984) 400.
14 R. E. Boehm and D. E. Martire, *Anal. Chem.*, 61 (1989) 471.
15 M. A. Quarry, M. A. Stadalius, T. H. Mourey and L. R. Snyder, *J. Chromatogr.*, 358 (1986) 17.
16 M. A. Quarry, M. A. Stadalius, T. H. Mourey and L. R. Snyder, *J. Chromatogr.*, 358 (1986) 1.
17 Cs. Horváth (Editor), *High-Performance Liquid Chromatography —Advances and Perspectives*, Vol. 4, Academic Press, New York, 1986, pp. 195–312.
18 C. H. Lochmüller and M. B. McGranaghan, *Anal. Chem.*, 61 (1989) 2449.
19 G. Glöckner and J. H. M. van den Berg, *J. Chromatogr.*, 352 (1986) 511.
20 G. Glöckner, *Chromatographia*, 23 (1987) 517.
21 M. A. Quarry, R. L. Grob and L. R. Snyder, *Anal. Chem.*, 58 (1986) 907.
22 R. K. Gilpin, D. J. Camillo and C. A. Janicki, *J. Chromatogr.*, 121 (1976) 13.
23 F. P. B. van der Maeden, M. E. F. Biemond and P. C. G. M. Janssen, *J. Chromatogr.*, 149 (1978) 539.
24 P. A. Bristow and J. H. Knox, *Chromatographia*, 10 (1977) 279.
25 J. A. Perry, *J. Liq. Chromatogr.*, 13 (1990) 1047.

Journal of Chromatography, 543 (1991) 171–177
Elsevier Science Publishers B.V., Amsterdam

CHROM. 23 082

Approach to direct chiral recognition of some terpenic hydrocarbon constituents of essential oils by gas chromatography systems via α-cyclodextrin complexation

RENATA J. OCHOCKA*
Medical Academy, Faculty of Pharmacy, Gen. J. Hallera 107, PL-80-416 Gdańsk (Poland)
and
DANUTA SYBILSKA, MONIKA ASZTEMBORSKA, JOANNA KOWALCZYK and JANINA GORONOWICZ
Institute of Physical Chemistry, Polish Academy of Sciences, Kasprzaka 44/52, PL-01-224 Warsaw (Poland)

(First received October 9th, 1990; revised manuscript received December 28th, 1990)

ABSTRACT

The application of a very selective chiral stationary phase (Celite coated with α-cyclodextrin in formamide solution) in gas chromatography is described. Using this phase it is possible to separate enantiomeric mixtures of α-pinene, β-pinene, limonene and camphene. The separation of these compounds in essential oils is also demonstrated.

INTRODUCTION

Terpenes are an important group of compounds found in large amounts in plants. For the separation and analysis of their very complex mixtures derived from natural sources such as essential oils, gas chromatography (GC) is the method of choice, especially for compounds with boiling points ranging from 140 to 300°C. Nevertheless, owing to the large number of possible isomers within each group of terpenes and the lack of pure standard compounds, the problem of the analysis of essential oils is too difficult to solve by simple classical GC methods [1]. For this reason, improved GC techniques have been applied, *e.g.*, capillary GC, GC–mass spectrometry [2,3] and GC–Fourier transform infrared spectrometry [4–6].

However, many of the terpenes are chiral compounds and hence they can be present in natural mixtures in one or two enantiomeric forms and in various proportions. The chirality of the terpenes may have a strong influence on their various biological interactions because antipodes often differ in their biological activity. This phenomenon is understandable in view of the high stereospecificity required by a "lock-and-key" type of relationship between two partners, when one of them has a rigidly defined chirality. As a consequence, the important problem of chiral

0021-9673/91/$03.50

discrimination leads to additional difficulties in the analysis of essential oils, especially when terpenic hydrocarbons are considered. To our knowledge, the chromatographic separation and direct chiral recognition of terpenic hydrocarbons in essential oils have not previously been attempted, mainly because of the lack of convenient enantioselective chromatographic stationary phases.

We found previously that using α-cyclodextrin (α-CD) under appropriate conditions of partition GC, very efficient separations of α-pinene and β-pinene into enantiomers can be achieved [7]. Recently, efficient separations of enantiomers of α-pinene and limonene achieved using permethylated β-cyclodextrin [8] or α-cyclodextrin [9] and the separation of enantiomeric camphenes [10] have been reported. The applications of cyclodextrins and their derivatives for the separation of enantiomers under GC conditions have been thoroughly reviewed by Schurig and Nowotny [11]. This paper reports our attempts to apply this method using α-CD for the chiral recognition of the above-mentioned enantiomeric hydrocarbons when they are present in complex mixtures such as essential oils.

Two essential oils from species of the conifer family Pinaceae were studied, silver fir needle oil obtained from *Abies alba* Mill. and pine needle oil obtained from *Pinus sylvestris* L. The chemical compositions of both oils have recently been studied by several workers [12–15], terpenic hydrocarbons, *i.e.*, α-pinene, β-pinene, limonene and camphene, were found to be the main components.

EXPERIMENTAL

Reagents

α-, β- and γ-CD were supplied by Chinoin (Budapest, Hungary). Celite (30–80 mesh) for GC was from BDH (Poole, U.K.). Silver fir needle oil and pine needle oil obtained by steam distillation of needles of *Abies alba* Mill. and *Pinus sylvestris* L., respectively, were from Herbapol (Łódź, Poland). All other materials were of analytical-reagent grade and were used without further purification.

Apparatus and procedure

Chromatographic studies were performed using a Hewlett-Packard Model 5890 gas chromatograph equipped with a dual flame ionization detector. The peak areas and retention times were measured by means of a Hewlett-Packard 3390A integrator. Glass columns (2 m × 4 mm I.D.) were used. The compounds (0.02–0.15 μl) were injected with Hamilton microsyringes separately or as mixtures. A constant inlet pressure (2.75 ± 0.05 atm) and helium flow-rate (40 ± 0.5 ml/min) were maintained. The column packings, *i.e.*, Celite (30–80 mesh) coated with a formamide solution of α-CD, β-CD and γ-CD, were prepared as described previously [16]. The amounts of formamide (4.54 g) and Celite (20 g) were constant. Stationary phases contained CDs as follows: I, none (control); II, α-CD (0.79 mol%); III, β-CD (0.23 mol%); and IV, γ-CD (0.79 mol%). The amount of coated support in each analytical column was *ca.* 11 g.

In contrast to the behaviour of β-CD and γ-CD, α-CD forms an efficient separating agent under GC conditions when its formamide solution contains 3–4% of water [16]. Consequently, the stationary phase for column II contained 4% of water and lithium nitrate (0.45 g) was added as the stabilizing agent. The contents of

formamide and water in the final packings were determined by thermogravimetric analysis with a DuPont Model 1090 thermal analysis system.

RESULTS AND DISCUSSION

Preliminary studies

In separate sets of experiments performed using a supplementary column with glycerine as stationary phase in the temperature range 70–80°C, it was found that the content of monoterpenic hydrocarbon was 88% in pine needle oil and 82% in fir needle oil. These data correspond with the earlier results of thermogravimetric studies [17]. These hydrocarbon fractions were the main objectives of our investigations. The remaining, more polar, terpenic derivatives in the oils (12 and 18%, respectively) were strongly adsorbed on columns containing formamide medium (at 30°C) and were not eluted in the form of distinguishable peaks.

Artificial mixtures

Fig. 1 shows the chromatogram of an artificial mixture of enantiomers of α-pinene, β-pinene, camphene and limonene obtained on chiral discriminating column II. A chromatogram of the same mixture obtained on the reference achiral column with pure formamide (I, F) is presented in Fig. 2.

Mixture I studied was prepared from pure compounds or from compounds of known composition and previously determined optical purity and contained, respectively, (+)- and (−)-α-pinene (13% and 5%), (+)- and (−)-β-pinene (6% and 22%), (+)- and (−)-limonene (23% and 19%) and (+)- and (−)-camphene (5% and 7%). The adjusted retention times of the compounds on columns with α-CD, β-CD and γ-CD are given in Table I. The data indicate that only α-CD recognizes distinctly enantiomers on the investigated monoterpenic hydrocarbons. In contrast, no distinguishable enantioselectivity could be observed for β-CD and γ-CD, although their

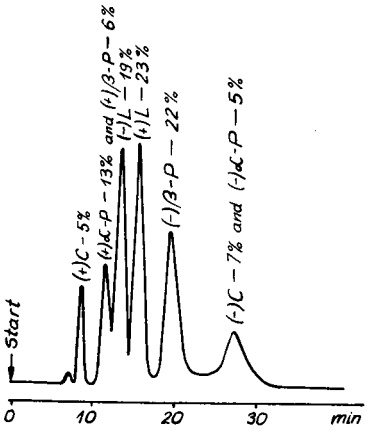

Fig. 1. Chromatogram of artificial mixture I containing (+)- and (−)-α-pinene (α-P), (+)- and (−)-β-pinene (β-P), (+)- and (−)-limonene (L) and (+)- and (−)-camphene (C) obtained at 30°C on column II. Injected sample, 0.12 μl.

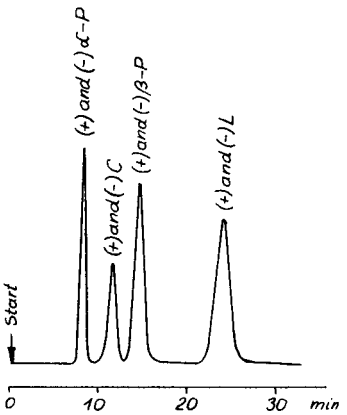

Fig. 2. Chromatogram of mixture I obtained at 30°C on reference column I. Injected sample, 0.04 μl.

complexes with α- and β-pinene, camphene and limonene are much more stable than the corresponding complexes wih α-CD.

For this reason, higher temperatures and lower β-CD concentration were applied to elute these compounds at reasonable retention times from β-CD (0.23 mol%) and γ-CD (0.79 mol%) columns, as can be seen in Table I. Overall these data seem to be satisfactory.

Under the experimental conditions very efficient discrimination of particular compounds can be achieved via α-CD complexation at 30 and 40°C on column II, *e.g.*, at 30°C with a separation factor $\alpha_{-/+} = 2.4$ for α-pinene, 1.7 for β-pinene, 3.2 for camphene and $\alpha_{+/-}$ 1.2 for limonene. Such high separation factors for enantiomers are very rarely encountered, especially when hydrocarbons are involved.

The chromatogram in Fig. 1 shows that the situation is less satisfactory for mixtures. In fact (+)-camphene, (+)-limonene, (−)-limonene and (−)-β-pinene are

TABLE I

ADJUSTED[a] RETENTION TIMES (t'_R, min) OF ENANTIOMERS OF α-PINENE, β-PINENE, LIMONENE AND CAMPHENE DETERMINED AT 30°C AND/OR 60°C COLUMNS I–IV

Compound	Column I		Column II, 30°C	Column III, 60°C	Column IV, 60°C
	30°C	60°C			
(+)-α-Pinene	8.0	1.9	11.4	10.0	13.0
(−)-α-Pinene	8.0	1.9	22.6	10.0	13.0
(+)-Camphene	11.4	2.4	8.5	20.7	35.2
(−)-Camphene	11.4	2.4	22.6	20.7	35.2
(+)-β-Pinene	14.4	2.8	11.4	23.6	28.8
(−)-β-Pinene	14.4	2.8	19.5	23.6	28.8
(+)-Limonene	23.9	3.9	15.5	17.9	9.3
(−)-Limonene	23.9	3.9	13.3	17.9	9.3

[a] Adjusted with the dead time of the column, t_0 ($t'_R = t' - t_0$ where t' is the observed retention time).

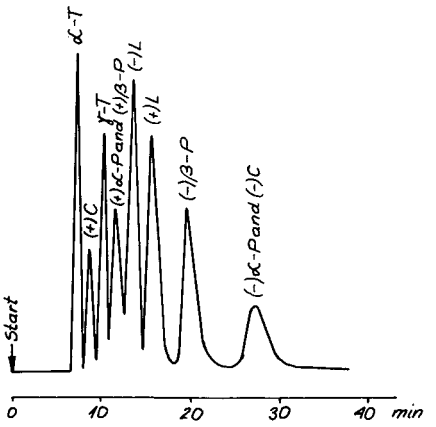

Fig. 3. Chromatogram of artificial mixture II, *i.e.*, mixture I supplemented with α-terpinene (α-T) and γ-terpinene (γ-T), obtained at 30°C on chiral column II with α-CD. Injected sample, 0.12 μl.

eluted as separate peaks and thus they can be directly identified and determined. (+)-α-Pinene give a combined peak with (+)-β-pinene and (−)-α-pinene gives a combined peak with (−)-camphene; hence they can only be determined as a sum. In order to overcome this difficulty, a supplementary achiral column was used, working in parallel, which allowed the separation of α-pinene, β-pinene and camphene. As indicated in Table I and from literature data, the problem of the separation of these three hydrocarbons is relatively simple and for this purpose reference column I (F) can be used. Further confirmations can be obtained by using column III (0.23 mol% β-CD) or IV (0.79 mol% γ-CD).

The results obtained on two columns (α-CD and reference) may serve as a basis for further approximate evaluations of the relative amounts of (+)-α-pinene and (+)-β-pinene in a mixture of unknown composition.

Preliminary studies of essential oils and literature data suggest that in addition to the above-mentioned compounds, other compounds may also be present, including achiral molecules. In order to investigate this problem, we studied mixture I supplemented with various terpenic hydrocarbons. This preliminary identification of unknown peaks is exemplified by Fig. 3.

Essential oils

Figs. 4 and 5 show chromatograms of pine needle oil and fir needle oil, respectively, obtained on column II (0.23 mol% α-CD) under similar conditions to those applied for standard mixtures (Figs. 1 and 3). Table II gives the contents of the main components as identified by direct measurements on the α-CD column and Table III those on the reference column. It is seen that the main components of fir needle oil (overall *ca.* 75.8%) are laevorotatory monoterpenic hydrocarbons: (−)-limonene (27.7%), (−)-β-pinene (14.4%), (−)-α-pinene and (−)-camphene (33.7%). In contrast, in the pine needle oil dextrarotatory hydrocarbons dominate (overall *ca.* 59.1%): (+)-α-pinene and (+)-β-pinene (56.3%), (+)-camphene (0.9%) and (+)-limonene (1.9%).

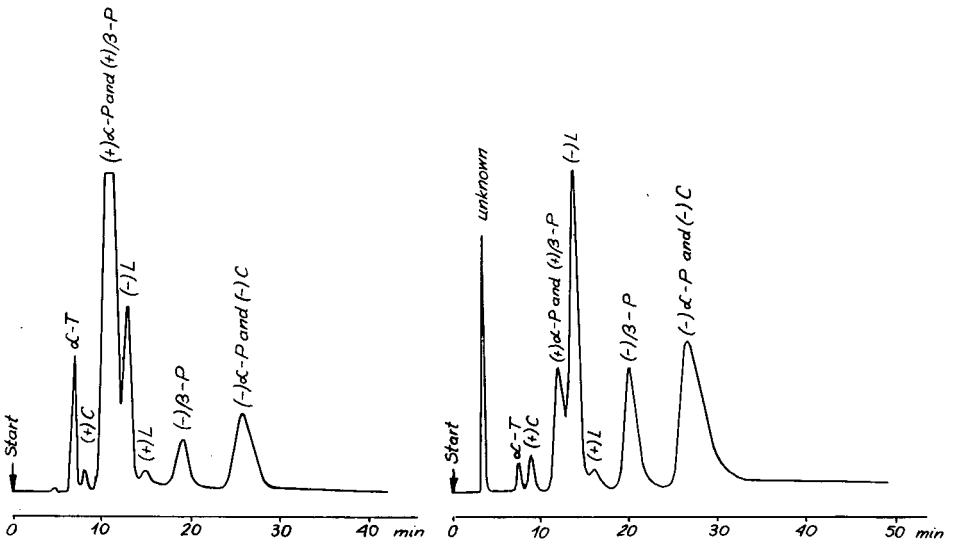

Fig. 4. Chromatogram of a 0.15-μl sample of pine needle oil obtained at 30°C on chiral column II with α-CD.

Fig. 5. Chromatogram of a 0.12-μl sample of fir needle oil obtained at 30°C on chiral column II with α-CD.

TABLE II

CONTENTS (%) OF THE MAIN COMPONENTS OF PINE NEEDLE OIL AND FIR NEEDLE OIL (IN %) AS DETERMINED ON CHIRAL COLUMN II WITH α-CD

Conditions as in Table I.

Compound	Pine needle oil	Fir needle oil
α-Terpinene	5.3	1.3
(+)-Camphene	0.9	1.2
(+)-α-Pinene and (+)-β-pinene	56.3	10.7
(−)-Limonene	12.4	27.7
(+)-Limonene	1.9	1.2
(−)-β-Pinene	5.8	14.4
(−)-α-Pinene and (−)-camphene	13.7	33.7

TABLE III

CONTENTS (%) OF THE MAIN COMPONENTS OF PINE NEEDLE OIL AND FIR NEEDLE OIL AS DETERMINED ON REFERENCE COLUMN I

Conditions as in Table I.

Compound	Pine needle oil	Fir needle oil
α-Terpinene	4.5	1.5
(+)-α-Pinene and (−)-α-pinene	35.8	35.1
(+)-β-Pinene and (−)-β-pinene	38.3	14.8
(+)-Limonene and (−)-limonene	14.5	27.2
(+)-Camphene and (−)-camphene	0.9	1.2

The results presented above suggest that the difficult problem of the direct recognition of enantiomers of particular terpenic hydrocarbons present in essential oils could be resolved on the basis of α-CD complexation. To achieve this goal very detailed optimization studies should be performed.

ACKNOWLEDGEMENT

This work was supported by Grant CPBR 3.20 from the Polish Academy of Sciences.

REFERENCES

1 E. von Rudloff, *Adv. Chromatogr.*, 10 (1974) 173.
2 B. A. Bierl-Leonhardt and E. D. De Vilbiss, *Anal. Chem.*, 53 (1981) 936.
3 R. P. Adams, M. Granat, L. R. Hogge and E. M. von Rudloff, *J. Chromatogr. Sci.*, 17 (1979) 75.
4 V. F. Kalasiński and J. T. McDonald, *J. Chromatogr. Sci.*, 21 (1983) 193.
5 P. R. Griffiths, J. A. de Haseth and L. V. Azarraga, *Anal. Chem.*, 55 (1983) 1361A.
6 V. F. Kalasiński, S. Pechsiri and K. S. Kalasiński, *J. Chromatogr. Sci.*, 24 (1986) 543.
7 T. Kościelski, D. Sybilska and J. Jurczak, *J. Chromatogr.*, 280 (1983) 131.
8 V. Schurig, M. Schleimer and H. P. Nowotny, *Naturwissenschaften*, 77 (1990) 133.
9 M. Lindström, T. Norin, I. Valterova and J. Vrkoc, *Naturwissenschaften*, 77 (1990) 134.
10 D. Sybilska, J. Kowalczyk, M. Asztemborska, T. Stankiewicz and J. Jurczak, *J. Chromatogr.*, 543 (1991) 397.
11 V. Schurig and H. P. Nowotny, *Angew. Chem., Int. Ed. Engl.*, 29 (1990) 939.
12 K. Bauer and G. Garbe, *Common Fragrances and Flavor Materials, Preparations, Properties and Uses*, VCH, Weinheim, 1985, pp. 134–135.
13 S. M. Lapp and E. von Rudloff, *Can. J. Bot.*, 60 (1982) 2762.
14 D. V. Banthorpe, O. Ekundayo and V. C. O. Njar, *Phytochemistry*, 23 (1984) 291.
15 S. Simard, J. M. Hachey and G. J. Collin, *J. Wood Chem. Technol.*, 8 (1988) 561.
16 D. Sybilska and J. Jurczak, *Carbohydr. Res.*, 192 (1988) 243.
17 R. J. Ochocka, M. Wesołowski and H. Lamparczyk, *Thermochim. Acta*, 173 (1990) 199.

Journal of Chromatography, 543 (1991) 179–186
Elsevier Science Publishers B.V., Amsterdam

CHROM. 23 080

Crown ethers as stationary phases in gas chromatography

Comparison between dibenzo-18-crown-6, dibenzo-24-crown-8 and dicyclohexano-24-crown-8 with respect to polarity, selectivity and stability[a]

NAGARAJ R. AYYANGAR*, AMRUTA S. TAMBE and SUJATA S. BISWAS
Division of Organic Chemistry—11, National Chemical Laboratory, Pune-411 008 (India)
(First received August 17th, 1990; revised manuscript received December 27th, 1990)

ABSTRACT

Chromatographic characteristics, including thermal stability, polarity and selectivity, of dibenzo-18-crown-6 (DB18C6), dibenzo-24-crown-8 (DB24C8) and dicyclohexano-24-crown-8 (DCH24C8) were compared. Phase transition studies were carried out by plotting graphs of log(specific retention volume) against the inverse of absolute temperature. Nitrochlorobenzene, nitrophenol, nitroaniline, chloroaniline, cresol, chlorophenol and dimethylphenol isomers were injected onto these crown ether stationary phases at 3%, 10% and 20% loadings. Dimethylphenol and nitrochlorobenzene isomers were separated well on 10% DB24CB and 10% DCH24C8 columns. DB18C6 is useful for the direct analysis of nitrophenol and nitroaniline isomers without any derivatization.

INTRODUCTION

Crown ether compounds have widely been used in analytical chemistry [1–3]. The use of crown ethers in chromatography was first reported by Blasius *et al.* [4] and Sousa *et al.* [5]. The effect of the hydrophobicity and cavity size of the crown ether in crown ether-containing mobile phases on the retention of amino compounds in reversed-phase high-performance liquid chromatography (RP-HPLC) has been studied [6]. RP-HPLC of substituted anilines utilizing the molecular recognition ability of crown ethers has been compared with ion-pair chromatography [7].

The use of crown ethers in gas chromatography (GC) has been rare. Vigalok and Bubachinkova [8] first reported the chromatographic characteristics of 18-crown-6. Ono [9] separated dichlorophenol isomers on 20% dibenzo-18-crown-6 coated on acid-washed firebrick C_{22} (2.25 m × 3 mm I.D. stainless-steel column). Li [10,11] tried to separate hydrocarbons, alcohols and amines on various crown ether stationary phases. Fine *et al.* [12] reported preparation and GC characterization of

[a] NCL Communication No. 4979.

0021-9673/91/$03.50

some silacrown ether stationary phases. Lee *et al.* [13] compared oligo(ethylene oxide)-substituted polysiloxanes with polyethylene glycol as stationary phase for capillary GC and found that crown ether-polysiloxanes have unique selectivity because of the size and shape of the crown ether cavity. Separations of aromatic hydrocarbons, chlorine-containing compounds, etc. on Carbochrome modified with dibenzo-18-crown-6 have been reported [14]. The chromatographic characteristics of some dipentadecylcrown ethers and *n*-undecyloxymethyl-18-crown-6–polysiloxane have been studied recently [15,16]. The inclusion properties of some crown ethers have been studied by GC [17].

In this study, the chromatographic characteristics of dibenzo-18-crown-6 (DC18C6), dibenzo-24-crown-8 (DB24C8) and dicyclohexano-24-crown-8 (DCH24C8) were compared.

EXPERIMENTAL

A Hewlett-Packard Model 5880A gas chromatograph equipped with a level 4 integrator and computing system and a flame ionization detector was used. Aldrich-grade crown ethers were used for making the stationary phases. The crown ethers (DB18C6, DB24C8 and DCH24C8) were coated on Chromosorb W AW DMCS (80–100 mesh) at concentrations of 3%, 10% and 20%. The coated supports were packed in stainless-steel columns (1.8 m × 3 mm O.D.). The maximum operating temperatures for the stationary phases were first established using thermogravimetry and differential scanning calorimetry (DSC) and the phases were then tested chromatographically by the method of Pulsipher *et al.* [18]. Nitrogen was used as the carrier gas at a flow-rate of 30 ml min^{-1}. The polarities of DB24C8 and DCH24C8 were measured at 120°C and that of DB18C6 at 180°C.

The column void volume was determined by the iterative method of Guardino *et al.* [19]. The efficiency of the crown ether columns was determined at 170°C and compared with that of Carbowax 20M. The selectivities of the crown ethers were characterized by injecting positional isomers of cresol, nitrochlorobenzene, chloroaniline, chlorophenol, dimethylphenol, nitrophenol and nitroaniline.

RESULTS AND DISCUSSION

Phase transition and thermal stability studies

The specific retention volume (V_g) for the test compound *p*-toluidine was calculated at 10°C intervals and a graph of $\log V_g$ *versus* $10^4/T$ was plotted for *p*-toluidine on DB18C6 and DCH24C8 columns (Fig. 1). There is no phase transition in DCH24C8, as indicated by the straight line. The temperature range from T_1 (140°C) to T_2 (153°C) is the transition range for DB18C6 as determined by GC. At temperatures below T_1, solute retention will depend essentially on adsorption processes, but as the temperature is raised above T_1, the stationary phase starts to melt and it attains the liquid state at T_2. At the latter temperature the retention of solutes is due to partition. This temperature matches the phase transition temperature obtained by DTA. Fig. 2 shows the plot of log V_g *versus* $10^4/T$ for acetonitrile on DB24C8. The phase transition temperature obtained from the graph (104°C) is in good agreement with that obtained by DSC (107.5°C). DB24C8 becomes a true liquid at 104°C.

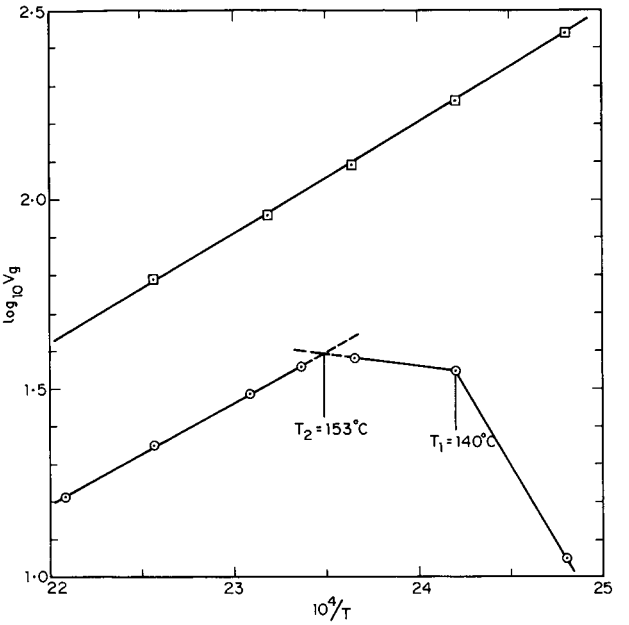

Fig. 1. Plots of log (specific retention volume) against inverse of absolute temperature for *p*-toluidine on (○) 10% DB18C6 and (□) 10% DCH24C8 columns.

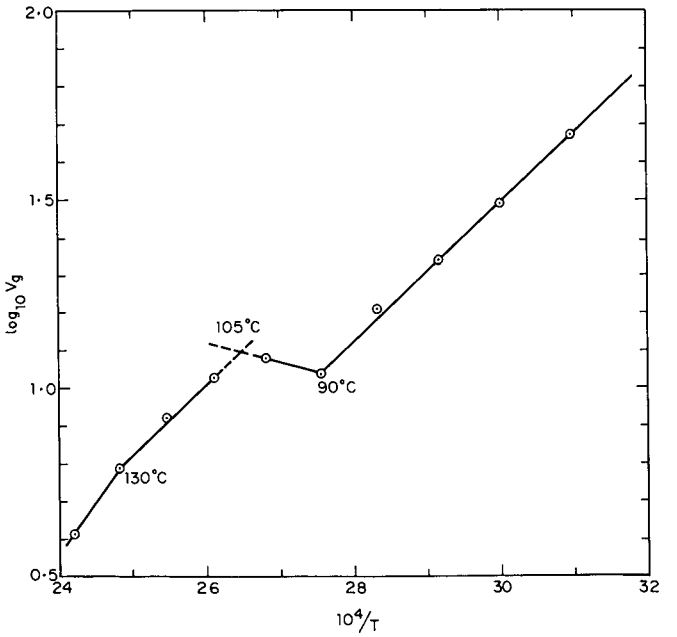

Fig. 2. Plot of log (specific retention volume) against inverse of absolute temperature for acetonitrile on 10% DB24C8 column.

TABLE I

COMPARISON OF PHASE TRANSITION TEMPERATURES AND MINIMUM AND MAXIMUM OPERATING TEMPERATURES

Stationary phase	Temperature at which decomposition starts[a] (°C)	Maximum allowable temperature (°C)	Phase transition temperature (°C)	
			By DTA[b]	By DSC[c]
DB18C6	210	190	151	161.25
DB24C8	185	175	60	85
			80	107.5
DCH24C8	199.5	180	–	–

[a] This temperature is determined by thermogravimetry.
[b] Differential thermal analysis.
[c] Differential scanning calorimetry.

The DB18C6 and DCH24C8 columns were first conditioned at 190°C for 4 h. The specific retention volume (V_g) for octadecane was then determined at 160°C. Subsequently stepwise conditioning was applied at 10°C intervals to establish whether there was any change in V_g. With 10% DB18C6 there was no change in the value of V_g whereas there was a 2.3% decrease in V_g for octadecane on 10% DB24C8 after conditioning at 190°C for 2 h. The 10% DB24C8 column was first conditioned up to 175°C and the specific retention volume for octadecane was then determined at 140°C. There was no change in V_g after stepwise conditioning of the column at 150, 160, 170 and 175°C.

Table I gives a comparison of the phase transition temperatures and maximum and minimum operating temperatures for the different crown ethers. A comparison of efficiencies in terms of total number of plates (N) and height equivalent to a theoretical plates (H) between various crown ethers and Carbowax 20M is shown in Table II.

Polarity and selectivity studies

McReynolds' constants (ΔI), retention indices (I), capacity factors (k') and average polarities of the various crown ethers together with the ΔI values for Carbowax 20M and tricresyl phosphate are given in Table III. The temperature for mea-

TABLE II

COMPARISON OF EFFICIENCY IN TERMS OF TOTAL NUMBER OF PLATES (N) AND HEIGHT EQUIVALENT OF THEORETICAL PLATES (H) BETWEEN VARIOUS CROWN ETHERS AND CARBOWAX 20M AT 170°C

Stationary phase	Octadecane		*o*-Nitrochlorobenzene		3,4-Dimethylphenol	
	N	H(cm)	N	H(cm)	N	H(cm)
10% DB18C6	331	0.54	465	0.38	243	0.74
10% DB24C8	798	0.23	1611	0.11	1247	0.14
10% DCH24C8	836	0.22	1697	0.106	1979	0.09
Carbowax 20M	611	0.29	1527	0.118	2283	0.08

TABLE III

CAPACITY FACTORS (k'), RETENTION INDICES (I), McREYNOLDS' CONSTANTS (ΔI) AND AVERAGE POLARITY FOR THE McREYNOLDS' PROBES ON VARIOUS CROWN ETHERS ALONG WITH THE ΔI VALUES FOR CARBOWAX 20M AND TRICRESYL PHOSPHATE

Stationary phase	Parameter	McReynolds' probes					Average polarity
		Benzene	*n*-Butanol	2-Pentanone	Nitropropane	Pyridine	
DCH24C8	ΔI	153	333	194	331	291	260
	I	806	923	821	983	990	
	k'	1.31	2.47	1.43	3.40	3.55	
Tricresyl phosphate	ΔI	176	321	250	374	299	284
DB24C8	ΔI	286	454	366	544	607	452
	I	939	1044	993	1196	1206	
	k'	0.81	1.44	1.09	3.29	3.49	
Carbowax 20M	ΔI	322	536	368	572	510	462
DB18C6[a]	ΔI	231	526	472	475	521	442
	I	1314	1558	1525	1580	1507	
	k'	0.56	2.57	2.09	2.95	1.87	

[a]McReynolds' constants for DB18C6 were determined at 180°C using high-temperature probes suggested by Vernon and Ogundipe [18], *i.e.*, *n*-butylbenzene, benzyl alcohol, acetophenone, nitrobenzene and aniline.

surement of these values was 120°C for DCH24C8 and 180°C for DB18C6 (DB18C6 is a solid at 120°C). Test probes used at high temperature (*i.e.* 180°C) were *n*-butylbenzene, benzyl alcohol, acetophenone, nitrobenzene and aniline, as suggested by Vernon and Ogundipe [20]. Comparison of the ΔI values shows that average polarity of DCH24C8 is similar to that of tricresyl phosphate and the latter retains ketones and nitro compounds more strongly. DB24C8 has an average polarity similar to that of Carbowax 20M and it retains proton-accepting compounds much more strongly whereas Carbowax 20M retains alcohols more strongly.

Since Ono [9] had reported the separation of dichlorophenol isomers on 20% DB18C6, we compared the selectivities of the crown ethers studied here with respect to dichlorophenols and similar compounds such as dimethylphenols, cresols, nitrophenols, nitrochlorobenzenes and chloranilines. DB24C8 has the largest ΔI value for nitro compounds and accordingly it gives the best separation of nitrochlorobenzene isomers, as is seen in Fig. 3. The analysis time is also much shorter (*ca.* 7 min) than that for the same separation on Carbochrome modified with DB18C6 (12 min) [14].

Previously we reported the determination of nitrochlorobenzene isomers on a 5% isopropylidenebisphenol diacetate column [21]. The separation of dimethylphenol isomers on the crown ether stationary phases is shown in Fig. 4. It was not possible to separate 2,4- and 2,5-dimethylphenol on any of the crown ethers and 2,3- and 3,5-dimethylphenol were only partially resolved. When the loading was increased to 20% the peaks became broad and the separation did not improve much. Separations of *o*-, *m*- and *p*-cresols and -chloroanilines were also tried, but without any success. When dichlorophenol isomers were injected onto the 10% DB18C6 column,

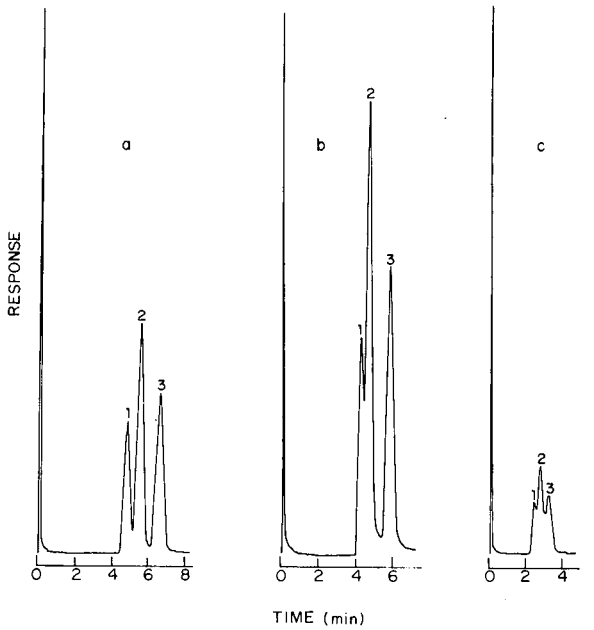

Fig. 3. Separation of nitrochlorobenzene isomers on various crown ethers at 170°C. Nitrogen flow-rate, 30 ml min^{-1}. Peaks: 1 = *m*-nitrochlorobenzene; 2 = *p*-nitrochlorobenzene; 3 = *o*-nitrochlorobenzene. (a) 10% DB24C8; (b) 10% DCH24C8; (c) 10% DB18C6.

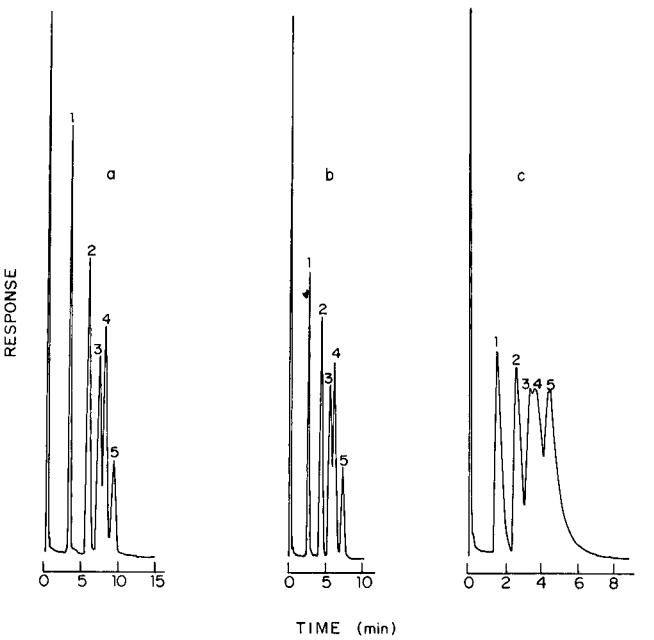

Fig. 4. Separation of dimethylphenols (DMP) on various crown ethers. Nitrogen flow-rate, 30 ml min^{-1}. Peaks: 1 = 2,6-DMP; 2 = 2,4 + 2,5-DMP; 3 = 2,3-DMP; 4 = 3,5-DMP; 5 = 3,4-DMP. (a) 10% DHC24C8 at 170°C; (b) 10% DB24C8 at 170°C; (c) 10% DB18C6 at 160°C.

post-tailing was observed. The retention times of these isomers depend on the amount injected. The DCH24C8 and DB24C8 columns gave symmetrical peaks but without any separation.

Nitrophenol and nitroaniline isomers were injected onto the 3% crown ether columns without any derivatization. *Ortho* isomers eluted immediately after the solvent peak whereas *meta* and *para* isomers were retained for a long time. The retention times of *p*-nitrophenol and *p*-nitroanilines are too long on DB24C8 and DCH24C8 at 170°C and 180°C, respectively, indicating that these molecules must fit well in the cavities of the crown ethers. The separation and analysis time for nitrophenols and nitroanilines on the 3% DB18C6 column is considerable and one can use a DB18C6 column for the direct analysis of nitrophenols (the coating can be even less, e.g., 1%). It is not necessary to derivatize the samples. The analysis of phenols is important owing to its practical applications in biochemical, clinical, forensic and wood chemistry and in food inspection and environmental pollution control. Table IV gives the retention indices of various positional isomers on the different crown ethers.

TABLE IV

RETENTION INDICES OF SOME POSITIONAL ISOMERS ON 10% CROWN ETHERS AT 170°C

Carrier gas, nitrogen at a flow-rate of 30 ml min^{-1}; injection temperature, 220°C; detector temperature, 250°C.

Solute	Stationary phase		
	DB18C6	DB24C8	DCH24C8
2,6-Dimethylphenol[a]	1741	1749	1593
2,5-Dimethylphenol	1858	1871	1724
2,4-Dimethylphenol	1858	1870	1721
2,3-Dimethylphenol	1919	1928	1767
3,5-Dimethylphenol	1935	1952	1789
3,4-Dimethylphenol	1976	1992	1820
o-Cresol	1785	1796	1593
m-Cresol	1858	1870	1655
p-Cresol	1849	1863	1651
o-Nitrochlorobenzene	1983	1968	1728
m-Nitrochlorobenzene	1918	1892	1661
p-Nitrochlorobenzene	1949	1927	1682
o-Chloroaniline	1835	1828	1640
m-Chloroaniline	2010	2011	1801
p-Chloroaniline	2005	2011	1796
o-Nitrophenol[b]	1839	1754	1761
m-Nitrophenol	2130	2647	2671
p-Nitrophenol	2183	2798	2804
o-Nitroaniline	2057	2335	2312
m-Nitroaniline	2124	2533	2504
p-Nitroaniline	2230	2816	2774

[a] Dimethylphenols were injected at 160°C on DB18C6.

[b] Nitrophenols were injected at 180°C on 3% DB18C6 and 3% DCH24C8 and at 170°C on 3% DB24C8.

CONCLUSIONS

The average polarities of DB24C8 and DCH24C8 are similar to those of Carbowax 20M and tricresyl phosphate, respectively. DB24C8 retains proton-accepting compounds much more strongly than Carbowax 20M. The efficiencies of DB24C8 and DCH24C8 are comparable to that of Carbowax 20M. Nitrochlorobenzene and dimethylphenol isomers are separated very well on DB24C8 and DCH24C8. DB18C6 can find applications in the direct analysis of nitrophenols and nitroanilines. The *para* isomers of nitrophenol and nitroaniline fit very well in the cavities of DB24C8 and DCH24C8, as is indicated by their long retention times on these crown ethers.

ACKNOWLEDGEMENTS

The authors thank Mr. S. S. Deo and Mr. V. V. Borker for technical assistance.

REFERENCES

1 I. M. Kolthoff, *Anal. Chem.*, 51 (1979) 1R.
2 E. Blasius and K. P. Janzen, in F. Vögtle and E. Webber (Editors), *Host Guest Complex Chemistry —Macrocycles; Synthesis Structures, Applications*, Springer, Berlin, Heidelberg, 1985, p. 189.
3 R. Huang and D. Zhang, *Fen Hsi Hua Hsuch*, 9 (1981) 615.
4 E. Blasius, W. Adrian, K. P. Janzen and G. Klautke, *J. Chromatogr.*, 96 (1974) 89.
5 L. R. Sousa, D. H. Hoffman, L. Kaplan and D. J. Cram, *J. Am. Chem. Soc.*, 96 (1974) 7100.
6 T. Nakagawa, H. Murata, A. Shibukawa, K. Murakami and H. Tanaka, *J. Chromatogr.*, 330 (1985) 43.
7 A. Shibuka, T. Nakagawa, A. Kaihara, K. Yagi and H. Tanaka, *Anal. Chem.*, 59 (1987) 2496.
8 R. V. Vigalok and L. F. Bubachinkova, *Usp. Gaz. Khromatogr. (Kazan)*, 6 (1981) 190.
9 A. Ono, *Analyst (London)*, 108 (1983) 1265.
10 R. Li, *Wuhan Daxue Xuebao, Zira Kexueban*, 4 (1985) 121.
11 R. Li, *Sepu*, 4 (1986) 304.
12 D. D. Fine, H. L. Gearhart, II, and H. A. Mottola, *Talanta*, 32 (1985) 751.
13 C. A. Rause, A. C. Finlinson, B. J. Tarbet, J. C. Pixton, N. M. Djordjevic, K. E. Markides and M. L. Lee, *Anal. Chem.*, 60 (1988) 901.
14 E. V. Zagorevskaya and N. V. Kovaleva, *J. Chromatogr.*, 365 (1986) 7.
15 Y. Jin, R. Fu and Z. Huang, *J. Chromatogr.*, 469 (1989), 153.
16 C. Y. Wu, C. M. Wang, Z. R. Zeng and X. R. Lu, *Anal. Chem.*, 62 (1990) 968.
17 A. Kohoutova, E. Smolkova-Keulemansova and L. Feltl, *J. Chromatogr.*, 471 (1989) 139.
18 M. A. Pulsipher, R. S. Johnson, K. E. Markides, J. S. Bradshaw and M. L. Lee, *J. Chromatogr. Sci.*, 24 (1986) 383.
19 X. Guardino, J. Albaiges, G. Firpo, R. Rodriguez-Vinals and M. Gassiot, *J. Chromatogr.*, 118 (1976) 13.
20 F. Vernon and C. O. E. Ogundipe, *J. Chromatogr.*, 132 (1977) 181.
21 N. R. Ayyangar, A. S. Tambe and S. S. Biswas, *J. Chromatogr.*, 483 (1989) 33.

Journal of Chromatography, 543 (1991) 187–194
Elsevier Science Publishers B.V., Amsterdam

CHROM. 23 108

Post-extraction solvent flush of the pressure restrictor in supercritical fluid extraction

CYNTHIA A. THOMSON and DAVID J. CHESNEY*
Department of Chemistry and Chemical Engineering, Michigan Technological University, Houghton, MI 49931 (U.S.A.)
(First received March 27th, 1990; revised manuscript received January 7th, 1991)

ABSTRACT

When using supercritical fluid extraction to isolate and concentrate pesticide residues from plant tissue samples, extraneous components of the plant matrix are extracted in sufficient quantity to cause intermittent obstruction of the pressure restrictor. In some cases, termination of the extraction occurs due to irreversible plugging of the restrictor. It has been determined that a post-extraction solvent flush of the pressure restrictor is sufficient to prevent restrictor obstruction in almost all cases.

INTRODUCTION

Supercritical fluid extraction (SFE) is increasingly being applied for the isolation of a wide variety of analytes from complex matrices [1]. Many applications involve the coupling of SFE and supercritical fluid chromatography (SFC) for a combined extraction and analysis with a single instrument [2,3]. Other on-line applications involve the interfacing of SFE with mass spectrometry [4] and capillary gas chromatography [5,6]. The coupling of SFE with SFC or other chromatographic modes has merit in many cases [3]. However, such on-line coupling can lead to complications involving undesired extract components which present chromatographic or detector-interference problems or which may be strongly retained on the column, requiring excessive flushing times for removal.

Off-line SFE is also performed whereby the sample extract is collected in a solid phase trap [7] or solvent [8,9] and then further treated to make it suitable for analysis by the appropriate instrumental technique. The use of off-line SFE has several practical advantages. A well-chosen trapping solvent can be evaporated to obtain a more concentrated solution for subsequent analysis. The extract solution can be subjected to chemical treatments such as liquid–liquid extraction or solid phase extraction which, properly chosen, will produce additional selectivity for the analyte of interest. Off-line SFE also provides maximum flexibility in the choice of the analytical technique, allowing optimization of both sensitivity and selectivity for the analyte of interest.

Off-line SFE is not without its problems, however. Potential sample losses due to aerosol formation have led some investigators to the use of liquid nitrogen cold

0021-9673/91/$03.50

traps to ensure complete collection of extracted components [10]. The use of pure carbon dioxide as a supercritical fluid extraction medium has also led to restrictor clogging problems due to the rapid cooling of the fluid which takes place upon expansion to atmospheric pressure [10].

A problem which we have encountered in our use of off-line SFE in the analysis of food crops for pesticide residues is the presence of undesired co-extracted components of the plant tissue matrix. This material collects in the pressure restrictor, causing unpredictable changes in its restrictive ability and intermittent plugging. In many cases, the flow of supercritical extractant has been stopped entirely. This co-extracted material was found to be soluble in organic solvents such as ethanol and isooctane and is most likely plant triglycerides which are known to be extracted from plant tissues at the SFE conditions employed [1,11].

Our interests lie in the determination of "bound" residues, which are incorporated into the plant matrix and thus difficult to extract. In such a situation, a constant flow-rate of supercritical extractant for extended periods of time is crucial for maximum extraction efficiency.

Our solution to this problem of restrictor plugging involves combining a suitable solvent with the supercritical fluid between the extraction cell and the pressure restrictor. This approach eliminates the intermittent plugging of the pressure restrictor due to the accumulation of extracted plant material. The solvent flush is also useful in providing additional enthalpy sufficient to prevent the freezing of the carbon dioxide at the pressure restrictor outlet. Secondary control of the extractant carbon dioxide flow-rate is also provided by varying the solvent flow-rate through the restrictor. This paper describes the apparatus and its operation. Data is presented to illustrate the improvement in consistency of the supercritical carbon dioxide flow-rate during extraction.

EXPERIMENTAL

Chemicals

Isooctane and ethanol were reagent grade and used after filtering through a 0.45-μm glass microfibre filter. 2,4-Dichlorophenol, 99% (Aldrich, Milwaukee, WI, U.S.A) was used without further purification. "Bone dry" welding-grade carbon dioxide was used as the supercritical fluid extractant.

Samples

Plant tissues were straw and seed of triticale and barley. All were stored in glass jars with aluminum foil seals at -20°C. Small amounts of material were ground 10 min in a small grain mill producing 2–4 mm lengths suitable for packing into the extraction cell. The individual portions were combined and thoroughly mixed to ensure a homogeneous sample of each matrix.

SFE instrumentation

The SFE apparatus was constructed in-house from available components and is shown in Fig. 1. A standard reciprocating high-performance liquid chromatography (HPLC) pump (Milton Roy MiniPump, Laboratory Data Control, Riviera Beach, FL, U.S.A.) was used to pressurize the carbon dioxide above its critical pressure. The

pump head and check valves were cooled by circulating a −15°C ethylene glycol–water mixture through an aluminium radiator machined to closely fit the pump head. Liquid carbon dioxide was delivered to the pump through 1/8-in. stainless-steel tubing. All other connecting tubing was 1/16-in. stainless-steel.

The extraction cells consisted of empty 5 cm × 4.6 mm HPLC columns (Alltech, Deerfield, IL, U.S.A.) with 2-μm stainless-steel frits on both the inlet and outlet ends. Knurl–Lok fittings (Alltech) with PEEK double-sided ferrules were used to secure the extraction cell in line. A Varian 1400 gas chromatograph oven was used for temperature controle. The extraction cell was preceded by a 10 m coil of 1/16-in. stainless-steel tubing to provide temperature equilibration for the supercritical carbon dioxide. The transfer line exiting the extraction cell was routed through the heated (70–85°C) injector port of the chromatograph oven.

The flushing solvent was pumped by a second MiniPump. Flushing solvent and supercritical carbon dioxide extractant were combined at a stainless-steel tee fitting and routed to the pressure restrictor. The delivery rates of the carbon dioxide and the flush solvent were adjusted independently to maintain a narrow range of extraction pressure.

The pressure restrictor was a 15 cm × 1/16 in. O.D. × 0.020 in. I.D. stainless-steel tubing crimped at the very end. The solvent line into the interfacing tee was replaced with a stainless-steel plug when extract collection without the solvent flush was desired. Collection of the sample extract was performed by placing the tip of the pressure restrictor in a small quantity of solvent contained in a 20 × 150 mm side-arm test tube. A rubber stopper served to seal the side-arm test tube and support the pressure restrictor. In this manner, flow-rates of the gaseous carbon dioxide could be monitored by a bubble flowmeter. A large beaker of tap water (35–40°C) provided

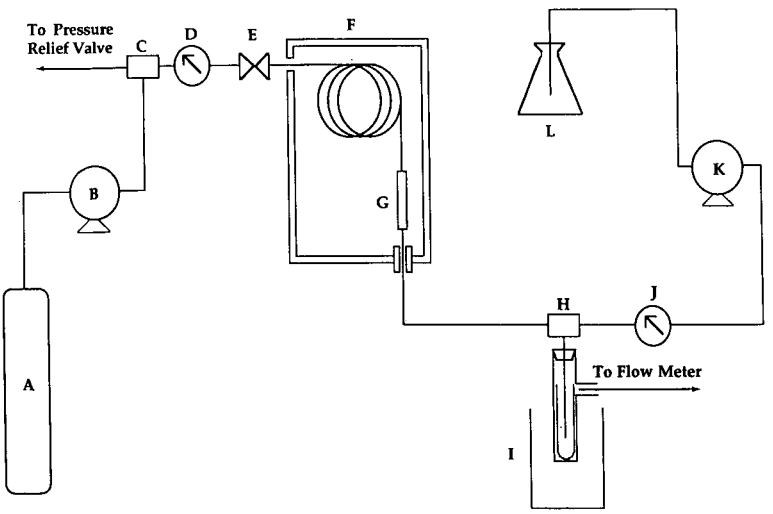

Fig. 1. Supercritical fluid extraction apparatus. See text for additional description. A = Liquid CO_2 cylinder; B = CO_2 pump with cooling assembly; C = tee fitting; D = pressure gauge; E = on/off needle valve; F = oven; G = extraction cell; H = CO_2/solvent interface tee; I = extract collection assembly; J = pressure gauge; K = flush solvent pump; L = solvent reservoir.

thermal mass to the collection apparatus to minimize the freezing of carbon dioxide at the restrictor tip. In cases where analyte was thought to be lost by volatilization from the collection tube, a second side-arm test tube with an impinger was placed in line before the bubble flowmeter.

Extraction

A clean, dry extraction cell was positioned vertically with only the outlet end fitting attached. Silanized glass beads (60–80 mesh, Alltech) were placed into the extraction cell to a depth of about 0.5 cm. This layer of glass beads served as a depth filter, preventing the compaction of the plant tissue sample against the outlet frit. The inlet end fitting was attached loosely to allow the extraction cell and glass beads to be weighed. The cell was opened and a sample of ground plant tissue was packed gently into the extraction cell. The inlet end fitting was replaced and the cell and its contents reweighed. For recovery studies, samples were spiked with 100 μl volumes (Hamilton Microliter syringe) of aqueous 2,4-dichlorophenol standards and then sealed tightly.

The restrictor tip was immersed in the collecting solvent prior to placing the extraction cell on line in the SFE oven. The oven and the carbon dioxide pump were turned on to allow the extraction cell to attain thermal equilibrium while the carbon dioxide pressure built up. When used, the solvent flush pump was turned on once the carbon dioxide pressure and flow were sufficient to prevent backflushing of solvent through the connecting tubing toward the extraction cell. The system generally took less than five min to reach the desired temperature and pressure. Extractions were run for 60 min, unless the carbon dioxide flow was reduced to zero before this time. During the extraction, minor adjustments of both pumps were typically required to maintain pressure within 20–50 p.s.i. of the initial setting.

The restrictor required occasional reconstruction, due to plugging by solid particles or physical damage to the tip. Restrictor calibration was required after reconstruction in order to keep the pump vernier settings approximately the same from one set of runs to the next. For calibration, the carbon dioxide line to the interfacing tee was replaced with a stainless-steel plug allowing only isooctane to be pumped through the restrictor. With an isooctane delivery rate of 0.23 ml/min, the restrictor tip was crimped to yield a back pressure reading of 400–500 p.s.i.

RESULTS AND DISCUSSION

We are exploring the use of off-line supercritical fluid extraction to isolate pesticide residues for subsequent HPLC analysis. Our initial attempts to extract plant tissues used ethanol as a flushing and trapping solvent. Upon dilution with water to provide a solution compatible with our mobile phase, substantial quantities of formerly dissolved plant extract precipitated, making the solution unsuitable for HPLC injection without further clean-up. This precipitated material was found to be soluble in isooctane. However, efforts to remove these components by liquid–liquid extraction with isooctane were unsuccessful due to the formation of a persistent emulsion.

It was suspected that this plant material was also responsible for the inconsistencies in carbon dioxide flow through the pressure restrictor during the course of an extraction. Isooctane was chosen as the flushing and trapping solvent since it retained the water-insoluble extract components while allowing the partitioning of polar and ionized analytes into an aqueous layer without forming an emulsion.

The gaseous carbon dioxide flow-rate during the course of several individual extractions is shown in Fig. 2–5. In each figure, solid symbols indicate extractions run with an isooctane solvent flush, while open symbols indicate no solvent flush. Matrices were extracted in the order in which they are presented. Individual samples follow the order: circle; triangle; square. All twelve samples with solvent flush were completed before the first run without solvent flush. Close operator attention is typically needed to manually adjust conditions at the start of each extraction, precluding immediate measurement of gaseous carbon dioxide flow-rates. The restrictor was reconstructed between the second and third triticale straw samples (Fig. 2) and following each sample without a solvent flush. Even when the restrictor was not changed or was reconstructed and calibrated, initial carbon dioxide flow-rates were seldom identical between sequential runs due to slight variations in cell packing.

As can be seen from the plots of the samples extracted without an isooctane flush in Figs. 2 and 3, a drastic decrease in carbon dioxide flow was observed shortly after the start of the extraction. This behavior was observed to some degree in all straw samples in which an isooctane flush was not used. The decrease in carbon dioxide flow caused by the accumulation of matrix materials in the restrictor without a solvent flush caused a concomitant pressure increase in the extraction cell. This required the operator to continually lower the vernier setting for the pump stroke, thereby maintaining the target pressure and density at the expense of carbon dioxide flow through the extraction cell. Obviously, this is not a desirable situation for efficient extraction. The samples run with a solvent flush exhibit relatively consistent carbon dioxide flow-rates from start to finish of each individual extraction. Without a solvent flush, this consistency is rarely observed. The similarity in the gaseous carbon dioxide flow-rate between samples run without a solvent flush in Fig. 3 is an exception among such extractions. The carbon dioxide flow behavior shown in Fig. 2 is more common.

The extraction pressure of 2300 p.s.i. did not produce the same level of co-extracted materials in seed as in straw. Consequently, extraction of seed samples without a solvent flush (Figs. 4 and 5) did not exhibit the same pattern of carbon

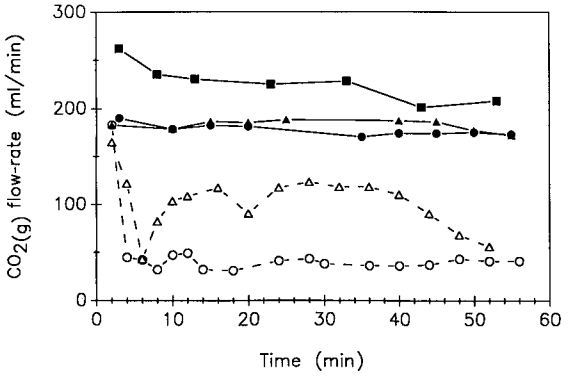

Fig. 2. Flow-rate of gaseous CO_2 for triticale straw extractions. Closed symbols: isooctane solvent flush, 0.23 ml/min (av.). Open symbols: no solvent flush of restrictor. Extraction (CO_2) conditions: 40°C; 2400 p.s.i. (av.), calculated density = 0.801 g/cm^3.

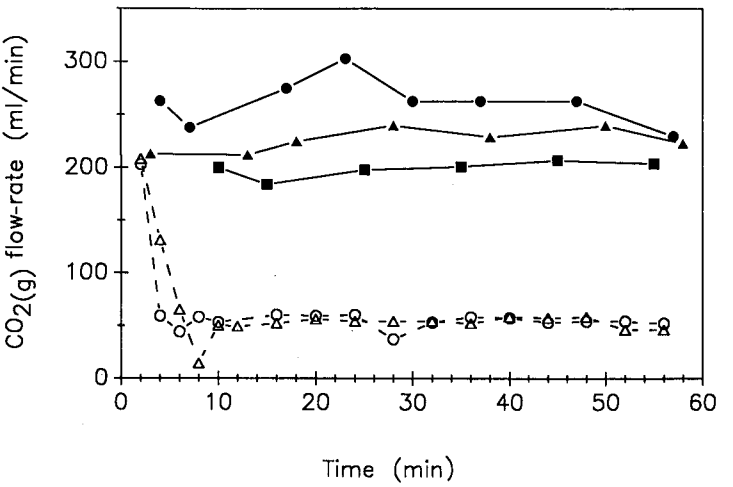

Fig. 3. Flow-rate of gaseous CO_2 for barley straw extractions. Closed symbols: isooctane solvent flush, 0.26 ml/min (av.). Open symbols: no solvent flush of restrictor. Extraction (CO_2) conditions: 40°C, 2400 p.s.i. (av.), calculated density = 0.801 g/cm^3.

dioxide flow. If the seed samples are extracted at a higher density, the extraction behavior with regard to gaseous carbon dioxide flow-rate is similar to that of the straw [12].

An additional problem which results from running extractions without a solvent flush is apparent is Figs. 4 and 5. The initial high flow-rate of carbon dioxide in these experiments was sufficient to evaporate the isooctane trapping solvent from the collection tube, leading to an accumulation of solid carbon dioxide at the restrictor tip and ultimately, to a plugging of the restrictor.

With the solvent flush, this problem was eliminated. At the solvent flush flow-rates used, the solvent added to the collection tube by the flush operation replaced

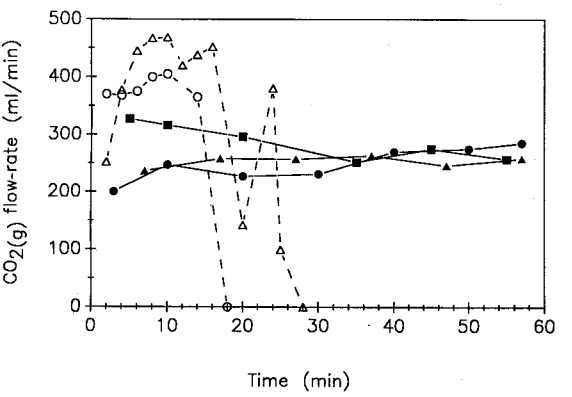

Fig. 4. Flow-rate of gaseous CO_2 for triticale seed extractions. Closed symbols: isooctane solvent flush, 0.28 ml/min (av.). Open symbols: no solvent flush of restrictor. Extraction (CO_2) conditions: 40°C, 2350 p.s.i. (av.), calculated density = 0.790 g/cm^3.

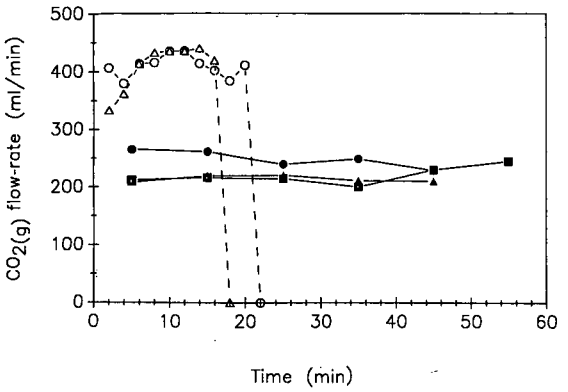

Fig. 5. Flow-rate of gaseous CO_2 for barley seed extractions. Closed symbols: isooctane solvent flush, 0.29 ml/min (av.). Open symbols: no solvent flush of restrictor. Extraction (CO_2) conditions: 40°C, 2280 p.s.i. (av.), calculated density = 0.774 g/cm^3.

solvent lost due to evaporation. Thus, the restrictor tip was never exposed and was always surrounded by a sufficient volume of solvent to prevent accumulation of solid carbon dioxide. In addition, the solvent flush provided additional thermal mass during the passage of extractant through the restrictor. Such benefits have already been noted for extraction co-solvents [10].

It should be emphasized that this solvent flush is not an extraction co-solvent. It is suspected that the flush solvent and the carbon dioxide extractant form a segmented two-phase system in the restrictor. Since this occurs after the extraction cell, the formation of such a two-phase system does not affect extraction efficiency. Indeed, such a situation may increase trapping efficiency of the extracted solutes by providing additional contact with the trapping solvent while the analyte is still being solvated and transported to the restrictor tip by supercritical carbon dioxide. This arrangement may help in minimizing analyte losses due to volatilization or the aerosol formation concomitant with expansion of the carbon dioxide to a gas.

As a consequence of running an extraction with a solvent flush, the total volume of supercritical carbon dioxide in contact with the sample during a complete run is increased, producing higher extraction efficiencies in a finite extraction period. Preliminary results with spiked samples indicate that extraction efficiency of 2,4-dichlorophenol is increased with the solvent flush [12]. However, such spikes are relatively easy to recover in a short period of time, since the spiked solute resides primarily on the surface of the plant matrix.

CONCLUSION

A post-extraction solvent flush of the pressure restrictor has been proven useful in minimizing excessive accumulation of co-extracted material. The choice of flushing solvent can be tailored to the sample matrix without affecting extraction efficiency. This approach should therefore be generally applicable to any supercritical fluid extraction in which the sample matrix yields materials capable of plugging the restrictor.

With isooctane competing for passage through the restrictor, secondary controle of the carbon dioxide flow is achieved. The overall gaseous flow-rate can be fine-tuned to a greater degree than is possible by adjustment of the carbon dioxide vernier alone. Only small adjustments of individual pump-stroke vernier settings are required to maintain the desired pressure. Thus, reasonably consistent flow-rates are obtained during the entire course of the extractions.

REFERENCES

1 J. W. King, *J. Chromatogr. Sci.*, 27 (1989) 355.
2 M. E. P. McNally and J. R. Wheeler, *J. Chromatogr.*, 435 (1988) 63.
3 M. R. Andersen, J. T. Swanson, N. L. Porter and B. E. Richter, *J. Chromatogr. Sci.*, 27 (1989) 371.
4 H. T. Kalinoski, H. R. Udseth, B. W. Wright and R. D. Smith, *Anal. Chem.*, 58 (1986) 2421.
5 S. B. Hawthorne, M. S. Kreiger and D. J. Miller, *Anal. Chem.*, 60 (1988) 472.
6 B. W. Wright, S. R. Frye, D. G. McMinn and R. D. Smith, *Anal. Chem.*, 59 (1987) 640.
7 M. Miller Schantz and S. N. Chesler, *J. Chromatogr.*, 363 (1986) 397.
8 S. B. Hawthorne and D. J. Miller, *Anal. Chem.*, 59 (1987) 1705.
9 S. B. Hawthorne and D. J. Miller, *J. Chromatogr. Sci.*, 24 (1986) 258.
10 B. W. Wright, C. W. Wright, R. W. Gale and R. D. Smith, *Anal. Chem.*, 59 (1987) 38.
11 S. T. Schaeffer, L. H. Zalkow and A. S. Teja, in K. P. Johnston and J. M. L. Penninger (Editors), *Supercritical Fluid Science and Technology* (*ACS Symposium Series*, No. 406), American Chemical Society, Washington, DC, 1989, Ch. 26, p. 416.
12 C. A. Thomson and D. J. Chesney, unpublished results.

Journal of Chromatography, 543 (1991) 195–200
Elsevier Science Publishers B.V., Amsterdam

CHROM. 23 088

Determination of the lipophilicity of arylsulphonylalkanoic and arylsulphonylcycloalkanecarboxylic acids by thin-layer chromatography

J. POLAŃSKI and A. RATAJCZAK*
Department of Organic Chemistry, Silesian University, Szkolna 9, 40-006 Katowice (Poland)
(First received October 17th, 1990; revised manuscript received December 31st, 1990)

ABSTRACT

The R_M values of arylsulphonylalkanoic and arylsulphonylcycloalkanecarboxylic acids were measured by thin-layer chromatography on a polyamide layer. The R_M *vs.* Rekker hydrophobicity relationship was analysed and some excellent correlations, especially within strictly congeneric sub-series, were established.

INTRODUCTION

Lipophilicity is one of the basic properties discussed in quantitative structure–activity relationship (QSAR) studies of biologically active compounds [1]. However, because of the complexity of the phenomena involved, no individual and simple procedure can be recommended as a unique quantitative measure of this property [2]. One of the parameters that appears to fit into the QSAR models of lipophilicity is the R_M value determined on polyamide layers [2,3]. This parameter has been found even more suitable for the description of the biological activity of some compounds than the Hansch hydrophobic constant [4], apparently owing to the similarity between the polyamide and the protein structures [5]. On the other hand, it has been established that the retention mechanism on the polyamide layers involved both partition and adsorption through the hydrogen bonds [6], the phenomena omnipresent in most natural processes.

The aim of this work was to study the dependence between the R_M parameters measured on polyamide layers and the Rekker hydrophobic constants for the series of α-arylsulphonylalkanoic and α-arylsulphonylcycloalkanecarboxylic acids (I–III), some of which have been found to stimulate a sweet taste receptor [7].

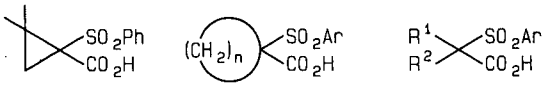

I II III

0021-9673/91/$03.50

EXPERIMENTAL

The title compounds were synthesized according to procedures described elsewhere [8].

For the determination of R_M values, polyamide 11 F_{254} (Merck, Darmstadt,

TABLE I

LIPOPHILICITY INDICES OF THE ACIDS I–III[a]

No.	Type of structure	Ar[b]	R^1/R^2[b] or n	R_M	$S(R_M)$[c]	Σf
1	III	Ph	H/H	−0.31	0.062	0.453
2	III	Ph	Me/H	0.15	0.064	0.860
3	III	Ph	Et/H	0.41	0.043	1.390
4	III	Ph	*n*-Pr/H	0.61	0.033	1.920
5	III	Ph	*i*-Pr/H	0.57	0.052	1.797
6	III	Ph	*s*-Bu/H[d]	0.81	0.077	2.327
7	III	Ph	*c*-Pn/H	0.93	0.050	2.513
8	III	Ph	Bz/H	1.07	0.051	2.740
9	III	Ph	*n*-Bu/H	0.84	0.021	2.450
10	III	Fc	*i*-Pr/H	0.88	0.041	—[e]
11	III	Ph	Me/Me	0.40	0.065	1.477
12	III	Ph	Et/Et	0.79	0.067	2.537
13	III	Ph	*n*-Pr/*n*-Pr	1.16	0.055	3.597
14	III	Ph	*n*-Pr/Et	0.98	0.124	3.067
15	III	Ph	Et/Me	0.58	0.087	2.007
16	III	Ph	*i*-Pr/Me	0.70	0.054	2.414
17	II	Ph	2	0.47	0.067	1.133
18	I	Ph	—	0.54	0.044	2.157
19	II	Ph	3	0.48	0.022	1.663
20	II	Ph	4	0.70	0.052	2.193
21	II	Ph	5	0.91	0.010	2.723
22	III	4-Me-Ph	*i*-Pr/H	0.72	0.056	2.301
23	III	4-Cl-Ph	*i*-Pr/H	0.88	0.044	2.521
24	III	4-Br-Ph	*i*-Pr/H	1.05	0.039	2.730
25	III	4-Et-Ph	*i*-Pr/H	0.90	0.022	2.831
26	III	4-*t*-Bu-Ph	*i*-Pr/H	1.16	0.041	3.855
27	III	4-*i*-Pr-Ph	*i*-Pr/H	1.05	0.016	3.238
28	III	4-MeO-Ph	*i*-Pr/H	0.70	0.035	1.868
29	III	3,4-Cl-Ph	*i*-Pr/H	1.22	0.022	3.186
30	II	4-MeO-Ph	5	1.05	0.009	2.794
31	II	4-Me-Ph	4	0.81	0.045	2.697
32	II	4-MeO-Ph	4	0.81	0.034	2.264
33	III[f]	Ph	Me/H	−0.35	0.084	0.680
34	II	Fc	4	0.96	0.020	—[e]

[a] The synthesis has been detailed elsewhere [8].

[b] Ph = phenyl; Me = methyl; Et = ethyl; Pr = propyl; Bu = butyl; Fc = ferrocenyl; *c*-Pn = cyclopentyl; Bz = benzyl; 3,4-Cl-Ph = 3,4-dichlorophenyl.

[c] Relative standard deviations of R_M (n = 8–10).

[d] Compound 6 consists of two diastereoisomers [7] which do not separate under the chromatographic conditions.

[e] The Rekker fragmental constant f for the ferrocene unit is not available in the literature.

[f] 2-Phenylsulphinylpropionic acid.

Germany) 20 × 20 cm plates were used as the stationary phase. The tested compounds were dissolved in methanol ad 40-μg samples were spotted randomly on the plates in order to avoid any systematic error. Four chromatographic plates placed in a holding frame were developed to a height of 15 cm after 2 h of saturating the chromatographic tank, and using citric buffer (pH 2)–methanol (1:1, v/v) as the mobile phase. The plates were then dried and spots were detected under UV light (254 nm). The reported R_M values, calculated from equation $R_M = \log(1/R_F - 1)$, are the averages of 8–10 measurements.

The Rekker hydrophobic constants, Σf, were calculated according to ref. 9.

RESULTS AND DISCUSSION

Table I gives the R_M values obtained from our experiments and the calculated Rekker hydrophobic constants, Σf. The relative standard deviations of the R_M values range from 1.0 to 12.4%.

Table II shows the established regression relationships for all the derivatives considered (eqn. 1) and for limited sub-sets of these compounds (eqns. 2–4a).

TABLE II

CORRELATION EQUATIONS[a] BETWEEN R_M AND Σ_f VALUES

$R_M = a\Sigma f + b$

Eqn. No.	a	b	n	r	s	F	Compounds considered
1	0.435	−0.272	32	0.937	0.132	216	All[b]
2	0.468	−0.262	8	0.995	0.033	588	2–9
3	0.364	−0.147	6	0.998	0.019	1064	11–16
4	0.406	−0.193	3	1.000[c]	0.004	5547	19–21
4a	0.291	0.080	4	0.951	0.079	19.10	17, 19–21

[a] All calculations were performed on a Texas Instruments SR 51 A calculator.
[b] Excluding 10 and 34: ferrocene derivatives whose f values are not available in the literature.
[c] 0.9999.

The relationship R_M *vs.* Σf for all the 32 derivatives considered is show in Fig. 1. The correlation coefficient is $r = 0.937$.

Fig. 2 shows the relationship R_M *vs.* Σf for the mono-(R_2 = H) and disubstituted (R^1,$R^2 \neq$ H) phenylsulphonylalkanoic acid derivatives. The results can be arranged in two separate straight-line plots, one for each type of derivative. The respective correlation coefficients are remarkably high (above 0.99) (eqns. 2 and 3, Fig. 2). It seems justified to conclude that these significantly good correlations indicate the congenericity of the aforementioned sub-sets of derivatives, as obtained from the definition of the congenericity [10]. Hence it seems reasonable to assume that within the two discussed sub-sets the adsorption processes are alike to such an extent that the retention differences are due to the differences in the partition mechanism only.

In contrast, a significantly poorer correlation is observed within the cyclic

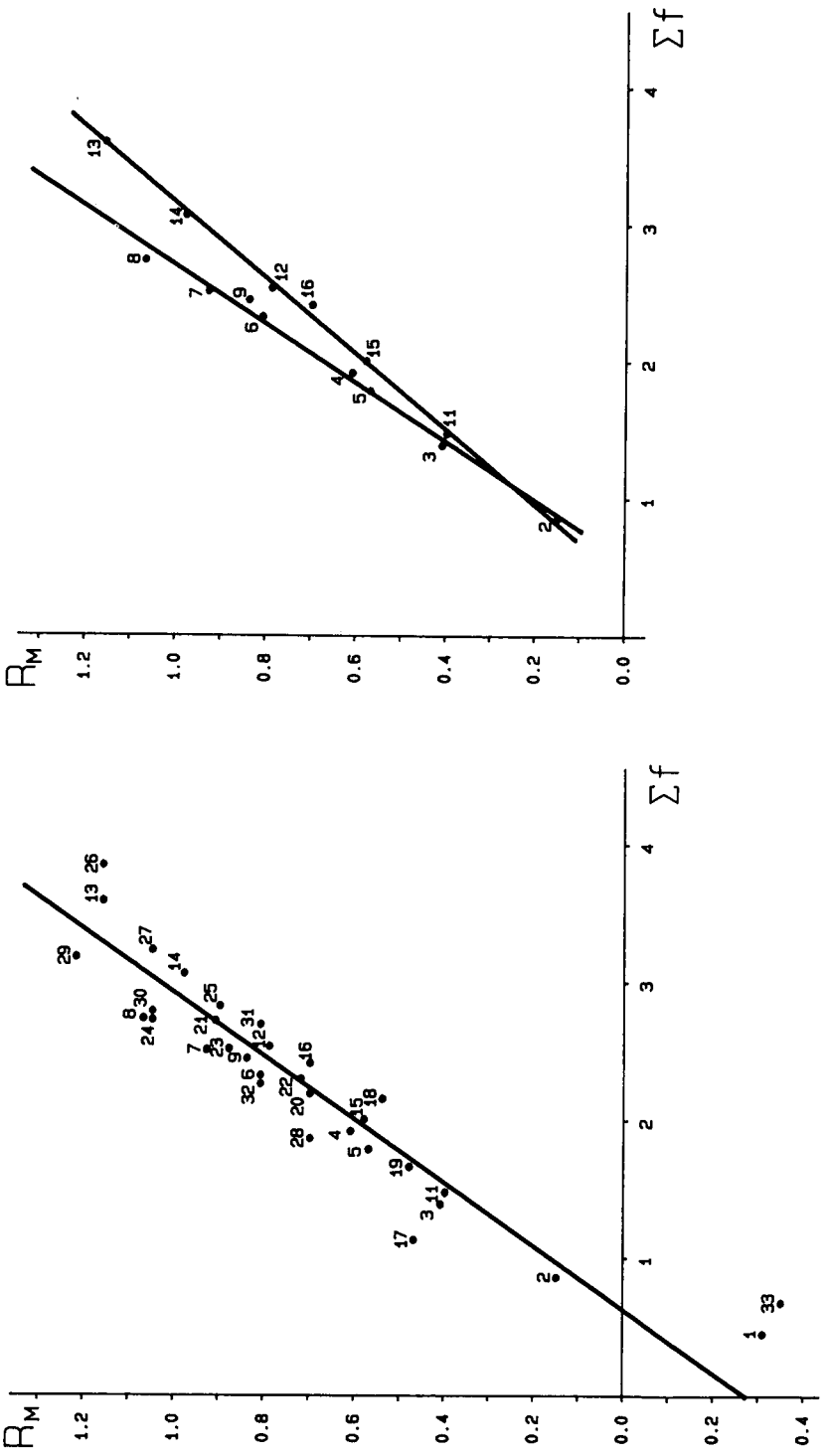

Fig. 1. Relationship between R_M and Σf values for all the 32 derivatives considered, as described by eqn. 1.

Fig. 2. Relationship between R_M and Σf values for mono- and disubstituted phenylsulphonylalkanoic acid derivatives, as described by eqns. 2 and 3, respectively.

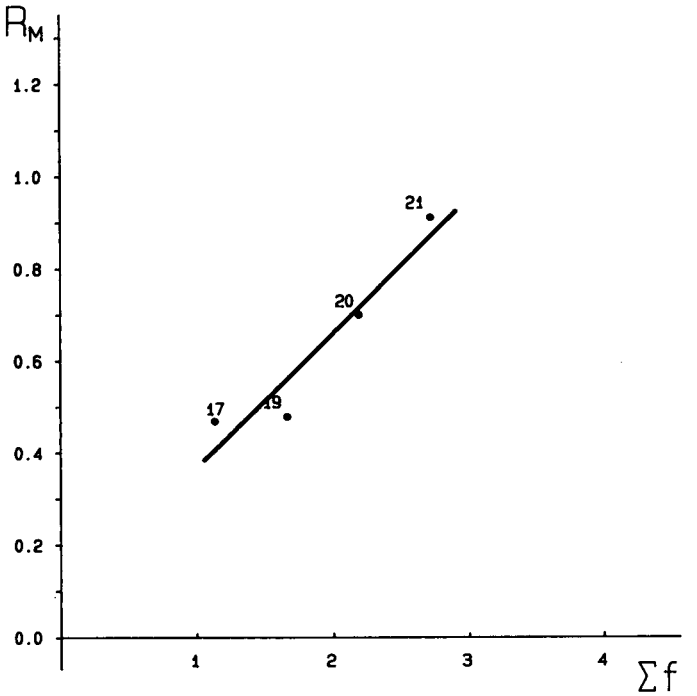

Fig. 3. Relationship between R_M and Σf values for phenylsulphonylcycloalkanecarboxylic acids, as described by eqn. 4a.

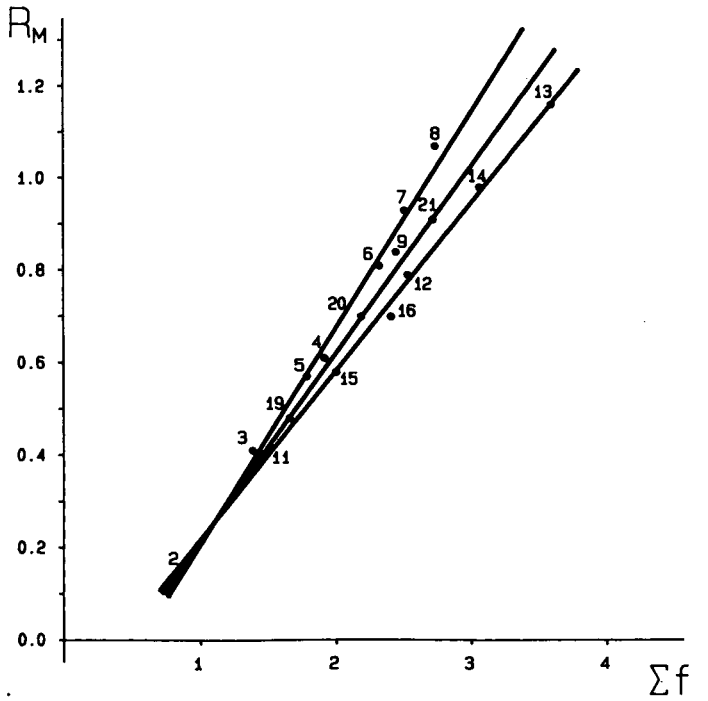

Fig. 4. Relationship between R_M and Σf values for mono-, disubstituted and cyclic phenyl derivatives, as described by eqns. 2, 3 and 4, respectively.

derivatives sub-set (eqn. 4a, Fig. 3). This phenomenon probably results from the change in the geometry of the polar $COOH/SO_2$ moiety induced by the cyclopropane ring. Hence the consecutive cyclic derivatives differ in respect of both the partition and adsorption mechanisms. Neglecting the cyclopropane derivative 17 gives eqn. 4, which describes excellently the R_M *vs.* Σf relationship for the cyclobutane to cyclohexane analogues. It is worth mentioning also that the three aforementioned straight-line plots (eqns. 2–4) intersect precisely at one point (Fig. 4).

CONCLUSIONS

The intermolecular interaction through hydrogen bonds and partition effects in the retention mechanism on polyamide seem to be similar and may simulate the intermolecular interaction in living systems which are usually based on lipophilicity and hydrogen bond effects. In fact, probably owing to the importance of these two factors in chemoreception processes [11], the established R_M values provide a significantly better fit in our QSAR (structure–taste) model than do the hydrophobicity constants [7,12].

REFERENCES

1 J. C. Dearden, *Environ. Health Perspect.*, 61 (1985) 203.
2 R. Franke, *Theoretical Drug Design Methods*, Akademie Verlag, Berlin, 1984, pp. 30–79.
3 R. F. Rekker, *The Hydrophobic Fragmental Constant*, Elsevier, Amsterdam, 1977, p. 20.
4 J. C. Dearden, A. M. Patel and J. M. Thubby, *J. Pharm. Pharmacol.*, 26, Suppl. (1974) 75P.
5 C. Hansch and F. Helmers, *J. Polym. Sci.*, 6 (1968) 3295.
6 C. F. Poole and S. A. Schuette, *Contemporary Practice of Chromatography*, Elsevier, Amsterdam, 1984, p. 687.
7 A. Ratajczak and J. Polański, in Abstracts of Papers of the *14th International Symposium on the Organic Chemistry of Sulfur, Łódź, Poland, September 1990*, D-0-2.
8 A. Ratajczak and J. Polański, *Pol. J. Chem.*, submitted for publication.
9 R F. Rekker, *The Hydrophobic Fragmental Constant*, Elsevier, Amsterdam, 1977, pp. 350–355.
10 R. F. Rekker, in M. Tichy (Editor), *QSAR in Toxicology and Xenobiochemistry*, Elsevier, Amsterdam, 1985, pp. 3–24.
11 H. D. Belitz, W. Chen, H. Jugel, W. Stempfl, R. Treleano and H. Wieser, in P. Schreier (Editor), *Flavour'81*, Walter de Gruyter, Berlin and New York, 1981, pp. 741–755.
12 J. Polański and A. Ratajczak, in preparation.

Journal of Chromatography, 543 (1991) 201–210
Elsevier Science Publishers B.V., Amsterdam

CHROM. 23 071

Determination of phospholipids on two-dimensional thin-layer chromatographic plates by imaging densitometry

HIROSHI YAMAMOTO*, KENJI NAKAMURA and MIHO NAKATANI
R&D Engineering Department, Analytical Instrument Division, Shimadzu Corporation, 1, Nishinokyo-Kuwabaracho, Nakagyo-ku, Kyoto 604 (Japan)
and
HIROSHI TERADA
Faculty of Pharmaceutical Sciences, University of Tokushima, Shomachi-1, Tokushima 770 (Japan)
(First received October 9th, 1990; revised manuscript received December 20th, 1990)

ABSTRACT

Data acquisition and image analysis by a flying-spot-based densitometer linked with a personal computer for the determination of compounds separated by thin-layer chromatography (TLC) were studied. This method was applied to the reflectance imaging densitometry of phospholipids separated two-dimensionally on a TLC plate. Phospholipids were determined with high accuracy and reproducibility, showing that the proposed method is very useful for the determination of compounds separated by two-dimensional TLC.

INTRODUCTION

Densitometry has been widely used for the quantitative assay of zones of light-absorbing compounds or fluorophores that have been separated on a supporting material, such as an electrophoretic gel or a thin-layer chromatographic (TLC) plate. Two techniques are available for densitometric scanning of separated zones. One is linear scanning with a slit-shaped light beam, which is widely used clinically for determining serum proteins. In this instance, the density distribution of the substance examined is assumed to be virtually uniform in the direction perpendicular to the scanning axis, and so the slit illumination should give the correct absorbance signal. However, on two-dimensional electrophoresis or TLC, the density distribution of a substance in a zone is usually not uniform, and the density is distributed randomly in the two-dimensional plane. In such instances, the alternative technique of two-dimensional scanning, rather than linear scanning, should be used.

Several types of densitometers that scan sample bands mechanically in two dimensions with a small light spot have been shown to be effective in eliminating errors due to irregular distribution of the sample [1–3]. Recently, new techniques of imaging densitometry using image detectors and computer image analysis techniques have been reported to be useful for the quantification of gel electropherograms or thin-layer

0021-9673/91/$03.50

chromatograms [4–10]. These techniques facilitate fast scanning and easy data handling, but have the common disadvantages of a narrow dynamic range of the video camera, difficulty with uniform illumination and lack of optical contrast on the image plane due to mutual optical interference of pixels. Taube and Neuhoff [11] reported methods for two-dimensional data acquisition using a scanning photometer and image processing of bands separated by chromatography or electrophoresis.

We have reported the technique of dual-wavelength, zig-zag scanning [12], in which a small light spot scans the sample bands two-dimensionally in a zig-zag manner so that a wide dynamic range of signal detection and high optical contrast are achieved. However, with this type of mechanical scanning system, a long time is required for scanning the whole TLC plate.

The densitometric determination of phospholipids on TLC plates, mainly those separated one-dimensionally, has been reported [13–17].

To improve the quantification, imaging densitometry using a black-and-white video camera has recently been applied in two-dimensional TLC [8]. However, this method seems to have the limitation of a narrow dynamic range. This paper describes an improvement of our mechanical scanning system for imaging densitometry and the application of this system to the determination of phospholipids separated two-dimensionally on TLC plates.

EXPERIMENTAL

Reagents

Soybean phospholipid was purchased from Wako (Osaka, Japan) and dissolved in chloroform to give a 0.05 g/ml solution. The phosholipids, L-α-phosphatidylcholine (PC), L-α-phosphatidylethanolamine (PE) and L-α-phosphatidylinositol (PI), all from soybeans, and synthetic L-α-phosphatidic acid (PA) were purchased from Sigma (St. Louis, MO, U.S.A.) and dissolved together in chloroform. Other reagents were of analytical-reagent grade.

Thin-layer chromatography

TLC was performed on silica gel high-performance TLC plates (10 × 10 cm) from E. Merck (Darmstadt, Germany). Mixtures of chloroform–methanol–7 *M* ammonia (65:30:4) and chloroform–methanol–acetic acid–water (170:25:25:6) were used for development in the first and second dimension, respectively. After development, the plates were allowed to dry, sprayed with copper(II) sulphate solution in 8% phosphoric acid and then charred by heating at 160°C for 20 min. Densitometry was carried out at 400 nm only, because the absorbance of the charred zones on the TLC plate was non-specific.

Flying-spot densitometry

A dual-wavelength flying-spot scanner (Shimadzu, Model CS-9000) linked with a personal computer was used for data acquisition and image processing. A minute monochromatic light beam (0.4 × 0.4 mm) was generated by an assembly of a fixed slit and spiral slit on a rotating disk located in the exit portion of a monochromator, as shown in Fig. 1. By reciprocating movement of the rotating disk, the light beam moved up and down, and was projected onto a TLC plate by collimating mirror optics to

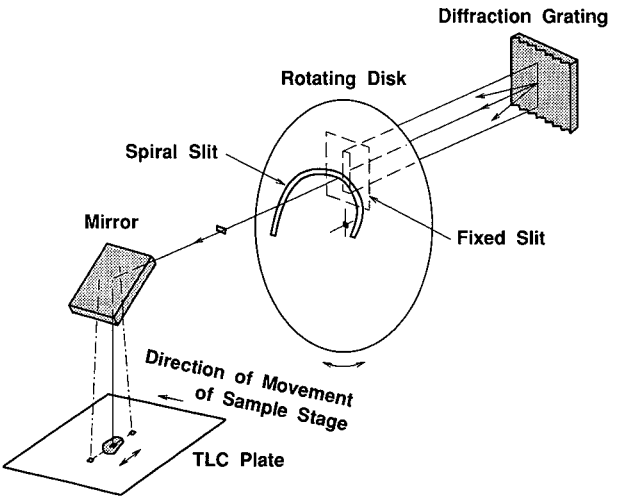

Fig. 1. Principle of flying-spot scanning.

illuminate an area of 0.4 × 0.4 mm on the plate surface and reciprocated for 10 mm in a stepwise manner at 0.2 mm pitch (Fig. 1). The sample stage was moved in the longitudinal direction with a 0.2 mm pitch at the end of each reciprocating movement of the light spot (= flying spot) so as to generate raster. For scanning the whole TLC plate, this raster scan of 10-mm width was repeated in the longitudinal direction by shifting the sample stage laterally in steps of 10 mm.

The diffusely transmitted portion of light under the plate was picked up by the photomultiplier PM_t and the other portion of light reflected from the plate was picked up by the photomultiplier PM_r, as shown in Fig. 2. The signals were converted to those

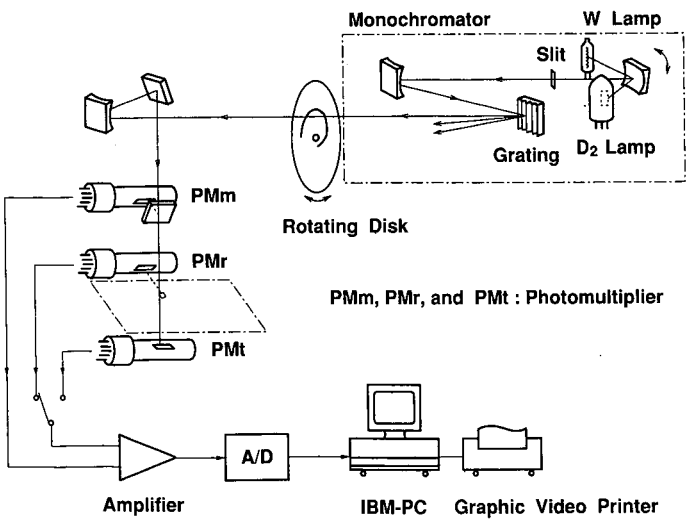

Fig. 2. Optical and signal conversion systems of the flying-spot densitometer.

of transmitted intensity (I_t) and reflected intensity (I_r). The photomultiplier PM_m detected a fraction of the irradiation light, and its signal I_m was used to compensate for fluctuations of the light source in terms of the ratios I_t/I_m and I_r/I_m.

The logarithmic signals, log (I_m/I_t) and log (I_m/I_r), were converted into binary values. These had the dynamic range of -0.8 and 4.0, which was digitized with 12-bit resolution.

Determination of phospholipids on TLC plates

For application of the above methods, we determined phospholipids on TLC plates by diffuse reflectance measurement. Zones on a TLC plate usually have specific absorption peaks in either the visible or ultraviolet region, or both. Therefore, the use of a monochromator that allows the selection of any desired wavelength is useful in the densitometric determination of zones on a TLC plate. Our scanning device offers continuous wavelength selection of monochromatic lights of 10-nm bandwidth over the range 200–700 nm. Therefore, it allows the selection of a optimum wavelength according to the optical characteristics of the sample compound.

The minute light spot moves laterally on the sample surface, as shown in Fig. 1, and so the angle and position of the incident beam on the photocathode of the photomultiplier also vary. Consequently, the local sensitivity differences of the photocathode of photomultipliers, PM_m, PM_r and PM_t (Fig. 2) must be compensated for each signal of either log (I_m/I_r)or log (I_m/I_t) for the sample compound. The data for correction were obtained by scanning a blank area of the TLC plate in the lateral direction for a 10-mm distance in 0.2-mm steps. These data were stored in the memory as a locality correction table and subtracted from subsequent real-time signals at the corresponding lateral positions. There was a *ca.* 20–30% change in local sensitivities on the photocathode, but this was compensated for by subtraction of the correction data.

Signals obtained by the procedure described above were led to an IBM PC-AT external computer, as shown in Fig. 2, and stored in a RAM disk as image data. The RAM disk had an 8 Mbyte capacity, which was sufficient to memorize sixteen full images from a plate of 100 × 100 mm area. The computer had an installed coprocessor to increase the calculation speed and a "mouse" for easy operation. In zones of interest diluted with a high background noise, it was sometimes necessary to smooh raw data. A Laplacian 3 × 3 two-dimensional smoothing function was used to help in eliminating noise and enhancing zone detection. This smoothing was repeated when necessary. The effect of smoothing on a zone of interest is exemplified in Fig. 3. Image data stored in the memory were subsequently processed to detect each zone and sum the absorbance values in the zone area.

Each zone could be detected either automatically or manually. In the automatic mode, the absorbance difference from one pixel to the next was calculated and each zone was detected through a computer algorithm according to either the discrimination level selected earlier or the sensitivity of curvature. In the manual mode, each zone was outlined by use of a "mouse"-controlled pointer on the CRT screen. Use of mapping images obtained at different discrimination levels and three-dimensional projection images or sectional images made manual assays easier. The pattern around the zone and its sectional images corresponding to the x-axis and y-axis cursors are shown in Fig 4. For accurate integration of the absorbance value in each zone, the

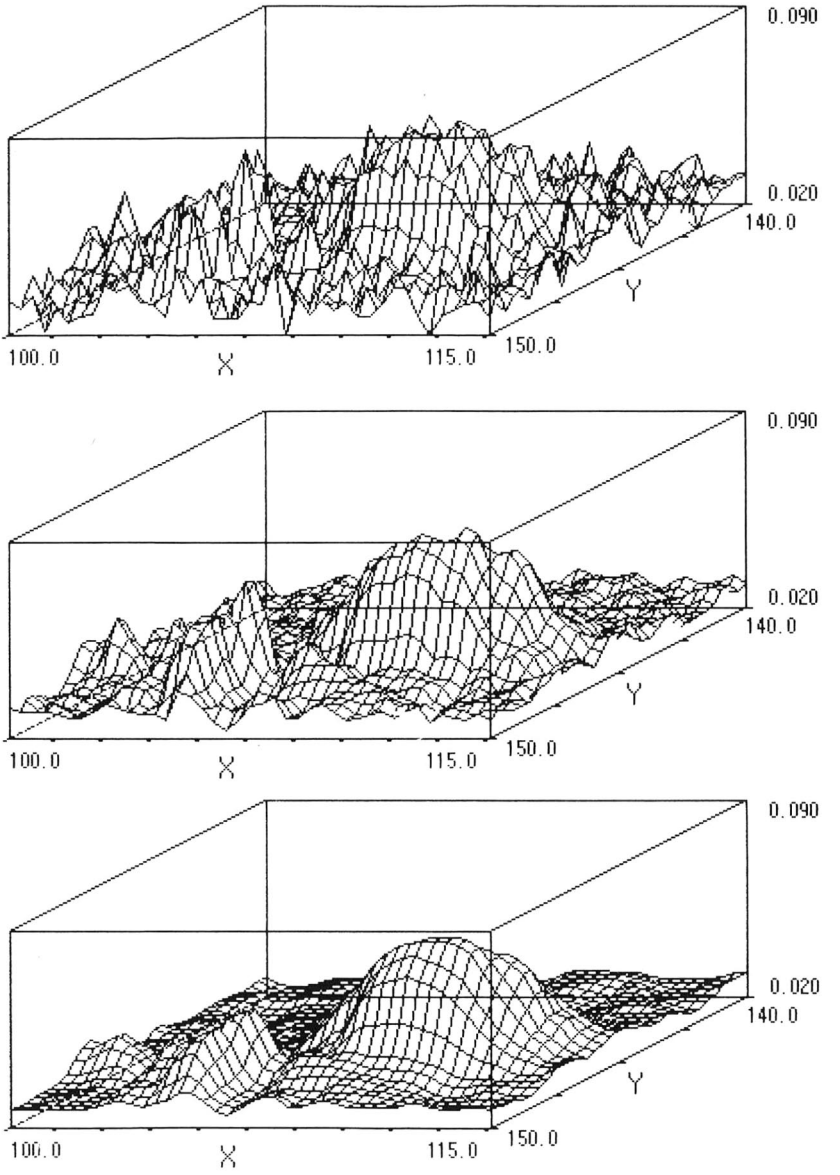

Fig. 3. Effect of Laplacian 3 × 3 smoothing. (a) Original data; (b) results smoothed once; (c) results smoothed five times.

background absorbance was subtracted. Three levels of background subtraction could be selected: the background absorbance could be taken as zero or the mean level on the border, or could be chosen by the operator. The background value, calculated as the product of the background absorbance and the area, was subtracted from the integrated absorbance value inside the border of each zone. Selection of the level of

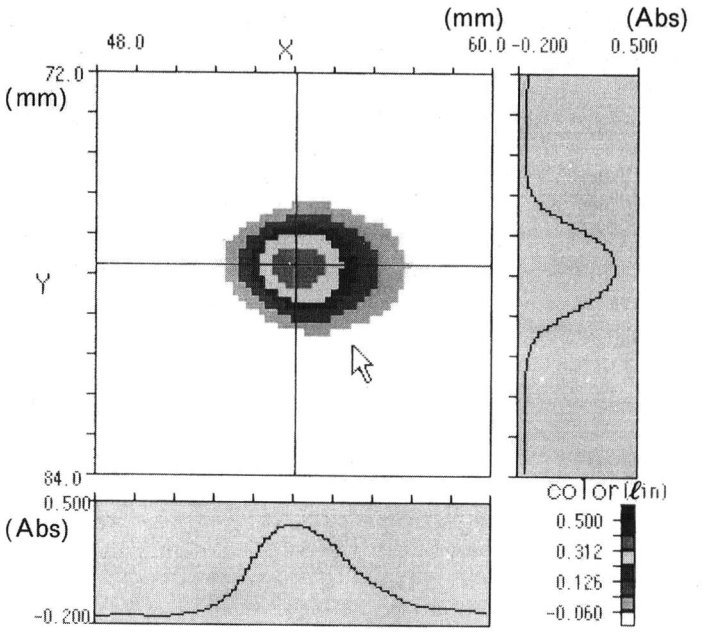

Fig. 4. Two-dimensional pattern around the zone and its sectional images corresponding to *x*- and *y*-axis cursors.

background subtraction depended on whether there were adjacent zones and on whether the background absorbance varied markedly.

RESULTS AND DISCUSSION

It is very important to minimize the data acquisition time for obtaining image data. The present method of flying-spot densitometry required about 15 min to scan a total area of 100 × 100 mm with a resolution of 0.2 mm in both the longitudinal and lateral directions, including the real-time locality correction process. Once the data had been stored in the memory, the time required for image processing of the 100 × 100 mm area was *ca.* 2 min, and this time could be greatly shortened by use of a faster computer.

Soybean phospholipids were separated by two-dimensional TLC, as shown in Fig. 5, then the whole area of the plate was scanned and image data were stored in the memory of the computer. Each zone was displayed as a contour map by preselecting a threshold level for the absorbance value. Detection of each zone and integration of absorbance in a zone were usually performed automatically by the computer algorithm alone. However, for the analysis of adjacent zones, manual determination was adequately adapted. Therefore, another borderline was drawn manually for a chosen discrimination level, which was determined by reference to sectional views corresponding to *x*- and *y*-axis cursors in which the start and end points of the peaks were found one-dimensionally (Fig. 4). The three-dimensional distribution of density was

observed visually so the borderline could be drawn to surround the entire zone. The contour line level for the mapping image was varied by 0.001 absorbance unit as the smallest unit when this borderline was being checked.

Two-dimensinal TLC of soybean phospholipid was performed in five runs, and densitometric determinations of four major components, PE, PC, PI and PA, and four minor components stearoylglucoside (SG), phosphatidylglycerol (PG), cerebroside (Ce) and X (not identified), as shown in Fig. 5, were carried out on each plate. TLC of standard phospholipids PC and PE was also performed. To eliminate errors caused by differences in the charring conditions for different plates, integrated values for the eight components were summed and the total value for each plate was taken as 100%, then the percentage densitometric values for each of the eight components and average values for the five TLC plates were calculated. These values are summarized in Table I. The relative standard deviations (R.S.D.) for the four major phospholipids PE, PC, PI and PA were in the range *ca.* 2–5%. This range is similar to that observed in one-dimensional TLC densitometry [14], indicating that this method is suitable for two-dimensional TLC densitometry.

Next we carried out two-dimensional TLC of mixtures of various amounts of PA, PE, PI and PC, from 0.25 to 3.0 μg, on six TLC plates. In this experiment, 5.0 μg of PC were applied separately to each plate as a standard. Fig. 6 shows the results of

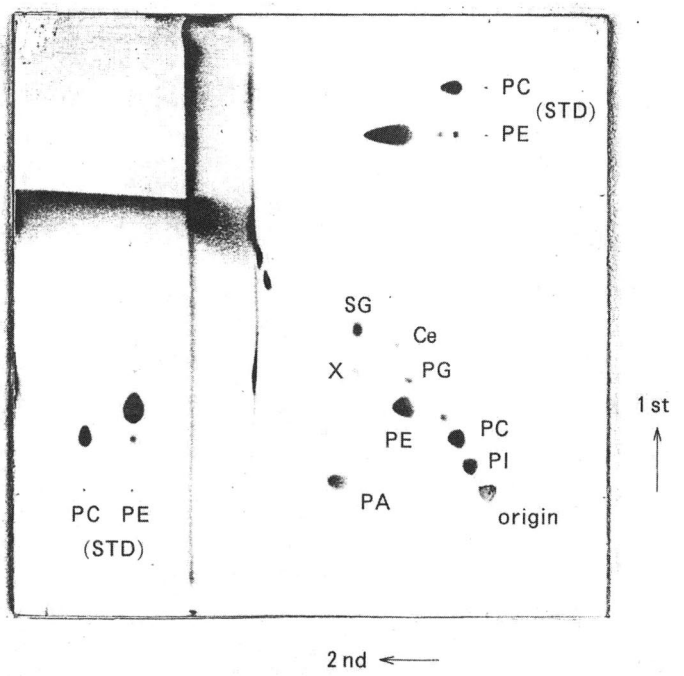

Fig. 5. Two-dimensional TLC of soybean phospholipids. PE = Phosphatidylethanolamine; PC = phosphatidylcholine; PI = phosphatidylinositol; PA = phosphatidic acid; SG = stearoylglucoside; PG = phosphatidylglycerol; Ce = cerebroside; *x* = unidentified substance.

TABLE I

INTEGRATED ABSORBANCES OF PHOSPHOLIPIDS FROM TWO-DIMENSIONAL HIGH-PERFORMANCE TLC PLATES DETERMINED BY FLYING-SPOT SCANNING[a]

Plate No.	Relative absorbance (%)[b]								
	PE	PC	PI	PA	SG	PG	Ce	X	Total
1	30.36	26.09	15.15	16.11	7.13	1.94	1.74	1.48	100
2	28.48	25.07	16.44	16.56	7.02	2.61	2.04	1.78	100
3	28.80	25.59	15.24	15.91	6.86	3.09	2.70	1.81	100
4	27.44	25.07	15.06	16.69	7.85	2.91	2.67	2.31	100
5	28.99	25.43	14.49	17.69	8.01	2.24	1.68	1.47	100
Average	28.80	25.45	15.28	16.59	7.37	2.56	2.17	1.77	100
S.D.	1.05	0.43	0.71	0.69	0.52	0.48	0.49	0.34	
R.S.D. %	3.65	1.67	4.67	4.17	7.06	18.56	22.85	19.31	

[a] Soybean phospholipid was separated by two-dimensional TLC. The plates were then charred and integrated absorbances of phospholipids were determined by flying-spot densitometry. Their values are shown as percentages of the total absorbance.

[b] PE = Phosphatidylethanolamine; PC = phosphatidylcholine; PI = phosphatidylinositol; PA = phosphatidic acid; SG = stearoylglucoside; PG = phosphatidylglycerol; Ce = cerebroside; X = unidentified substance.

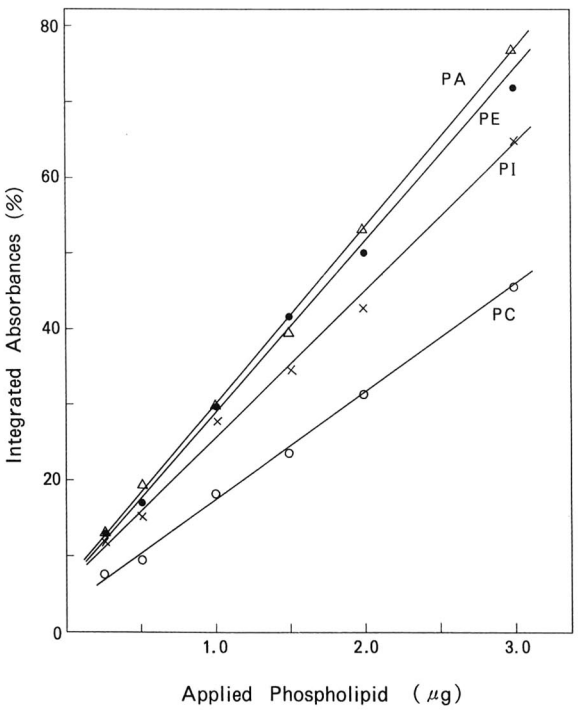

Fig. 6. Linear relationships between integrated absorbances of phospholipids and their amounts applied to two-dimensional TLC plates. Integrated absorbances are expressed as percentages of that of the standard sample of PC. Abbreviations as in Fig. 5.

TABLE II

LINEAR RELATIONSHIP BETWEEN INTEGRATED ABSORBANCES AND AMOUNTS OF PHOSPHOLIPIDS APPLIED ON TWO-DIMENSIONAL TLC[a]

Phospholipid	Linear relationship[b]	γ[c]
PA	$y = 23.18x + 7.07$	0.999
PE	$y = 21.69x + 7.43$	0.999
PI	$y = 14.03x + 3.13$	0.998
PC	$y = 18.93x + 7.06$	0.997

[a] Two-dimensional TLC of various concentrations of samples of PA (phosphatidic acid), PE (phosphatidylethanolamine), PI (phosphatidylinositol) and PC (phosphatidylcholine) was carried out on six plates. The plates were then charred and flying-spot densitometry was performed. A typical chromatogram is shown in Fig. 5.

[b] Results of regression analyses of the relationships between the amounts (in μg) of phospholipid applied (x) and the integrated absorbances relative to that of standard PC (y).

[c] Correlation coefficient.

densitometry represented by integrated absorbances relative to that of the standard PC (%) as functions of the amounts of phosholipids applied. As can be seen, with all four phospholipids the integrated absorbance was linearly related to the amount of phospholipid applied, although the plots did not pass through the origin. The calibration graphs obtained by densitometry of charred zones using one-dimensional TLC have also been reported not to pass through the origin [18–20]. The results of regression analyses of these results are summarized in Table II: very significant linear relationships were obtained between the integrated absorbance and the amount of phospholipid applied for all the phospholipids, indicating that the present method is suitable for the determination of phospholipids.

To confirm this, we next carried out densitometry of the two-dimensional TLC plates to which known amounts of several phosholipids had been applied with 5.0-μg samples of PC and PE as references. The results were quantified according to the relationships in Table II and are summarized in Table III. The differences between the

TABLE III

DETERMINATION OF PHOSPHOLIPIDS BY TWO-DIMENSIONAL TLC AND FLYING-SPOT DENSITOMETRY ACCORDING TO THE RESULTS OF REGRESSION ANALYSES SHOWN IN TABLE II

Phospholipid[a]	Amount of phospholipid (μg)			
	Sample 1		Sample 2	
	Applied	Determined	Applied	Determined
PA	1.00	0.92	3.00	3.08
PE	3.00	3.09	2.00	1.93
PI	2.00	1.97	2.00	1.85
PC	2.00	1.81	1.00	0.95

[a] PA = Phosphatidic acid; PE = phosphatidylethanolamine; PI = phosphatidylinositol; PC = phosphatidylcholine.

calculated amounts and amounts applied in different runs were always less than 10%, confirming that the calculated values were within acceptable limits for practical use of the method [17,18,20].

REFERENCES

1 J. Goldman and R. R. Goodall, *J. Chromatogr.*, 40 (1969) 345.
2 J. Goldman and R. R. Goodall, *J. Chromatogr.*, 47 (1970) 386.
3 V. Pollack and A. A. Boulton, *J. Chromatogr.*, 50 (1970) 30.
4 S. Pongor, *J. Liq. Chromatogr.*, 5 (1982) 1583.
5 D. D. Rees, K. E. Fogarty, L. K. Levy and F. S. Fay, *Anal. Biochem.*, 144 (1985) 461.
6 M. L. Gianelli, J. B. Callis, N. H. Andersen and G. D. Christian, *Anal. Chem.*, 53 (1981) 1357.
7 M. L. Gianelli, D. H. Burns, J. B. Callis, G. D. Christian and N. H. Andersen, *Anal. Chem.*, 55 (1983) 1858.
8 T. S. Ford-Holevinski and N. S. Radin, *Anal. Biochem.*, 150 (1985) 359.
9 D. H. Burns, J. B. Callis and G. D Christian, *Trends Anal. Chem.*, 5 (1986) 50.
10 R. M. Belchamber, H. Read and J. D. M. Roberts, *J. Chromatogr.*, 395 (1987) 47.
11 D. Taube and V. Neuhoff, *J. Chromatogr.*, 437 (1988) 411.
12 H. Yamamoto, T. Kurita, J. Suzuki, R. Hira, K. Nakano, H. Makabe and K. Shibata, *J. Chromatogr.*, 116 (1976) 29.
13 W. L. Erdohl, A. Stolyhwo and O. S. Privett, *J. Am. Oil Chem. Soc.*, 50 (1973) 513.
14 M. Goppelt and K. Resch, *Anal. Biochem.*, 140 (1984) 152.
15 L. Kolarovic and N. C. Fournier, *Anal. Biochem.*, 156 (1986) 244.
16 T. Nagata, L. L. Poulsen and D. M. Ziegler, *Anal. Biochem.*, 171 (1988) 248.
17 J. C. Touchstone and J. G. Alvarez, *J. Chromatogr.*, 429 (1988) 359.
18 J. Bitman and D. L. Wood, *J. Liq. Chromatogr.*, 4 (1981) 1023.
19 B. R. Mullin, C. M. B. Poore and B. H. Rupp, *J. Chromatogr.*, 278 (1983) 160.
20 G. Schmitz, G. Assmann and D. E. Bowyer, *J. Chromatogr.*, 307 (1984) 65.

Journal of Chromatography, 543 (1991) 211–219
Elsevier Science Publishers B.V., Amsterdam

CHROM. 23 105

Simple procedure involving derivatisation and thin-layer chromatography for the estimation of trace levels of halogenated alkylamines and their hydrolysis products in drug substances and formulations

P. H. LEIGH and M. J. BOWKER*

Analytical Chemistry Laboratories, Dagenham Research Centre, Rhône-Poulenc Rorer, Dagenham, Essex, RM10 7XS (U.K.)

(First received August 7th, 1990; revised manuscript received December 27th, 1990)

ABSTRACT

Thin-layer chromatographic methods are described for the assessment of residues of aminoalcohols in promethazine, gallamine and mepyramine (pyrilamine) injections using chromogenic/fluorogenic reagents. Detection limits of 8 ppm have been established for 2-dimethylaminopropan-1-ol and 1-dimethylaminopropan-2-ol in promethazine injection, 7 ppm for 2-diethylaminoethanol in gallamine injection and 1 ppm for 2-dimethylaminoethanol in mepyramine injection. These methods enable the assessment of residues of β-chloroalkylamine alkylating agents. The simplicity and sensitivity of these methods compare favourably with the few literature methods and offer scope for adaptation for other β-chloroalkylamines in basic drugs.

INTRODUCTION

Halogenated alkylamines are widely used throughout the pharmaceutical industry as alkylating agents in the manufacture of drug substances. Their use frequently occurs at an early stage in the manufacturing route, allowing subsequent stages for unreacted residues or their hydrolysis product, the aminoalcohol, to be removed by recrystallisation, extraction etc.

The chemistry of these simple molecules is relatively complex and received much concerted effort in the late 1940s and early 1950s [1–9]. From these studies, which mainly concerned their reaction kinetics, it can be inferred that: (i) in alkaline solution they are prone to intramolecular cyclisation with the rate of reaction dependent on the size of the ring formed; such cyclisation reactions occur rapidly even at ambient temperature (half-lives typically 1–10 min), (ii) although theoretically so, these cyclisations are rarely reversible because the competing hydrolysis reaction causes ring fission to the corresponding aminoalcohol.

The lowest member of the homologous series of such alkylating agents, 2-chloroethylamine, is extremely unstable and the alkylating agent of choice is

0021-9673/91/$03.50

normally the intramolecular cyclisation product, aziridine. Analytical methods have been reported for aziridine using derivatisation/spectrophotometry [10–12]; aziridine and its hydrolysis product, ethanolamine, can be analysed by ligand exchange chromatography [13]. Residues of 2-chloroethylamine and aziridine have recently been analysed in pharmaceuticals [14] by derivatisation gas chromatography.

Dialkylaminoethyl and propyl halides are more frequently employed as alkylating agents in the pharmaceutical industry but analytical procedures for their estimation have not been reported. Cyclisation of these dialkylaminoalkyl halides yields quaternary aziridinium ions which readily hydrolyse in solution to give tertiary aminoalcohols (Fig. 1).

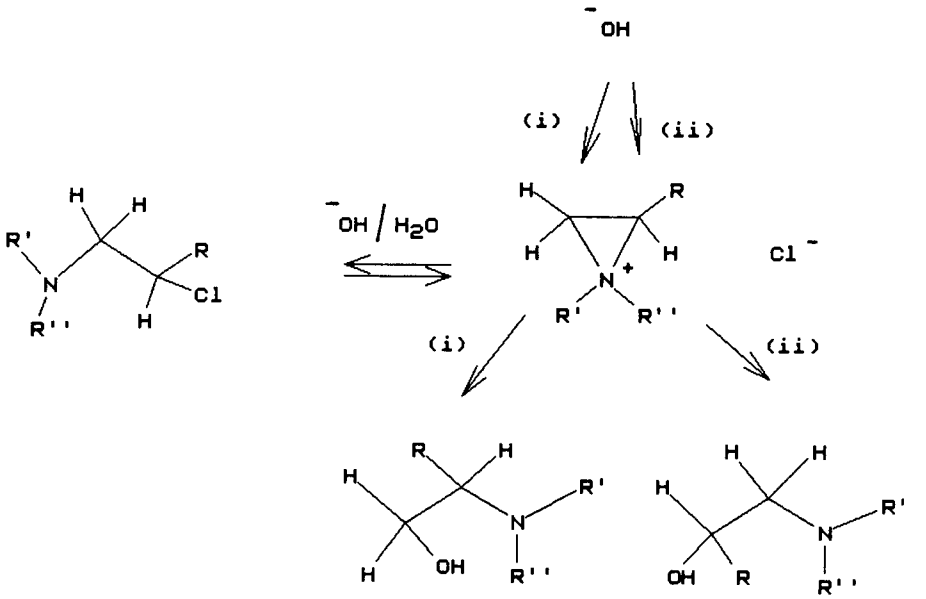

Fig. 1. Hydrolysis of β-chloroalkylamines to aminoalcohols. Key: R, R′, R″ = CH_3 (promethazine synthesis); R = H, R′, R″ = C_2H_5 (gallamine synthesis); R = H, R′,R″ = CH_3 (mepyramine synthesis).

The aziridinium ion derived from intramolecular cyclisation of 1-dimethylamino-2-chloropropane can yield two isomeric aminoalcohols on cleavage of the intermediate aziridinium ion, although attack at the least hindered carbon atom (route *i*), yielding 2-dimethylaminopropan-1-ol is favoured.

The derivatisation reaction schemes for the aminoalcohols are shown in Fig. 2.

This paper describes methods for the determination of trace amounts of the pharmaceutically important alkylating agents, 1-dimethylamino-2-chloroethane, 1-diethylamino-2-chloroethane and 1-dimethylamino-2-chloropropane via their corresponding aminoalcohols.

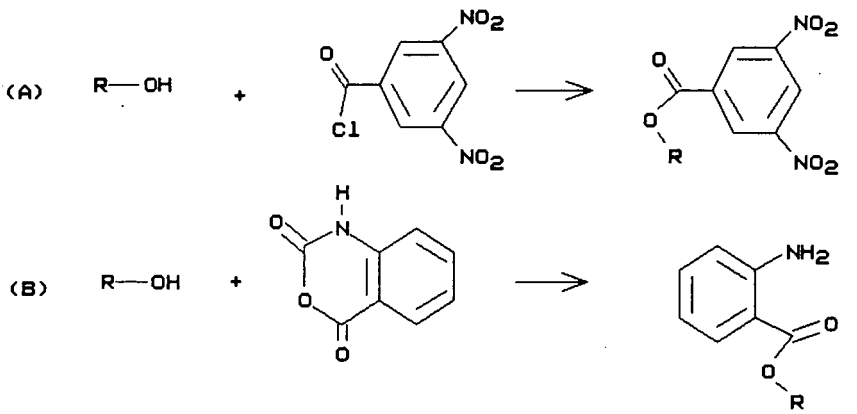

Fig. 2. Reaction schemes for derivatisation reactions. (A) Promethazine injection BP and gallamine injection BP; (B) mepyramine injection. R–OH represents the relevant aminoalcohol for each product.

EXPERIMENTAL

Samples

Samples of promethazine injection BP (British Pharmacopeia) [Phenergan injection 2.5% (w/v)], gallamine injection BP [Flaxedil injection 4.0% (w/v)] and mepyramine (pyrilamine) injection 2.5% (w/v) (Anthisan injection) were obtained from in-house stored check samples of production batches.

Chemicals

Aminoalcohols, aminoalcohol hydrochlorides, 3,5-dinitrobenzoyl chloride, 3,5-dinitrobenzoic acid and isatoic anhydride were all obtained from Aldrich (Gillingham, U.K.). 2-Dimethylaminopropan-1-ol was obtained from the Alfred Bader Library of Rare Chemicals (Aldrich).

Potassium carbonate (anhydrous) and potassium bicarbonate (anhydrous) were both Pronalys grade analytical reagents from the May & Baker range of laboratory chemicals (Rhône-Poulenc, Manchester, U.K.).

All other chemicals were of general reagent grade quality from May & Baker.

Apparatus

Octadecylsilyl (C_{18}) and silica sample preparation cartridges are part of the Sep-Pak range manufactured by Waters Associates and were obtained in the U.K. from Phase Separations (Queensferry, U.K.). Thin-layer chromatographic (TLC) plates, 20 × 20 cm, silica-gel GF_{254}, 0.25 mm thick manufactured by Merck were obtained from BDH (Dagenham, U.K.). These plates were activated for 1 h at 105°C before use. All other equipment is that generally found in an analytical chemistry laboratory.

Sample preparation —Promethazine injection BP

Condition a C_{18} Sep-Pak with 5 ml methanol followed by 5 ml deionised water. Attach the cartridge to a 20-ml glass syringe. Transfer 5 ml of injection solution into

the barrel of the glass syringe. Using the syringe plunger, elute the sample through the cartridge, collecting the eluate in a 100-ml amber separator containing 5 ml of 1 *M* hydrochloric acid solution. Elute the cartridge with 2 × 5 ml water, collecting the eluates in the separator. Discard the cartridge.

Extract the acidified eluate with 6 × 20 ml dichloromethane, shaking each aliquot for approximately 1 min. Discard the dichloromethane extracts and add 10 ml of 2.5 *M* sodium hydroxide solution. Transfer the solution to the barrel of a 20-ml glass syringe fitted with a new, conditioned C_{18} Sep-Pak cartridge. Collect the eluate in a second 100-ml amber separator. Elute the cartridge with 2 × 5 ml water, collecting the eluates in the separator. Discard the cartridge. Extract the solution with 4 × 5 ml dichloromethane and run each aliquot through anhydrous sodium sulphate into a 50-ml round-bottomed flask containing a solution of approximately 5 mg of 3,5-dinitrobenzoic acid in 1 ml diethyl ether[a].

Evaporate the dried dichloromethane extracts to dryness at ambient temperature using a rotary evaporator. Re-dissolve the residue in *ca.* 1 ml diethyl ether and add 10 mg of 3,5-dinitrobenzoyl chloride. Add 2 µl triethylamine as catalyst and stopper the tube to permit the derivatisation to proceed.

After 30 min, add 1 ml of 1.25 *M* (5%, w/v) sodium hydroxide solution, stopper and shake for approximately 1 min to destroy excess derivatising agent. Transfer the ether phase, using a Pasteur pipette, to a 5-ml pear-shaped flask. Repeat the extraction with a further 1 ml aliquot of ether, transferring the ether phase to the pear-shaped flask. Evaporate the ethereal solution to dryness and re-dissolve the residue in 100 µl of chloroform. The sample solution is now ready for spotting onto a TLC chromatoplate.

To prepare a "spiked" sample, transfer, by microsyringe, 10 µl *each* of 1-dimethylaminopropan-2-ol and 2-dimethylaminopropan-1-ol into a 100-ml measuring cylinder containing 100 ml of deionised water. Stopper and shake thoroughly. Pipette 10 ml into a second 100-ml measuring cylinder, dilute to volume with water and mix thoroughly ("spiking" solution). Carry out the extraction procedure as described above after adding 1 ml of "spiking" solution to the 5 ml bulked injection solution at the first stage of the procedure.

Sample preparation —Gallamine injection BP

The procedure for the sample solution is as described above for promethazine injection BP with the following amendment: a 4-ml sample of product is taken, equivalent to 160 mg of gallamine triethiodide contained in two 2-ml ampoules.

To prepare a "spiked" sample, transfer, by microsyringe, 10 µl of 2-diethylaminoethanol into a 100-ml measuring cylinder containing 100 ml of deionised water. Stopper and shake thoroughly. Pipette 10 ml into a second 100-ml measuring cylinder, dilute to volume with water and mix thoroughly ("spiking" solution). Carry out the extraction procedure as described above for promethazine injection BP after adding 1 ml of "spiking" solution to the 4 ml bulked injection solution at the first stage of the procedure.

---

[a] The purpose of adding 3,5-dinitrobenzoic acid to the eluate prior to evaporation is to minimise evaporative loss of aminoalcohols known to otherwise occur.

Sample preparation —Mepyramine injection

Transfer 6 ml of injection solution into a 25-ml separator containing 2 ml of 2 *M* potassium carbonate solution. Extract the resulting mepyramine base suspension with 4 × 5 ml aliquots of dichloromethane, (1 min shaking for each aliquot). Discard the dichloromethane extracts and transfer the aqueous phase to a 25-ml measuring cylinder. Wash the separator with 1 ml of 2 *M* potassium hydrogen carbonate solution followed by 1 ml of deionised water and add both to the measuring cylinder.

Dissolve 50 mg isatoic anhydride in 5 ml acetonitrile in a sample tube then add it to the aqueous extract in the measuring cylinder; mix for about 30 s then heat at 75°C for 15 min in order to complete derivatisation.

Allow the mixture to cool to ambient temperature, add about 2 ml of acetonitrile and shake the cylinder for about 30 s. The upper (water in acetonitrile) layer is removed and introduced into a 100-ml round-bottomed flask. The extraction is repeated with a further 2 × 5 ml aliquots of acetonitrile which are combined in the round-bottomed flask. Evaporate the contents of the flask to dryness under vacuum at about 40°C. (*Care*: bumping may occur in the initial stages of evaporation.) The residue is triturated with about 15 ml dichloromethane and the suspension transferred to a 100-ml separator containing 50 ml of 0.5 *M* sodium hydroxide solution. Shake the contents of the separator for about 1 min and transfer the lower organic layer into a 100-ml round-bottomed flask via a plug of anhydrous sodium sulphate. Re-extract with a further 15 ml aliquot of dichloromethane. Finally, wash the sodium sulphate with about 5 ml of dichloromethane adding this to the combined extracts. Concentrate the solution to about 2 ml by evaporation under vacuum. Wash a silica sample preparation cartridge with 10 ml of dichloromethane. Transfer the concentrated dichloromethane extract into the barrel of a 20-ml glass syringe attached to the cartridge. Transfer the sample onto the cartridge by means of the syringe plunger and discard the eluate. Wash the round-bottomed flask and syringe barrel with further aliquots of dichloromethane (up to 10 ml) and elute the washings through the cartridge. Discard the eluates. Elute the cartridge with 10 ml dichloromethane followed by 10 ml acetonitrile and discard the eluates. Elute the cartridge with 10 ml methanol and collect the eluate in a 100-ml round-bottomed flask.

Evaporate the methanol eluate to dryness under vacuum, re-dissolve the residue in about 1 ml of dichloromethane and transfer the solution to a 5-ml pear-shaped flask. Evaporate to dryness under vacuum and repeat the procedure by introducing a further 1 ml aliquot of dichloromethane used to wash the round-bottomed flask.

Re-dissolve the residue in 100 μl of dichloromethane. The sample solution is now ready for spotting onto a chromatoplate.

To prepare a "spiked" solution, transfer 5 μl of 2-dimethylaminoethanol into a 100-ml measuring cylinder containing 100 ml water. Stopper and shake thoroughly, ("spiking" solution). Carry out the extraction procedure as described above after adding 100 μl of "spiking" solution to the 6 ml bulked injection solution at the first stage of the procedure.

Adaptation to drug substances and synthetic intermediates

Residual levels of β-chloroalkylamines in drug substances or synthetic intermediates may be calculated indirectly from experimentally determined aminoalcohol contents of autoclaved injection solutions, as described earlier. However, these

experimental methods may be readily adapted to provide direct assessment of β-chloroalkylamine residues. Hydrolysis of β-chloroalkylamines in alkaline solution (pH > 12) at 75°C for 15 min has been shown to produce quantitative yields of the corresponding aminoalcohols.

Adaptation of the methods described for Phenergan injection 2.5% (w/v) and Flaxedil injection 4.0% (w/v) for the estimation of 1-dimethylamino-2-chloropropane and 1-diethylamino-2-chloroethane respectively has been achieved by introducing an hydrolysis step after the addition of 10 ml of 2.5 *M* sodium hydroxide. Aliquots of promethazine hydrochloride, 125 mg or gallamine triethiodide, 160 mg are dissolved in 5 ml of water and are analysed according to the respective methods for the injection solutions with the additional hydrolysis steps.

Analysis of β-chloroalkylamine residues in promethazine *base* may be accomplished by dissolving 110 mg of the drug substance in 4 ml of 0.1 *M* hydrochloric acid rather than water.

The method for Anthisan injection is also readily adapted for estimating residues of 1-dimethylamino-2-chloroethane in mepyramine maleate drug substance. Dissolve 150 mg of mepyramine maleate in 6 ml of water in a 50-ml measuring cylinder. Add 2 ml of 2 *M* potassium carbonate solution and heat at 75°C for 15 min. Allow to cool and extract with 4 × 5 ml portions of dichloromethane as described above.

Thin-layer chromatography

Sample spots (40 μl and 20 μl) and "spiked" sample spots (20, 10, 5, 2 and 1 μl) are spotted onto activated silica-gel layers (0.25 mm thickness). The plates are eluted for 10 cm in 100% acetone (promethazine and gallamine) or 100% methanol (mepyramine). The TLC tanks are saturated with their respective solvents.

Detection is made under 254 nm irradiation (aminoalcohol residue derivatives from promethazine and gallamine) or under 366 nm irradiation (aminoalcohol residue derivative from mepyramine). The estimation of aminoalcohol content is achieved by calculating the proportion of the weight of aminoalcohol detected in sample chromatograms to the weight of drug substance taken and expressing the result as ppm. The β-chloroalkylamine content may then be calculated from the relative molecular weights of β-chloroalkylamine and aminoalcohol. In the case of injection solutions, a correction should be made for the expected degree of hydrolysis of β-chloroalkylamines during autoclaving (see Results and Discussion).

RESULTS AND DISCUSSION

The aminoalcohols could not all be determined using the same method since 2-dimethylaminoethanol remained preferentially in an alkaline aqueous phase and was also lost during evaporation in the final stage of the concentration process.

A possible alternative method for 2-dimethylaminoethanol residues in Anthisan injection was that previouly reported for traces of glycols, polyols and hydroxylamines in aqueous media [15]. It has been shown that these residues can be isolated by the use of C_{18} sample preparation cartridges, dried with nitrogen and subsequently desorbed with a polar organic solvent such as acetonitrile. However, although this method could be applied successfully to traces of 2-dimethylaminoethanol in water, it failed to retain the aminoalcohol in the presence of mepyramine maleate drug substance. The method

finally developed involved the minimum of sample handling and permitted the derivatisation to take place in an aqueous/organic medium.

The 3,5-dinitrobenzoate ester derivatives of the aminoalcohol residues from Phenergan and Flaxedil injections were not very stable and readily underwent hydrolysis or solvolysis in the presence of protic solvents. Further investigation confirmed that isatoic anhydride would readily form an anthraniloate ester with 2-dimethylaminoethanol with the advantage that it was effective in aqueous/organic solutions [16,17], yielding a stable, highly fluorescent derivative. This reagent was thus adopted for use with samples of Anthisan injection.

The chromatographic properties of the various derivatives were investigated using TLC with 100% acetone for elution of the 3,5-dinitrobenzoate esters and 100% methanol for the anthraniloate ester. Linear intensity gradients for absorption at 254 nm against concentration were found for the 3,5-dinitrobenzoate esters of 1-dimethylaminopropan-2-ol, 2-dimethylaminopropan-1-ol and 2-diethylaminoethanol over the *apparent* range 0.4–3.2 μg with respect to the underivatised aminoalcohols (*i.e.* complete derivatisation cannot be assumed). A linear intensity gradient for fluorescence emission intensity was also found for 2-dimethylaminoethyl anthraniloate over the *apparent* range 0.05–1.0 μg with respect to the underivatised aminoalcohol.

When applied to solutions containing either promethazine hydrochloride or gallamine triethiodide, the procedure separated the 3,5-dinitrobenzoate esters of the aminoalcohols from excess reagent, 3,5-dinitrobenzoic acid (solvolysis by-product and also added to avoid evaporative loss of aminoalcohol) and from traces of co-extracted drug substance. Approximate R_F values are given in Table I. The TLC method for the anthraniloate ester of 2-dimethylaminoethanol enables separation of the derivative from excess reagent, anthranilic acid and from traces of co-extracted drug substance. Approximate R_F values are given in Table II.

All derivatives can be positively identified by spraying with Dragendorff's reagent [18], producing a red–brown colouration of the insoluble tertiary-amino iodo-bismuthate salt.

Because of the likelihood of traces of both the β-chloroalkylamine and the

TABLE I

APPROXIMATE R_F VALUES FOR COMPONENTS IN ACETONE (100%) MOBILE PHASE

Component	Approximate R_F
3,5-Dinitrobenzoate esters of:	
2-Dimethylaminopropan-1-ol	0.20
1-Dimethylaminopropan-2-ol	0.38
2-Diethylaminoethanol	0.32
3,5-Dinitrobenzoyl chloride (reagent)[a]	0.04–0.16 (streak)
3,5-Dinitrobenzoic acid[b]	0.04–0.19 (streak)
Promethazine	0.05–0.15 (streak)
Gallamine	baseline–0.11 (streak)

[a] Excess reagent is mostly destroyed during sample work-up.
[b] This component remains in an aqueous (discarded) phase during sample work-up.

TABLE II

APPROXIMATE R_F VALUES FOR COMPONENTS ELUTED IN METHANOL (100%) MOBILE PHASE

Component	Approximate R_F
2-Dimethylaminoethyl-anthraniloate	0.28
Isatoic anhydride (reagent)[a]	0.70
Anthranilic acid[b]	0.66
Mepyramine	0.13–0.25 (streak)

[a] Excess reagent is mostly destroyed during sample work-up.
[b] This component remains in an aqueous (discarded) phase during sample work-up.

corresponding aminoalcohol being present together in autoclaved injection solutions, simulated autoclaving experiments were carried out on samples of the parent β-chloroalkylamines for each product studied in order to assess the degree of hydrolysis to the corresponding aminoalcohols. Dilute stock solutions of the β-chloralkylamines were prepared in 0.01 *M* hydrochloric acid in order to inhibit hydrolysis prior to the autoclaving experiments. Table III contains details of autoclave conditions, weights of β-chloroalkylamine taken, the experimental pH values and the approximate degrees of conversion to aminoalcohols (by comparison with TLC spot intensities of derivatives from known amounts of aminoalcohols).

The different pHs chosen for simulated autoclave experiments reflect those extremes of pH commonly found in samples of injection solutions containing the drug substances.

The limits of detection for the aminoalcohols, combined with the observed degrees of hydrolysis of the β-chloroalkylamines enable the limits of detection for the β-chloroalkylamines (as hydrochlorides) in the drug substances to be calculated indirectly. These limits are given in Table IV.

TABLE III

APPROXIMATE PERCENTAGE CONVERSION OF β-CHLOROALKYLAMINES UNDER CONDITIONS SIMULATING THE PRODUCTION OF INJECTIONS

Autoclave conditions	Name and weight of β-chloroalkylamine	pH	Aminoalcohol(s) produced	Approx. conversion (%)
121°C/20 min	1-Dimethylamino-2-chloropropane (25 μg)	5.0	1-Dimethylaminopropan-2-ol 2-Dimethylaminopropan-1-ol	None detected 40
121°C/20 min	1-Dimethylamino-2-chloropropane (25 μg)	6.0	1-Dimethylaminopropan-2-ol 2-Dimethylaminopropan-1-ol	None detected 80
121°C/20 min	1-Diethylamino-2-chloroethane (14 μg)	5.5	2-Diethylaminoethanol	25
121°C/20 min	1-Diethylamino-2-chloroethane (13 μg)	7.5	2-Diethylaminoethanol	50
115°C/30 min	1-Dimethylamino-2-chloroethane (8 μg)	6.0	2-Dimethylaminoethanol	100

TABLE IV

LIMITS OF DETECTION FOR AMINOALCOHOLS IN INJECTION SOLUTIONS AND β-CHLOROALKYLAMINES IN DRUG SUBSTANCES

Injection	Drug substance	Limit of detection, ppm[a]	
		Aminoalcohol(s)	β-Chloroalkylamine (as hydrochloride)
Phenergan	Promethazine hydrochloride	8 (for each)	15–30 (for each)[b]
Flaxedil	Gallamine triethiodide	7	20–40[b]
Anthisan	Mepyramine maleate	1	1

[a] ppm with respect to the nominal content of drug substance.
[b] The range represents the uncertainty due to the effect of product pH upon the degree of hydrolysis of β-chloroalkylamine to aminoalcohol.

Samples of five batches of Phenergan injection manufactured between May 1985 and May 1987 contained no detectable trace (limit 8 ppm) of either 2-dimethylaminopropan-1-ol or 1-dimethylaminopropan-2-ol.

Samples of nine batches of Flaxedil injection manufactured between October 1984 and September 1987 contained no detectable trace (limit 7 ppm) of 2-diethylaminoethanol.

Samples of three batches of Anthisan injection manufactured in 1985 contained no detectable trace (limit 1 ppm) of 2-dimethylaminoethanol.

REFERENCES

1 G. Salomon, *Trans. Faraday Soc.*, 33 (1936) 153.
2 P. D. Bartlett, S. D. Ross and C. G. Swain, *J. Am. Chem. Soc.*, 69 (1947) 2971.
3 W. E. Hanby, G. S. Hartley, E. O. Powell and H. N. Rydon, *J. Chem. Soc.*, (1949) 519.
4 B. Cohen, E. R. Van Artsdalen and J. Harris, *J. Am. Chem. Soc.*, 70 (1948) 281.
5 B. Hansen, *Acta Chem. Scand.*, 16 (1962) 1945.
6 B. Cohen, E. R. Van Artsdalen and J. Harris, *J. Am. Chem. Soc.*, 74 (1952) 1875.
7 P. D. Bartlett, J. W. Davis, S. D. Ross and C. G. Swain, *J. Am. Chem. Soc.*, 69 (1947) 2977.
8 P. D. Bartlett, S. D. Ross and C. G. Swain, *J. Am. Chem. Soc.*, 71 (1949) 1415.
9 B. Cohen, E. R. Van Artsdalen and J. Harris, *J. Am. Chem. Soc.*, 74 (1952) 1878.
10 T. R. Crompton, *Analyst (London)*, 90 (1965) 107.
11 E. Sawicki and C. R. Sawicki, *Ann. NY Acad. Sci.*, 163 (1969) 895.
12 D. J. Evans, R. J. Mayfield and I. M. Russell, *J. Chromatogr.*, 115 (1975) 391.
13 K. Shimomura, T.-J. Hsu and H. F. Walton, *Anal. Chem.*, 45 (1973) 501.
14 P. E. De Haan, D. De Jong, J. H. M. Van Den Berg and C. G. Kruse, *J. High Resolut. Chromatogr.*, 12 (1989) 604.
15 D. Valdez and J. C. Reier, *J. Liq. Chromatogr.*, 10 (1987) 863.
16 A. R. Moorman and R. H. Abeles, *J. Am. Chem. Soc.*, 104 (1982) 6785.
17 M. E. Kargacin, G. Bassell, P. J. Ryan and T. W. Honeyman, *J. Chromatogr.*, 393 (1987) 454.
18 E. Stahl (Editor), *Thin-layer Chromatography —A Laboratory Handbook*, Springer, Berlin, 2nd ed., 1969, spray reagent No. 97, p. 873.

Journal of Chromatography, 543 (1991) 220–225
Elsevier Science Publishers B.V., Amsterdam

CHROM. 23 192

Short Communication

Automated aflatoxin analysis of foods and animal feeds using immunoaffinity column clean-up and high-performance liquid chromatographic determination

MATTHEW SHARMAN and JOHN GILBERT*
Ministry of Agriculture, Fisheries and Food, Food Science Laboratory, Colney Lane, Norwich NR4 7UQ (U.K.)
(Received January 22nd, 1991)

ABSTRACT

A commercially available system is described for the fully automated clean-up and high-performance liquid chromatographic (HPLC) analysis of aflatoxins in foods and animal feeds. The system marketed primarily for handling solid-phase extraction columns has modified software to facilitate use with immunoaffinity columns. Sample extract clean-up followed by injection onto an HPLC column with post-column iodination and fluorescence detection is carried out completely unattended. A coefficient of variation of 5.1% for aflatoxin B_1 analysis was obtained, and the accuracy of the system was demonstrated by the analysis of peanut butter certified reference material.

INTRODUCTION

Contamination of foods and animal feeds with aflatoxins B_1, B_2, G_1 and G_2 is controlled by tolerance limits in at least 50 countries worldwide [1]. Monitoring for these mycotoxins is carried out not only by enforcement authorities but also for purposes of commercial trade and for quality control of foods and animal feed constituents. There is thus a considerable requirement for large numbers of aflatoxin determinations, this demand being further exacerbated by difficulties of sampling which means that it is often necessary to analyse large numbers of replicate samples from the same batch or consignment of material. Although rapid immunologically-based screening tests and enzyme-linked immunosorbent assay (ELISA) methods are available for determining aflatoxins, they do not normally allow for simultaneous monitoring of both individual and total aflatoxin levels [2,3]. There is therefore some advantage in adopting the approach of instrumental analysis by high-performance liquid chromatography (HPLC) where aflatoxins are separated and then individually quantified. This approach becomes even more attractive if the procedure can be automated.

0021-9673/91/$03.50

Immunoaffinity columns comprise an anti-aflatoxin antibody bound to a gel material contained in a small plastic cartridge. Crude extract is forced through the column and the aflatoxins are left bound to the recognition site of the immunoglobulin. Extraneous material can be washed off the column with water and the aflatoxins can be recovered in purified form by liberating the bound analyte from the antibody with an elution solvent such as methanol or acetonitrile. Immunoaffinity columns are commercially available and have been routinely employed for determining aflatoxins B_1, B_2, G_1 and G_2 in nuts, nut products and dried fruit [4,5], as well as for determining aflatoxin M_1 in milk [6] and cheese [7]. These columns have the advantages of speed and simplicity compared to conventional clean-up and of high specificity thereby producing extracts free of interferences. A disadvantage can be the need to push the sample extract through the column at a slow but steady rate, which is tedious when carried out manually and can be a source of variable recoveries when not properly controlled [4].

The simplicity of analysis using immunoaffinity columns makes this approach particularly amenable to automation, which in turn overcomes any problems associated with sample loading onto the column. In this paper we describe modification to the design of the plastic immunoaffinity cartridges to fit the rack of a commercially available automated sample preparation system (ASPEC). Changes to the software of the system have also been made to permit the operation of conditioning, loading, washing and eluting from the columns. The system has been fully intregrated with the HPLC analysis, using post-column iodination [8] with fluorescence detection to determine aflatoxins. The ruggedness of the system has been proved over several months in routine unattended operation in surveillance work monitoring aflatoxins in imported dried figs and pistachio nuts.

EXPERIMENTAL

Materials

Total aflatoxin immunoaffinity columns ASPEC type TD110 were obtained from Biocode (York, U.K.). Acetonitrile, methanol and chloroform were purchased from Rathburn (Walkerburn, U.K.). All water was deionised and distilled. Aflatoxins B_1, B_2, G_1 and G_2 standards were purchased individually from Sigma (Poole, U.K.) and buffer salts were from BDH (Poole, U.K.). Peanut butter certified reference materials (CRMs) [9] containing aflatoxins B_1, B_2, G_1 and G_2 (CRMs 385 and 401) were purchased from the Community Bureau of Reference (BCR) of the Commission of the European Communities (Brussels, Belgium).

Sample preparation

Nuts and nut products (peanut butter). A finely ground sample of the product (30 g) was weighed accurately into a 400 ml beaker to which was added acetonitrile–water (6:4, v/v; 90 ml). The mixture was homogenised with an IKA Ultra Turrax blender at high speed for 3–5 min. Water (135 ml) was added and the sample was homogenised for a further 2 min to produce a slurry which was subsequently filtered through Whatman 113V filter paper into a conical flask (250 ml). A portion of the filtrate (15 ml) was diluted with phosphate-buffered saline (PBS) (135 ml, pH 7.4). An aliquot (*ca.* 52 ml) of this solution was transferred into a plastic Falcon tube No. 2070 (Philip Harris, London, U.K.) and placed in the rack (code 24) of the ASPEC system.

Dried fruit (figs). Samples were prepared by passing the dried fruit through a meat mincer (Butcher Boy TM22) and then slurrying with water (5:3, w/w) in a pilot-plant electric food mixer (Crypto Peerless EB60) for 0.5 h. A sample of the slurry (80 g) was weighed into a 400-ml beaker to which was added acetonitrile–water (68.75:31.25, v/v; 120 ml). The mixture was homogenised with an IKA Ultra Turrax blender at high speed for 3–5 min to produce a slurry which was subsequently filtered through Whatman 113V filter paper into a conical flask (250 ml). A portion from the top layer of the filtrate (5 ml) was diluted with PBS (120 ml, pH 7.4). An aliquot (*ca.* 52 ml) of this solution was transferred into a plastic Falcon tube and placed in the rack (code 24) of the ASPEC system.

Animal feedingstuffs. A sample of the feed (30 g) was weighed accurately into a 250-ml beaker to which was added chloroform (150 ml) and water (5 ml). The mixture was homogenised with an IKA Ultra Turrax blender at high speed for 3–5 min to produce a slurry which was subsequently filtered through Whatman 113V filter paper into a conical flask (250 ml). A portion of this filtrate was transferred to a round bottomed flask (500 ml) and the chloroform was removed under vacuum at 30°C. The residue was redissolved by the addition of methanol (5 ml) and PBS (145 ml) followed by gentle swirling. After the addition of hexane (*ca.* 50 ml) and further gentle swirling the mixture was transferred to a separating funnel and shaken gently for 10 s. The lower layer was collected and an aliquot (*ca.* 52 ml) of this solution was transferred into a plastic Falcon tube and placed in the rack (code 24) of the ASPEC system.

Automatic clean-up and chromatography

The automated HPLC system (from Anachem, Luton, U.K.) consisted of a Gilson 307 isocratic pump, a Gilson ASPEC (an automatic solid phase extraction system fitted with a Rheodyne 7010 injector and a Gilson 401 dilutor), an LKB 2150 isocratic pump (Pharmacia, Milton Keynes, U.K.) a Colora water bath thermostatted at 80°C, and a Perkin-Elmer (Beaconsfield, U.K.) LC240 fluorescence detector set at 364 nm excitation and 434 nm emission wavelengths. The detector, the Gilson pump and the ASPEC were linked via a Gilson 506B system interface module to an IBM Model 30 PC. The use of Gilson 712 HPLC software allowed both collection of data and the control of the interfaced equipment.

A Spherisorb ODS1 analytical column (5 μm particle size, 250 × 4.6 mm I.D.) was employed and this was protected by an inline filter (A315, Upchurch) fitted with a 2-μm frit (A101, Upchurch) and a C_{18} guard column (C752, Upchurch). The mobile phase of water–acetonitrile–methanol (58:30:12) was pumped at 0.86 ml/min. Post-column iodination as described elsewhere [8], employed a 5 m × 0.3 mm I.D. reaction coil maintained at 80°C. Eluent from the HPLC column was mixed in the reaction coil with a saturated solution of iodine in water pumped at 0.7 ml/min through a Valco T-piece (Chrompack, No. 22458).

RESULTS AND DISCUSSION

The Gilson ASPEC system was primarily designed and marketed for the use of solid-phase extraction columns for the automated clean-up of samples. The system as supplied comprised the following units: (1) A rack containing 250-ml plastic bottles of water, PBS and acetonitrile. (2) Two racks (code 24) for holding up to 24 Falcon tubes

(50 ml maximum volume containing diluted extracts) and up to four standards in 20-ml vials. (3) A rack (code 30) for holding 2-ml amber crimp cap vials (2CVA, Chromacol) which are used to retain a portion of the sample extract for future reference purposes if required. (4) A DEC rack designed to hold 500 mg/3 ml Bond Elut solid-phase extraction columns (Analytichem).

The operation of the ASPEC system is shown schematically in Fig. 1, and consists of initial washing of the immunoaffinity columns with 9.0 ml of PBS at 6.0 ml/min. The sample extract (50 ml) is then loaded from rack code 24 onto the immunoaffinity column at 6.0 ml/min. The column is washed with water (2.0 ml) at 6 ml/min and air dried (2.0 ml) prior to the elution of the aflatoxins into a plastic collection tube. The elution step is carried out by application of 0.5 ml of acetonitrile onto the column at 1.5 ml/min followed by a wait period of 12 s and a further addition and elution with 1.0 ml of acetonitrile. Air (1.0 ml) is used to recover any solvent remaining on the column and the eluted sample is mixed by bubbling air (3.0 ml) through the solution in the collection vial. A portion of this solution (0.5 ml) is transferred to a sealed amber vial in rack code 30 for retention. The remaining acetonitrile solution (1.0 ml) is diluted with water (2.0 ml) and mixed with air bubbling (3.0 ml). Sample extract (400 μl) is injected using partial loop fill into a 800-μl loop.

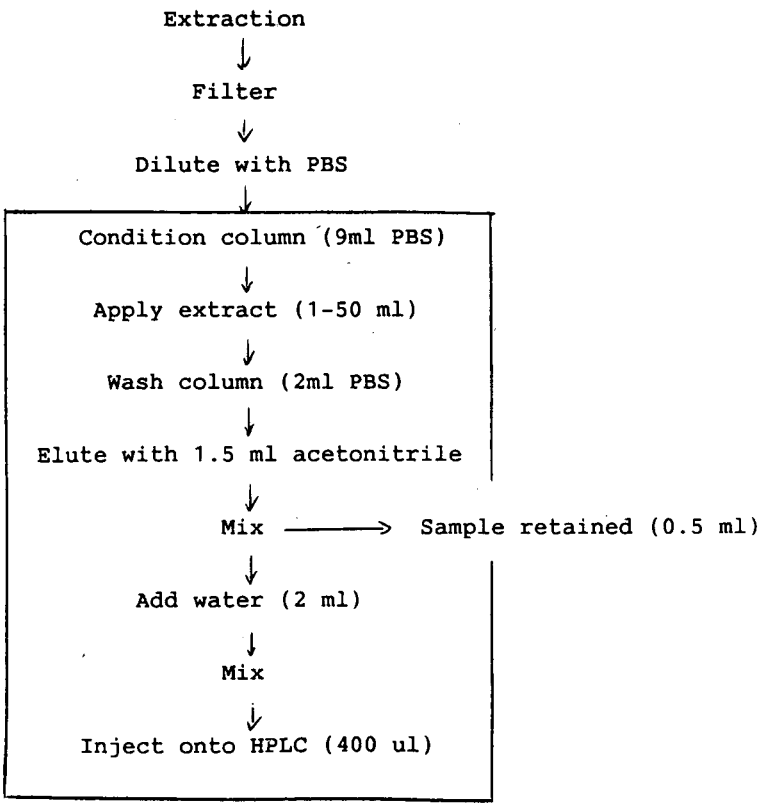

Fig. 1. Schematic illustrating the automated analysis of aflatoxins. Operations within the box are fully automated.

The running sequence for the ASPEC includes the injection of four standards to construct a calibration curve. During the chromatography of the last standard the first sample is prepared and preparation of all subsequent samples is then carried out whilst the previous sample is being separated on the HPLC system. This allows a sample to be injected and quantified every 22 min.

Quality assurance checks in relation to instrumental stability are programmed into the system by running a standard after every fourth sample extract has been prepared and injected. The ASPEC system also has considerable flexibility and will respond to highly contaminated extracts which are found to be above the working range of the detector/integrator by reinjection of 100 μl of the prepared solution directly from the plastic collection tubes in the DEC rack.

The performance of the system was evaluated by replicate analyses ($n = 20$) of a sample of well homogenised naturally contaminated dried fig slurry where the coefficient of variation (C.V.) for aflatoxin B_1 was = 5.1% (8.5 μg/kg), for aflatoxin B_2 = 6.2% (1.6 μg/kg), for aflatoxin G_1 = 10.3% (4.7 μg/kg) and for aflatoxin G_2 = 15.0% (1.5 μg/kg). The accuracy of the system was tested by examining peanut butter reference materials where it can be seen from Table I that the results were found to be in good agreement with the certified values for the aflatoxins.

The system has proved to be rugged and reliable in routine survey work where in a period of 6 months some 2000 samples were analysed (4000 determinations including standards and replicates). There were no instrumentation failures in that period or software difficulties, the only problem encountered being the failure of needle seals which did not lead to loss of samples. At present with a run time of 22 min and a sample carousel capacity for 20 sample tubes, in unattended operation the system runs for about 11 h. For the future a possible improvement would be a larger sample carousel to extend the running time during unattended operation.

TABLE I

RESULTS OF AUTOMATED AFFINITY COLUMN HPLC ANALYSIS OF AFLATOXINS IN CERTIFIED REFERENCE MATERIALS

Certification data (μg/kg) from ref. 9.

	CRM 385				CRM 401			
	B_1	B_2	G_1	G_2	B_1	B_2	G_1	G_2
Mean	7.1	1.4	1.9	0.4	<0.2	<0.1	<0.1	<0.1
Replicates (n)	6	6	6	6	6	6	6	6
S.D.	0.7	0.16	0.26	0.08	–	–	–	–
95% CL[a]	1.4	0.32	0.51	0.16	–	–	–	–
Certified level	7.0	1.1	1.7	0.3	<0.2	<0.2	<0.3	<0.2
S.D.	0.42	0.09	0.16	0.09	–	–	–	–
95% CL	0.80	0.20	0.30	0.20	–	–	–	–

[a] CL = Confidence limit.

CONCLUSIONS

An automated system for aflatoxin analysis using immunoaffinity columns for sample clean-up, has shown excellent accuracy and precision in routine operation. Although the system has been used primarily for the analysis of foods contaminated with aflatoxins, the ASPEC system is versatile and one attraction of this approach to automation is the ease with which the system can be readily tailored to other immunoaffinity column-based analyses. The conditioning of the immunoaffinity columns can be set from 1 to 20 ml, sample load volume from 1 to 250 ml, the transfer of reference sample from 0 to 2000 μl and the elution of the aflatoxin by acetonitrile from 100 to 3000 μl. The speed of aspiration/dispensing can be varied in the range 0.18 ml/min to 96 ml/min and the wait time for the elution of aflatoxins in steps of 0.01 min. Finally the injection volume can be varied from 50 μl to 800 μl. This flexibility means that the system can be readily adapted to the analysis of other mycotoxins such as zearalenone and ochratoxin A where immunoaffinity columns are already available, or can be used in other areas of contaminant analysis such as veterinary drug residues where there is a demand for automated analysis and this approach is becoming accepted.

ACKNOWLEDGEMENTS

The authors gratefully acknowledge the assistance of P. Arnold (Biocode Ltd.) for the provision of modified affinity columns and M. Lindsay (Anachem Ltd) for modification of the software for the ASPEC system.

REFERENCES

1 H. P. van Egmond, *Food Add. Contam.*, 6 (1989) 139.
2 D. E. Koeltzow and S. N. Tanner, *J. Assoc. Off. Anal. Chem.*, 73 (1990) 584.
3 M. J. Shepherd, D. N. Mortimer and J. Gilbert, *J. Assoc. Publ. Anal.*, 25 (1987) 129.
4 A. L. Patey, M. Sharman and J. Gilbert, *Food Add. Contam.*, 7 (1990) 515.
5 M. Sharman, A. L. Patey, D. A. Bloomfield and J. Gilbert, *Food Add. Contam.*, 8 (1991) in press.
6 D. N. Mortimer, J. Gilbert and M. J. Shepherd, *J. Chromatogr.*, 407 (1987) 393.
7 M. Sharman, A. L. Patey and J. Gilbert, *J. Chromatogr.*, 474 (1989) 457.
8 M. J. Shepherd and J. Gilbert, *Food Add. Contam.*, 1 (1984) 325.
9 J. Gilbert, M. Sharman, G. M. Wood, A. Boenke and P. J. Wagstaffe, *Food Add. Contam.*, 8 (1991) in press.

Journal of Chromatography, 543 (1991) 226–232
Elsevier Science Publishers B.V., Amsterdam

CHROM. 23 185

Short Communication

High-performance liquid chromatography of sulfur-containing amino acids and related compounds with amperometric detection at a modified electrode

JAMES A. COX* and EWA DABEK-ZLOTORZYNSKA
Department of Chemistry, Miami University, Oxford, OH 45056 (U.S.A.)
(Received June 14th, 1990)

ABSTRACT

Organic disulfides generally are not oxidized at bare electrodes under conditions that are suited to routine amperometric detection, and thiols are typically oxidized in a manner that leads to partial blockage of the surface. Modification of a carbon electrode with a film of Ru(III,IV) oxide stabilized with cyano-cross-links permits the amperometric detection of cystine, cysteine, glutathione, methionine, and glutathione disulfide under conditions compatible with their chromatographic separation on a strong cation-exchange column. Detection limits of 0.2–0.6 μM and linear dynamic ranges of at least 1–50 μM were obtained. The electrode was stable for at least 11 days with a pH 1 citrate, phosphate mobile phase.

INTRODUCTION

Electrochemical detectors are attractive for high-performance liquid chromatography (HPLC) because of their sensitivity and wide linear dynamic range. A limiting factor is that many species which have standard potentials in the range that is appropriate for redox at an electrode are not significantly electroactive at usual surfaces although they are redox active in homogeneous solution. In some cases the difference in behavior is due to slower charge transfer kinetics at electrode surfaces than in homogeneous solution. A second factor is adsorption of an intermediate of the electrochemical reaction that blocks further electrolysis.

Modification of electrode surfaces by immobilizing reversible redox couples thereon provides a route to permit amperometric detection of many of these species. For example, in the study described herein, we use a glassy carbon electrode modified by electrodeposition of a 1–5 monolayer film of a mixed-valence ruthenium oxide polymer cross-linked with cyanide, mvRuCN [1,2]. The Ru-species present at 0.92 V *vs.* a silver–silver chloride electrode is a sufficiently strong oxidizing agent to react with species such as As(III) [1], cysteine [3], glutathione [3], cystine, insulin [4] and

0021-9673/91/$03.50

thiocyanate [5]. These species are not electrochemically oxidized at bare surfaces in a manner that is suitable for analytical methodology. Quantitative results are obtained at the mvRuCN electrode because the current which flows as a result of re-oxidation of the ruthenium is directly proportional to the concentration of the analyte in solution over a wide range.

Another means of overcoming the above-stated limitations of bare electrodes is to step the potential to values that sequentially generate a reactive oxide layer on a surface of Pt or Au which promotes electrolysis and then electrochemically restore the surface to its initial state [6,7]. This pulsing program is repeated for each point displayed in the recorded chromatogram. An example of the applicability of this pulsed detector which is related to the present study is the elimination of the passivation of a Pt surface during the oxidation of thiourea and related compounds [8]. The product of the two-electron oxidation of thiourea is an adsorbed dimer that blocks further charge transfer at a bare electrode. By generating a reactive oxide of the electrode metal, the dimer is further oxidized, and electrode activity is retained.

The first report of application of a modified electrode to amperometric detection in a flow system involved the determination of hydrazine [9]. A carbon paste electrode into which a metallophthalocyanine was mixed was used as a detector for flow-injection analysis and HPLC. Baldwin and co-workers applied this electrode to several other analytes including thiols [10], oxalic acid and α-keto acids [11] and carbohydrates [12]. The practical application of the metallophthalocyanine-loaded carbon paste electrodes is limited by lack of long-term stability without pulsing the potential. We reported the determination of nitrite by flow-injection amperometry at a platinum electrode modified with a film of quaternized poly(4-vinylpyridine) which was impregnated with a redox mediator, hexachloroiridate; however, this complex-loaded ionomer also was not sufficiently stable for practical application [13].

Prahbu and Baldwin recently discussed the relative merits of a modified electrode at constant potential and a classical electrode used in the pulsed mode as electrochemical detectors for carbohydrates [14], which are not generally electroactive at constant potential. Using a copper-based chemically modified electrode [14], 1.2 pmol of glucose was determined by HPLC, and the electrode showed less than 10% loss of sensitivity after 5 h. The useful lifetime of the modified electrode was 2–3 days under constant-potential application. The merits of this system relative to pulsed amperometric detectors for carbohydrates were stated as superior detection limits and compatibility with the most common instrumentation for electrochemical detection in HPLC (that is, current measurement at constant applied potential).

The amperometric detector based on the mvRuCN electrode, which is used in the present study, also operates in a true potentiostatic mode. It yields sensitivities at the pmol level in flow systems [3–5] and is stable for periods up to three months in solutions which are optimized for electrochemical measurements [5]. However, prior to the present study it had not been demonstrated that the mvRuCN electrode retains these characteristics under conditions that are compatible with separation of mixtures by HPLC. In this article, conditions are described that permit both HPLC separation and amperometric detection at the mvRuCN electrode for a set of analytes which are important in bioanalytical chemistry. These compounds are not all detected by any other reported electrode at constant potential although certain thiols are directly oxidized at carbon electrodes [15] and are detected with a gold amalgam electrode by their promotion of the oxidation of mercury [16].

EXPERIMENTAL

The liquid chromatographic system consisted of a dual-piston pump, which was taken from a Dionex 2010i ion chromatograph; a 100-μl loop injector; a 250 × 4.6 mm I.D. Partisil SCX (10 μm) strong cation-exchange analytical column (Alltech), and a Bioanalytical Systems (BAS) electrochemical detector. This detector comprised an MF 1000 glassy carbon electrode which was modified as described below, an MF 2020 silver–silver chloride reference electrode and an MF 1018 stainless-steel block as the auxiliary electrode. A BAS CV 37 potentiostat was used to apply the potentials and measure the currents, which were monitored *vs.* time on an Esterline Angus Speed Servo II strip chart recorder. All chromatograms were recorded using the amperometric detector, modified as described below, with an applied potential of 0.92 V *vs.* silver–silver chloride.

Unless otherwise noted, the chemicals were ACS reagent grade and were used without further purification. The $RuCl_3 \cdot 3H_2O$ was obtained from Pfaltz and Bauer, and the $K_4Ru(CN)_6 \cdot 3H_2O$ was from Alpha Products. The L-cysteine hydrochloride hydrate (99%) and glutathione (reduced form), 98%, were from Aldrich. L-Cystine and methionine in comparable purities were obtained from Sigma, and the oxidized form of glutathione was from Boehringer Mannheim. The cysteine and oxidized form of glutathione were stored in a desiccator at 4°C. The water used was house-distilled and further purified by passing it through a Barnstead NANOpure II system.

The cystine stock solution was prepared in dilute NaOH. Serial dilutions were made using the mobile phase. Stock solutions of methionine and other individual compounds were made immediately before use by dissolving the compound in the mobile phase solution. All mobile phases were made up fresh each day. Prior to use all mobile phases were filtered through a 0.45-μm Metricel membrane filter (Gelman) and were deaerated with oxygen-free nitrogen for 1 h.

The electrodes were prepared by electrochemical deposition of a mixed-valence ruthenium oxide film that was stabilized with cyano-cross-links [1,2]. Prior to surface modification, the glassy carbon electrodes were polished successively using 1-μm, 0.3-μm and 0.05-μm alumina (Mark V Laboratory, East Granbury, CT, U.S.A.) on a metallographic polishing cloth (Buehler, Evanston, IL, U.S.A.) with deionized water as the lubricant. The electrodes were thoroughly rinsed and sonicated using deionized water (sonication time, 10 min). Freshly prepared electrodes were assembled in a flow cell which was filled with a plating solution containing 2 m*M* $RuCl_3$, 2 m*M* $K_4Ru(CN)_6$ and 0.5 *M* KCl with the pH adjusted to 2.0 using HCl. The glassy carbon indicator was then cycled between 500 mV and 1100 mV *vs.* Ag/AgCl at a scan rate of 50 mV/s for a total of forty cycles. The initial and final potentials were 500 mV. The cell was then filled at open circuit with the mobile phase and stored in this condition until needed.

RESULTS AND DISCUSSION

The analytes selected were cysteine (CSH), cystine (CSSC), glutathione (GSH), the oxidized (disulphide) form of glutathione (GSSG) and methionine (MET). The initial chromatographic experiments were based on conditions reported by Eggli and Asper [17] and by Werkhoven-Goewie *et al.* [18]. The eluents were citric acid (0.090 *M*)

TABLE I

HPLC OF GSH, CSH AND MET IN CITRATE–PHOSPHATE BUFFERS WITH AMPEROMETRIC DETECTION AT A MODIFIED ELECTRODE

$V_{1/2}$ = half width volume; k' = capacity factor; correlation coefficients (r^2) and standard deviations of slopes are based on six replicate experiments; calibration data were not obtained in the pH 2.6 buffer at 0.3 ml/min.

Analyte	pH	Flow-rate (ml/min)	k'	$V_{1/2}$ (ml)	Conc. range (μM)	Slope (nA/μM)	r^2
GSH	2.6	1.0	1.6	0.4	1–100	5.7 ± 0.2	0.998
CSH	2.6	1.0	1.7	0.4	1–100	9.4 ± 0.2	0.999
MET	2.6	1.0	2.8	0.8	1–200	3.9 ± 0.1	0.999
GSH	2.6	0.3	1.6	0.14	–	–	–
CSH	2.6	0.3	1.6	0.14	–	–	–
MET	2.6	0.3	2.7	0.32	–	–	–
GSH	2.2	0.3	1.8	0.16	1–100	7.7 ± 0.1	0.999
CSH	2.2	0.3	1.9	0.16	1–100	9.9 ± 0.2	0.999
MET	2.2	0.3	3.3	0.35	2–200	3.9 ± 0.1	0.999

and Na_2HPO_4 (0.022 M) buffers at pH 2.6 and 2.2, respectively. With a subset of GSH, CSH and MET, alone and in mixtures, chromatograms were obtained at 1.0 and 0.3 ml/min on the Partisil SCX column. In addition, calibration curves were obtained for each of these analytes. The results are summarized in Table I.

In these experiments, mixtures of GSH and CSH were not resolved, but the data in Table I demonstrate that the detector response was sensitive (*ca.* 4–10 nA/μM) and was directly proportional to concentration over a wide range. With the pH 2.6 buffer and a flow-rate of 1.0 ml/min, the detection limits, which were taken as the concentration that yielded a signal of three times the background noise, were 0.25 μM, 0.15 μM and 0.45 μM for GSH, CSH and MET, respectively.

Changing the mobile phase to 18.6 mM ammonium citrate–60.7 mM H_3PO_4 at pH 2.4 [17] did not result in separation of GSH and CSH on the Partisil SCX column. Hence, the effect of pH of the citric acid–phosphate system on the chromatographic behavior was further investigated. A a result, a mobile phase of 0.04 M citric acid–0.1 M Na_2HPO_4 at pH 2.0 was identified as suitable for the resolution of a mixture of

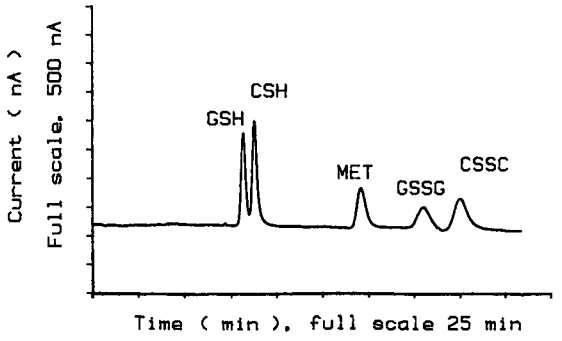

Fig. 1. HPLC of a five-component mixture with a pH 2.0 citrate–phosphate buffer as the mobile phase and amperometric detection at the mvRuCN electrode at 0.92 V *vs.* Ag/AgCl.

GSH, CSH, CSSC, GSSG and MET (Fig. 1) on this Partisil SCX column. All further work on the performance of the mvRuCN eletrode as an amperometric detector for these compounds was performed with this HPLC eluent.

The reproducibility of the detector response was investigated by injecting seven samples of a mixture of GSH, CSH and MET, where each concentration was 25 μM. The respective peak currents were 178 $\pm$ 1, 223 $\pm$ 4 and 93 $\pm$ 2 nA. Calibration curves were linear for all of the investigated analytes, as shown in Table II.

To test the stability of the detector in the selected mobile phase, chromatograms were obtained on a single preparation of the modified electrode over an eleven-day period. The total working time was about 50 h. Calibration curves for GSH, CSH and MET were obtained each day using the concentration range 1–100 μM. The results are summarized in Table III. Although the data are statistically constant over this period, the useful lifetime of that particular electrode preparation did not extend beyond eleven days. For example, on day 13, the slopes of calibration curves for GSH, CSH and MET decreased to 4.8, 6.0 and 2.9 nA/μM, respectively.

The detectability of the amperometric detector based on the mvRuCN electrode was compared to other reported detectors for the selected compounds. For example, HPLC experiments on GSH and CSH with amperometric detection have been performed using the oxidation of mercury as the anodic response [16,19,20]. With a Zorbax ODS column (5 μm, 250 $\times$ 4.6 mm), an eluent of 0.05 M trichloroacetate (1% CH_3OH) at pH 2.0, and a 100-μl injection volume, the detection limits for GSH and CSH were 1.8 and 1.2 pmol [20], respectively, compared to 18 pmol GSH and 15 pmol CSH in the present study. The electrode areas were the same in both cases. Differences in the chromatographic system may account, in part, for the poorer detection limits in the present study. A post-column ligand-exchange detection system [18] also provided detection limits that are superior to those with the mvRuCN detector for GSH, CSH, MET and CSSC. The following detection limits were reported in ref. 18 for GSH, CSH, MET and CSSC, respectively (values from the present study are in parenthesis): 16 (18), 3.2 (15), 20 (38) and 9.6 (42) pmol.

We are continuing to work toward optimizing the mvRuCN electrode as the indicator in an amperometric detector (constant potential) for HPLC. A factor that is somewhat deleterious to the detection limit is the high background that results because

TABLE II

HPLC CALIBRATION CURVES FOR SELECTED THIOLS AND DISULFIDES WITH AMPEROMETRIC DETECTION AT THE MODIFIED ELECTRODE IN A pH 2.0 CITRATE–PHOSPHATE MOBILE PHASE

Analyte	Range (μM)	Slope (nA/μM)	S.D. of slope (nA/μM, n = 6)	r^2	LOD[a] (μM)
GSH	1–100	6.9	0.2	0.999	0.18
CSH	1–100	8.7	0.1	0.999	0.15
MET	1–200	3.6	0.1	0.999	0.38
GSSG	1–50	2.0	0.1	0.999	0.63
CSSC	1–50	3.0	0.1	0.999	0.42

[a] LOD (limit of detection) = concentration that yields a current of three times the background noise.

TABLE III

TEST OF THE STABILITY OF THE MODIFIED ELECTRODE IN A pH 2.0 CITRATE–PHOSPHATE MOBILE PHASE

General conditions are same as those in Table II.

Day	Calibration curve slope (nA/μM)		
	GSH	CSH	MET
1	7.1	8.9	3.7
2	7.0	8.9	3.6
3	7.1	8.9	3.7
4	7.1	8.7	3.6
5	7.1	8.6	3.6
6	7.0	8.6	3.6
7	7.0	8.4	3.7
8	6.8	8.2	3.6
9	7.0	8.4	3.8
10	6.9	8.0	3.6
11	6.5	7.8	3.6

this surface catalyzes the oxidation of water (Fig. 1). Variation of the formulation of the modifier may permit the use of a lower applied potential which perhaps would result in a decrease in background without compromising the other performance characteristics of this electrode. But another important factor is that the HPLC system that we assembled is unlikely to duplicate state-of-the-art systems in overall stability and, therefore, detectability.

CONCLUSION

The described modified electrode permits the determination of GSH, CSH, MET, GSSG and CSSC in the μM range by HPLC with amperometric detection at constant potential. This set of analytes is not electroactive at other surfaces. The electrode is stable in a mobile phase suitable for the HPLC separation of these compounds for about ten days without cleaning or reactivation.

ACKNOWLEDGEMENT

The work was supported by the National Institutes of Health under grant 1R15GM39948-01.

REFERENCES

1 J. A. Cox and P. J. Kulesza, *Anal. Chem.*, 56 (1984) 1021.
2 P. J. Kulesza, *J. Electroanal. Chem.*, 220 (1987) 295.
3 J. A. Cox and T. J. Gray, *Electroanalysis*, 2 (1990) 107.
4 J. A. Cox and T. J. Gray, *Anal. Chem.*, 61 (1989) 2462.
5 J. A. Cox, T. J. Gray and K. Kulkarni, *Anal. Chem.*, 60 (1988) 1710.
6 S. Hughes and D. C. Johnson, *Anal. Chim. Acta*, 132 (1981) 11.

7 G. C. Neuburger and D. C. Johnson, *Anal. Chem.*, 59 (1987) 150.
8 T. Z. Polta and D. C. Johnson, *J. Electroanal. Chem.*, 209 (1986) 159.
9 K. M. Korfhage, K. Ravichandran and R. P. Baldwin, *Anal. Chem.*, 56 (1984) 1514.
10 M. K. Halbert and R. P. Baldwin, *Anal. Chem.*, 57 (1985) 591.
11 L. M. Santos and R. P. Baldwin, *Anal. Chem.*, 58 (1986) 848.
12 L. M. Santos and R. P. Baldwin, *Anal. Chem.*, 59 (1987) 1766.
13 J. A. Cox and K. R. Kulkarni, *Talanta*, 33 (1986) 911.
14 S. V. Prabhu and R. P. Baldwin, *Anal. Chem.*, 61 (1989) 852.
15 J. A. Cox and A. Przyjazny, *Anal. Lett.*, 10 (1977) 869.
16 L. A. Allison and R. E. Shoup, *Anal. Chem.*, 55 (1983) 8.
17 R. Eggli and R. Asper, *Anal. Chim. Acta*, 101 (1978) 253.
18 C. E. Werkhoven-Goewie, W. M. A. Niessen, U. A. Th. Brinkman and R. W. Frei, *J. Chromatogr.*, 203 (1981) 165.
19 R. Saetre and D. L. Rabenstein, *Anal. Chem.*, 50 (1978) 276.
20 D. Shea and W. A. MacCrehan, *Anal. Chem.*, 60 (1988) 1449.

Journal of Chromatography, 543 (1991) 233–240
Elsevier Science Publishers B.V., Amsterdam

CHROM. 23 197

Short Communication

High-performance liquid chromatographic separation of racemic and diastereomeric mixtures of 2,4-pentadienoate–iron tricarbonyl derivatives

MINREN XU and CHIEU D. TRAN*
Department of Chemistry, Marquette University, Milwaukee, WI 53233 (U.S.A.)
(Received January 24th, 1991)

ABSTRACT

β-Cyclodextrin chiral stationary phase facilitates the chiral separation of the (±)-methyl-5-formyl-2,4-pentadienoate–iron tricarbonyl (*1*) racemic mixture. The separation of oxazolidine derivatives *2* and *3* diastereomers were achieved with a C_{18} column but the compounds underwent in-column hydrolysis to give (−)- and (+)-*1*, respectively. This hydrolysis was exploited for the determination of *2* and *3* by the β-cyclodextrin column, namely *2* and *3* were initially and completely hydrolyzed in the column to give (−)- and (+)-*1* and this racemic mixture was then separated by this chiral column.

INTRODUCTION

Methyl-5-formyl-2,4-pentadienoate–iron tricarbonyl (**1**) has been proved to be an important intermediate in the syntheses of many chiral compounds, for instance chiral polyenes [1,2]. Introduction of the iron tricarbonyl to the formyl pentadienoate produces a chiral center on the molecule which is very useful in asymmetric syntheses [3]. The absolute configuration of enantiomers **1** has been determined by X-ray crystallography [4]. The structures of (−)- and (+)-**1** are given below:

Several chemical resolutions of racemic mixture (±) **1** into enantiomers have been reported [5,6]. For example, the racemic mixture **1** can be resolved by the initial

0021-9673/91/$03.50

conversion of **1** into diastereomeric oxazolidine derivatives **2** and **3** through a reaction with a chiral compound (−)-ephedrine and the subsequent isolation of **2** and **3** through fractional crystallization in diethyl ether and *n*-hexane, respectively.

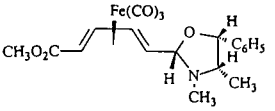

2

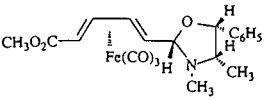

3

The final hydrolyses of the diastereomers **2** and **3** in the presence of silica gel and water give the optically active (−)- and (+)-**1**. This procedure is tedious, time consuming and more importantly, cannot be easily performed with a small amount of sample. It is thus, important to develop a novel separation method which can separate not only the (−)- and (+)-**1** enantiomers but also the **2** and **3** diastereomers as well.

Cyclodextrin (CD)-bonded stationary phases are well known for their efficient in the separation of chiral compounds [7–10]. The chiral separation is accomplished because CDs which are the optically active, doughnut shaped molecules, selectively form inclusion complexes with the analyte. Since **1**, **2** and **3** are relatively hydrophobic and have the required functional groups to interact with CDs, it is expected their separation can be achieved with the use of the chiral stationary phase CD column. It will be reported, for the first time, in this communication that (−)- and (+)-**1** enantiomers can be separated by a β-CD column. The diastereomeric **2** and **3** can also be separated by the same column by initially allowing this compounds to undergo in-column hydrolysis to give a racemic mixture of (±)-**1**.

EXPERIMENTAL

Reagents and materials

High-performance liquid chromatography (HPLC)-grade methanol was obtained from Burdock & Jackson (Muskegon, MI, U.S.A.). Deionized water was distilled from all glass distillation apparatus. Mobile phase was filtered through a nylon 0.45-μm membrane filter and degassed with sonication and vacuum.

Chiral compound (−)-**1**, (+)-**1** and their racemic mixture as well as diastereomers **2**, **3** and their mixture were synthesized and purified according to ref. 5. Optical rotations in methanol were determined to be $[\alpha]_D^{25} = -62°$ and $+62°$ for (−)- and (+)-**1**, and $-365°$ and $+100°$ for **2** and **3**, respectively. These values are in agreement with the literature data [5]. The melting points of **2** and **3** were found to be 111.0°C and 104.0°C which agree well with the literature values of 111.0°C and 104.0°C, respectively [5]. All samples were dissolved in absolute methanol prior to injection.

Apparatus and procedure

The HPLC separations were performed with a Shimadzu isocratic pump (Model LC-600), a Rheodyne Model 7125 sample injector equipped with a 20-μl loop, and a variable-wavelength detector operated at 351 nm.

The chromatograms of (±)-, (−)- and (+)-**1** were obtained using a β-CD

bonded column (250 × 4.6 mm I.D., ASTEC, Whippany, NJ, U.S.A.) at 23°C as a chiral stationary phase and water–methanol (9:1, v/v) as a mobile phase. The chromatograms of diastereomeric mixture, their single component **2** and **3** were performed with a C_{18} bonded column (250 × 4.6 mm I.D., Custom LC, Houston, TX, U.S.A.) at 23°C and a mobile phase which consists of methanol–0.06 *M* phosphate buffer pH 8.0 (85:15, v/v). The flow-rate of 1.0 ml/min was used in all the experiments. The void volume of the columns was determined by injecting 20 μl pure methanol or water when pumping with a mixture mobile phase. The change of reflective index caused by the injected solvents was used as the marker.

RESULTS AND DISCUSSION

The chromatogram in Fig. 1a shows a near base-line separation of the racemic mixture (±)-**1**. The chromatograms of the pure optically active (−)- and (+)-

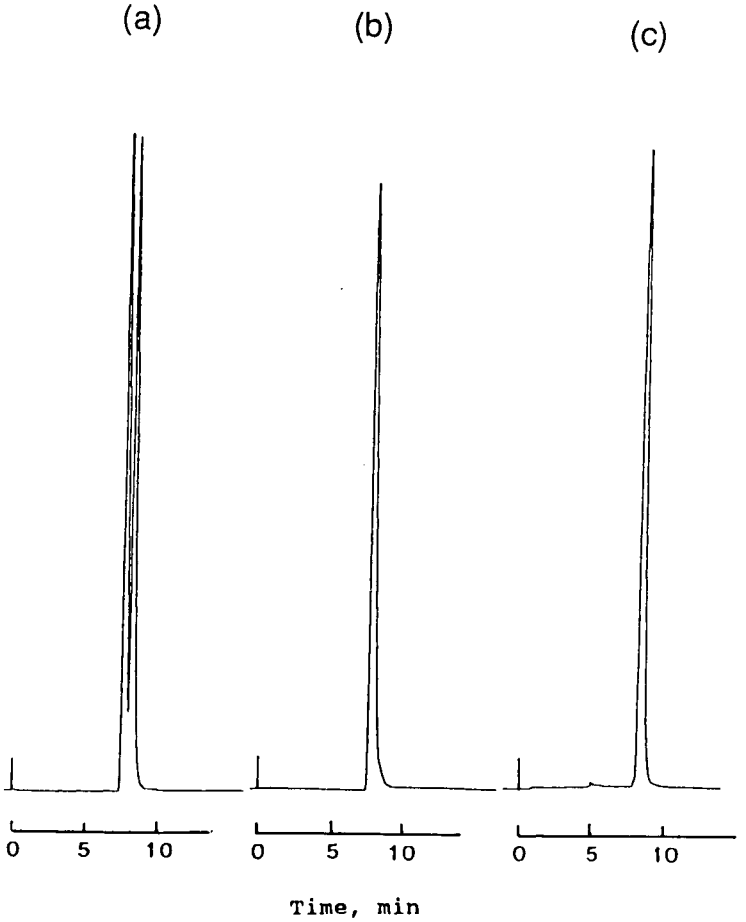

Fig. 1. Chiral separation of (±)-methyl-5-formyl-2,4-pentadienoate–iron tricarbonyl (compound **1**) on a β-CD bonded chiral stationary phase. Mobile phase: water–methanol (9:1, v/v); flow-rate: 1.0 ml/min. (a) Racemic mixture; (b) (−)-enantiomer; (c) (+)-enantiomer.

enantiomers, which are given in Fig. 1b and c, confirm the chiral resolution and enable the assignment of the peaks. Accordingly, the first peak, eluted with a retention time at 7.5 min is due to the (−)-enantiomer following by the (+)-enantiomer with a retention time of 8.1 min. The separation factor α and the resolution R_s are calculated to be 1.11 and 0.93.

The β-CD column was also used to separate the diastereomeric mixture of **2** and **3**. The results, obtained with the mobile phase consists of water–methanol (9:1, v/v) at pH 6.5, is shown in Fig. 2a. For reference, the chromatogram of the pure **2** and **3**

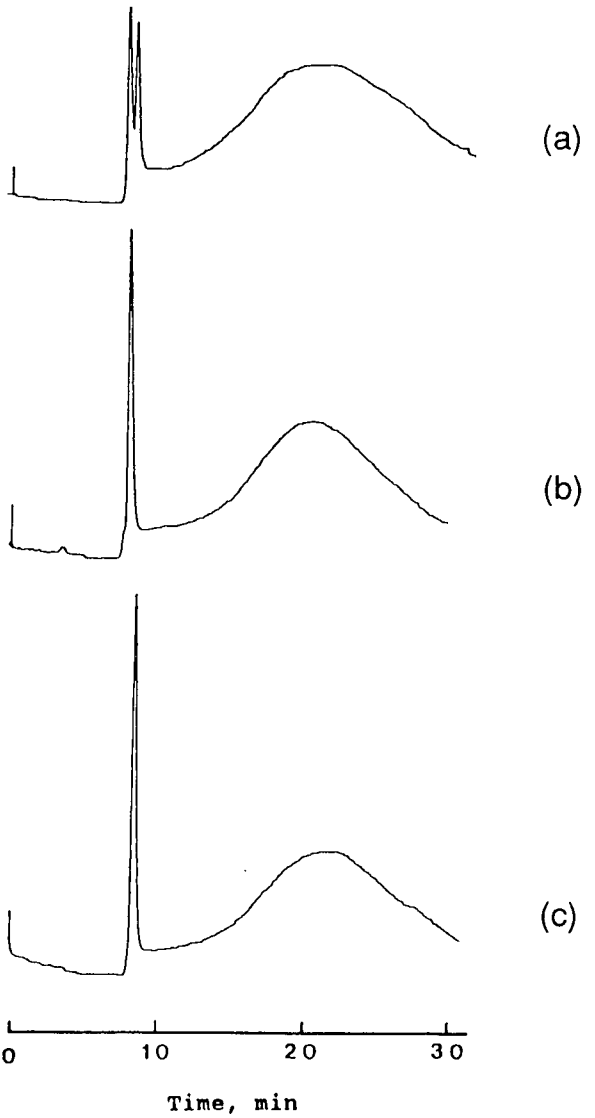

Fig. 2. Separation of diastereomeric oxazoline derivatives **2** and **3** on the β-CD chiral stationary phase. Mobile phase: water–methanol (9:1, v/v), pH 6.5; flow-rate: 1.0 ml/min. (a) Mixture of **2** and **3**; (b) pure **2**; (c) pure **3**.

obtained using the same conditions, are also shown in Fig. 2b and c. Based on the optical rotations, melting points and NMR data, **2** and **3** are considered to be pure. It is therefore, possible that they undergo decomposition in the column. In fact, it is likely that compounds **2** and **3** decompose in the column to give (−)- and (+)-**1** in the column because: (1) there is some unreacted silica in the β-CD column and (2) as explained earlier, these diastereomers are known to undergo hydrolysis in the presence of silica gel and water. From Fig. 2a–c and the chromatograms of the optically pure (−)- and (+)-**1** shown in Fig. 1a–c, it is evident that the broad peaks in Fig. 2 are due to the diastereomers **2** and **3**. These compounds decomposed in the column to give (−)- and (+)-**1**, respectively. The decomposed product (±)-**1** are then undergone chirally separated by the β-CD column to give a chromatogram (Fig. 2a) similar to those of the pure racemic mixture (±)-**1**. Moreover, the similarity between the peak at 7.5 min in Fig. 2b [from the (−)-**1** generated by **2**] and that of the pure (−)-**1** shown in Fig. 1b, and between the peak at 8.1 min in Fig. 2c [from the (+)-**1** generated by **3**] and that of the pure (+)-**1** shown in Fig. 1c further confirms our explanation. Since the in-column hydrolysis of **2** and **3** is unavoidable, it may be possible to quantitatively determine **2** and **3** by selecting experimental conditions in such a way that **2** and **3** undergo completely hydrolysis to give (−)- and (+)-**1**. The hydrolyzed products can then be determined by the β-CD column. We have, in fact, successfully implemented this possibility by performing the separation at pH 4.5 and the results obtained for the mixture of **2** and **3**, and also for the pure **2** and **3** are shown in Fig. 3. As shown in these figures, **2** and **3** underwent complete hydrolysis to give (−)- and (+)-**1** which were then quantitatively and chirally separated by the β-CD column.

The diastereomeric mixture of **2** and **3** was also separated on a C_{18} bonded phase using methanol containing 15% phosphate buffer at pH 8.0 as mobile phase. The chromatogram obtained, shown in Fig. 4a, is rather complex. For reference, the chromatograms of the pure **2**, **3** and **1** are also given in Fig. 4b, c and d. From these chromatograms it is evident that **2** and **3** also underwent hydrolysis in this column. The peaks having retention times of 6.7 and 8.1 min in Fig. 2a are due to compounds **2** and **3**, respectively, while the peak at 3.1 min is similar to the single chromatogram peak of the pure compound **1** (Fig. 4d) and is due to the hydrolyzed product **1**. There is only one peak in Fig. 4a which corresponds to compound **1** in spite of the fact that **2** and **3** are known to undergo hydrolysis to give (−)- and (+)-**1**, respectively. This is hardly surprising because while (−)- and (+)-**1** enantiomers are produced by **2** and **3**, they cannot be separated by the achiral C_{18} column used.

It has been demonstrated that the racemic mixture of the compound **1** can be near baseline separated into enantiomers by use of the β-CD chiral stationary column. The corresponding diastereomers **2** and **3** were also separated by this chiral column. However, these diastereomers undergo in-column hydrolysis to give a racemic mixture of **1**. However, the diastereomers can be determined by this method by performing the separation at pH 4.5 because at this pH, they undergo complete hydrolysis to give a racemic mixture of **1** which is then quantitatively and chirally separated. A C_{18} column can also separate the diastereomers. However, since the in-column hydrolysis is unavoidable and this column cannot chirally separate the racemic mixture of **1**, it is not as useful as the β-CD chiral stationary phase column.

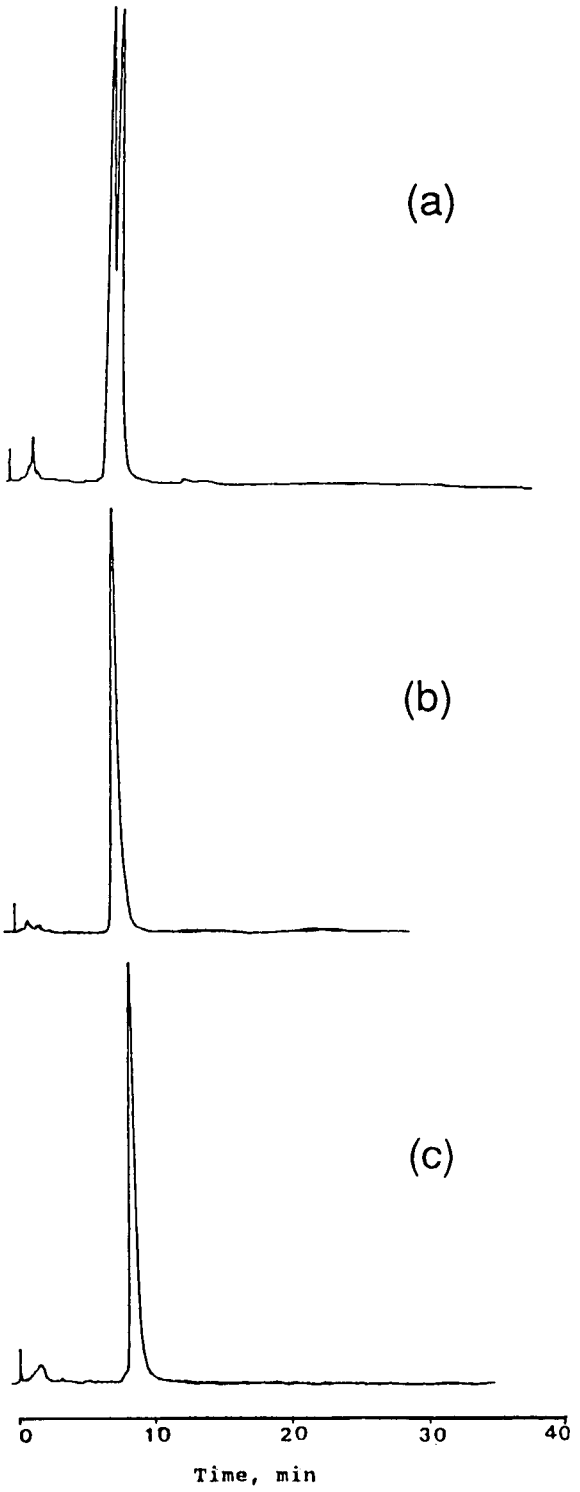

Fig. 3. Separation of diastereomeric oxazoline derivatives **2** and **3** on the β-CD chiral stationary phase. Same conditions as in Fig. 2 except pH was 4.5. (a) Mixture of **2** and **3**; (b) pure **2**; (c) pure **3**.

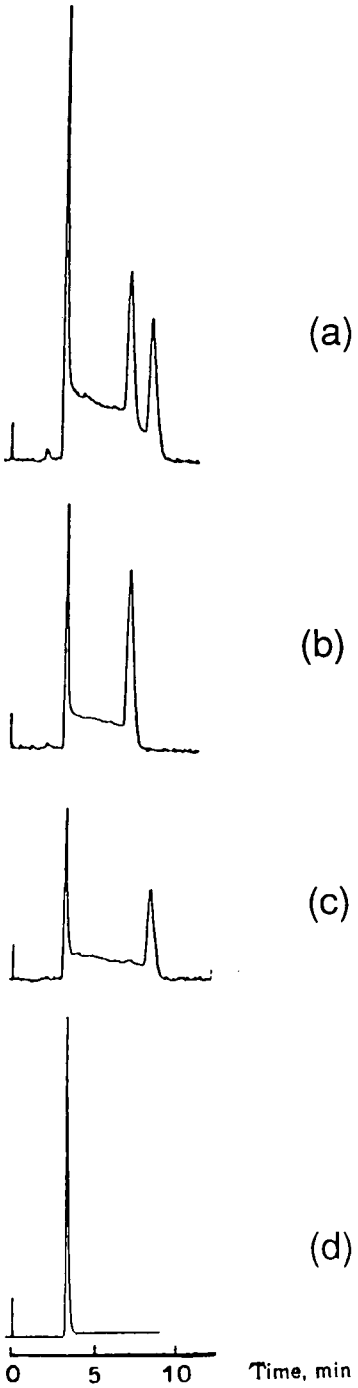

Fig. 4. Separation of diastereomeric oxazolidine derivatives **2** and **3** on a C_{18} column. Mobile phase: methanol–0.06 *M* phosphate buffer pH 8.0 (85:15, v/v); flow-rate: 1.0 ml/min. (a) Mixture of **2** and **3**; (b) pure **2**; (c) pure **3**; (d) pure **1**.

ACKNOWLEDGEMENT

The authors are grateful to Professor William Donaldson and Mr. Chunlin Tao for the gift of compounds **1**, **2** and **3**, and Advanced Separation Technologies (ASTEC) for the gift of the Cyclobond I column. Financial support for this work is provided by the National Institutes of Health.

REFERENCES

1 A. Monpert, J. Martelli, R. Gree and R. Carrie, *Nouv. J. Chim.*, 7 (1983) 345.
2 R. Gree, J. Kessabi, P. Mosset, J. Martelli and R. Carrie, *Tetrahedron Lett.*, 25 (1984) 3697.
3 K. Nunn, P. Mosset, R. Gree and R. W. Saalfrank, *Angew. Chem., Int. Ed. Engl.*, 27 (1988) 1188.
4 J. Morey, P. Mosset, D. Gree, R. Gree and L. Tonpet, *Tetrahedron Lett.*, 28 (1987) 2959.
5 A. Monpert, J. Martelli, R. Gree and R. Carrie, *Tetrahedron Lett.*, 22 (1981) 1961.
6 R. L. Markezich, *Ph.D. Dissertation*, University of Wisconsin, Madison, WI, 1971.
7 D. W. Armstrong, *Sep. Purif. Methods*, 14 (1985) 212.
8 W. L. Hinze and D. W. Armstrong, *Ordered Media in Chemical Separations*, American Chemical Society, Washington, DC, 1987.
9 D. W. Armstrong, *Anal. Chem.*, 59 (1987) 84A.
10 D. W. Armstrong and S. M. Han, *CRC Crit. Rev. Anal. Chem.*, 19 (1988) 175.

Journal of Chromatography, 543 (1991) 241–243
Elsevier Science Publishers B.V., Amsterdam

CHROM. 23 089

Short Communication

Identification of vitamin D_2 by thermospray-interface mass spectrometry

KAZUNORI TAKAMURA* and HIROKO HOSHINO
Seitoku Junior College of Nutrition, 1–4–6, Nishi-shinkoiwa, Katsushika-ku, Tokyo 124 (Japan)
NORIAKI HARIMA
JASCO International Co., Ltd., 2–4–21, Sennin-cho, Hachioji City, Tokyo 193 (Japan)
TATSUYUKI SUGAHARA
Kagawa Nutrition College, 3–24–2, Komagome, Toshima-ku, Tokyo 170 (Japan)
and
HISAO AMANO
Toho University School of Medicine, 5–21–16, Ohmori-nishi, Ohta-ku, Tokyo 143 (Japan)
(First received July 16th, 1990; revised manuscript received December 11th, 1990)

ABSTRACT

In order to identify vitamin D_2 contained in shiitake mushroom (*Lentinus edodes*), which is taken routinely in Japan, vitamin D_2 was isolated by thin-layer liquid chromatography and high-performance liquid chromatography and identified by thermospray-interface mass spectrometry; this procedure prevents the decomposition of vitamin by heat, which is a common problem in the gas chromatography–mass spectrometry of vitamin D_2.

INTRODUCTION

The identification of vitamin D_2 [1] (hereafter called D_2) and the determination of vitamin D_3 [2] metabolites have usually been conducted by gas chromatography–mass spectrometry (GC–MS). It is well known, however, that the heating process during GC causes ring closure of a steroid ring between the 9- and 10-positions, converting D_2 into pyro D_2 and isopyro D_2 [3] (Fig. 1). In order to identify D_2 contained in shiitake mushroom (*Lentinus edodes*), which is taken routinely in Japan, we isolated D_2 by thin-layer liquid chromatography (TLC) and high-performance liquid chromatography (HPLC) and the isolated substance was identified by thermospray-interface mass spectrometry (TSP-MS). We have subsequently succeeded in obtaining a mass spectrum of D_2 that does not suffer from thermal ring closure.

0021-9673/91/$03.50

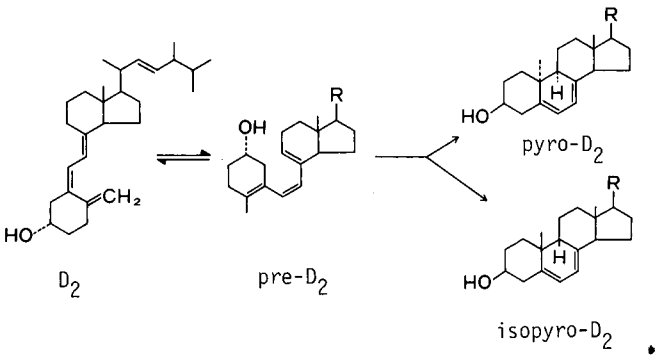

Fig. 1. Thermal isomerization of vitamin D_2.

EXPERIMENTAL

All reagents were of analytical-reagent grade from Wake (Osaka, Japan). Shiitake mushroom (brand name Koshin) produced in Japan from March to May was used as a sample. A 500-g sample was ground with a homogenizer (one fifth at a time), and all of it was placed in a digestion flask and decomposed by heating at 80°C for 30 min after addition of absolute non-aldehyde ethanol (400 ml), pyrogallol (40 g) and 50% potassium hydroxide solution (100 ml). After cooling to room temperature, unsaponifiable matter was extracted with 1000 ml of benzene, followed by washing once each with 500 ml of 1 *M* and 300 ml of 0.5 *M* potassium hydroxide solution and then four times with 100 ml of water [4]. The upper benzene layer was separated by TLC using a Wako-gel B5FM silica gel TLC plate (Wako) with benzene–acetone (95:5) as developing solvent and UV detection (254 nm) so as to obtain a D_2 fraction.

This D_2 fraction was extracted with chloroform and evaporated to dryness below 35°C. To the resulting residue 2 ml of methanol–acetonitrile (1:1) were added and this solution was further purified twice by HPLC on an NSLC Model 100A chromatograph (Nihon Seimitsu Kagaku). In the first step a LiChrosorb RP-18 column (250 × 7.5 mm I.D.) was used with methanol–acetonitrile (1:1) as eluent and in the second step a Nucleosil 100-5 column column (150 × 4.6 mm I.D.) with *n*-hexane containing 0.1% of *n*-amyl alcohol and 0.4% of isopropyl alcohol as eluent.

Finally, the isolated substance was dissolved in 0.5 ml of 0.1 *M* ammonium acetate–methanol (4:6) and directly subjected to identification of D_2 by TSP-MS on a VG Model 12-250 instrument (VG Analytical) without any HPLC column, under the following conditions: solvent flow-rate, 0.4 ml/min; source temperature, 230°C; probe temperature, 250°C; electron energy, 70 eV.

RESULTS AND DISCUSSION

Fig. 2 is a TSP mass spectrum the purified extract of shiitake mushroom. A major peak was detected at *m/z* 397, $[M+H]^+$, but little fragmentation was observed. Similar results were obtained with standard D_2. Pyro D_2 and isopyro D_2 were also subjected to TSP-MS under the same conditions as those employed for the

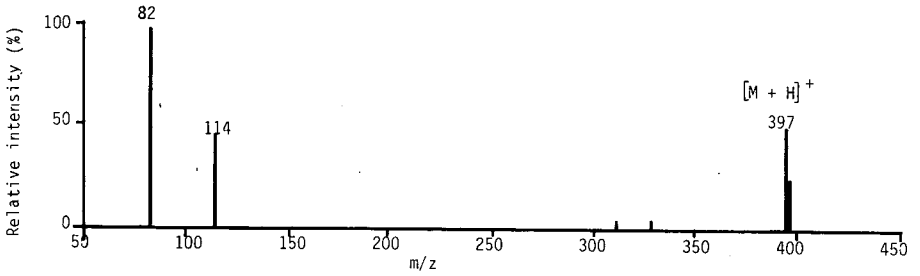

Fig. 2. Mass spectrum of the purified D_2 fraction obtained from shiitake mushroom (concentration 5 μg/μl). Injection volume, 3 μl.

standard D_2. No peak at *m/z* 397 was obtained with these samples, indicating that D_2 suffering no thermal ring closure can be identified by TSP-MS.

The identification of aldosterone and corticosterone, each having a steroid ring similar to that in vitamin D_3, by LC–MS [5,6] (measurement concentration 1 μg in 100 μl) and the determination of vitamin D_3 metabolites (1,25-dihydroxy-vitamin D_3 and 24,25-dihydroxy-vitamin D_3) by GC–MS [7,8] (determination concentration 0–250 ng/l) have been reported previously. In contrast to dihydroxy-vitamin D_3, the measurement concentration employed in this study was as high as 5 μg/μl, as D_2 is poorly ionized in TSP-MS as there are few functional groups. Previously D_2 has not been identified by TSP-MS.

REFERENCES

1 A. Takeuchi, T. Okano, S. Teraoka, Y. Murakami, M. Sayamoto, S. Sawamura and T. Kobayashi, *Bitamin*, 58 (1984) 439.
2 J. Fohlman, P. A. Peterson, I. Kamensky, P. Hakansson and B. B. Sundqvist, *Nucl. Instrum. Methods. Phys. Res.*, 198 (1982) 169.
3 P. Busse, *Hoppe-Seyler's Z. Physiol. Chem.*, 214 (1933) 211.
4 F. J. Mulder, E. J. DeVries and K. J. Keuning, *Pharm. Weekbl.*, 100 (1965) 1457.
5 D. Watson, G. W. Taylor, S. Laird and G. P. Vinson, *Biochem. J.*, 242 (1987) 109.
6 P. R. Das, B. N. Pramanik, R. D. Malchow and K. J. Ng, *Biomed. Environ. Mass Spectrom.*, 15 (1988) 253.
7 I. Bjorkhem, I. Holmberg, T. Kristiansen and J. I. Pedersen, *Clin. Chem.*, 25 (1979) 584.
8 R. D. Coldwell, D. J. H. Trafford, H. L. J. Makin, M. J. Varley and D. N. Kirk, *Clin. Chem.*, 30 (1984) 1193.

Journal of Chromatography, 543 (1991) 244–249
Elsevier Science Publishers B.V., Amsterdam

CHROM. 23 129

Short Communication

Direct determination of metamitron in surface water by large sample volume injection

RENÉ B. GEERDINK

Institute for Inland Water Management and Waste Water Treatment, P.O. Box 17, 8200 AA Lelystad (The Netherlands)

(First received July 24th, 1990; revised manuscript received November 13th, 1990)

ABSTRACT

For a number of applications, *e.g.*, monitoring of surface water quality, trace components which can be detected at levels of 0.1–1 ng do not need preconcentration. However, the determination of these components is usually performed after liquid–liquid or solid-phase extraction, which is time consuming. Injection of the sample directly into the separation system not only saves time (allowing higher sample throughputs), but is also uncomplicated and thus automatable. Metamitron was determined by direct injection of (surface) water samples onto an analytical C_{18} column. With a 2-ml loop injection, the detection limit was 0.15 μg/l in surface water. No significant peak broadening compared with a 20-μl loop injection was observed. The linearity of the method was satisfactory ($r^2 = 0.9985$) and the relative standard deviation for seven replicate 2-ml injections at 2 μg/l was 3%. The total analysis time was only 10 min.

INTRODUCTION

So far, only a few low-level multicomponent methods [1–4] for surface water analysis have been reported. Especially for early warning systems these methods should be fast, reliable and capable of determining a broad range of relevant individual substances. The time available to decide whether the quality of a water is good enough, *e.g.*, for preparing drinking water, may not be more than 1–2 days after the first signal of an accidental discharge. For unknown components, this time is probably too short. Often the analyst tries to determine the component(s) by applying existing methods. Recoveries using, *e.g.*, extraction and/or derivatization are more or less unknown, so one can only determine the trend of a concentration profile rather than actual concentrations. In such events, an uncomplicated analytical method that does not involve any isolation or derivatization step is needed.

On June 14th, 1990, Dutch authorities were warned by the International Commission for Protection of the Rhine against Pollution (ICPR) about an accidental discharge (*ca.* 3 ton) of metamitron (4-amino-4,5-dihydro-3-methyl-6-phenyl-1,2,4-triazin-5-one), an agricultural herbicide, at Leverkusen (Germany). Our existing

0021-9673/91/$03.50

multicomponent methods were not applicable to this compound. Moreover, from literature it was known that the extraction efficiency using dichloromethane was poor and irregular [1–3]. Because the results obtained on a C_{18} concentration column [2] were good (85%), we decided to determine this component by direct injection of large volumes (2 ml) of surface water into an analytical C_{18} column, allowing simplicity and speed of analysis.

Data on large-volume injections are only sparingly available in the literature and usually refer to biological fluids [5–8]. The technique of direct concentration on the top of the column was more effective in reversed-phase compared to normal-phase chromatography [7], and data have been reported for injection volumes up to 2 ml. Direct aqueous injection has also been reported for the determination of N-methyl-carbamates [9,10]. No loss of resolution was found and with large injection volumes detection limits at the ng/l level were expected.

In this paper we report our results obtained by direct injection, achieving a detection limit of 0.15 μg/l (150 ng/l) with a total analysis time of *ca.* 10 min.

EXPERIMENTAL

Reagents

High-performance liquid chromatographic (HPLC) grade acetonitrile and water were obtained from Mallinckrodt (St. Louis, MO, U.S.A.) and perchloric acid from Baker (Deventer, The Netherlands).

Metamitron was obtained from Riedel-de Haën (Hannover, Germany).

Apparatus

For sample analysis the HPLC apparatus consisted of a Milton Roy (Riviera Beach, FL, U.S.A.) ConstaMetric 3000 pump to deliver the mobile phase and Pye Unicam Model 4110 and LC3 variable-wavelength UV absorbance detectors (Philips, Eindhoven, The Netherlands), set at 310 and 230 nm, respectively. For validation of the method the HPLC apparatus consisted of an LKB (Bromma, Sweden) Model 2150 pump and an LKB Model 2141 variable-wavelength UV absorbance detector.

Samples were injected using a Rheodyne injection valve with 0.02-, 0.1- and 2-ml loops. Chromatograms were recorded and integrated by a data station (Millipore, Bedford, MA, U.S.A.) using Baseline 810 software.

Procedures

Stock solutions of metamitron were freshly prepared each week by weighing followed by dissolution in acetonitrile. These solutions were diluted using HPLC-grade water to obtain standard solutions.

No pretreatment of surface water samples was performed except checking the pH, which should be between 6.5 and 7.5. The samples were separated on a reversed-phase column (LiChrospher 100 RP-18, 5 μm) (250 × 4 mm I.D.) using acetonitrile–water (40:60, v/v) acidified to pH 2.7 with perchloric acid at a flow-rate of 1 ml/min.

RESULTS AND DISCUSSION

Chromatography

Metamitron can be detected at low concentrations using UV absorption at 230 or 310 nm, fluorescence or electrochemical [1] detection. The limit of detection is *ca.* 0.1–1 ng absolute [1,2]. On a C_{18} column using acidified (perchloric acid) acetonitrile–water (40:60, v/v) mobile phase at pH 2.7 we found this component elutes with $k' = 2$.

With both UV detectors in series we first determined the response ratio (310/230 nm) for confirmation (identification); this value turned out to be 3.5. With loop injections of 0.02, 0.1 and 2 ml no significant band broadening in the system used (see Fig. 1) was observed.

From Table I, it can be seen that the peak width at half height ($w_{\frac{1}{2}}$) and at the peak base is the same for all volumes injected, indicating that metamitron is very efficiently concentrated from the aqueous sample on the top of the column. The increase in retention time from 4 to 6 min on going from 0.02 to 2 ml is in good agreement with the results of Broquaire and Guinebault [6], who reported a linear increase in retention time with the volume injected for components in non-eluting solvents.

From the results using 0.1- and 2-ml injections, the minimum detectable amount

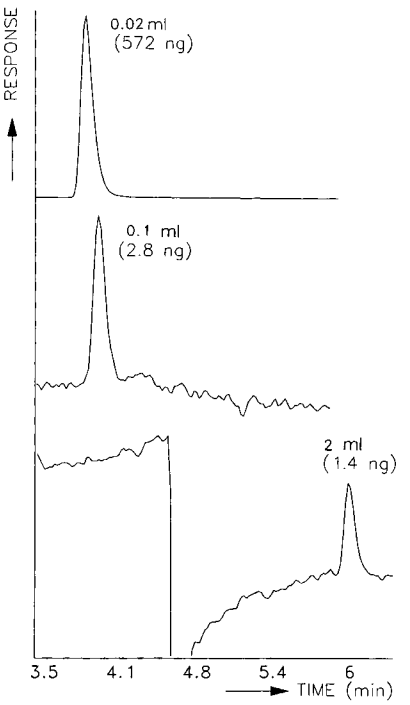

Fig. 1. HPLC of metamitron standard solutions using varying concentrations and loop volumes. Column, 250 × 4 mm I.D. LiChrosphere 100 RP-18, 5 μm; eluent, acetonitrile–water (40:60) at pH 2.7; flow-rate, 1.0 ml/min. UV detection at 310 nm.

TABLE I

DEPENDENCE OF RETENTION TIME AND PEAK WIDTH ON INJECTION VOLUME

Injection volume (ml)	Concentration (μg/l)	t_R (min)	Peak width (min)	
			$w_{\frac{1}{2}}$	Base
0.02	28600	3.92	0.11	0.21
0.1	28.6	4.03	0.12	0.19
2	0.7	6.05	0.10	0.17

of metamitron was calculated to be *ca.* 0.3 ng, indicating that with large injection volumes of 2 ml no further concentration of the analyte of interest was necessary and that the detection limit (signal-to-noise ratio = 3) in surface water was *ca.* 0.15 μg/l.

The direct injection of 2-ml surface water samples showed that a wavelength of 310 nm was much more selective than 230 nm (see Fig. 2). From the inset in Fig. 2 it can also be seen that the response ratio (310/230 nm) at this low level (*ca.* 1.5 μg/l) may be used for confirmation (especially in the case when a warning has been issued against pollution by a particular compound, the concentration of which is far greater than that of all other unknown compounds in the water). Owing to the presence of dissolved organic constituents (DOC) in the surface water samples, metamitron is expected to be dragged along, resulting in a shorter retention time compared with a standard solution. This phenomenon was confirmed by comparing spiked with non-spiked surface water; the retention shift of metamitron was 32 s. From Table II it can be seen that the concentration profile in the river Rhine could easily be followed. Because this

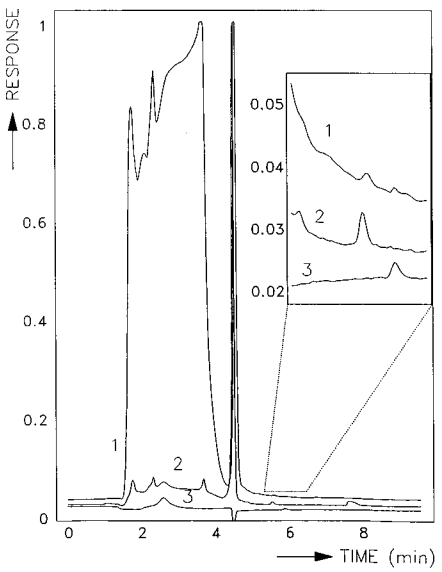

Fig. 2. HPLC of *ca.* 1.5 μg/l metamitron samples using a 2-ml injection volume. (1) Surface water, detection at 230 nm; (2) surface water, detection at 310 nm; (3) standard, detection at 310 nm.

TABLE II

CONCENTRATIONS OF METAMITRON IN RHINE WATER AT LOBITH AFTER AN ACCIDENTAL SPILL

Sample data[a]	Time (h)	Concentration (μg/l)
17.06.90	06.00–12.00	0.4
	12.00–18.00	0.6
	18.00–24.00	0.9
18.06.90	00.00–06.00	1.4
	06.00–12.00	1.6
	12.00–18.00	1.3
	18.00–24.00	1.2
19.06.90	00.00–06.00	1.3
	06.00–12.00	0.7
	12.00–18.00	0.5
	18.00–24.00	0.4
20.06.90	00.00–06.00	<0.2
	08.10	<0.2

[a] Composite or grab samples.

component is subject to EC regulation and the maximum admissible concentration (of any one pesticide) in drinking water is 100 ng/l, the intake of surface water for preparing drinking water was stopped for some time.

The validation of the method was determined using the LKB apparatus (see Experimental). The calibration graph (see Fig. 3) in the "real concentration" range (1–10 μg/l) was linear (r^2 = 0.9985). From the 95% confidence curve it can be seen that the limit of detection is 0.45 μg/l. Measurements using dual-wavelength detection, however, are much less sensitive than analyses at fixed wavelength owing to an increased noise level (more than a factor of ten according to the specifications). Two detectors in series might be the method of choice in trace analysis.

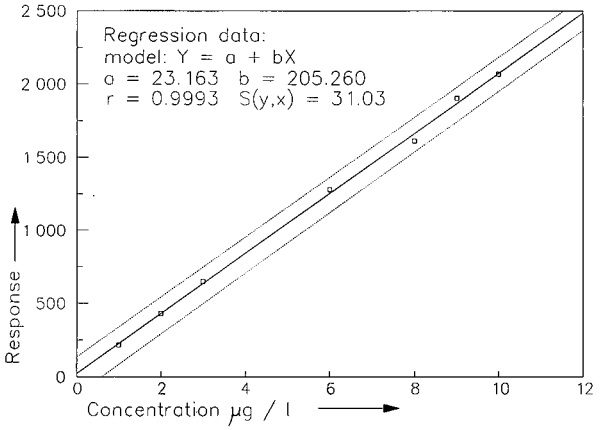

Fig. 3. Calibration graph with regression data and 95% confidence interval for metamitron. Injection volume, 2 ml.

The repeatability of 2-ml sample injections at 2 μg/l was good (relative standard deviation 3%; $n = 7$). The mean recovery of spiked surface water at 2 μg/l was 100.1%. More than 40 surface water injections of 2000 μl were applied to the analytical column without a significant decrease in performance. Neither clogging of the analytical column with particulate matter nor other adverse effects such as irreversible adsorption or memory effects were observed.

CONCLUSION

The determination of metamitron has been achieved by large-volume injections of samples of surface water directly into the analytical column. The limit of detection was 0.15 μg/l using UV detection at 310 nm and applying 2 ml of aqueous sample to the column. The method is reliable and fast (*ca.* 10 min). The calibration graph showed a linear behaviour ($r^2 = 0.9985$) and the repeatability of 2-ml injections at 2 μg/l showed a relative standard deviation of 3%.

The method is simple and indicates that components having sufficient retention on C_{18} columns and having good detectability can be determined very rapidly at low levels. This might be the preferred method if rapid decisions about water quality are necessary with regard to preparing drinking water.

REFERENCES

1 W. Schüssler, *Chromatographia,* 27 (1989) 431.
2 R. Reupert and E. Plöger, *Wasser,* 72 (1989) 211.
3 R. Reupert and E. Plöger, *Fresenius' Z. Anal. Chem.,* 331 (1988) 503.
4 C. J. Miles and H. A. Moye, *Chromatographia,* 24 (1987) 628.
5 M. C. Rouan, *J. Chromatogr.,* 426 (1988) 335.
6 M. Broquaire and P. R. Guinebault, *J. Liq. Chromatogr.,* 4 (1981) 2039.
7 P. R. Guinebault and M. Broquaire, *J. Chromatogr.,* 217 (1981) 509.
8 P. R. Guinebault, M. Broquaire and R. A. Braithwaite, *J. Chromatogr.,* 204 (1981) 329.
9 P. D. McDonald, W. P. Leveille, A. E. Sims, W. J. Wildman, V. R. Zener, A. D. Scarchilli and A. David, *Proceedings, Water Quality Technology Conference, Philadelphia, PA, November 12–16, 1989,* American Water Works Association, Denver, CO, 1991, pp. 631–649.
10 D. L. Foerst, *Method 531, EPA/600/4-85/054,* U.S. Environmental Protection Agency, Environmental Monitoring and Support Laboratory, Cincinnati, OH, 1985.

Journal of Chromatography, 543 (1991) 250–256
Elsevier Science Publishers B.V., Amsterdam

CHROM. 23 070

Short Communication

Determination of the anticancer drug bruceoside-A in the Chinese drug Yadanzi (*Brucea Javanica* Merr.)

HUA CHI*, YUN-PING WANG and TONG-HUI ZHOU
Institute of Materia Medica, Chinese Academy of Medical Sciences, 1 Xian Nong Tan Street, 100050 Beijing (China)
and
CHUN-LIAN JIN
Beijing Tong Ren Tang Second Drug Factory, 100075 Beijing (China)
(First received July 17th, 1990; revised manuscript received December 18th, 1990)

ABSTRACT

A high-performance liquid chromatographic method was developed for the determination of bruceoside-A in the Chinese drug Yadanzi (*Brucea javanica* Merr.). After being boiled in ethanol for the lysis of enzyme, nuts of the fruits of Yadanzi were ground and refluxed with light petroleum (b.p. 60–90°C) to remove the oil, then sonicated in methanol for 1 h and the methanolic solution was left overnight. The resulting solution was analysed using a high-performance liquid chromatograph equipped with a reversed-phase ODS-bonded column and eluted with methanol–water (41:59, v/v) at a flow-rate of 1 ml/min with UV detection at 254 nm.

INTRODUCTION

The fruits of Yadanzi (*Brucea javanica* Merr.) are a common drug in Chinese traditional medicine. Bruceoside-A (Fig. 1) extracted from the fruits has been reported to have anticancer activity [1–3]. Several studies have been reported on the identifi-

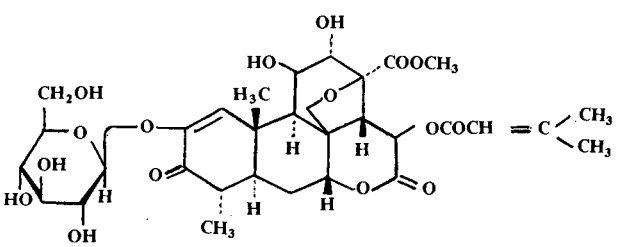

Fig. 1. Structure of bruceoside-A.

0021-9673/91/$03.50

cation of chemical components in the fruits [1–7]. However, to our knowledge, no method has been reported for the determination of bruceoside-A in the fruits. The quality of the fruits of Yadanzi is dependent on the place of production and storage conditions. Information about the bruceoside A content in the fruits is needed for the correct administration of the drug. This paper describes a high-performance liquid chromatographic (HPLC) method for the determination of bruceoside-A in the fruits of Yadanzi.

EXPERIMENTAL

Materials

Bruceoside-A standard was a kind gift from Professor Xian Li (Shenyang Pharmaceutical Institute, Shenyang, China) and Professor Jing-Xi Xie, (Institute of Materia Medica, Chinese Academy of Medical Sciences, Beijing, China). Samples of fruits of Yadanzi were purchased from Beijing, Tianjin, Yunnan, Haikang and Hainandao (China). Chemicals were of analytical-reagent grade.

High-performance liquid chromatography

A Waters Model 510 pump was used together with a 25 cm × 5 mm I.D. reversed-phase bonded column packed with 10-μm ODS material (C_{18}-YWG, Tianjin, China). The sample loop had a volume of 10 μl and the Shimadzu SPD-2A ultraviolet detector was set at 254 nm (0.02 a.u.f.s.). The mobile phase was methanol–water (41:59, v/v) at a flow-rate of 1 ml/min.

Analytical procedure

The shells of Yadanzi fruits were removed and 1.3 g of the nuts was boiled in 10 ml of ethanol for the lysis of enzyme on the surface of the fruits. After grinding, 0.25 g of the nuts was wrapped in a piece of filter-paper and refluxed with 30 ml of light petroleum (b.p. 60–90°C) for 3 h to remove the oil. The nuts were then sonicated in 15 ml of methanol for 1 h and the solution was left overnight. A 5-μl volume of the methanolic solution was injected into the HPLC system and the amount of bruceoside-A in the nuts was calculated from a calibration graph. The ethanolic solution used for the lysis of enzyme was also injected into the HPLC system and the amount of bruceoside-A obtained from this solution was added to that obtained from the methanolic solution to give the total amount of bruceoside-A in the nuts.

RESULTS AND DISCUSSION

Optimization of HPLC conditions

A column packed with reversed-phase ODS C_{18} was tried with eluents consisting of different combinations of methanol and water for the separation of bruceoside-A from the fruits of Yadanzi. Bruceoside-A was well separated with methanol–water (41:59, v/v), as shown in Fig. 2. When the proportion of methanol was decreased, the separation could be further improved. In such a case, more sample could be injected for the collection of bruceoside-A from the outlet of the column.

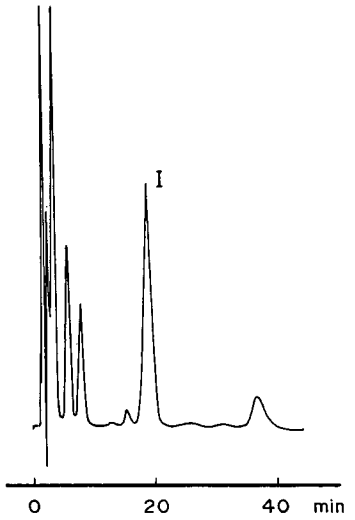

Fig. 2. HPLC of the extracts from the nuts of Yadanzi fruits obtained from Tianjin. For chromatographic conditions, see Experimental. Peak I: bruceoside-A.

Identification of chromatographic peak corresponding to bruceoside-A

The eluate corresponding to peak I in Fig. 2 was collected and evaporated to dryness under vacuum with gentle heating, and further dried in a bottle over phosphorus pentoxide for 3 days. The IR spectrum of the dried powder shown in Fig. 3 was identical with that obtained by Li and Xian, who reported the spectrum for the structural elucidation of bruceoside-A [4], and the NMR spectrum in Fig. 4 coincided

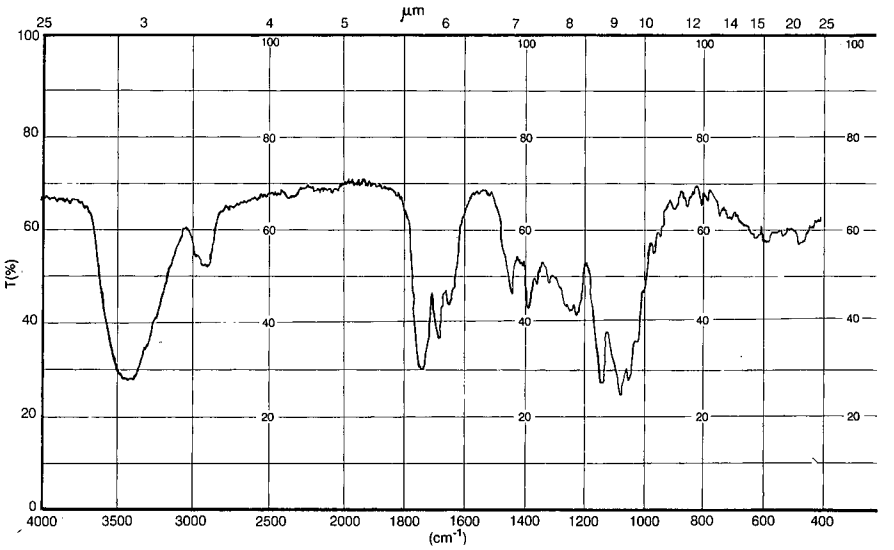

Fig. 3. IR spectrum of bruceoside-A (KBr pellet).

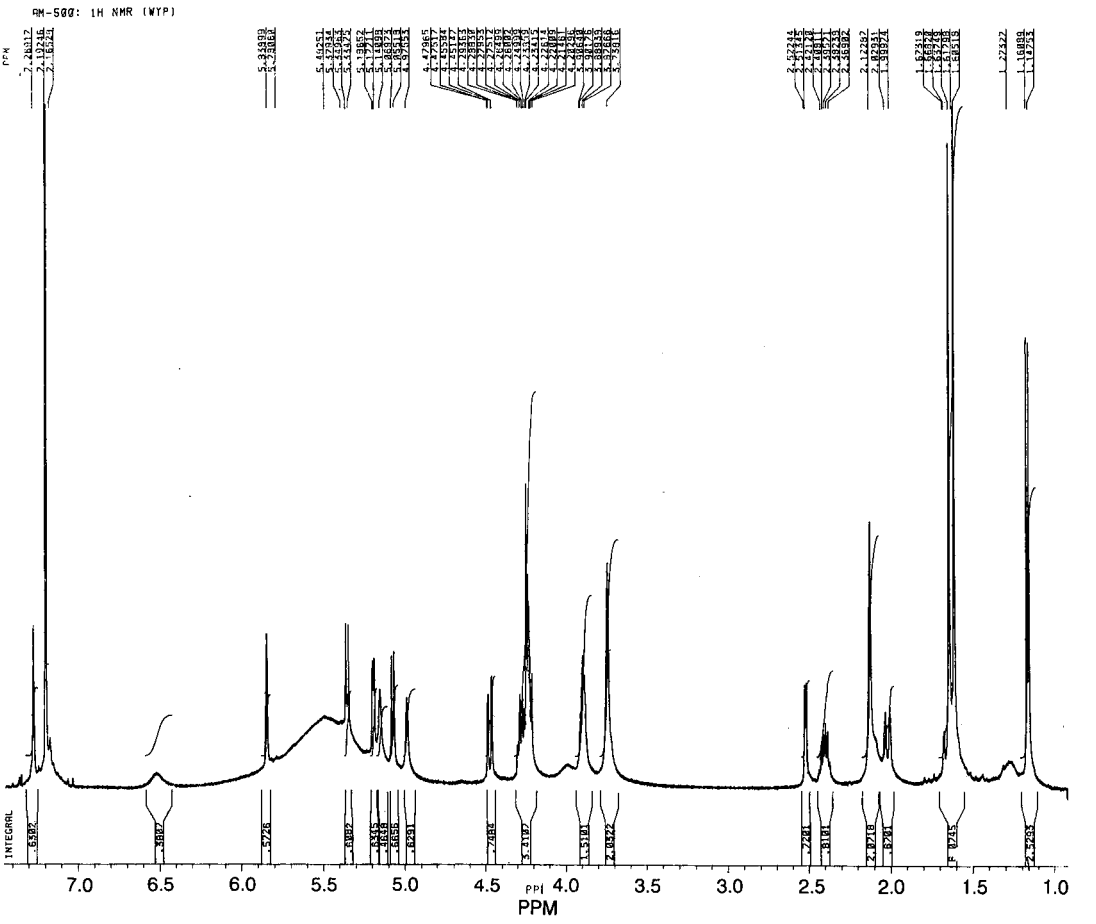

Fig. 4. NMR spectrum of bruceoside-A. Solvent: deuterated pyridine. Reference: tetramethylsilane.

with that obtained by Lee *et al.* [1] for the identification of bruceoside-A. The mass spectrum obtained with fast atom bombardment yielded an ion of *m/z* 705, which might be from $M^+ + 23$ (23 is the atomic weight of sodium), and addition of potassium to the sample yielded an ion of *m/z* 721, which might be from 682 + 39 (39 is the atomic weight of potassium). The molecular mass of bruceoside-A is 682. The retention time of the component collected corresponding to peak I in Fig. 2 was identical with that of the bruceoside-A standard obtained from Professor Jing-Xi Xie and Professor Xian Li. The compound collected from the eluate corresponding to peak I in Fig. 2 was thus identified as bruceoside-A.

Calibration

The calibration graph for bruceoside-A was prepared by injection of 0.22–1.10 μg of bruceoside-A. The resulting graph was linear within this range, with a correla-

tion coefficient of 0.998 ($n = 5$). The regression equation is $y = 0.2 + 65.1x$, where y is the amount of bruceoside-A, x is the peak height.

Optimization of experimental conditions for the removal of oil in the fruits of Yadanzi

A 700-mg amount of ground nuts of Yadanzi fruits was placed in 30 ml of light petroleum (b.p. 60–90°C), followed by refluxing, sonication or being left at room temperature. The weights of the nuts were checked to calculate the amount of oil removed. It was found that refluxing for 3–4 h was the most efficient method for the removal of the oil, and a period of 3 h was adopted.

Comparison of different methods of extraction

Methanol and ethanol were tried for the extraction fo bruceoside-A from the nuts of Yadanzi fruits. After refluxing for 30 min, the amount of bruceoside-A extracted by ethanol was 89% of that extracted by methanol. Extraction with methanol was further studied with different treatments. As shown in Table I, bruceoside-A was stable during reflux and after being refluxed for 1 h the peak height of bruceoside-A ceased to increase. Extraction by sonication followed by leaving the solution overnight yielded the same results as those obtained by refluxing for 1 h. The latter was simpler and therefore used in later experiments.

Recovery

The recovery of bruceoside-A in the extraction procedure was studied by the addition of bruceoside-A to Yadanzi nuts from which the oil had been removed, then the extraction was carried out by adding 15 ml of methanol to the samples and sonication for 1 h and the solutions were left overnight. The resulting solutions were examined by HPLC to check the content of bruceoside-A. As shown in Table II, five runs yielded an average recovery of 98.2% with a relative standard deviation of 4.0%.

Determination of bruceoside-A in samples obtained from different districts in China

Yadanzi fruit samples obtained from Beijing, Tianjin, Yunnan, Haikang and Hainandao were analysed according to the analytical procedure. The results are shown in Table III. The chromatograms were very similar to each other, as shown in Fig. 2.

TABLE I

COMPARISON OF DIFFERENT METHODS FOR THE EXTRACTION OF BRUCEOSIDE-A FROM THE NUTS OF YADANZI FRUITS

Method	Peak height of bruceoside-A (mm) ($n = 2$)
Sonicated with methanol for 1 h	40.0, 41.0
Left in methanol overnight	40.0, 40.0
Sonicated in methanol for 1 h then left overnight	48.0, 49.0
Refluxed in methanol for 30 min	45.0, 50.0
Refluxed in methanol for 1 h	46.0, 51.0
Refluxed in methanol for 2 h	46.0, 51.5
Refluxed in methanol for 3 h	45.0, 51.0

TABLE II

RECOVERY OF BRUCEOSIDE-A IN THE EXTRACTION PROCEDURE

No.	Content of bruceoside-A (mg)	Bruceoside-A added (mg)	Bruceoside-A found (mg)	Recovery (%)
1	4.042	2.754	6.918	104.43
2	4.042	2.550	6.444	94.20
3	4.042	2.562	6.538	97.42
4	4.042	2.225	6.257	99.55
5	4.042	2.290	6.226	95.37

Five analyses of bruceoside-A in the sample obtained from Tianjin yielded an average value of 1.43% with a standard deviation of 0.06%. As shown in Table III, the amounts of bruceoside-A in samples from different sources varied widely.

TABLE III

DETERMINATION OF BRUCEOSIDE-A IN THE FRUITS OF YADANZI OBTAINED FROM DIFFERENT DISTRICTS IN CHINA

Source	Bruceoside-A found (%)	*n*
Beijing	0.50, 0.47	2
Hainandao	1.04 ± 0.05	3
Haikang	1.11 ± 0.04	3
Yunnan	0.85 ± 0.04	4
Tianjin	1.43 ± 0.06	5

CONCLUSION

A proposed HPLC method for the determination of bruceoside-A in the fruits of Yadanzi provides a means of elucidating the quality of the Chinese drug Yadanzi and would be useful for guidance regarding administration of the drug in the correct dosage.

ACKNOWLEDGEMENTS

We are grateful to Professor K. H. Lee of the School of Pharmacy, University of North Carolina, U.S.A., for sending an NMR spectrum of bruceoside-A and to Professor Xian Li of Shenyang Pharmaceutical Institute, Shenyang, China, for providing the bruceoside-A standard and an IR spectrum.

REFERENCES

1 K. H. Lee, Y. Imakura and H. C. Huang, *J. Chem. Soc., Chem. Commun.*, (1977) 69–70.
2 K. H. Lee, Y. Imakura, Y. Sumida, R. Y. Wu, I. H. Hall and H. C. Huang, *J. Org. Chem.*, 44 (1979) 2180–2185.
3 X. J. Xi and J. Zheng, *Acta Pharm. Sin.*, 16 (1981) 53–55.
4 L. Xian and Z. S. Xian, *Zhong Cao Yao*, 11 (1980) 530–533.
5 L. Xian and Z. S. Xian, *Acta Shenyang Pharm. Inst.*, 17 (1983) 45–47.
6 L. A. Qiu, L. S. Rong, J. Zheng and X. J. Xi, *Acta Beijing Educ. Coll.*, 3 (1982) 71–73.
7 S. S. Qing, W. L. Qun and Z. L. Ping, *Zhong Cao Yao*, 14 (1983) 5–7.

Journal of Chromatography, 543 (1991) 257–261
Elsevier Science Publishers B.V., Amsterdam

CHROM. 23 122

Short Communication

Re-examination of the fatty acid composition of *Biota orientalis* seed oil by gas chromatography–mass spectrometry of the picolinyl ester derivatives

MARCEL S. F. LIE KEN JIE* and CANDY Y. C. CHOI
Department of Chemistry, University of Hong Kong, Pokfulam Road, Hong Kong (Hong Kong)
A. BERGER
223 Food Science and Technology Building, University of California, Davis, CA 95616 (U.S.A.)
and
R. G. BERGER
Institut für Lebensmitteltechnologie und Analytische Chemie der Technischen Universität München, Munich (Germany)
(First received September 11th, 1990; revised manuscript received January 14th, 1991)

ABSTRACT

Re-examination of the fatty acid composition of *Biota orientalis* (*Platycladus orientalis* or *Thuja orientalis* or *Arbor-vitae*) by gas chromatography–mass spectrometry of the picolinyl ester derivatives showed the presence of 20:3(5*c*,11*c*,14*c*) (4.3%) and 20:3(11*c*,14*c*,17*c*) (0.4%), which was not in agreement with the results published previously. The positions of the unsaturated centres in the alkyl chain of the fatty acids were readily determined by examining the mass spectral fragmentation pattern of the picolinyl derivatives.

INTRODUCTION

Gas chromatography–mass spectrometry (GC–MS) of picolinyl ester derivatives of unsaturated fatty acids has proved to be a reliable means of determining the chain length and the position of the unsaturated centres in long-chain fatty acids. Similarly to the methyl ester derivatives of unsaturated fatty acid molecules, the picolinyl esters are readily separated by GC on polar and non-polar stationary phases. Also, prior to GC analysis, reversed-phase high-performance liquid chromatography can be utilized to fractionate the picolinyl esters to enhance the detectability of minor components present in natural samples [1,2]. However, unlike methyl ester derivatives, there is no double bond migration during mass spectral analysis of the picolinyl esters

0021-9673/91/$03.50

of unsaturated fatty acids. This observation permits the direct analysis of a mixture of picolinyl esters of saturated and unsaturated fatty acids without the need to derivatize the unsaturated centres prior to mass spectral analysis in order to determine the positions of the ethylenic bonds present [3–7]. This method is also applicable to highly unsaturated fatty acids as demonstrated by Christie [8] in the structural elucidation of 18:3(5*c*,9*c*,12*c*).

The fatty acid composition of the seed oil of *Biota orientalis* (also known as *Platycladus orietalis* or *Thuja orientalis* or more commonly as *Arbor-vitae*) [9] was reported earlier by our group to contain a relatively high proportion of 20:4 (5*c*,11*c*,14*c*,17*c*) (10.5%) [10]. This seed oil is used in Chinese medicine to alleviate problems related to the male reproductive system [11]. Our purpose in re-examining the fatty acid composition stems from our intensive investigations into the biological effects of this seed oil on rats maintained on an essential fatty acid-free diet [12].

EXPERIMENTAL

Materials

B. orientalis seeds were purchased from herb shops in Guangzhou, China. Isolation of the oil and conversion of the neutral lipid–glycolipid fraction to the free fatty acid and methyl ester derivatives and separation of methyl esters by silver ion thin-layer chromatography as described previously [10]. 1,1′-Carbonyldiimidazole, 3-hydroxymethylpyridine and 4-pyrrolidinopyridine were purchased from Aldrich (Milwaukee, WI, U.S.A.). All solvents were distilled before use.

Preparation of picolinyl ester derivatives

1,1′-Carbonyldiimidazole in dichloromethane (75 μl, 100 mg/ml) was added to the free fatty acid mixture (5 mg) in dichloromethane (75 μl). After standing for 1 min at room temperature, a solution of 3-hydroxymethylpyridine (7.5 mg) and 4-pyrrolidinopyridine (1.5 mg) in dichloromethane (75 μl) was added, followed by triethylamine (75 μl). The mixture was left for 10 min at 37°C, then evaporated to dryness in a stream of nitrogen. The products were dissolved in *n*-hexane (5 ml), washed with water (2 ml) and dried over sodium sulphate. The *n*-hexane solution was loaded on a column of Florisil (0.5 g) in *n*-hexane contained in a pasteur pipette and eluted with 8 ml of *n*-hexane–diethyl ether (95:5, v/v) to remove non-polar material. The column was then eluted with 10 ml of *n*-hexane–diethyl ether (1:4, v/v), which gave the required picolinyl ester derivatives after evaporation of the solvent of the eluent under reduced pressure.

GC–MS

GC–MS was carried out on a Hewlett-Packard Model HP5970 gas chromatograph fitted with a 12 m × 0.2 mm I.D. capillary glass column (0.33 μm film thickness, cross-linked methylsilicone gum, Ultra 1), with helium as the carrier gas at a flow-rate of *ca.* 2 ml/min and temperature programming from 170 to 240°C at 5°C/min. The outlet of the column was connected to a Hewlett-Packard mass-selective detector.

GC of the methyl ester derivatives was carried out on the same chromatograph, fitted with a 30 m × 0.25 mm I.D. glass capillary column (0.20 μm film thickness, SP2330) isothermally at 220°C using helium as the carrier gas at a flow-rate of *ca.*

2 ml/min and a flame ionization detector. A mixture of methyl esters of 14:0, 16:0, 18:0, 20:0 and 22:0 fatty acids was used as an external standard.

RESULTS AND DISCUSSION

The fatty acid composition of the *B. orientalis* seed oil was compared to that obtained in a previous study [10], which utilized a microbore non-polar column and a 2-m SP2300 packed column (Table I). The present investigation showed the clear separation of the picolinyl ester derivatives of the 20:3 component into two distinct positional isomers (Fig. 1), which were identified by GC–MS as 20:3(5*c*,11*c*,14*c*) (4.3%) and 20:3(11*c*,14*c*,17*c*) (0.4%). The relative abundance of these two isomers is consistent with that occurring in the seed oils of many gymnospermae [13]. The mass spectra of these isomers are presented in Figs. 2 and 3, respectively. In the mass spectum of 20:3(5*c*,11*c*,14*c*), the unsaturated centre at the C-5/C-6 position was confirmed by the gap between m/z = 178 and 204, and positions C-11/C-12 and C-14/C-15 were determined from gaps at m/z = 260 and 286 and m/z = 300 and 326, respectively (Fig. 2). The mass spectrum of 20:3(11*c*,14*c*,17*c*) displayed gaps at m/z = 262 and 288, m/z = 302 and 328 and m/z = 342 and 368, which confirmed the positions of the double bonds at C-11/C-12, C-14/C-15 and C-17/C-18, respectively (Fig. 3). Three minor components [20:1(11*c*) (0.4%), 20:2(5*c*,11*c*) (0.8%) and 20:2 (11*c*,14*c*) (0.8%)] were also identified by GC–MS of the picolinyl ester derivatives, which eluded our earlier investigation. The structure of 20:4 (11.3%) was reconfirmed by mass spectral analysis of the picolinyl derivative (Fig. 4). In the mass spectral analysis of 20:4(5*c*,11*c*,14*c*,17*c*), the unsaturated centre at the C-5/C-6 position was confirmed by the gap between m/z = 178 and 204, while the positions C-11/C-12, C-14/C-15 and C-17/C-18 were determined from the gaps at m/z = 260 and 286, m/z = 300 and 326 and m/z = 340 and 366, respectively.

From the above results, it is evident that GC–MS of picolinyl ester derivatives of

TABLE I

FATTY ACID COMPOSITION OF *BIOTA ORIENTALIS* SEED OIL

Fatty acid	Content (mol%)	
	This work	Ref. 10
16:0	4.7	5.1
18:0	3.5	3.4
18:1(9*c*)	11.6	15.3
18:2(9*c*,12*c*)	26.0	25.6
18:3(9*c*,12*c*,15*c*)	36.2	34.7
20:0	Trace	Trace
20:1(11*c*)	0.4	–
20:2(5*c*,11*c*)	0.8	Trace
20:2(11*c*,14*c*)	0.8	Trace
20:3(5*c*,11*c*,14*c*)	4.3	–
20:3(11*c*,14*c*,17*c*)	0.4	4.9
20:4(5*c*,11*c*,14*c*,17*c*)	11.3	10.5

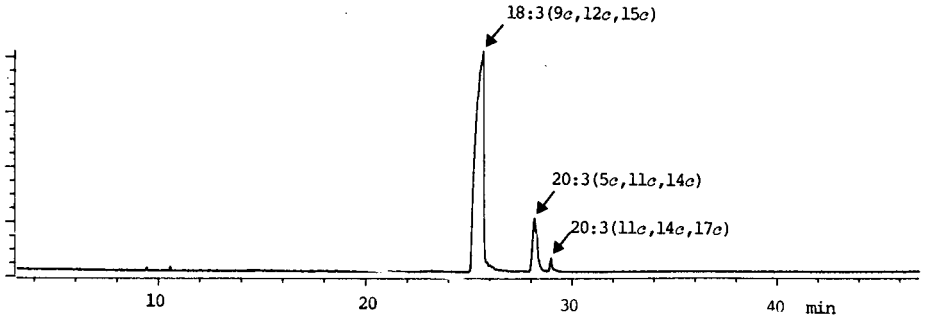

Fig. 1. Chromatogram of picolinyl esters of 18:3 and 20:3 components of *Biota orientalis* seed oil. For conditions, see *GC–MS*.

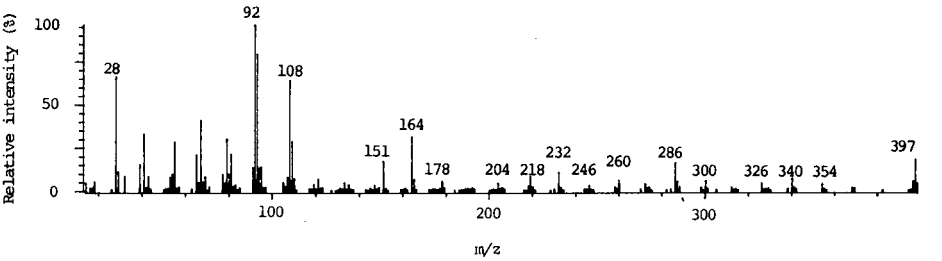

Fig. 2. Mass spectral analysis of picolinyl ester of 20:3(5*c*,11*c*,14*c*).

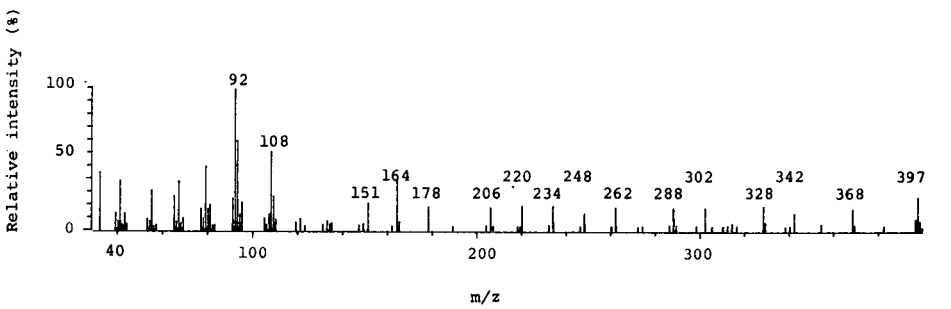

Fig. 3. Mass spectral analysis of picolinyl ester of 20:3(11*c*,14*c*,17*c*).

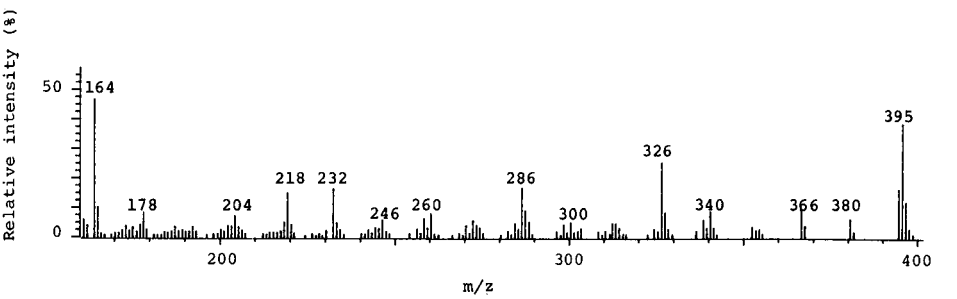

Fig. 4. Mass spectral analysis of picolinyl ester of 20:4(5*c*,11*c*,14*c*,17*c*).

fatty acids constitutes a facile and reliable method for determining the chain length and the positions of the unsaturated centres in the alkyl chain of fatty acid molecules.

ACKNOWLEDGEMENTS

This study was supported by the Lipid Research Fund and the Strategic Research Grants Committee of the University of Hong Kong. The authors thank Dr. Bruce German and Mr. Richard Creveling of the University of California, Davis, Lipid Research Laboratory, for assistance in lipid analyses.

REFERENCES

1 W. W. Christie and K. Stefanov, *J. Chromatogr.*, 392 (1987) 259.
2 W. W. Christie, E. Y. Brechany and K. Stefanov, *Chem. Phys. Lipids*, 46 (1987) 127.
3 D. J. Harvey, *Biomed. Mass Spectrom.*, 9 (1982) 33.
4 W. W. Christie, E. Y. Brechany and R. T. Holmăn, *Lipids*, 22 (1987) 224.
5 W. W. Christie, E. Y. Brechany, F. D. Gunstone, M. S. F. Lie Ken Jie and R. T. Holman, *Lipids*, 22 (1987) 664.
6 W. W. Christie, E. Y. Brechany and M. S. F. Lie en Jie, *Chem. Phys. Lipids*, 46 (1988) 225.
7 M. S. F. Lie Ken Jie and C. Y. C. Choi, *J. Int. Fed. Clin. Chem.*, submitted for publication.
8 W. W. Christie, in R. C. Cambie (Editor), *Fats for the Future*, Ellis Horwood, Chichester, 1989, pp. 335–344.
9 L. H. Bailey and E. Z. Bailey, *Hortus Third: a concise dictionary of gardening, general horticulture and cultivated plants in North America*, Macmillan, New York, 1976.
10 M. S. F. Lie Ken Jie, H. B. Lao and Y. F. Zheng, *J. Am. Oil Chem. Soc.*, 65 (1988) 597.
11 *Chongyao da Zidian*, Shanghai Science Technology Publishing Co., Shanghai, 1978.
12 M. S. F. Lie Ken Jie and M. Sugano, unpublished results.
13 T. Takagi and Y. Itabashi, *Lipids*, 17 (1982) 716.

Journal of Chromatography, 543 (1991) 262–265
Elsevier Science Publishers B.V., Amsterdam

CHROM. 23 110

Short Communication

Enthalpy of transfer in supercritical fluid chromatography

MICHAL ROTH
Institute of Analytical Chemistry, Czechoslovak Academy of Sciences, 61142 Brno (Czechoslovakia)
(First received October 23rd, 1990; revised manuscript received January 10th, 1991)

ABSTRACT

The enthalpy of solute transfer from the mobile to the stationary phase in supercritical fluid chromatography has often been calculated from the plot of solute retention against the reciprocal absolute temperature at a constant density of the mobile phase fluid. In this treatment it has been assumed that the enthalpy of solute transfer is directly proportional to the slope of this plot.

In the present report, the above procedure is proven to be incorrect. A thermodynamic analysis shows that the slope of a constant-density plot is related neither to enthalpy nor to internal energy of solute transfer between the two phases.

The temperature dependence of solute retention in supercritical fluid chromatography has been studied at a constant pressure or at a constant density of the mobile phase fluid. The temperature dependence of the logarithm of the solute capacity factor, k, is strongly curved and displays a maximum when observed at a constant pressure [1–4]. On the other hand, the plots of ln k against the reciprocal of absolute temperature, $1/T$, at a constant density of the mobile phase are nearly linear [5]. Several workers [5–9] have employed constant-density plots to calculate the molar enthalpy of transfer of the solute from the mobile to the stationary phase, ΔH_t, according to the equation

$$\Delta H_t = -R[\partial \ln k/\partial(1/T)]_{\rho_m} \quad (1)$$

where R is the molar gas constant and ρ_m is the density of the mobile phase fluid. However, a rigorous thermodynamic support for eqn. 1 has never been presented. Further, Martire and Boehm [10] have related the slope of a constant-density plot to the internal energy of transfer, ΔU_t, rather than to the enthalpy of transfer. Therefore, an attempt to elucidate the actual thermodynamic background of the slope of a constant-density plot appeared worthwhile.

0021-9673/91/$03.50

Considering $\ln k$ as a function of the reciprocal of absolute temperature, $1/T$, and of the pressure, P, one may write the total differential of $\ln k$ as

$$\mathrm{d}\ln k = \left[\frac{\partial \ln k}{\partial(1/T)}\right]_P \mathrm{d}(1/T) + \left(\frac{\partial \ln k}{\partial P}\right)_T \mathrm{d}P \tag{2}$$

It follows directly from eqn. 2 that the derivative of $\ln k$ with respect to $1/T$ at a constant density of the mobile phase fluid is given by

$$\left[\frac{\partial \ln k}{\partial(1/T)}\right]_{\rho_m} = \left[\frac{\partial \ln k}{\partial(1/T)}\right]_P + \left(\frac{\partial \ln k}{\partial P}\right)_T \left[\frac{\partial P}{\partial(1/T)}\right]_{\rho_m} \tag{3}$$

Eqn. 3 may be rewritten in a more convenient form:

$$\left[\frac{\partial \ln k}{\partial(1/T)}\right]_{\rho_m} = -T^2(\partial \ln k/\partial T)_P - T^2\gamma_{mV}(\partial \ln k/\partial P)_T \tag{4}$$

where

$$\gamma_{mV} = (\partial P/\partial T)_{\rho_m} \tag{5}$$

is the thermal pressure coefficient [11] of the mobile phase fluid. The derivatives on the right-hand side of eqn. 4 are given by [12]

$$(\partial \ln k/\partial T)_P = (\bar{h}_{1s}^{\infty} - \bar{h}_{1m}^{\infty})/(RT^2) + \alpha_{mP} + (V_s/V_m)\alpha_{sP} + C(\partial x_{3s}/\partial T)_P \tag{6}$$

$$(\partial \ln k/\partial P)_T = (\bar{v}_{1m}^{\infty} - \bar{v}_{1s}^{\infty})/(RT) - \beta_{mT} - (V_s/V_m)\beta_{sT} + C(\partial x_{3s}/\partial P)_T \tag{7}$$

where

$$C = 1/(1 - x_{3s}) - \partial \ln \varphi_{1s}^{\infty}/\partial x_{3s} \tag{8}$$

$\bar{h}_{1m}^{\infty}$ and $\bar{h}_{1s}^{\infty}$ are the infinite-dilution partial molar enthalpies of the solute in the mobile and the stationary phase, respectively, $\bar{v}_{1m}^{\infty}$ and $\bar{v}_{1s}^{\infty}$ are the infinite-dilution partial molar volumes of the solute in the two phases, V_m and V_s are the volumes of the two phases in the column, α_{mP} and α_{sP} are the isobaric expansivities of the two phases, β_{mT} and β_{sT} are the isothermal compressibilities of the two phases, x_{3s} is the equilibrium mole fraction of the mobile phase fluid in the stationary phase and φ_{1s}^{∞} is the infinite-dilution fugacity coefficient of the solute in the stationary phase.

Substituting from eqns. 6 and 7 into eqn. 4 and employing the identity [11]

$$\alpha_{mP} = \beta_{mT}\gamma_{mV} \tag{9}$$

one obtains

$$\left[\frac{\partial \ln k}{\partial(1/T)}\right]_{\rho_m} = -[\bar{h}_{1s}^{\infty} - \bar{h}_{1m}^{\infty} - T\gamma_{mV}(\bar{v}_{1s}^{\infty} - \bar{v}_{1m}^{\infty})]/R + T^2(V_s/V_m)(\beta_{sT}\gamma_{mV} - \alpha_{sP}) -$$

$$CT^2[(\partial x_{3s}/\partial T)_P + \gamma_{mV}(\partial x_{3s}/\partial P)_T] \quad (10)$$

If the terms containing V_s, V_m and x_{3s} are neglected, one arrives at a final approximate relationship

$$\left[\frac{\partial \ln k}{\partial(1/T)}\right]_{\rho_m} \approx -(\Delta H_t - T\gamma_{mV}\Delta V_t)/R \quad (11)$$

where ΔH_t and ΔV_t are the molar enthalpy and molar volume of solute transfer from the mobile to the stationary phase, respectively:

$$\Delta H_t = \bar{h}_{1s}^{\infty} - \bar{h}_{1m}^{\infty} \quad (12)$$

$$\Delta V_t = \bar{v}_{1s}^{\infty} - \bar{v}_{1m}^{\infty} \quad (13)$$

The internal energy of solute transfer is given by

$$\Delta U_t = \Delta H_t - P\Delta V_t \quad (14)$$

The term in parentheses on the right-hand side of eqn. 11 would be equal to ΔU_t if

$$T\gamma_{mV} = P \quad (15)$$

In general, however, eqn. 15 applies only to an ideal gas. In a supercritical fluid the situation can be very different. For example, in carbon dioxide at 345 K and 150 bar, the Lee–Kesler correlation [13,14] yields $\gamma_{mV} = 1.88$ bar/K, so that $T\gamma_{mV} \approx 650$ bar.

CONCLUSIONS

The plots of ln k against $1/T$ at a constant density of the mobile phase fluid should be interpreted with care. The principal virtue of such plots is their apparent linearity as correctly predicted by the unified molecular theory of chromatography [10]. However, the linearity alone does not imply that the slope of a constant-density plot has a simple physical significance. It appears that the slope of such a plot is related neither to enthalpy nor to internal energy of solute transfer between the two phases. Instead, the slope is a composite parameter given by eqn. 10 or 11.

REFERENCES

1 S. T. Sie and G. W. A. Rijnders, *Sep. Sci.*, 2 (1967) 729.
2 S. T. Sie and G. W. A. Rijnders, *Sep. Sci.*, 2 (1967) 755.
3 D. Leyendecker, F. P. Schmitz and E. Klesper, *J. Chromatogr.*, 315 (1984) 19.

4 T. L. Chester and D. P. Innis, *J. High Resolut. Chromatogr. Chromatogr. Commun.*, 8 (1985) 561.
5 H. H. Lauer, D. McManigill and R. D. Board, *Anal. Chem.*, 55 (1983) 1370.
6 C. R. Yonker and R. D. Smith, *J. Chromatogr.*, 351 (1986) 211.
7 D. Leyendecker, D. Leyendecker, B. Lorenschat, F. P. Schmitz and E. Klesper, *J. Chromatogr.*, 398 (1987) 89.
8 T. A. Berger, *J. Chromatogr.*, 478 (1989) 311.
9 D. R. Luffer, W. Ecknig and M. Novotny, *J. Chromatogr.*, 505 (1990) 79.
10 D. E. Martire and R. E. Boehm, *J. Phys. Chem.*, 91 (1987) 2433.
11 J. S. Rowlinson and F. L. Swinton, *Liquids and Liquid Mixtures*, Butterworth, London, 3rd ed., 1982, pp. 11–19.
12 M. Roth, *J. Phys. Chem.*, 94 (1990) 4309.
13 B. I. Lee and M. G. Kesler, *AIChE J.*, 21 (1975) 510.
14 B. I. Lee and M. G. Kesler, *AIChE J.*, 21 (1975) 1040.

PUBLICATION SCHEDULE FOR 1991

Journal of Chromatography and Journal of Chromatography, Biomedical Applications

MONTH	D 1990	J	F	M	A	M	
Journal of Chromatography	535/1 + 2	536/1 + 2 537/1 + 2 538/1	538/2 539/1 539/2	540/1 + 2 541/1 + 2 542/1	542/2 543/1	543/2 544/1 + 2 545/1	The publication schedule for further issues will be published later
Cumulative Indexes, Vols. 501–550							
Bibliography Section				560/1			
Biomedical Applications		562/1 + 2 563/1	563/2	564/1	564/2 565/1 + 2	566/1 566/2	

INFORMATION FOR AUTHORS

(Detailed *Instructions to Authors* were published in Vol. 522, pp. 351–354. A free reprint can be obtained by application to the publisher, Elsevier Science Publishers B.V., P.O. Box 330, 1000 AH Amsterdam, The Netherlands.)

Types of Contributions. The following types of papers are published in the *Journal of Chromatography* and the section on *Biomedical Applications:* Regular research papers (Full-length papers), Review articles and Short Communications. Short Communmications are usually descriptions of short investigations, or they can report minor technical improvements of previously published procedures; they reflect the same quality of research as Full-length papers, but should preferably not exceed six printed pages. For Review articles, see inside front cover under Submission of Papers.

Submission. Every paper must be accompanied by a letter from the senior author, stating that he/she is submitting the paper for publication in the *Journal of Chromatography*.

Manuscripts. Manuscripts should be typed in double spacing on consecutively numbered pages of uniform size. The manuscript should be preceded by a sheet of manuscript paper carrying the title of the paper and the name and full postal address of the person to whom the proofs are to be sent. As a rule, papers should be divided into sections, headed by a caption (*e.g.*, Abstract, Introduction, Experimental, Results, Discussion, etc.). All illustrations, photographs, tables, etc., should be on separate sheets.

Introduction. Every paper must have a concise introduction mentioning what has been done before on the topic described, and stating clearly what is new in the paper now submitted.

Abstract. All articles should have an abstract of 50–100 words which clearly and briefly indicates what is new, different and significant.

Illustrations. The figures should be submitted in a form suitable for reproduction, drawn in Indian ink on drawing or tracing paper. Each illustration should have a legend, all the *legends* being typed (with double spacing) together on a *separate sheet.* If structures are given in the text, the original drawings should be supplied. Coloured illustrations are reproduced at the author's expense, the cost being determined by the number of pages and by the number of colours needed. The written permission of the author and publisher must be obtained for the use of any figure already published. Its source must be indicated in the legend.

References. References should be numbered in the order in which they are cited in the text, and listed in numerical sequence on a separate sheet at the end of the article. Please check a recent issue for the layout of the reference list. Abbreviations for the titles of journals should follow the system used by *Chemical Abstracts.* Articles not yet published should be given as "in press" (journal should be specified), "submitted for publication" (journal should be specified), "in preparation" or "personal communication".

Dispatch. Before sending the manuscript to the Editor please check that the envelope contains four copies of the paper complete with references, legends and figures. One of the sets of figures must be the originals suitable for direct reproduction. Please also ensure that permission to publish has been obtained from your institute.

Proofs. One set of proofs will be sent to the author to be carefully checked for printer's errors. Corrections must be restricted to instances in which the proof is at variance with the manuscript. "Extra corrections" will be inserted at the author's expense.

Reprints. Fifty reprints of Full-length papers and Short Communications will be supplied free of charge. Additional reprints can be ordered by the authors. An order form containing price quotations will be sent to the authors together with the proofs of their article.

Advertisements. Advertisement rates are available from the publisher on request. The Editors of the journal accept no responsibility for the contents of the advertisements.

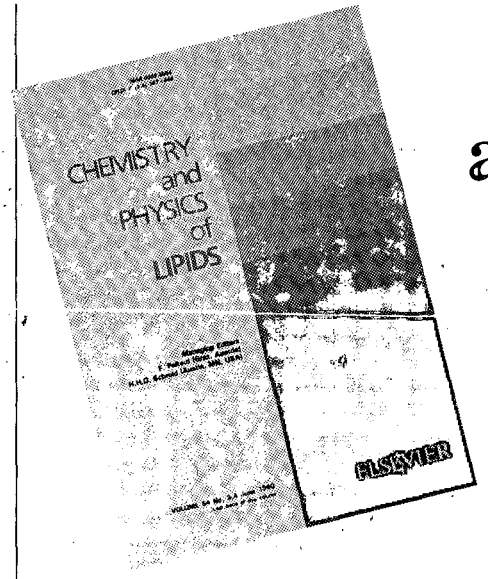

CHEMISTRY and PHYSICS of LIPIDS

Aims and Scope :
CHEMISTRY and PHYSICS of LIPIDS publishes papers and review articles in the field of molecular biology which emphasize chemical and (bio)physical aspects of lipids. Accordingly, the journal covers: advances in synthetic lipid methodology; chemical and (bio)physical characterization of isolated structures; physicochemical studies into lipid-lipid and lipid-protein interactions in lipoproteins and in natural and model membranes; thermodynamics, phase behaviour, topology and dynamics of lipid assemblies; structure-function relationships; and the role of lipids in the regulation of biological processes. Reviews, original research communications and short communications will be considered for publication in each issue. Special issues devoted to high interest topics appear each year.

Supported by an international Advisory Editorial Board

Subscription Information:
1991: Volumes 55-58 (4 vols. in 12 issues)
Price: US$ 712.00 plus US$ 68.00 postage and handling
ISSN 0009-3084

Abstracted/Indexed in: Biological Abstracts; Chemical Abstracts; Current Contents (Life Sciences); Excerpta Medica (EMBASE); Index Medicus; PASCAL M; Reference Update.

ELSEVIER SCIENCE PUBLISHERS

SEND YOUR ORDERS TO:
ELSEVIER SCIENTIFIC PUBLISHERS IRELAND, LTD., P.O. BOX 85, LIMERICK, IRELAND
Requests for free sample issues should be addressed to:
ELSEVIER SCIENCE PUBLISHERS B.V., P.O. Box 1527, 1000 BM Amsterdam, The Netherlands. Fax: (020) 5803-342
or: Journal Information Center, ELSEVIER SCIENCE PUBLISHING CO. INC., P.O. Box 882,
Madison Square Station, New York, NY 10159, U.S.A. Tel: (212) 633-3750
The US $ price is definitive

91/JO/020/E